Modelling of Arterial and Haemogenic Endothelium Development from Mouse and Human Pluripotent Stem Cells



Juan Pablo Ruiz Villalobos

Pembroke College

University of Oxford

A thesis submitted for the degree of

Doctor of Philosophy

Michaelmas 2018

For Sofía and Isabel,
Who in less than nine months in the womb did something experts in this field have attempted to recreate for decades.

And for their whole generation,
May we be judged justly for the world we leave you behind.

Acknowledgments

Like the haematopoietic stem cell (HSC), human beings are at their fullest potential when surrounded and supported by others, their niche, as it were. And so, though the work presented here is my own, it would be remiss of me to not thank those who played critical support roles through the years of experiment design, tissue culture, lab meetings, moving overseas, deep dinner conversations, heartache, and bliss.

I would like to thank and acknowledge my mentors, who took on this somewhat peculiar scientist on their team. For their patience through my periods of intense excitement and my literally running through lab screaming, singing, or dancing, and through my periods of likewise intense disinterest, distraction, and depression. Roger and Catherine, the lessons I learned in developmental biology during my time at Oxford were indispensable throughout my thesis work, and a newfound love and interest I will maintain throughout my life. André, for your positivity and encouragement; without your understanding and patience with me during my periods of mental health struggles and willingness to listen, I would not be finishing this thesis. I would also like to thank Herman and Jeff, who have guided and mentored me in the past and continue to support me in my scientific journey.

To the Porcher, Patient, Larochelle, and Vyas labs: The community and friendships built during these years played a large role in the person and scientist I have become; from conversations in the cafeteria, pubs, and late-night tissue culture…they all go with me on this next journey. Especially though, I would like to thank the postdocs and staff scientists: Hedia and Rick for their technical expertise and willingness to drop their own projects at any point to help me with any questions and concerns I had regarding my own; Aldo, Arif, and Rui for their theoretical expertise and putting up with the plethora of questions I threw at them regarding developmental biology and experimental design.

Flow Cytometry played an important role during my time as a PhD student, and I came to enjoy it and gain expertise in it as my favourite assay to characterise cells. It was a learning process that involved many, across labs and continents: Paul from the WIMM FACS facility, and Kevin, for his initial training and support, many times conversational and emotional more than technical. Jörg, for fostering that passion and answering my questions in Belgium. I found that same kind of support at the NIH, both with Keyvan at the haematology branch Flow facility, and with Pradeep, Venina, and Steve at the NHLBI Flow Cytometry Core. I also want to thank Helen, who with her flow expertise from yet another lab, the Jacobsen group, gave me a very thorough lesson in setting up new panels with proper controls.

During these years, I was surrounded by people far and wide that formed a support net and niche in which I found stability, and for them, I will always be grateful. Specifically, I'd like to thank the counsellors and therapists that supported me during my time at Oxford and NIH: Ruth, Julia, and Laurie, you were all much-needed guardian angels. Likewise, all Friends in London, US, Spain, and Mexico, who continue to push and challenge me on the path. Specifically, I'd like to thank Anatolio, Mike, Adam, Jo, Wes, Tom, Cornelia, Ana María, Mario, Cristina, and of course, Arif.

I'd like to thank my family, for their incomparable love, support, and patience in what has been the most emotionally turbulent half-decade of my life. Specifically, I'd like to thank my mother, who has been a source of strength, learning, patience, love, porras, and apapachos. Sin ti Mami, nunca hubiera llegado tan lejos. Mis logros son tuyos. I will always be grateful for your perseverance, strength, and desire to learn and listen. I'd also like to thank my aunt Tessy, who helped me start an important chapter in my journey of

self-discovery and learning. And to Paola, for her example in self-love and bravery amidst so much adversity: true love breaks boundaries and paradigms. And to my sisters, father, grandparents, aunts, uncles, and brother-in-law, for accepting me as I am, difficult though that may be for them sometimes.

I am grateful for the other strong women in my life, for their friendships and mentorships throughout the years. To my three wonderful and magical partners throughout the course of this thesis: Pam, Rachel, and Katie, who in your own unique struggles and adversity shared beautiful moments of vulnerability and connection with me and continue to inspire me on this path of personal and relational growth. May we all find people who can love us in a way that feels nurturing, whole, exciting, safe, and satisfying, and may we find the courage and strength to communicate when our relational needs are not met and boundaries not respected.

To Victoria, my fairy godmother, for all the kvelling that kept me going. To Isabel, Nina, Catherine, So, and Estefanía for the comfort, the conversations, and laughter. To my Oxford Doñas: Dan, Mary, and Kiki, who welcomed me into their home and girl's nights; for the kitchen dancing and support with my ups and downs. To the Three Fold Chord: Heather and Kacey; for MMM nights with sangritas and your patient listening to the crazy musings of my heart.

To the men in my life, who not only give me hope for the future of masculinity, but challenge me with their examples, mentorship, and friendship to be a better man: Bokki Sæll, Matt, Josh, and Sylvain. You have all filled different aspects of that need for companionship we all have. But especially, to the brothers who walked with me during the PhD years: Tomek, thank you for the music, it was a beautiful privilege to be your second wife; Will, "min broðr, hwæt!" Malte, for the solidarity and understanding; Adam, for the reminder that it's ok for the Who to be more important than the What, and bringing me into your DC family. And of course Pedro, my shield-brother: AL SM NA

I would also like to thank those who, like me, have a dream for a more egalitarian, inclusive, and diverse scientific enterprise, that we may have the freedom to dream up our wild experiments without having first to think of what will get us into Science or Nature. There were many who advised me to stop the passion work I was doing on the side with Labmosphere, to put my head down, publish my science, and change things when in power. In wanting to prove them wrong, I was only spurred further. Had I listened to them, I would never have joined the Board of Directors at Future of Research, or publicly challenged Drs. Lawrence Tabak and Francis Collins on their handling of the GSI initiative. But there were also those who encouraged me, and it is them I thank by name: Gary, Jessica, Adriana, and the rest of the board at Future of Research, as well as Chris Pfund, Kenny, Chris Pickett, Stephani, Angela, Susanna, and all others who bravely speak up and challenge a deeply broken system, regardless of career stage. Being a scientist in this day and age means engaging with the social, political, and environmental injustices of our time, both inside and outside of our own Ivory Tower. I remain deeply grateful to my entire HHMI Gilliam cohort and family. Never would I have imagined that I'd have the privilege to develop and grow as a scientist alongside such inspiring, incredible people.

Finally, I'd like to acknowledge and thank the Great Storyteller and Beloved. In front of me, You continue to place the great Unknown that fuels our questions and thirst for discovery in science and personal growth in life. Behind me lie the synchronic coincidences and challenges You've arranged; they form the mosaic of this strange and unique Way I tread upon. Yes, even Your ironic sense of humour is greatly appreciated and loved, if sometimes in retrospect.

Note on Spelling Conventions

Working across continents brings with it a multitude of joys and difficulties, some bigger than others. As an avid writer, storyteller, and linguist at heart, I hold language and the stories we tell with it to be important. Given this thesis is being presented at Oxford University, spelling and grammar conventions used in the United Kingdom were chosen. As the most striking and recurring example, *haematopoiesis* is used instead of *hematopoiesis*. Where this convention is not followed, it is due to typographical errors, as opposed to a deliberate choice by the DPhil candidate.

Research Declaration

The work presented in this thesis is my own unless indicated. All text, figures, tables, data, or results which are not wholly my own work are indicated and the sources acknowledged.

Materials and Methods

Scl:mCherry cell line was developed in collaboration with Dr. Philip Hublitz of the WIMM Genome Editing Facility. Dr. Hublitz was in charge of study design, guide RNA design, cloning, and surveyor assays. Cell line validation (Figure 2.1) was done in collaboration with Drs. Maiken Kristiansen and Hedia Chagraoui. Dr. Kristiansen performed the western blots, and Dr. Chagraoui the FACS and subsequent RT-qPCR, as well as the blast colony assay.

Normal human iPSC lines used in this thesis were generated by Dr. Luigi Alvarado in collaboration with Dr. Jizhong Zou and Dr. Jeanette Beers of the National Institutes of Health iPSC core facility. Teratoma assay and histology, were done by Dr. Chengyu Liu of the NHLBI Transgenic Core Facility. Karyotyping was coordinated by Husam Qanash in collaboration with WiCell at the University of Wisconsin. Erythroid cell differentiation, globin extraction, and HPLC experiments for globin experiments for Figure 5.6d were carried out by Dr. Juan Haro-Mora of the Cellular and Molecular Therapeutics lab at NHLBI.

Word Count: **~43,000**

Abbreviations

ActA	Activin A
AF	Alexa Fluor
AP	Alkaline Phosphatase
BI	Blood Islands
BL-CFC	Blast Colony Forming Cells
bFGF	Fibroblast Growth Factor, basic
BMP4	Bone Morphogenic Protein 4
Br-cAMP	8-Bromoadenosine 3',5' – cyclic monophosphate sodium salt
BV	Brilliant Violet
CD	Cluster of Differentiation
CFU	Colony Forming Unit
CHO	Chinese Hamster Ovarian
COUP-TFII	Chicken Ovalbumin Upstream Promoter TF II (*NR2F2*)
DA	Dorsal Aorta
Dlc	Delta C
Dld	Delta D
DLL4	Delta-like ligand 4
DLP	Dorsal Lateral Plate (mesoderm)
EB	Embryoid Body
EC	Endothelial Cell
EHT	Endothelial to haematopoietic transition
EMP	Erythromyeloid progenitor
ESC	Embryonic Stem Cell
ES-HSPC	Embryonic Stem cell-derived Haematopoietic Stem Cells
FACS	Flow-assisted Cell Sorting
FL	Fetal Liver
FLK1	Fetal Liver Kinase 1 (KDR; VEGFR2)
FLT3-L	Fms-related tyrosine kinase 3 ligand
FMO	Fluorescence minus One
GFP	Green Fluorescent Protein
GOI	Gene of Interest
GPR	G Protein-coupled Receptor
HCT	Haematopoietic stem Cell Transplant
HE	Haemogenic endothelium
HED	Haematoendothelial Differentiation media
hESC	Human Embryonic Stem Cell
h-iPSC	Human induced pluripotent stem cell
HPC	Haematopoietic progenitor cell
HSC	Haematopoietic stem cell
HSPC	Haematopoietic stem and progenitor cell
iPSC	Induced pluripotent stem cell
Jag1	Jagged 1
KDR	Kinase insert Domain Receptor (VEGFR2; Flk-1)
KO	Knock-out
LIF	Leukaemia Inhibitory Factor
LP	Lateral Plate (Mesoderm)

MACS	Magnetic Assisted Cell Sorting
mESC	Mouse Embryonic Stem Cell
MFI	Mean Fluorescence Intensity
NHLBI	National Heart, Lung, and Blood Institute
NIH	National Institutes of Health
NR2F2	Nuclear Receptor Subfamily 2, group F, member 2 (COUP-TFII)
NO	Nitric Oxide
NRP1	Neuropilin 1
PB	Peripheral Blood
PDGFRα	Platelet-derived growth factor alpha
PGE2	Prostaglandin E2
PSC	Pluripotent Stem Cell
pSMAD	phosphorylated SMAD
Rspo1	R-spondin 1
SCF	Stem Cell Factor; Kit Ligand
Scl/Tal1	Stem cell leukaemia/T-cell acute lymphoblastic leukaemia 1
SD	Standard Deviation
SEM	Standard Error of the Mean
SFD	Serum-free Differentiation
SHH	Sonic Hedgehog
TF	Transcription Factor
Tgfβ	Transforming growth factor beta
TPO	Thrombopoietin
VE	Vascular Endothelium
VE-Cad	Vascular Endothelial Cadherin
VEGFA	Vascular Endothelial Growth Factor
VEGFR-2	VEGF Receptor 2 (KDR, Flk-1)
WIMM	Weatherall Institute of Molecular Medicine
WT	Wildtype

Table of Contents

Acknowledgments....ii
Note on Spelling Conventions....iv
Research Declaration.... v
Abbreviations vi
Table of Contents....viii
List of Figures and Tables....xii
Abstract xiv
1. Introduction.... 1
1.1. Haematopoietic Stem Cells: Promises and Challenges.... 2
1.2. Developmental Haematopoietic Waves.... 5
1.2.1. First Wave: Primitive Haematopoiesis.... 7
1.2.2. Second Wave: Definitive Yolk Sac Haematopoiesis.... 7
1.2.3. Third Wave: Intraembryonic Haematopoiesis.... 11
1.2.4. Tracing Haematopoietic Waves *in vitro* 13
1.2.5. A Note on *Fate* and *Potential* 14
1.3. Developmental Haematoendothelial Populations 19
1.3.1. The Haemangioblast.... 19
1.3.2. Haemogenic Endothelium (HE) and the Endothelial to Haematopoietic Transition (EHT).... 20
1.4. Signalling Pathways Necessary for HSC Development.... 27
1.4.1. Arterial Programme Specification: VEGFA, Notch, and Circulation 27
1.4.2. Notch Regulation of EHT.... 29
1.4.3. Somitic Signals: Haematopoietic Regulation Independent of Arterial Development33
1.4.4. Hox and Notch: Independent Regulation and Requirement.... 35
1.5. HE Differentiation Models.... 37
1.6. Thesis Objectives.... 44
2. Materials and Methods.... 46
2.1. Media Formulations and Molecular Reagents 47
2.1.1. Cell Culture Cytokines, Growth Factors, and Small Molecules 47
2.1.2. Cell Culture Media Formulations 47
2.1.3. Flow Cytometry Antibodies and Isotype Controls 49
2.1.4. Taqman™ RT-qPCR primer and probe sets.... 51
2.2. Cell Line Generation and Maintenance 52

2.2.1. CHO-LIF Cells 53
2.2.2. Mouse Embryonic Stem Cells (mESCs) 53
2.2.2.1. Cell Passaging 53
2.2.2.2. Cell Freezing 54
2.2.2.3. Cell Thawing 55
2.2.3. *Scl:mCherry* mESC 55
2.2.3.1. Guide RNA and Plasmid Design and Cloning 55
2.2.3.2. Transfection and Cell Cloning 56
2.2.3.3. Clone Validation and Sequencing 57
2.2.3.4. Line Maintenance 58
2.2.4. Human Induced Pluripotent Stem Cells (h-iPSCs) 59
2.2.4.1. Human CD34+ haematopoietic stem and progenitor cells (HSPCs) 59
2.2.4.2. Line Generation and Validation 59
2.2.4.3. Cell Passaging 60
2.2.4.4. Cell Freezing 60
2.2.4.5. Cell Thawing 61
2.3. Pluripotent Stem Cell Differentiation 61
2.3.1. Mouse HSPC Differentiation 61
2.3.1.1. Days -1 – 3.5 EB Formation and Mesodermal Specification 62
2.3.1.2. Days 4.5 – 5.5 HE Specification 63
2.3.1.3. Days 5.5 – 5.5+6 EHT Culture 63
2.3.2. Human HSPC Differentiation 64
2.3.2.1. Days -1 – 3.5 Cluster Formation and Mesodermal Specification 64
2.3.2.2. Days 3.5 – 21 Hematopoietic Specification and Culture 65
2.3.2.3. High VEGFA treatment 66
2.3.2.4. Sample Collection and Preparation 66
2.4. Flow Cytometry and Flow Assisted Cell Sorting (FACS) 67
2.4.1. Analyzers and Sorters 67
2.4.2. Sample Preparation and Staining 67
2.4.3. Fluorescence Minus One, Isotype, and Single Stain Controls 68
2.4.4. Antibody Titration for Cell Sorting 69
2.4.5. Intracellular staining 69
2.5. Colony Forming Unit (CFU) Assay 70
2.5.1. Mouse CFU Assays 70
2.5.2. Human CFU Assays 71
2.6. Mouse Transplantation Assays 71
2.6.1. Mouse Strains 71

2.6.2. Irradiation and Transplantation 71
2.6.3. Animal Euthanasia and Sample Collection 72
2.7. RNA Preparation and Analysis 73
2.7.1. Standard RNA Collection and Processing 73
2.7.2. Reverse Transcription and RT-qPCR 73
2.8. Data Analysis and Statistics 73
2.8.1. Flow Cytometry 73
2.8.2. RT-qPCR 75
2.8.2.1. CT Thresholds and Values 75
2.8.2.2. ΔC_T Calculations and 95% Confidence Interval 75
2.8.3. Multiple Sample Comparsion 76
2.8.4. CFU 76
2.8.5. Significance 76
3. Modelling Wave Two of Murine Haematopoiesis 77
3.1. Introduction 78
3.2. Late-stage FLK1^{+} haematoendothelial precursors lack *Brachyury* and PDGFRα expression 81
3.3. FLK1^{High} cells express a Haematoendothelial Phenotype 84
3.4. Day 3.5 FLK1^{+} and FLK1^{-} Cells Equally Contribute to Day 5.5 FLK1^{High} Population 90
3.5. FLK1^{High} Cells Arise in Response to VEGFA without an Arterial Niche or Identity 98
3.6. FLK1^{High} cells produce HSPCs immunophenotypically resembling second wave haematopoiesis. 105
3.7. Discussion 113
4. Modelling Arterial Murine Haematopoiesis 118
4.1. Introduction 119
4.2. Treatment of FLK1^{+} cells with high VEGFA concentrations leads to activation of Notch signalling and initiation of an arterial programme 122
4.3. Short-term exposure to high VEGFA levels leads to activation and maintenance of key arterial genes in culture 129
4.4. Global arterial programme leads to no differences in HSPC phenotype and function 138
4.5. An *in vitro* DLL4+ HE with haematopoietic progenitor potential 143
4.6. Discussion 148
5. Modelling Human Arterial Haematopoiesis 152
5.1. Introduction 153
5.2. *In vitro* system produces HSPCs 156
5.3. HSPCs arise in two waves of erythromyeloid potential 159

5.4. Differentiation leads to low percentages of endothelial niche in monolayer ... 164
5.5. Mesodermal patterning activates *HOX* code in VE and HSPC populations but is insufficient for engraftment ... 168
5.6. High VEGFA in culture leads to sustainable arterial niche and arterial HE ... 172
5.7. Discussion ... 181
6. Conclusion ... 185
6.1. The Mesodermal Conundrum: Driving Wave 3 Haematopoiesis ... 187
6.2. The Arterial Conundrum: Arterial Programming of HE ... 192
Appendix I: Supplementary Figures ... 196
References ... 205

List of Figures and Tables

Figure 1.1 Roadblock to HSC Therapy ... 3
Figure 1.2 Consecutive Developmental Waves of Haematopoiesis ... 6
Figure 1.3 HE to HSC Progression ... 13
Figure 1.4 Waddington Representation of a Cell's Developmental Landscape ... 15
Figure 1.5 Endothelial to Haematopoietic Transition ... 23
Figure 1.6 Complex spatio-temporal Notch regulation of EHT ... 31
Figure 1.7 Differing Models for HE Specification from Different Waves ... 40
Figure 2.1. Generation and characterisation of Scl:mCherry reporter cell line ... 56
Figure 2.2. Differentiation scheme for mouse HSPC differentiation ... 61
Figure 2.3. Differentiation scheme for h-iPSCs into HSPCs ... 64
Figure 2.4 Representative plot of flow cytometry pre-gating for further analysis on all samples collected ... 74
Figure 3.1 Characterisation of Two-Wave System ... 83
Figure 3.2. Day 5.5 FLK1^{High} cells present a Hematoendothelial Phenotype ... 86
Figure 3.3 Scl expression using Scl:mCherry mESCs ... 89
Figure 3.4. Population Tracing Experimental Design ... 92
Figure 3.5 Sorting Strategy for Population Tracing Experiment ... 94
Figure 3.6 Population-Tracing Reveals Mixed Origin of Day 5.5 FLK1^{High} cells ... 97
Figure 3.7 Day 5.5 FLK1^{High} cell response to VEGFA addition at Day 4.5 ... 101
Figure 3.8. HE specifies after day 4.5 outside of an arterial Notch context ... 103
Figure 3.9. Sorted FLK1^{High} Cells Differentiate Into Haematopoietic-Like Clusters 107
Figure 3.10 Replated FLK1^{High} Cells Develop Haematopoietic Immunophenotype 108
Figure 3.11 FLK1^{High} HE differentiates into second wave-like HSPCs ... 110
Figure 3.12 Mutually Exclusive Expression of VE-Cad and CD16/32 in cKIT^{+}CD41^{+} cells at Day +6 ... 112
Figure 4.1. High Concentration of VEGFA leads to an increase in FLK1^{High} percentages and decreased FLK1 expression ... 123
Figure 4.2 High Concentration of VEGFA leads to an Increase in DLL4 Expression and downstream Notch signalling ... 127
Figure 4.3 Long-term exposure to high VEGFA levels is detrimental to FLK1^{High} cells ... 130
Figure 4.4. Decreasing levels of VEGFA partially rescues haematopoiesis ... 132
Figure 4.5 High levels of VEGFA lead to sustained global arterial programme ... 135
Figure 4.6 Downstream Effects of VEGFA Titration at Day 4.5 ... 137
Figure 4.7. Type I and Type II Pre-HSCs in culture ... 139
Figure 4.8 LSK SLAM Immunophenotype and CFU ... 142
Figure 4.9 Haematopoietic Potential of DLL4^{-} and DLL4^{+} HE ... 145
Figure 4.10. Haematopoietic output of DLL4^{+} HE ... 147
Figure 5.1 HSPC Differentiation from h-iPSCs ... 157
Figure 5.2 HSPCs arise in two waves of erythromyeloid potential ... 161
Figure 5.3 Adult HSC Immunophenotype Does Not Distinguish Engrafting HSPCs arising in h-iPSC System ... 163
Figure 5.4 Monolayer Characterisation ... 166
Figure 5.5 Characterisation of Mesenchymal-like Stroma ... 167
Figure 5.6 Mesodermal patterning activates Hox code ... 170

Figure 5.7 Mesodermal Patterning is Insufficient for iPSC-derived HSPC engraftment 171
Figure 5.8 HSPC and Monolayer in h-iPSC Treatment Conditions 173
Figure 5.9 HSPC Characterisation in h-iPSC Treatment Conditions 175
Figure 5.10 HSPC Characterisation in h-iPSC Treatment Conditions (Continued) 176
Figure 5.11 Monolayer Characterisation in h-iPSC Treatment Conditions 178
Figure 5.12. VE Characterisation in h-iPSC Treatment Conditions 180
Figure 6.1 Chapter 4: VEGFA regulation of DLL4^{+}/DLL4^{-} HE 193

Supplementary Figure 3.1 Associated with Figure 3.8 197
Supplementary Figure 3.2 Associated with Figures 3.9, 3.10, and 3.11 198
Supplementary Figure 4.1 HSPC Characterization Associated with Figure 4.7 199
Supplementary Figure 4.2 Gating Strategy and Purity Checks Associated with Figure 4.9 200
Supplementary Figure 5.1 FMO Controls Associated with Figures 5.1 and 5.2 201
Supplementary Figure 5.2 FMO Controls Associated with Figure 5.2 and Monolayer CD235a Expression 202
Supplementary Figure 5.3 FMO Controls Associated with Figure 5.3 203
Supplementary Figure 5.4 Additional FMO Controls Associated with Figure 5.3. 204

Table 2.1 Cell culture reagents 47
Table 2.2 Solutions and media formulations 48
Table 2.3 Flow cytometry reagents 49
Table 2.4 Taqman™ primers and probes and Molecular Biology Reagents 51

Abstract

One of the most promising objectives of clinical haematology is to derive transplantable autologous haematopoietic stem and progenitor cells (HSPCs) from human pluripotent stem cell (PSC) sources *in vitro*, but efficient and clinically relevant methodologies remain unavailable. Observations in the developing vertebrate embryo indicate that the haematopoietic stem cells (HSCs) capable of long-term engraftment are produced by the third and last wave of haematopoietic development. This occurs in the developing dorsal aorta (DA) from haemogenic endothelium (HE) in close association with an arterial vascular endothelial niche. Notch and Vascular endothelial growth factor A (VEGFA) signalling pathways are critical regulators of arterial identity and HSPC development.

To better understand the lack of engrafting HSCs in *in vitro* PSC differentiation protocols, we further characterised a previously published, serum-free murine embryonic stem cell (mESC) embryoid body (EB) differentiation system. Results showed lack of a robust arterial niche and Notch signalling, and production of HSPCs resembling the erythro-myeloid progenitors (EMP) normally detected during one of the earlier, extra-embryonic waves of haematopoietic development. We then showed that transiently culturing cells with high concentrations of VEGFA led to activation of an arterial programme in cultured cells, though this was insufficient to drive HSC differentiation. Importantly, we showed the haematopoietic potential of arterial delta-like 4 (DLL4) expressing cells depends on VEGFA concentrations in the culture, demonstrating the potential of arterial cells to become HE.

To adapt these findings to a more clinically-translatable setting, we also characterised a serum-free, monolayer-based system for the differentiation of human HSPCs previously developed in the lab, commercially available as STEMdiff™ Hematopoietic Kit. Similar to results in the murine system, the supporting niche showed limited arterial vascular endothelium differentiation and was instead primarily composed of mesenchymal stromal-like cells. Culturing cells in high concentrations of VEGFA markedly enhanced arterial endothelium formation throughout culture, and concurrently decreased mesenchymal stroma. Likewise, we observed the presence of immunophenotypic $DLL4^{+}$ HE at early stages in cultures treated with high VEGFA concentrations, confirming data obtained from the mESC system. Despite lack of engraftment capacity of HSPCs, our studies contribute potential insights to the question of the haematopoietic potential of arterial endothelium. This will guide further improvement of currently available protocols to support *in vitro* HSPC differentiation.

1. Introduction

1.1.Haematopoietic Stem Cells: Promises and Challenges

The haematopoietic stem cell (HSC) is a rare, self-renewing cell found in the adult bone marrow that produces the haematopoietic cells throughout a healthy adult's life (Jordan and Lemischka 1990; Lemischka 1991; Spangrude et al. 1991). Because of this, these cells are a promising therapy for patients who present in the clinic with various haematopoietic disorders, including bone marrow failures and haematopoietic malignancies. For many of these patients, allogeneic haematopoietic stem cell transplants (HCT) from HLA-matched donors is a life-saving, last resort treatment (de la Morena and Gatti 2011).

However, lack of matching donor availability, along with immune rejection and graft versus host disease (GVHD), present significant hurdles to providing all patients with these types of therapies (de la Morena and Gatti 2011). While autologous, gene-corrected HCT is theoretically one way to overcome these hurdles, many patients with various bone marrow failures lack HSC populations to begin with. Likewise, expanding HSCs to clinically relevant numbers outside of their bone marrow niche without a loss of their self-renewal and multipotency remains difficult, despite improvements in HSC culture and expansion through the use of small molecules and bioreactors (Fares et al. 2014; Goessling et al. 2011; Ohishi, Varnum-Finney, and Bernstein 2002). Since the advent of induced pluripotent stem cells (iPSC) (Takahashi and Yamanaka 2006) and readily-available gene editing technologies such as CRISPR-Cas9 (Cong et al. 2013), producing autologous, gene-corrected HSCs *ex vivo* as a treatment for various congenital bone marrow disorders has become a possibility (Figure 1.1).

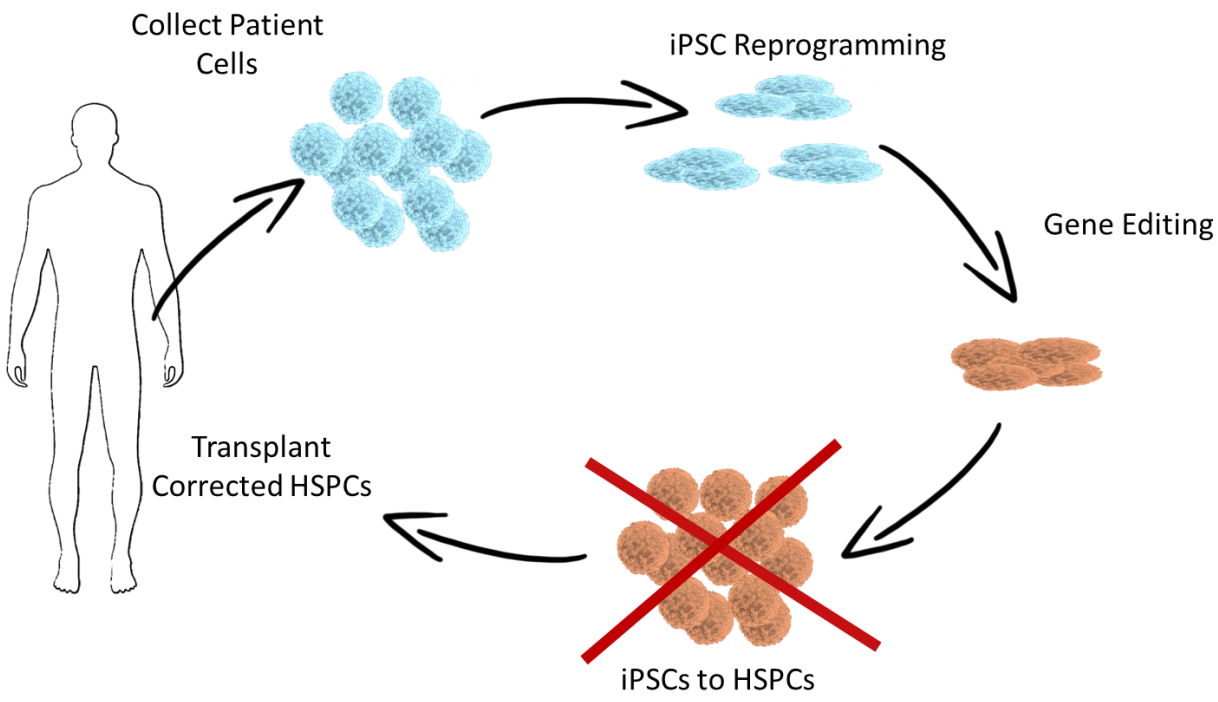

Figure 1.1 Roadblock to HSC Therapy
The advent of iPSC and gene editing technologies has made personalized HSC therapies for patients with genetic bone marrow failures a possibility. In theory, somatic cells can be collected from a patient and reprogrammed into iPSCs using clinical-grade approaches. Cells can then be cultured, expanded, and gene-corrected using gene editing technologies such as CRISPR-Cas9. The current technological roadblock stands at the iPSC to HSC differentiation stage, as no clinical-grade, scalable protocols for the differentiation of HSCs from iPSCs has been developed to date.

Unfortunately, producing engrafting HSCs *in vitro* continues to be a significant hurdle in the delivery of these therapies to the clinic (Figure 1.1). Only three very recent studies have reported differentiating HSCs *in vitro* (Lis et al. 2017; Sugimura et al. 2017; Guyonneau-Harmand et al. 2017). Of these, two use potentially oncogenic lentiviral vectors for the ectopic expression of transcription factors (TF) (Lis et al. 2017; Sugimura et al. 2017), making them clinically unsafe. The third study's manuscript was uploaded to a pre-print archive and has therefore yet to be peer-reviewed, validated, and replicated (Guyonneau-Harmand et al. 2017).

To overcome these roadblocks and develop protocols for the differentiation of HSCs from pluripotent stem cells (PSCs), the field of developmental haematopoiesis, which studies the processes by which HSCs arise in the embryo, has advanced tremendously in the past few years: *in vitro* differentiation studies along with *in vivo* studies in model organisms have provided insights required to mechanistically understand HSC development, maintenance, and expansion. While these topics have been extensively reviewed previously (Ivanovs et al. 2017; Crisan and Dzierzak 2016; Ditadi, Sturgeon, and Keller 2016; de Bruijn and Dzierzak 2017; Mikkola and Orkin 2006; Dzierzak and Speck 2008; Slukvin 2016; Costa, Kouskoff, and Lacaud 2012), this introduction will also cover them, followed by a more specific discussion on the important relationship between concomitantly developing HSCs and their arterial endothelial niche, which is the focus of this thesis.

1.2. Developmental Haematopoietic Waves

During development in higher vertebrates, blood is produced in the embryo in consecutive waves which occur both in the yolk sac (YS) vascular plexus (Kovach et al. 1967; Frame et al. 2016; Lux et al. 2008; Palis et al. 1999) as well as in intra-embryonic arterial regions (de Bruijn et al. 2000). In mammals, haematopoietic stem and progenitor cells (HSPCs) colonize the haematopoietic foetal liver (FL) (Medvinsky and Dzierzak 1996; Kumaravelu et al. 2002) and share the expression of many immunophenotypic markers (McGrath et al. 2015). This has historically made tracing their site of origin difficult once circulation in the embryo has been established. However, and as discussed below, the majority of studies in the developing embryo agree that, of these waves, only the final one produces fully functional and engraftable HSCs (Müller et al. 1994; Medvinsky and Dzierzak 1996; de Bruijn et al. 2000) (Figure 1.2).

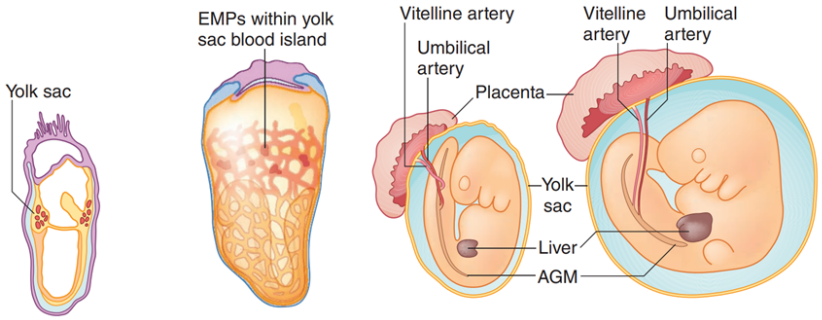

Timing (Mouse)	E7.5	E8.5 – 9.5	E10.5
Output	• Red Blood Cells (Embryonic Globins) • Macrophage and Megakaryocyte Progenitors	• Erythromyeloid Progenitors (EMPs) (Fetal and Adult Globins) • Lymphoid and Lympho-myeloid progenitors (LMPs)	• Haematopoeitic Progenitors (HPCs) • Pre-HSC Types I and II • Haematopoietic Stem Cells (HSCs)
Primitive/Def	Primitive	Definitive	Definitive
Location	Yolk Sac (Extra-Embryonic)	Yolk Sac (Extra-Embryonic)	AGM (Intraembryonic) Vitelline and Umbilical Arteries
3 - Wave	Wave 1	Wave 2	Wave 3
Engrafting/Adult Haematopoiesis	No	Yes^{+} Yes*	Yes

Figure 1.2 Consecutive Developmental Waves of Haematopoiesis
Haematopoiesis occurs in the embryo in consecutive waves, beginning at E7.5 and continuing through E10.5. Different, overlapping forms of categorising these waves are shown above and have historically been based on either the morphology of red blood cells arising from these waves or the location in which they initiate. Coloured brackets indicate where categorisation overlap can lead to confusion or conflation of terms (Blue = Primitive; Red = Definitive; Purple = Yolk Sac/Extraembryonic; Orange = AGM/Intraembryonic) Last row indicates each wave's engrafting properties or contribution to adult haematopoiesis.
(+) Macrophages from the YS at this stage of haematopoiesis have been shown to contribute to the adult pool of some specialised tissue cells, such as microglia (Schulz et al. 2012b; Hoeffel et al. 2012; Gomez Perdiguero et al. 2015; Hoeffel et al. 2015).
(*) Definitive YS HSPCs which arise at E8.5 – 9 have long-term engraftment potential only when transplanted into neonatal hosts (Johnson and Yoder 2005) or transfected ectopically to constitutively express *Hoxb4* (Kyba, Perlingeiro, and Daley 2002), suggesting intrinsic as well as niche requirements for acquiring engraftment and reconstitution potential. EMPs at this stage have been shown to have short-term engraftment capacity and produce erythrocytes with predominantly adult globins (McGrath et al. 2015). Illustrations of developmental stages adapted from (Yoder 2014).

1.2.1. First Wave: Primitive Haematopoiesis

The first wave, which originates in the early YS blood islands (BI) in mammals, is marked by rapid production of nucleated red blood cells expressing embryonic globins that provide oxygen to the developing tissues (Kovach et al. 1967; Palis et al. 1999). This wave also produces megakaryocyte and macrophage progenitors. In the mouse, this occurs at embryonic day 7.5, commonly labelled as E7.5 (Figure 1.2, first column). Red cells from this wave have been shown to arise from mesodermal precursors specified prior to gastrulation (Padrón-Barthe et al. 2014). Historically, red blood cells, and subsequently, the waves from which they arise in the embryo, were categorized morphologically based on their size and nucleation (Craig and Russell 1964; Kovach et al. 1967). This first wave of erythrocytes was labelled as *primitive*, given the fact that erythrocytes were large and nucleated, similar to the erythrocytes of birds, fish, and reptiles (Palis 2014). Additionally, these cells can be distinguished by their expression of mostly embryonic globin with some foetal globin. Though nucleated primitive erythrocytes cannot easily be detected in the embryo beyond E9.0 (Palis et al. 1999), studies have shown that these particular erythrocytes do eventually enucleate, and can be detected in circulation as late as five days following birth (Kingsley et al. 2004).

1.2.2. Second Wave: Definitive Yolk Sac Haematopoiesis

The first wave is then followed by a second wave starting at E8.5, composed of Erythromyeloid Progenitors (EMPs) (Palis et al. 1999; Frame et al. 2016; Lux et al. 2008), also arising in the YS (Figure 1.2, second column). As their name suggests, these progenitors have multi- and unipotent erythromyeloid differentiation potential: erythroid, megakaryocyte, macrophage, and granulocytic cells

differentiate from these cells in *ex vivo* assays (Inlay et al. 2014; Frame et al. 2016). Because erythrocytes that arise in this and later waves express foetal and adult globins and persist through late foetal and postnatal life, they, and the waves they arise from, are described as *definitive* (Palis 2014) (Figure 1.2, second row). The fact that third-wave HSCs also fall under the category of *definitive* haematopoiesis however, has led some in the field to implicitly associate *definitive* waves with the promise of *engrafting* potential, though the two are not necessarily related. As progenitors, EMPs and other Wave 2 HSPCs cells lack the long-term engrafting capacity associated with HSCs. Despite this, a few distinct populations of tissue-resident macrophages in adult mice have been traced to this wave of YS haematopoiesis (Schulz et al. 2012a; Hoeffel et al. 2012; Gomez Perdiguero et al. 2015; Hoeffel et al. 2015). Likewise, YS progenitors are able to reconstitute irradiated neonatal hosts (Johnson and Yoder 2005), and can also gain HSC-like long-term engraftment and reconstitution potential when transfected with constitutively active Homeobox B4 gene (*Hoxb4*) (Kyba, Perlingeiro, and Daley 2002) (Figure 1.2, second column, final row). Studies have also found that, at this stage (mouse E9.5), the YS contains lymphoid and lympho-myeloid progenitors (Cumano, Furlonger, and Paige 1993; Böiers et al. 2013; Yoshimoto et al. 2011; Yoshimoto et al. 2012) that arise prior to the HSC-dependent lymphoid progenitors found in the FL (Douagi, Vieira, and Cumano 2002).

Following the discovery that the potential to fully engraft and reconstitute the irradiated bone marrow of adult mice first developed in the aorta-gonad-mesonephros (Müller et al. 1994; Medvinsky and Dzierzak 1996), and later, more specifically, within the developing dorsal aorta (de Bruijn et al. 2000; de Bruijn et al. 2002), discussed in more detail in the following section, the distinction between

Yolk Sac and *Intraembryonic* haematopoiesis, in addition to *primitive* and *definitive*, began to be used. Rows three and four of Figure 1.2 show how the overlap between the *primitive/definitive, YS/AGM*, and *intra-/extraembryonic* classifications can lead to some confusion. This distinction between *Extra-* and *Intraembryonic* haematopoiesis was not fully adopted as some groups continued attempting to show that the YS also produced HSCs and contributed to adult haematopoiesis (Yoder, Hiatt, and Mukherjee 1997; Yoder and Hiatt 1997; Matsuoka et al. 2001; Kyba, Perlingeiro, and Daley 2002; Samokhvalov, Samokhvalova, and Nishikawa 2007; Lee et al. 2016). In the case of both Yoder and Hiatt studies listed above, engraftment ability was tested in irradiated newborn recipients, suggesting engraftment potential when the right micro-environmental cues are present (Yoder, Hiatt, and Mukherjee 1997; Yoder and Hiatt 1997). Matsuoka and colleagues used a stromal line derived from AGM explants to co-culture YS cells collected pre-circulation and once again show that, given the right micro-environmental cues, YS cells could produce long-term engrafting multi-lineage stem cells, though secondary transplants were not tested (Matsuoka et al. 2001). Kyba, Perlingeiro, and Daley, as mentioned above, transfected YS-derived cells with constitutively active *Hoxb4* to give long-term, serial, engraftment capacity to these cells, though this gave them a myeloid bias (Kyba, Perlingeiro, and Daley 2002). While all of these studies show that YS precursors might harbour the ability to produce cells with engrafting potential at some stage in their development, they do not prove that *in vivo* conditions promote YS cells to produce HSCs that contribute to adult haematopoiesis. Samokhvalov and colleagues used a *Runx1*$^{+/-}$ mouse line to conditionally trace *Runx1* expression from the YS in an attempt to show YS contribution to adult haematopoiesis (Samokhvalov, Samokhvalova, and

Nishikawa 2007). However, seven years earlier, a study had shown that *Runx1* haploinsufficiency led to both precocious HSC development, as well as presence of HSCs in the YS, (Cai et al. 2000) and therefore limited the conclusions of Samokhvalov et.al., who also used a *Runx1* haploinsufficent model, specifically to this context. Finally, Lee and colleagues used LYVE-1 (lymphatic vessel endothelial hyaluronan receptor-1) as a specific marker to establish contribution of Wave 2 YS cells to fetal and adult HSCs (Lee et al. 2016). Importantly, a recent study showed that AGM cells do also express this marker, and that YS explants, cultured in the same conditions as AGM explants do not produce fully-engrafting HSCs when AGM explants do (Ganuza et al. 2018). Therefore, none of these studies were able to definitely prove the *de novo* generation of HSCs in the YS and their contribution to adult haematopoiesis in unperturbed conditions *in vivo*.

The presence of multiple haematopoietic progenitors – primitive and, later, definitive EMPs and lymphoid progenitors – within the YS (Palis et al. 1999; Lux et al. 2008; Inlay et al. 2014; McGrath et al. 2015) makes the description of haematopoiesis as arising in waves, with HSC potential residing in only the third wave, slightly more precise than classifications of *definitive/primitive* or *intraembryonic/extraembryonic*. A three-wave classification, however, also leads to some potentially problematic overlap with the other classifications as Wave 2, which gives rise to EMPs, falls under the classification of *definitive*, giving rise to red blood cells expressing mostly foetal and some adult globins (Palis et al. 1999). There have also been some suggestions in the literature to further categorize haematopoietic development into four or even more waves (Dzierzak and Speck 2008; Ditadi, Sturgeon, and Keller 2016) given the independent EMP and lymphoid progenitors found in the YS. Because haematopoiesis occurs not discretely, but

along a spatio-temporal continuum, adding more waves can indeed provide a more precise depiction of the way in which HSPCs arise, but at the expense of simplicity. In convention with most current studies, this thesis will also use the three-wave model. In this case, Wave 1 refers to any primitive YS haematopoiesis, Wave 2 to definite YS haematopoiesis (erythro-myeloid, lymphoid, and lympho-myeloid progenitors), and Wave 3 to intraembryonic haematopoiesis (Figure 1.2, third row) as outlined in these sections.

1.2.3. Third Wave: Intraembryonic Haematopoiesis

It is only after endothelial cells from the lateral plate (LP) mesoderm have migrated towards the midline and fused to form the dorsal aorta (DA) that engrafting HSCs arise in clusters within the ventral wall of the DA at E10.5 (de Bruijn et al. 2000; de Bruijn et al. 2002; Taoudi and Medvinsky 2007) (Figure 1.2, third column). In mice, HSC activity during this last haematopoietic wave has also been shown to take place at low levels in the vitelline and umbilical (Gordon-Keylock et al. 2013; de Bruijn et al. 2000) arteries, though the possibility of seeding from intraembryonic sites following circulation or contamination from the AGM during sample preparation in these studies cannot be dismissed (Gordon-Keylock et al. 2013). By E12, it has been calculated that the entire mouse embryo contains roughly 66 definitive HSCs capable of engraftment, most of which are found in the foetal liver. Just a day prior to this, however, only about 3 engrafting HSCs are present (Kumaravelu et al. 2002). These cells have been shown to be slow-cycling (Batsivari et al. 2017), and are therefore an unlikely source for the 66 engrafting HSCs present a day later. In fact, it is cells fated to become HSCs in further need of maturation, termed Pro- and Type I and Type II Pre-HSCs (Taoudi et al. 2008;

Rybtsov et al. 2011; Rybtsov et al. 2014) that are present from as early as E9.5 that contribute to this pool of engrafting cells (Rybtsov et al. 2016). However, *ex vivo* engraftment potential may not be the most accurate measure of the total *in vivo* number of pre-HSCs and HSCs that contribute to adult haematopoiesis, as recent studies using lineage-tracing techniques have calculated this number to be between ~330 and ~719 per embryo, depending on the developmental stage at which they are counted (Ganuza et al. 2017; Fatima, Zhou, and Sorrentino 2018). Pre-HSCs have been shown to be dependent on stem cell factor (SCF) to complete their maturation to HSCs, as well as IL-3 at later stages (Rybtsov et al. 2014). As can be seen in Figure 1.3, progression from haemogenic endothelium (HE), described in detail in section 1.3.2, to HSCs includes a gradual activation of haematopoietic cell surface marker integrin subunit alpha 2b, also known as cluster of differentiation (CD) 41 (CD41), which is slowly lost as cells mature (Liakhovitskaia et al. 2014). Haematopoietic surface markers sialophorin (CD43) and protein tyrosine phosphatase, receptor type C (CD45) are also gradually upregulated during this transition (Rybtsov et al. 2014). Further characterisation from other groups has shown that endothelial protein C receptor (CD201) can be used in addition to these other makers to distinguish Type I and II Pre-HSCs (Zhou et al. 2016), while TNF-receptor superfamily member CD27 also marks Type II Pre-HSCs specifically (Li et al. 2017). When Type I and Type II pre-HSCs are purified from AGM embryos using these markers, they can be cultured *ex vivo* to mature into HSCs with engrafting potential (Taoudi et al. 2008; Rybtsov et al. 2011; Rybtsov et al. 2014; Zhou et al. 2016), making the immunophenotype potentially promising for identifying equivalent populations in *in vitro* systems.

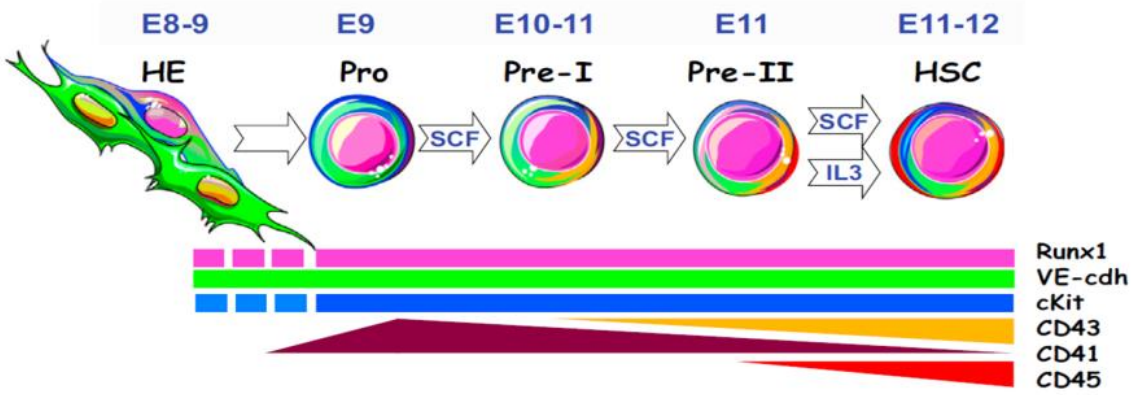

Figure 1.3 HE to HSC Progression
Early HE is marked by *Runx1* expression, as well as endothelial VE-Cad and stem cell marker cKIT. CD41 is the first haematopoietic marker to be expressed, as early as the HE stage before EHT commences (Liakhovitskaia et al. 2014). Cells transition through levels of specification before becoming fully engrafting HSCs. *In vitro* these cells are dependent on SCF and later, IL3 before fully maturing, and gradually lose CD41 while acquiring CD43, and later, CD45 expression. Resourced from (Rybtsov et al. 2014)

1.2.4. Tracing Haematopoietic Waves *in vitro*

In recent years, studies trying to map distinct haematopoietic progenitors *in vitro* have used the same terminology as used to describe *in vivo* haematopoiesis (Sturgeon et al. 2014; Irion et al. 2010; Kennedy et al. 2012). However, given the lack of *in vitro* spatial and structural equivalents of the YS and AGM, as well as the shared immunophenotypes among HSPCs arising from different waves (McGrath et al. 2015), this has proven challenging. In lieu of distinguishable immunophenotypes or engraftment studies, which are the gold standard to show the presence of HSC functionality in both mouse and human cells to date, other assays have been employed to characterise differentiating HSPCs *in vitro*, at least along the lines of *primitive* vs *definitive*. By differentiating progenitors arising *in vitro* in either blast colony assays or erythroid colony assays, globin expression can be assayed both at the gene expression as well as protein level. Most studies manipulating *in vitro* systems to produce later definitive waves employ this strategy

along with those listed below (Irion et al. 2010; Clarke et al. 2013; D'Souza, Kumar, and Slukvin 2018; Ng et al. 2016).

Both *in vitro* and *in vivo*, Notch signalling through NOTCH1 has been shown to be required for definitive, engrafting haematopoiesis (Kumano et al. 2003; Hadland et al. 2004). While definitive haematopoietic output from the YS is not impaired in *Notch1*$^{-/-}$ embryonic stem cells (ESCs) and embryos, long-term haematopoiesis is. Because of this, some *in vitro* studies have also indirectly used Notch dependence to suggest improvement in protocols that more closely resemble definitive, and potentially engrafting, haematopoiesis (Clarke et al. 2013; Ditadi et al. 2015; Uenishi et al. 2018).

Likewise, some *in vitro* studies have also used the potential to give rise to lymphoid progeny *in vitro* as a hallmark of definitive haematopoiesis that more closely resembles third-wave haematopoiesis (Kennedy et al. 2012; Park et al. 2018; Clarke et al. 2013). However, both B-cells (Yoshimoto et al. 2011) and T-Cells (Yoshimoto et al. 2012; Böiers et al. 2013) arise in the developing YS independent of HSC activity. Lymphoid potential *in vitro*, therefore, is also not necessarily a marker for a system's ability to produce engrafting HSCs. While all of these studies might point towards the creation of definitive waves, recapitulating definitive waves does not necessarily mean improvements towards recapitulating the final wave of engrafting HSCs.

1.2.5. A Note on *Fate* and *Potential*

When discussing developmental biology, particularly within the context of stem cells and their developmental trajectories, the distinction between *fate* and *potential* becomes important. This is because a cell's developmental trajectory is better

represented as a continuous, fluid process towards differentiated or “lower energy” states, as opposed to a set of discrete cell fate decisions and identities (Waddington, 1957). The best way to visualise this is through the model originally proposed in 1957 by C.H. Waddington (Figure 1.4a), in which a cell’s epigenetic landscape, and with it, its differentiation trajectory, is represented by a series of hills and troughs, and the cell itself by a marble on this landscape. Unperturbed in its wildtype, homeostatic, and *in vivo* context, a cell will differentiate down the path of least resistance dictated by both the signals it receives from its environment, as well as its own internal epigenome. However, perturbations to the system can provide enough energy to “push” the marble off course. The more differentiated the cell, the more stable its identity (visualized by deeper valleys) and the higher the energy required to push the cell towards a distinct identity.

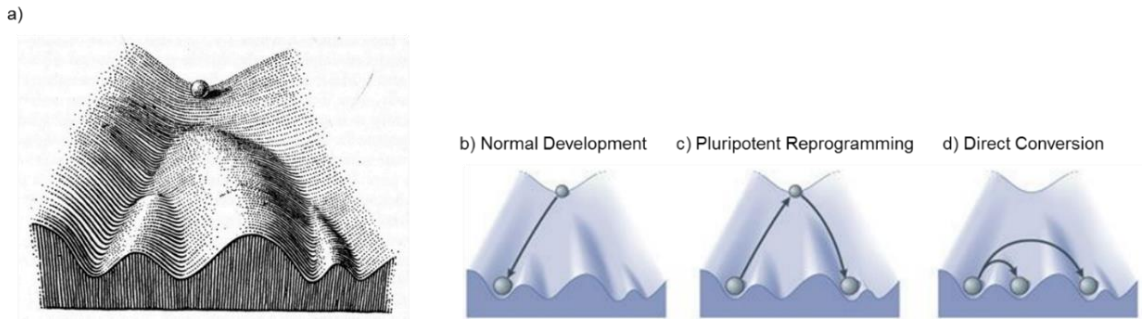

Figure 1.4 Waddington Representation of a Cell’s Developmental Landscape
a) Original drawing representing a creode, a metaphor depicting a cell’s epigenetic and developmental energy landscape. The word is a portmanteau of the Greek roots chre (χρή), meaning necessary or fitting, and hodos (ὁδός), meaning path or way. Sourced from (C.H. 1957). b) Normal development or differentiation, in which a cell rolls down to the path of lowest energy but can be altered by signals from its environment towards a different path. c) In pluripotent reprogramming or direct conversion (d), cells are taken from their low energy, differentiated state back to a high energy pluripotent state and back towards another differentiated state, or directly from one differentiated state to another. Sourced from (Ladewig, Koch, and Brüstle 2013).

In the context of this thesis, then, a cell’s *fate* is the path of least resistance, and one it will take in unperturbed circumstances *in vivo* (Figure 1.4b). Because of

this, it cannot be observed or determined until after the cell has undertaken that path. Anything other than a post-hoc observation will, by definition, be a perturbation to said path and could (to different degrees) affect the *fate* of the cell. An example of this is the lineage-tracing experiments described above in section 1.2.2, in which *LacZ* was introduced into one allele of the *Runx1* locus in a way that led to haploinsufficiency. In this context, the authors traced *Runx1*$^{+}$ YS cells and presented data in favour of YS contribution to adult haematopoiesis, an observation absent from wildtype embryos (Samokhvalov, Samokhvalova, and Nishikawa 2007). It is precisely because of the *Runx1* haploinsufficiency that the YS contributes to adult haematopoiesis, though whether this is due to direct effects on HSPC populations in the YS or earlier circulation of AGM HSC precursors has not been determined (Cai et al. 2000). Regardless of the mechanism, the Samokhvalov study is an example of conclusions being made regarding the *fate* of cells in a lineage-tracing system that, by design, perturbed the *in vivo* system in a way that affected the observed results.

On the other hand, a cell's *potential* is encompassed by all the differentiation possibilities, or low energy paths, available to it at any given point. This can be simulated at the single-cell level by removing cells from their *in vivo* context and placing them in media that promotes expected differentiation outcomes. This approach however, is limited by the following assumptions:

1) The stem cell or progenitor is bi-, oligo-, or multipotent, and has the ability to divide asymmetrically as it differentiates (Symmetric divisions, by definition, lead to two daughter cells identical to each other).

2) The conditions in which the cells are plated promote, if not all, most or many of the potential fates.

3) Related to 2, the downstream potentials being assayed do not require mutually exclusive differentiation conditions (E.g. Macrophage, Granulocytic, and Erythroid potential can be assayed in myeloid differentiation conditions, which do not normally promote lymphoid differentiation, even if the cell has lymphoid potential).

While it could be argued that the advent of iPSC and direct conversion technology (Takahashi and Yamanaka 2006) showed all cells have the potential to become any other cell type (Ladewig, Koch, and Brüstle 2013), these technologies involve extrinsic manipulations to the epigenome of a cell (pushing a marble up the hill or to another valley) (Figure 1.4c,d) as opposed to manipulations to their signals and environment (pushing a marble to the side on its way down the hill) (Figure 1.4b). Because of this, these are not considered when discussing a cell's potential in the context of this thesis.

Importantly, most *fate* tracing experiments rely on post-hoc observation of a cell's identity (most commonly through retrospective lineage tracing, in which a cell retains some label of the cell of interest from which it differentiated), while *potential* experiments rely on ad-hoc perturbations to the stem or progenitor cell to observe as many outcomes as possible, if not all. Because of this, a study which proves that a cell type has the potential to differentiate towards or through another specific cell type has neither proved that the cell is fated to differentiate down this path *in vivo*, nor that this path is necessary for downstream wildtype phenotype and function. Conversely, if a lineage-tracing *fate* experiment reveals that a cell, such as an HSC, is fated to become multiple cell types, it could also be said that it has those *potentials*. Along these lines, some studies use the term *biased* to describe multipotent cells with one predominant or overriding fate at steady state (Sanjuan-

Pla et al. 2013), while others use the term *competent* to describe cells with specific potentials (Swiers et al. 2013). Because differentiation during development is a continuous process along spatio-temporal axes, the timing of when cells are labelled or collected for either of these types of experiments is also important. Despite these limitations and caveats, the ability to study cells at the single-cell and population level has led to many interesting insights regarding the fate and potential of cell populations from the mesodermal level all the way to the adult HSC, some of which will be discussed in sections below.

1.3. Developmental Haematoendothelial Populations

1.3.1. The Haemangioblast

The close developmental relationship between endothelial and haematopoietic cells was described over one-hundred years ago with the observation of clusters of haematopoietic cells in close contact with the endothelium of developing vessels of the yolk sac—the yolk sac blood islands (BI)—and with the intraembryonic endothelium in the embryos of various vertebrates (Jordan 1917), including humans (Minot et al. 1913). Following this, studies observed that “angioblasts [in the developing chicken YS BI] not only give rise to endothelium and blood plasma but also produce the red blood-corpuscles” (Sabin 1920). It was these studies, showing both haematopoietic and endothelial cells from the same mesodermal population could develop into endothelium and blood (Sabin 1920; Murray 1932), that originally gave rise to the idea of a bipotential progenitor, the haemangioblast, which could differentiate into both haematopoietic and endothelial cells (Keller 2001). In support of this model, *in vivo* populations of mesodermal cells in the dorsal lateral plate (DLP) of the fish and frog co-express haematopoietic and endothelial genes (Thompson et al. 1998; Gering et al. 1998; Brown et al. 2000) and give rise to both of these lineages at the population level (Ciau-Uitz, Walmsley, and Patient 2000), while downstream vascular endothelial and haematopoietic cells share expression of transcription factors such as *Gata2* (Dorfman et al. 1992), *Lmo2* (Gering et al. 2003), and *Scl/Tal1* (Gering et al. 2003).

In later studies, embryoid bodies (EBs) differentiated from mouse embryonic stem cells (mESCs) were found to contain a haemangioblast-like population that was purified based on the expression of Vascular Endothelial Growth Factor

Receptor 2 (VEGFR2), also known as Fetal Liver Kinase 1 (FLK1) (Choi et al. 1998; Faloon et al. 2000), and had the ability to give rise to both haematopoietic as well as endothelial cells at the clonal level in a blast colony assay. This population was termed the blast colony forming cell (BL-CFC), and shown to be dependent on SCL/TAL1 to produce haematopoietic progeny (D'Souza, Elefanty, and Keller 2005). Cells with a similar bipotent potential to the BL-CFC were also isolated from gastrulating embryos (E7.0 – E7.5), and were found in highest numbers in the posterior primitive streak (Huber et al. 2004) seemingly confirming the presence of an *in vivo* haemangioblast. However, chimeric studies later found that *in vivo*, haematopoietic and endothelial cells in the YS BI were polyclonal in nature. While these studies could not fully discount the presence of a bipotent *in vivo* haemangioblast, they did show that its contribution to YS BI development in a clonally bipotent manner occurred rarely, if at all (Ueno and Weissman 2006). Later lineage-tracing studies *in vivo* confirmed these conclusions by showing that mesodermal progenitors are specified and fated to become either primitive blood or YS endothelium, but not both, prior to gastrulation and ingress into the primitive streak (Padrón-Barthe et al. 2014). Therefore, $FLK1^{+}$ mesodermal progenitors are fated towards restricted haematopoietic or endothelial fates *in vivo*, and the bipotent nature of these so-called haemangioblasts and their *in vitro* BL-CFC counterparts is revealed only as an artefact of the *in vitro* blast colony assay.

1.3.2. Haemogenic Endothelium (HE) and the Endothelial to Haematopoietic Transition (EHT)

Another population of cells with endothelial characteristics ($FLK1^{+}VE\text{-}Cad^{+}CD45^{-}$) and haematopoietic potential was also identified *in vitro* (Nishikawa et al. 1998).

When isolated from the YS of developing embryos, these VE-Cad^{+}CD45^{-} endothelial cells were shown to have haematopoietic potential (Oberlin et al. 2002; Nishikawa et al. 1998), however given that CD41^{+} cells were not excluded from sorted populations, it is likely that contaminating haematopoietic cells were present in the sorted cells in this particular study. Yet other labelling and fate-tracing experiments showed that haematopoietic cells did indeed originate from endothelial precursors (Jaffredo et al. 1998; Jaffredo et al. 2000; Sugiyama et al. 2003; Fraser et al. 2003; Zovein et al. 2008). These studies supported the theory of haemogenic endothelium (HE) proposed by earlier studies (Smith and Glomski 1982) hypothesizing that, unlike the bipotent haemangioblast, HE was an endothelial cell fated to become haematopoietic (Dieterlen-Lievre et al. 2002).

The process by which HE cells gain haematopoietic potential and morphology at the expense of their endothelial identity is known as the endothelial to haematopoietic transition (EHT) (Figure 1.5) (Zovein et al. 2008; Lancrin et al. 2009; Eilken, Nishikawa, and Schroeder 2009; Kissa and Herbomel 2010; Swiers et al. 2013; Bos, Hawkins, and Zovein 2015; Bertrand et al. 2010b; Boisset et al. 2010). The first time-lapse visualization of EHT was done in a mouse ES differentiation model (Eilken, Nishikawa, and Schroeder 2009), followed shortly by visualization in developmental zebrafish (Bertrand et al. 2010b; Kissa and Herbomel 2010) and mouse models (Boisset et al. 2010). These *in vivo* studies showed the process by which cells resembling vascular endothelium in both morphology and phenotype in the lumen of the dorsal aorta underwent morphological changes to resemble haematopoietic cells and entered circulation.

HE and EHT have also been shown to be associated with EMP and lymphoid progenitor waves during YS haematopoiesis (Yoshimoto et al. 2011;

Frame et al. 2016) as well as HSPC differentiation *in vitro* (Lancrin et al. 2009; Eilken, Nishikawa, and Schroeder 2009; Yvernogeau et al. 2016). In contrast to this, there is strong evidence to suggest that the first wave of haematopoiesis occurs directly from a mesodermal precursor specified prior to primitive streak migration and is independent of HE and EHT (Padrón-Barthe et al. 2014). While all haematopoietic activity during development except for the first primitive wave has been shown to be associated with an HE precursor stage (Padrón-Barthe et al. 2014; Zovein et al. 2008; Kissa and Herbomel 2010; Nishikawa et al. 1998; Frame et al. 2016), it should be noted that some studies have claimed that primitive erythrocytes develop from the haemangioblast through an HE intermediate (Lancrin et al. 2009; Stefanska et al. 2017). The main evidence provided both *in vitro* and *in vivo* is the expression of immunophenotypic HE markers in these populations. However, given that mesodermal haemangioblast and BL-CFC populations have been shown to express endothelial markers (Choi et al. 1998; Ema et al. 2006) as well as take-up acetylated LDL (Choi et al. 1998), the argument becomes circular, and one of semantics. Whether these early mesodermal populations, which express endothelial markers yet have been shown to be strictly biased towards either a haematopoietic or endothelial fate *in vivo* (Padrón-Barthe et al. 2014; Ueno and Weissman 2006) are to also be considered HE depends on how HE is specifically defined in this and other contexts. These progenitors, for example, have a multipotent nature *in vitro* at the clonal level, unlike definitive HE, which is clonally committed to a haematopoietic fate *in vitro* (Swiers et al. 2013). Recent RNA sequencing data at the single cell level from developing E6.5 to E8.5 cells suggests that, “unlike the second haematopoietic wave, the first wave does not transit through a molecular state with classical characteristics of mature

endothelial cells, such as high expression of *Cdh5* and *Pecam1*"(Pijuan-Sala et al. 2019).

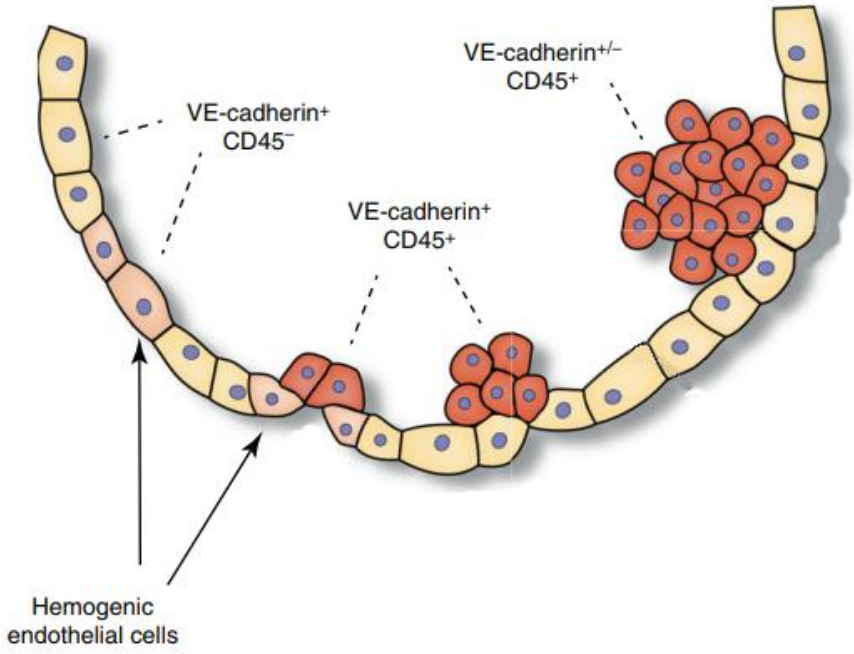

Figure 1.5 Endothelial to Haematopoietic Transition
Both endothelial cells (yellow) and HE cells (pink) express VE-Cadherin and other endothelial markers and originally lack haematopoietic markers. As HE undergoes EHT, it begins budding out of the endothelium and expressing haematopoietic markers, such as pan-haematopoietic CD45, thus activating both morphological as well as genetic blood characteristics. Cells in haematopoietic clusters further expand and begin downregulating VE-Cad and other endothelial markers. Adapted from (Costa, Kouskoff, and Lacaud 2012).

During EHT, HE cells activate haematopoietic TF *Runx1* (North et al. 1999), which is essential for normal definitive haematopoiesis (Okuda et al. 1996; Wang et al. 1996). This leads to upregulation of other haematopoietic genes at the expense of endothelial ones (Swiers et al. 2013; Lizama et al. 2015), while morphological changes, also a result of *Runx1* activation, lead to the formation of clusters (Cai et al. 2000; North et al. 1999; Bos, Hawkins, and Zovein 2015). RUNX1 has been suggested to act as a genetic landscape remodeler, opening previously inaccessible genetic neighbourhoods to haematoendothelial

transcription factors, such as LMO2, SCL/TAL1, and GATA2 that are already expressed in developing endothelial cells (Lichtinger et al. 2012).

In transgenic mice containing a reporter construct with the Runx1 +23 enhancer region cloned downstream of the *LacZ* gene, *LacZ* expression is detected as early as E8, prior to DA fusion and *Runx1* expression, in specific endothelial cells in aortic and YS regions that later develop hematopoietic potential (Nottingham et al. 2007). At this stage, in embryos with GFP expression driven by +23 enhancer activity, GFP^+ cells in the aorta have the potential to form endothelial tubules, but not haematopoietic colonies at the single cell level (Swiers et al. 2013). GFP^+ cells harvested later, at E9.5 and E10.5, after the onset of *Runx1* activation, have either endothelial or haematopoietic potential, but never both. HE then, is not a bipotential progenitor at the clonal level, with the ability to differentiate into both endothelium and haematopoietic cells, but a unipotent cell fated to become haematopoietic. Other studies also confirmed this with single-cell assays of their own (Bos, Hawkins, and Zovein 2015; Ditadi et al. 2015). After E9.5, the frequency of GFP^+ endothelial cells (EC) with haematopoietic potential increases over time, while the frequency of GFP^+ EC cells with endothelial potential decreases (Swiers et al. 2013). Post-hoc, temporal analysis of single cell gene expression showed a transition of endothelial to haematopoietic gene expression from GFP^- ECs through GFP^+ ECs towards $CD41^+$ early hematopoietic progenitors and $CD45^+$ hematopoietic cells. Given this, the authors suggested a model in which cells with an active +23 *Runx1* enhancer are “Competent” HE, with the potential to activate *Runx1*, while cells that then activate *Runx1* are specified as HE and initiate commitment to a haematopoietic fate. Not every developing EC is therefore “competent,” or has the potential for *Runx1* activation. Likewise, not every EC able

to activate *Runx1* will eventually activate the gene and undergo EHT. Committed HE is therefore a developing EC cell that has gone through at least two discrete steps—a competence and a commitment step—to differentiate itself from other EC progenitors and activate a haematopoietic programme.

Other single cell studies that have looked at the EHT process both *in vivo* and *in vitro* report similar findings, in which differentiating HE progressively lose an endothelial signature in favour of a haematopoietic one (Zhou et al. 2016; Kartalaei et al. 2015; Guibentif et al. 2017). Of particular interest, one study found that, at least *in vitro*, downstream haematopoietic lineage fate could be specified in cells as early as those undergoing EHT. Differentiating human iPSCs (h-iPSC) undergoing EHT sorted based on haematopoietic *WAS* gene expression had different haematopoietic lineage potentials (Guibentif et al. 2017). Another study found that at the EHT stage, a large portion of the genes that are up and downregulated were related to cytoskeleton and migration pathways, consistent with the morphological changes that cells experience at this stage (Kartalaei et al. 2015).

In YS HE, GFI1 and GFI1B, repressive factors downstream of *Runx1*, act to downregulate endothelial genes, particularly those related to morphology. HE in *Runx1*$^{-/-}$ ES cells and embryos with induced expression of GFI1 and GFI1B is able to go through a morphological EHT, though cells have reduced haematopoietic potential (Lancrin et al. 2012). In a converse experiment, *Gfi1* and *Gfi1b* double knock-out (KO) embryos and ES cells were shown to contain cells that did not undergo EHT, but upon dissociation and replating had nearly unperturbed haematopoietic potential (Lancrin et al. 2012). This suggests the activation of a haematopoietic programme might be regulated independently of the morphological

and cytoskeletal changes that allow the transitioning cell to escape the endothelium into the lumen, and later, circulation, though both programmes are downstream of *Runx1*. In AGM HE however, similar studies also showed that GFI1 and GFI1B act in concert to downregulate endothelial genes and bring about the morphological and cytoskeletal changes required for EHT, but that, in this case, GFI1 and GFI1B are also required for activation of a haematopoietic programme (Thambyrajah et al. 2016). This difference in gene signalling pathway requirements between YS and AGM HE has also been shown for Notch (Hadland et al. 2004; Kumano et al. 2003) and Ly6a (Chen et al. 2011), and supports the model for the existence of different kinds of HE.

Further study using DamID revealed that GFI1 and GFI1B act in concert with LSD1 and other coREST proteins as well as RUNX1 in order to repress endothelial genes, independent of *Runx1* activation of a hematopoietic programme (Thambyrajah et al. 2016). Of note, many of the novel genes discovered as GFI1 and GFI1B targets in this study also contained RBPJ-binding motifs, which suggests crosstalk with Notch regulation of EHT, described in more detail in further sections. The power of GFI1 and RUNX1 to remodel the endothelial epigenetic landscape and activate EHT has been shown by experiments in which ectopic expression of GFI1 and RUNX1 in concert with TFs FOSB and SPI1 can be used to reprogram adult mouse endothelium from various tissues to go through EHT and give rise to engrafting HSCs (Lis et al. 2017).

1.4. Signalling Pathways Necessary for HSC Development

1.4.1. Arterial Programme Specification: VEGFA, Notch, and Circulation

During early vertebrate development following gastrulation, endothelial precursor cells, also termed angioblasts, which express FLK1 (Drake and Fleming 2000), differentiate from the Lateral Plate (LP) mesoderm. Zebrafish and *Xenopus* studies have shown these cells then migrate towards the midline of the embryo to form the developing Dorsal Aorta (Cleaver and Krieg 1998; Zhong et al. 2001; Jin et al. 2005). In *Xenopus*, high concentrations of the small isoform of Vascular Endothelial Growth Factor A ($Vegfa_{122}$) secreted from the hypochord (Cleaver and Krieg 1998) act as a chemokine for the migrating cells. Hedgehog (Gering and Patient 2005; Vokes et al. 2004) and Bmp (Reese, Hall, and Mikawa 2004) signalling have also been shown to play a role in angioblast migration towards the midline. In zebrafish (Jin et al. 2005) and *Xenopus* (Cleaver and Krieg 1998), endothelial cells migrate as single cells, while in avian (Pardanaud et al. 1987; Coffin and Poole 1988), and mammalian embryos (Chong et al. 2011) cells have formed lumenised vessels (termed paired dorsal aortae), prior to migration.

Likewise at E8.25 in the mouse, cells already express Notch signalling gene *Dll4*, a specific marker of arterial identity in endothelial cells (Villa et al. 2001), and other arterial markers at the population level: *Notch1*, *Notch4*, *Hey1*, *Hey2*, *Nrp1*, *Jag1*, *Efnb2*, *Cx37*, *Cx40* (Chong et al. 2011). Beyond its chemokine properties, VEGFA lies at the top of the arterial fate specification cascade, its dose-dependent (Zhang et al. 2008a; Sriram et al. 2015) signalling leading to expression of arterial Notch ligand *Dll4*, among others (Lanner, Sohl, and Farnebo 2007; Hayashi and Kume 2008). DLL4 signalling through NOTCH1 and later, NOTCH4 receptors, in

concert with endothelial SOX transcription factors, then suppresses venous transcription factor COUP-TF II (Swift et al. 2014) expression and therefore, venous fate (Lawson et al. 2001). The mechanisms underlying arteriovenous specification have previously been reviewed in more detail, and involve feedforward loops initiated by Notch and maintained by shear stress in the developing arteries (Torres-Vázquez, Kamei, and Weinstein 2003; Fish and Wythe 2015).

The developing heart tube begins beating at E8.5, before the paired DA have fused. The shear stress from laminar flow experienced by endothelial cells plays an important role in the further differentiation (le Noble et al. 2003) and maintenance of arterial identity, signalling via nitric oxide (NO) through both Notch (Masumura et al. 2009) and c-AMP (Diaz et al. 2015), another pathway shown to work in concert with VEGFA to drive arterial cell specification (Yamamizu et al. 2010; Yurugi-Kobayashi et al. 2006). Studies have shown that in embryos lacking circulation, *Dll4* in developing arteries is expressed normally, but expression of downstream arterial genes, such as *Cx40*, is abrogated (Chong et al. 2011). Chick/quail experiments have also shown the plasticity of arterial cells and their dependence on shear stress from flow when transplanted into donor sites. Those that integrate into arterial regions maintain an arterial identity, while those that integrate into venous regions adopt a venous one (Moyon et al. 2001; Othman-Hassan et al. 2001). This suggests not only a certain plasticity within endothelial cells of the DA and other developing arteries, but also that local niche signals, in this case, Notch signalling and shear stress, are important to drive and maintain arterial cell identity. Interestingly, shear stress has also been shown to be required for the development of HSCs from intra-aortic clusters (Diaz et al. 2015; North et

al. 2009), through some of the same pathways that drive arterial specification. Studies in zebrafish showed that embryos with a lack of blood flow had reduced HSC numbers, and that this effect was mediated through NO, which could rescue HSC numbers in these embryos (North et al. 2009). This same study likewise found conservation of this NO-mediated effect in murine models of development. The effect of sheer stress on HSC development has likewise been linked to signalling through prostaglanding E2 (PGE2) and cyclic-AMP (Diaz et al. 2015). In *in vitro* mouse differentiation assays, the addition of PGE2 leads to the amplification of multipotent progenitors (North et al. 2007). Though PGE2 is not sufficient to produce HSCs on its own, these data suggest modulation of shear stress pathways, missing in static *in vitro* culture systems, could help derive cells with HSC-like engraftment capacity. Notch signalling has also been shown to be required, in addition to arterial development, for the development of HSCs (Ayllón et al. 2015; Butko, Pouget, and Traver 2016; Gama-Norton et al. 2015; Hadland et al. 2004; Hadland et al. 2015; Richard et al. 2013) and will be described in greater detail in the following section.

1.4.2. Notch Regulation of EHT

The important and complex role that Notch signalling plays in HSC differentiation has been recently described in detail (Butko, Pouget, and Traver 2016). While studies have clearly shown that Notch signalling is required for arterial specification, the data on Notch activation of *Runx1* and EHT can seem contradictory at a glance. Some studies have shown a Notch signalling requirement for AGM haematopoiesis (Robert-Moreno et al. 2005; Ayllón et al. 2015; Hadland et al. 2004; Kumano et al. 2003), while others show that blocking

or decreasing Notch signalling is required for EHT to progress (Richard et al. 2013; Huang et al. 2013; Zhang et al. 2015; Gama-Norton et al. 2015). *In vitro*, multiple studies using mouse, rhesus macaque, and human cells have all shown that Notch signalling from either an arterial endothelial stroma or exposure to immobilized Notch ligand DLL1 can support the differentiation and expansion of engrafting HSPCs from either *in vivo* or PSCs sources (Hadland et al. 2004; Hadland et al. 2017; Hadland et al. 2015; Kumano et al. 2003; Gori et al. 2015; Lu et al. 2016).

At the single cell level, down-regulation of the arterial endothelial programme is sufficient to induce HE specification and EHT in developing endothelial cells. Endothelial TF *Sox17*, which has been shown to be required for HE specification (Clarke et al. 2013), drives an endothelial programme, and is repressive of haematopoietic *Runx1* and *Gata2*. However, once these are expressed, then *Sox17* is repressed and EHT initiated (Lizama et al. 2015) (Figure 1.6a). Notch signalling is capable of further driving either of these programmes (Lizama et al. 2015; Gama-Norton et al. 2015).

In *in vitro* differentiations of human ESCs (hESCs), Notch activation in $DLL4^{low/-}$ HE from $DLL4^{High}$ endothelial cells increases the number of cells that will give rise to haematopoietic colonies (Ayllón et al. 2015). Both *in vitro* as well as *in vivo*, Notch signalling has been observed surrounding HSPC clusters, but never directly below them (Ayllón et al. 2015; Richard et al. 2013). These data point towards a model in which signalling from surrounding arterial cells activates *Runx1* and other haematopoietic genes in competent HE through Notch signalling (Figure 1.6b). The fact that Notch can signal through lateral inhibition (Sjöqvist and Andersson 2017) would support this model, in which Notch signalling from arterial

cells adjacent to competent HE would repress an arterial programme in favour of a haematopoietic one (Lizama et al. 2015).

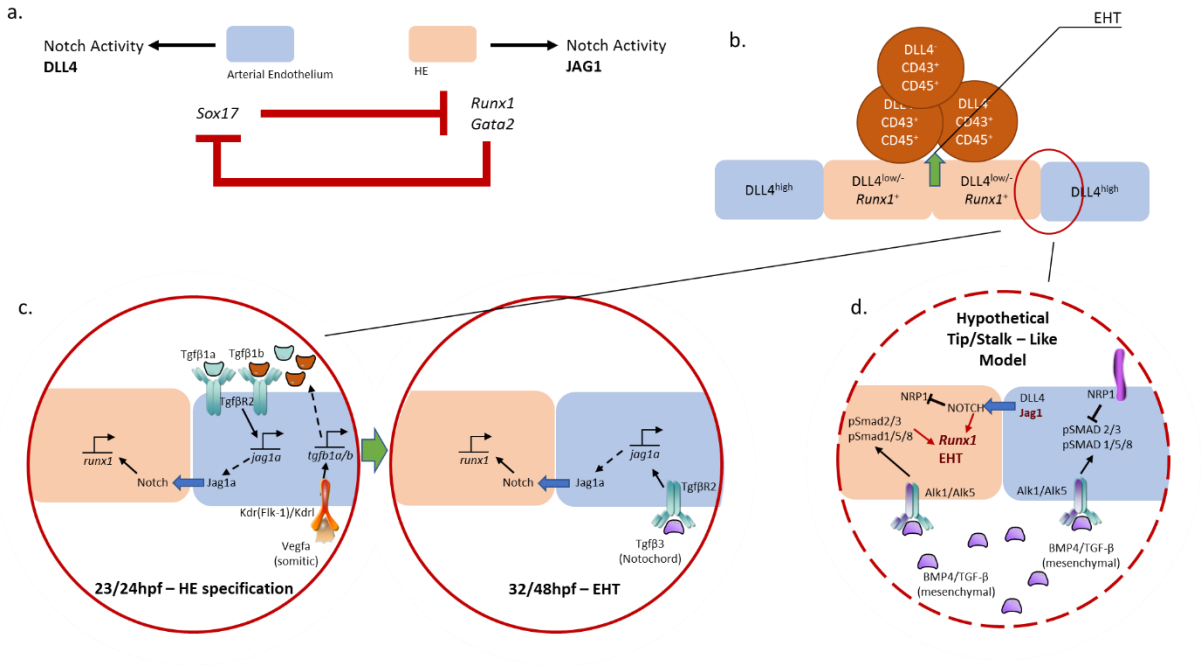

Figure 1.6 Complex spatio-temporal Notch regulation of EHT
a) Endothelial *Sox17* has been shown to downregulate haematopoietic *Runx1* and *Gata2* which in turn negatively regulate *Sox17*. Upon *Sox17* downregulation, *Runx1*, and therefore, EHT, is initiated. Notch signalling further activates both haematopoietic and endothelial fates, depending on cell type (Lizama et al. 2015). Other authors have shown JAG1 signalling leads to haematopoietic fate, while DLL4 signalling leads to an arterial endothelial programme (Gama-Norton et al. 2015). Blue coloured cells represent arterial endothelium while salmon coloured cells to HE fated to undergo EHT.
b) Some studies in mouse have shown DLL4^{High} expression to identify cells fated towards an arterial or endothelial cell fate, while DLL4$^{-/low}$ cells to be those expressing *Runx1* and fated to undergo EHT. Adapted from (Ayllón et al. 2015)
c) In zebrafish models, Notch signalling in the DA required for runx1 expression has been shown to be downstream of Tgfβ signalling at two stages: for HE specification and EHT. Both of these signals are through the Jag1a ligand, shown in mice to lead to a haematopoietic fate. Expression of Tgfβ in this case is activated by somitic Vegfa in the earlier stage, and through Tgfβ3 from the Notochord in the latter (Monteiro et al. 2016).
d) In migrating endothelial cells in angiogenic vessels, stalk/tip identity is tightly regulated by the interaction of VEGFA, NRP1, and phosphorylated SMADs (pSMADs) through either BMP or TGFβ signalling (Aspalter et al. 2015). Given the role that all of these signals have also been shown to play in developing HE in the aorta, a hypothetical model for Notch regulation of EHT based on the stalk/tip model is provided. Red font represents hypothetical downstream pathways/genes.

Jagged1 (JAG1) is another Notch ligand expressed by developing arterial endothelial cells in the AGM (Robert-Moreno et al. 2005). Unlike DLL4, JAG1 is

not required for the formation or arterial specification of the DA, but is required for downstream activation of *Gata2* and EHT (Robert-Moreno et al. 2008). As will be further explored in the following section, work in zebrafish has shown that this expression of arterial *jag1* is driven by Tgf-β, which is in turn activated by somitic Vegfa. At later stages, Tgf-β from the notochord also activates *jag1* and further drives *Runx1* and *Gata2* in developing HE (Figure 1.6c)(Monteiro et al. 2016).

A study in mouse embryos found that these distinct Notch signals are regulated at the molecular level based on affinity and signal strength. While the JAG1 ligand has a higher affinity than DLL4 to Notch1 and therefore outcompetes it in binding to the receptor, it signals at attenuated levels. This study also found that while DLL4 signalling drives an endothelial programme in AGM cells (in this case cells taken at E11.5, after EHT has primarily taken place), JAG1 signalling drives a haematopoietic one and inhibits the endothelial one (Gama-Norton et al. 2015) (Figure 1.6a). Other studies in the zebrafish have also found that G protein-coupled receptor (GPR) 183 modulates Notch signalling to facilitate EHT through degradation of the Notch1 receptor in HE cells (Zhang et al. 2015), confirming the results of a study that found overexpression of NOTCH1 in mouse VE-Cad^{+} endothelium led to abrogation of haematopoiesis (Tang et al. 2013). Studies have shown that HSCs become Notch independent following their maturation in the AGM region, likewise suggesting the timing of Notch signalling to be critical (Souilhol et al. 2016).

Work in migrating endothelial cells during angiogenesis also suggests tight interplay between Notch, VEGFA, and BMP4/TGF-β SMAD signalling to specify endothelial cell identity. Neuropilin1 (NRP1), a $VEGFA_{165}$ co-receptor, was shown to block SMAD signalling in cells with a stalk cell phenotype, while Notch signalling

from these cells blocked *Nrp1* expression in adjacent cells and therefore permitted SMAD signalling by Alk1 and Alk5 through BMP and TGF-β to drive the tip cell phenotype (Aspalter et al. 2015). Given the data that shows the importance of tight timing and gradients of VEGFA, TGF-β, BMP4, and Notch on EHT onset (Vargel et al. 2016; Crisan et al. 2015; Nostro et al. 2008; Monteiro et al. 2016; Gama-Norton et al. 2015; Zhang et al. 2015; Souilhol et al. 2016), it is tempting to speculate whether a similar lateral feedback and regulatory mechanism is not also occurring in adjacent HE and arterial endothelium in the AGM (Figure 1.6d).

1.4.3. Somitic Signals: Haematopoietic Regulation Independent of Arterial Development

In zebrafish embryos, endothelial progenitors migrating towards the midline come in contact with Notch signals from the developing somites. This signalling is potentiated through Dlc and Dld, their expression in turn driven by Wnt16 through a non-canonical Wnt signalling pathway (Clements et al. 2011). This pathway is specifically required for *runx1* activation in the DA and EHT, as abrogation of *dlc/dld* or *wnt16* translation in morphant embryos causes lack of haematopoiesis but does not affect expression of arterial genes in a normally developing DA. Notch signalling requires cell to cell contact, as ligands are bound to the membrane of signalling cells and the mechanical tension caused by the binding of signal to receptor has been shown to be required for signalling (Kopan and Ilagan 2009). It is the actual contact of migrating endothelial progenitors with the developing somites that is thought to allow this signalling to occur.

Similarly, studies in *Xenopus* have shown the independent roles that Vegfa isoforms play in haematopoietic and arterial differentiation. As has been previously

mentioned, Vegfa$_{122}$, the short and non ECM-bound isoform of Vegfa, is required for endothelial cell migration towards the midline and arterial specification of the DA (Cleaver and Krieg 1998). Independently, the medium and long isoforms of Vegfa, Vegfa$_{170}$ and Vegfa$_{190}$, are also expressed in the somites and required for *runx1* and EHT but not for DA development (Leung et al. 2013). Though Vegfa signalling does not require cell to cell contact, the medium and long isoforms of Vegfa are locally bound to the ECM surrounding the cells that produce it, a mechanism thought to aid in spatial distribution and concentrated release of the growth factor during angiogenesis (Park, Keller, and Ferrara 1993; Chen et al. 2010; Goerges and Nugent 2004; Ruhrberg et al. 2002). In this case however, it means that cells also need to be in close proximity to, if not completely touching, the developing somites to access these Vegfa reserves (Leung et al. 2013).

Studies in zebrafish in turn have found that this somitic Vegfa is upstream of DA *tgf-β* expression, which potentiates *runx1* expression and EHT independent of arterial specification (Monteiro et al. 2016) (Figure 1.6c), providing further mechanistic insights to the similar observations made in *Xenopus*. Further studies have shown that both *wnt16*, and therefore somitic *dlc/dld*, and somitic *vegfaa* expression require expression of R-spondin1 (Rspo1) (Genthe and Clements 2017). This points to a common regulatory pathway for the somitic signals that regulate EHT independent of the signals that regulate arterial specification and development.

Unequal exposure of migrating endothelial progenitors to both Notch and VEGFA signalling from the somites could therefore be what leads to heterogeneous *Runx1* activation of competent HE, or even heterogenous HSC and HPC potential of developing clusters. However, whether or not this somitic Notch

and Vegfa requirement is conserved in mammalian haematopoiesis remains to be shown.

1.4.4. Hox and Notch: Independent Regulation and Requirement

The first *Homeobox* (*Hox*) genes are initially activated downstream of BMP4 during gastrulation and mesodermal specification (Lengerke et al. 2008). *Hox* genes are then activated in a sequential manner, with later genes activating further down towards the posterior of the embryo (Pindyurin and van Steensel 2012). The four mammalian *Hox* clusters (paralogs to each other) are expressed in an anterior to posterior fashion (Forlani, Lawson, and Deschamps 2003) and are ultimately expressed in adult bone marrow HSPCs (Sauvageau et al. 1994). Many of them, including *Hoxa6* (Dickson et al. 2009)*, Hoxa9* (Lawrence et al. 2005)*,* and *Hoxb4* (Kyba, Perlingeiro, and Daley 2002; Zhang et al. 2008b) have been implicated in normal HSC function (Dou et al. 2016), as well as malignant haematopoiesis (Alharbi et al. 2012). Further analysis of the transcriptional programme of adult HSCs in both human and mice revealed that *HOXA* genes are not only important to the HSC transcriptional signature, but also that these genes are likely distinctly regulated from key haematopoietic genes such as *Gata2* and *Meis1* (McKinney-Freeman et al. 2012) during ontogeny. One interesting study in particular found that *HoxA3* is expressed as early as E8.25 in developing DA endothelium, but not in YS endothelium. This study then went on to describe how *HoxA3* is able to repress *Runx1* expression and haematopoietic commitment in HE both *in vivo* and *in vitro*, and can even reverse committed haematopoietic CD41 and CD45 expressing cells to an endothelial morphology and immunophenotype, suggesting

another pathway through which endothelial and haematopoietic fates mutually exclude and regulate each other in developing HE (Iacovino et al. 2011).

While engrafting HSC-like cells can be derived by inducing ectopic HOXB4 expression in differentiating mouse ES cells, these have been shown to have limited lymphoid potential (Kyba, Perlingeiro, and Daley 2002), likely due to their lack of a Notch transcriptional signature when compared directly to adult HSCs (McKinney-Freeman et al. 2012). When these cells are differentiated on stromal cells expressing Notch ligand DLL1, they are able to reconstitute both the myeloid and lymphoid lineages of irradiated host mice (Lu et al. 2016). This niche effect is both dosage and timing specific, again pointing to the requirement and specificity of Notch signals during HSC ontogeny, in agreement with other studies (Hadland et al. 2015; Hadland et al. 2004; Gori et al. 2015). These studies suggest that Hox and Notch programmes are activated and regulated independently, with the Hox code being specified as early as the mesodermal stage and the Notch programme at distinct stages of arterial specification and development. Likewise, these and other *in vitro* studies which fail to develop fully engrafting HSCs from PSC sources seem to suggest that while both of these programmes might be necessary, neither is independently sufficient for full HSC development (Sturgeon et al. 2014; Ditadi et al. 2015; Ng et al. 2016; Kyba, Perlingeiro, and Daley 2002; McKinney-Freeman et al. 2012).

1.5. HE Differentiation Models

It is still unknown to what extent the HE from which HSCs develop needs to activate an intrinsic arterial programme or merely be found in an arterial niche to receive Notch and other signals. Studies published during the course of this thesis of HE differentiating from human PSC sources have shown that low or negative expression of arterial DLL4 marks definitive HE (Ditadi et al. 2015; Ayllón et al. 2015). Likewise, they showed that vascular endothelium in these cultures could be separated into arterial, venous, and haemogenic endothelial populations based on the expression of endothelial CD73 and arterial CXCR4 (Ditadi et al. 2015). Even more recently however, similar studies have shown that definitive HE is not only Notch dependent, but also transitions through a stage of arterial DLL4 expression (Park et al. 2018; Uenishi et al. 2018). Work in the mouse has found similar findings, with HE expressing low to no levels of DLL4 giving rise to HPCs, while $DLL4^{+}$ HE giving rise to engrafting HSC populations (Hadland et al. 2017).

While these studies might point to the potential of $DLL4^{+}$ or $DLL4^{-}$ cells to activate *RUNX1* and undergo EHT though, none of them answer the question of whether HE fated to give rise to HSCs requires expression of some levels of an intrinsic arterial programme. DLL4 expression on its own cannot be used as proof of an arterial identity, and though these studies also assay the expression of arterial *EFNB2* and CXCR4, these differences could be an issue of timing or culture conditions. Recent studies have found that, though found within arterial regions, HE from the placenta and vitelline artery (Lee et al. 2016), as well as the AGM (Ganuza et al. 2018), express Lyve-1, a lymphatic marker, at some point during ontogeny prior to HSPC emergence. Indirectly, both of these studies show that the traditional lineage markers used to identify adult endothelial cell populations might

not be precise in doing the same for endothelial cells during ontogeny and/or that HE has a certain plasticity at these stages, and calls to question whether a full cell-intrinsic arterial programme is required for HSC development. In fact, single-cell RNA-sequencing of developing cells in the AGM found residual and shared expression of both arterial and venous genes in Type I and Type II Pre-HSCs with the potential to differentiate into engrafting HSCs (Zhou et al. 2016). These data suggest a model similar to that of HE in the YS, at least at the clonal level, in which HE arises from endothelium prior to its specification towards an arterial or venous lineage (Frame et al. 2016).

These different and sometimes seemingly contradictory data have led to the generation of different models and theories for the specification of HE (Figure 1.7). In one model, it is theorized that early mesoderm lineage separation between YS and Intraembryonic endothelium leads to the differences seen in HSPC potential arising from YS and AGM HE (Figure 1.7a). Data from *Xenopus* which shows the lineages from which YS and DLP blood arise are specified as early as the blastocyst stage support this model, as do *in vitro* experiments which show patterning of differentiating mesodermal cells leads to definitive and even AGM-like HE and HSPCs (Ciau-Uitz, Walmsley, and Patient 2000; Ng et al. 2016; Sturgeon et al. 2014). In some iterations, this model also posits that in order to give rise to HSCs, HE must derive from an arterial endothelial cell, similar to $DLL4^{+}$ cells that give rise to definitive HSPCs identified *in vitro* (Uenishi et al. 2018; Park et al. 2018). Recent data which claim to show extra-embryonic endothelial progenitors ingressing back into the embryo following gastrulation and contributing to AGM haematopoiesis in the developing mouse would seem to counter this model (Eliades et al. 2016). However, video data tracking these “ingressing,” cells is

neither clear nor conclusive, and it is also unclear whether the data itself is an artefact of extracted embryos developing *in vivo.*

In the differing niches model (Figure 1.7b), the theory is that “all HE is created equal,” in potential, and it is the surrounding niche cells, such as YS endothelium or arterial endothelium in the AGM, that provide the signals that HE needs in order to produce fully engrafting HSCs. The fact that cells derived from the YS prior to circulation have the ability to engraft, reconstitute, and contribute to adult haematopoiesis when transplanted into conditioned newborn recipients (Johnson and Yoder 2005; Yoder and Hiatt 1997; Yoder, Hiatt, and Mukherjee 1997) suggests that, given the right niche, these cells have the potential to give rise to engrafting HSCs. Data which shows that arterial endothelium and HE derive from different lineages *in vitro* also supports this model (Ditadi et al. 2015), as do studies that are able to derive HSCs *in vivo* from iPSC teratomas (Amabile et al. 2013; Suzuki et al. 2013). However, the fact that no Pre-HSCs are detected in the YS (Rybtsov et al. 2016) suggests that at least *in vivo*, the YS does not contain cells that will contribute to long-term adult haematopoiesis. It is likely that the cells identified in the previous studies, which, under proper conditions can develop into cells with HSC-like engrafting properties, do not share the same immunophenotype as Pre-HSCs found in the developing AGM. Likewise, the fact that E11.5 AGM cells *in vivo* retain some plasticity in their potential to activate either arterial or haemogenic programmes upon exposure to different Notch ligands also suggests a tighter relationship between arterial and HE fates (Gama-Norton et al. 2015).

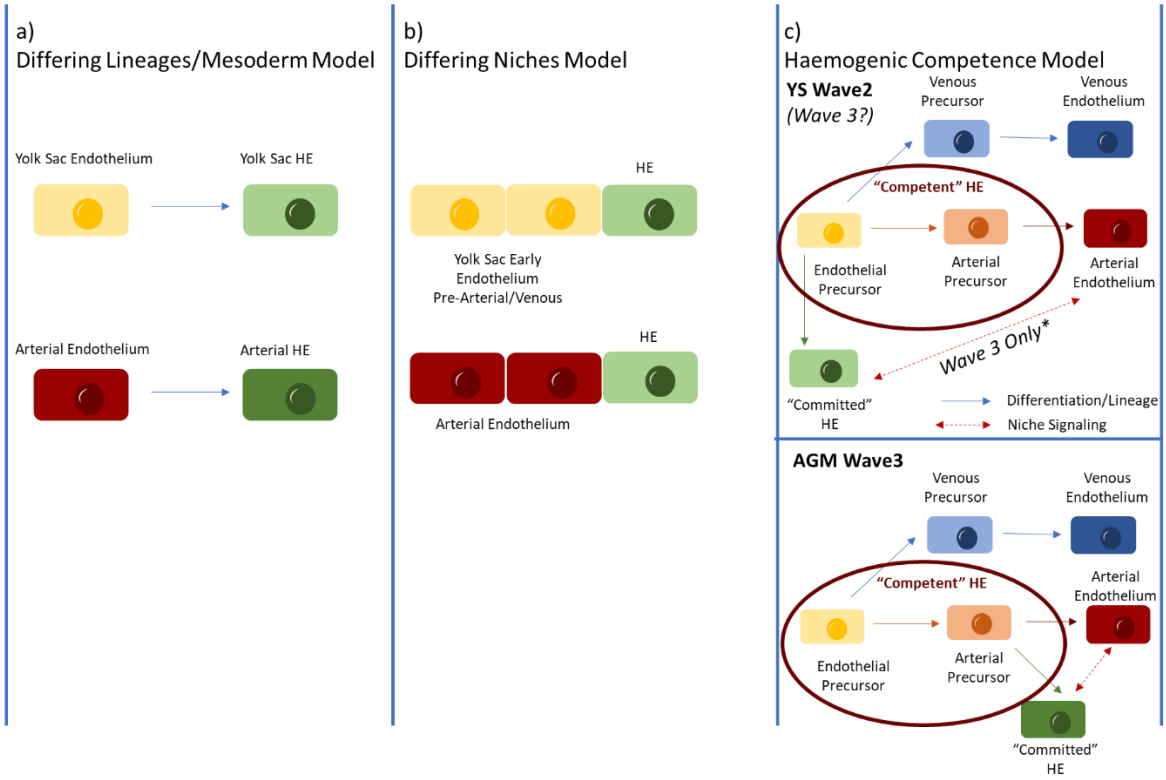

Figure 1.7 Differing Models for HE Specification from Different Waves
a) Differing Lineages/Mesoderm model of HE, in which early separation of AGM and YS endothelial progenitors lead to different HE lineages. b) Differing niches model, in which "all HE is created equal," and it is niche differences that drive different HSPC fates and potentials. c) Putative haemogenic competence model for YS and AGM HE, in which different endothelial progenitor populations have the potential to activate *Runx1*. Both cell-autonomous as well as niche differences lead to different HSPC fates and potentials.

As described in earlier sections, the idea of competent and committed HE in the mouse DA was proposed by (Swiers et al. 2013), where competent HE is marked in a GFP line by the *Runx1* +23 enhancer and committed HE marked by actual *Runx1* expression. Theoretically, I propose an extension of this model to one of haemogenic competence as a reconciliation of some aspects of the previous two models discussed above (Figure 1.7c). In this model, endothelial precursors in both the YS (Figure 1.7c, top panel) and the AGM (Figure 1.7c, bottom panel) can differentiate down a venous, arterial, or HE lineage. As they differentiate down an arterial fate, however, the window of haematopoietic "competence," would potentially remain open and able to be tracked through activity of the *Runx1* +23

enhancer. At any point in this window, extrinsic niche and environmental signals can activate *Runx1* and lead to haemogenic commitment and EHT. Data which point to the differences in timing of *Runx1* activation in the YS and AGM through various mechanisms, such as *Runx1* repression (and therefore late expression, compared to YS) in the AGM by *HoxA3* (Iacovino et al. 2011) and precocious haematopoiesis in the AGM of *Runx1* haploinsufficient embryos (Cai et al. 2000) and mES cells (Lacaud et al. 2004), seem to support the idea that endothelial cells maintain a window of plasticity for *Runx1* expression and HE commitment that might affect downstream HSPC function. In this sense then, it is the combination of mesoderm lineage (YS cells are never exposed to somitic Notch and Vegfa signalling, for example), partial differentiation down an arterial programme, and the presence in an arterial niche that all lead to HSC potential and functionality. This model allows for the seemingly contradictory *in vitro* data showing differing haematopoietic potential in DLL4 positive and negative cells (Ditadi et al. 2015; Uenishi et al. 2018), as well as allows for the existence of heterogeneous HE that gives rise to different HSPC populations, which has not only been proposed before (Slukvin 2016), but also observed *in vitro* (Guibentif et al. 2017).

Of course, this model has its own caveats and considerations. First and foremost, it is possible that DLL4^{+} cells in the AGM do not produce HSCs or even commit to HE, and that the arterial and haematopoietic lineages separate earlier, as has been suggested by *in vitro* data (Figure 1.7, top panel) (Ditadi et al. 2015). This caveat does not preclude the fact that it is still likely that both differences in mesodermal specification and HE niche lead to differences in downstream HSPC function between the YS and AGM. Second, it must be noted that while the migrating mesoderm that develops into AGM HE and HSCs in fish and *Xenopus*

comes in contact with localized somitic Notch and VEGFA signals necessary for HSC development, it is unknown whether this necessity is conserved in mammals, and whether the mesoderm that contributes to HSCs through the vitelline and umbilical arteries is exposed to such signals. Third, it must be noted that the window of haematopoietic competence of endothelial cells is transient, rather than permanent. In other words, it is unlikely that adult endothelial cells have haematopoietic competence. In fact, ectopic expression of *Runx1* is insufficient to efficiently generate HSPCs from adult human endothelial cells, a process which requires at minimum activation of *FOSB*, *GFI1*, *RUNX1*, and *SPI1* (Sandler et al. 2014). Finally, the study which first proposed HE competence did so with data on AGM HE (Swiers et al. 2013), not YS HE, and thus it remains to be seen whether an active +23 enhancer marks competent HE in the YS in cells with similar unipotent fates as in the AGM. On a similar note, in returning to the *in vitro* data that shows BL-CFCs produce primitive haematopoietic cells through an HE intermediate (Lancrin et al. 2009; Stefanska et al. 2017), it again becomes a question of definition whether we consider the window of haematopoietic competence in this model to stretch as far back as the mesodermal BL-CFC (*Runx1* is dispensable for first wave haematopoiesis, so it is unlikely that any of its enhancers are active at this stage and could mark “competence”). To do so would lead to a simplified model in which one could consider cells differentiating from multipotent mesoderm to specified adult arterial endothelial precursors as traveling on a highway with three exits (representing each haematopoietic wave) towards haematopoietic commitment and the distance once has travelled on that arterial endothelial “highway” determining HSPC function through signals acquired along the way. In other words, the cellular niches that form at different developmental

stages provide the signals that instruct the distinct properties of developing HE and the stages at which it exits this endothelial “highway.” This simplified model also points to the crux of many of the debates surrounding HSC ontogeny *in vivo* and their production *in vitro*. At least where their *in vitro* production is concerned, it is not so much the descriptions and definitions we use to refer to the different stages of HSC progenitors that matters so much as the signals, both cell-intrinsic and -extrinsic, that give rise to these populations, and whether or not they can be faithfully recapitulated *in vitro*.

1.6. Thesis Objectives

While the large number of past studies across model organisms on the development of HSPCs has led to the ability to differentiate HSPCs *in vitro* from both mouse and human PSCs, the clinical applications of these protocols is limited. As previously mentioned, there are currently two peer-reviewed protocols that describe the *in vitro* generation of engrafting HSCs (Sugimura et al. 2017; Lis et al. 2017) both of which have limitations that make them clinically unfeasible.

Up until the commencement of this thesis, most *in vitro* studies were heavily invested in the generation of HE and HSPCs and the characterisation of these cells in downstream phenotypic and functional assays. It is only until recently that studies have shifted focus towards analysing and characterising the *in vitro* niche that HSPCs develop in, and the particular relationship that arterial endothelium and HE have *in vitro* (Frame et al. 2016; Gori et al. 2015; Ditadi et al. 2015; Lu et al. 2016; Uenishi et al. 2018). And while studies showed that Notch signalling *in vitro* from an arterial stromal niche conferred long-term engrafting potential to HSPCs derived from HPC sources, using xenografts, even as a niche, makes these protocols unfeasible for clinical applications (Gori et al. 2015), prompting the need for synchronous generation of an arterial niche from PSC sources.

Given that Notch regulation required for HE development from the nascent arterial niche in the AGM is time- and dosage-specific, and the possibility that AGM HE needs to pass through an arterial intermediary step, this thesis sought to improve existing protocols for *in vitro* development of HSPCs and develop a well-characterised system for concomitant arterial and HE differentiation in which some

of these hypotheses could be tested. The objectives of the thesis, then, as divided into thesis chapters, were to:

1. More fully characterise a previously-published mESC protocol that gives rise to a *primitive* and *definitive* wave of HSPCs:
    a. FLK1^{+} definitive mesodermal progenitors from a previously described protocol were further characterised, as was their haematopoietic output following EHT.
    b. The endothelial niche in which these cells differentiated and underwent EHT was also characterised for the presence of arterial endothelium and Notch signalling.
2. Establish an mESC protocol for concomitant differentiation of arterial endothelium and HE.
    a. VEGFA concentrations in the differentiation system were modulated to promote arterial differentiation alongside EHT.
    b. The haematopoietic potential of DLL4^{+} endothelium was assayed.
3. Fully characterise and modify a commercially available human iPSC to HSC differentiation kit.
    a. The HSPC and monolayer fractions of the kit were characterised for haematopoietic output as well as presence of concomitantly developing arterial niche.
    b. VEGFA concentrations were modulated, as in previous chapters, to promote arterial development concomitant to HE specification.

2. Materials and Methods

2.1. Media Formulations and Molecular Reagents

2.1.1. Cell Culture Cytokines, Growth Factors, and Small Molecules

All cytokines and growth factors were reconstituted, aliquoted, and stored frozen as per manufacturer's instructions.

Table 2.1 Cell culture reagents

Name and Abbreviation	Description	Company and Catalogue Number
8-Bromoadenosine 3',5' -cyclic monophosphate sodium salt (br-cAMP)	Stable cAMP mimic	*Sigma B7880*
AA	L-Ascorbic Acid	*Sigma A4403*
Activin A (ActA)	Recombinant human/mouse/rat (CHO cell-derived)	*R&D Systems 338-AC*
Bone Morphogenic Protein 4 (BMP4)	Recombinant human (NS0-derived)	*R&D Systems 314-BP*
CHIR99021 (CHIR)	Canonical Wnt/β-catenin pathway agonist	*Sigma SML1046*
DAPT	γ-secretase and Notch inhibitor	*Sigma D5942*
DMSO	Dimethyl Sulfoxide	*Sigma D2650*
Fibroblast Growth Factor basic (bFGF)	Recombinant human (E. coli-derived)	*R&D Systems 233-FB*
Flt-3 Ligand (Flt3-L)	Recombinant mouse (NS0-derived)	*R&D Systems 427-FL*
SB431542 hydrate (SB)	Activin/Nodal and TGF-β antagonist	*Sigma S4317*
SCR7	Non-homologous end joining (NHEJ) inhibitor	*Xcessbio M60082*
Stem Cell Factor (SCF)	Also known as Kit Ligand; recombinant murine	*Peprotech 250-03-10*
Thrombopoietin (TPO)	Recombinant mouse (NS0-derived)	*R&D Systems 488-TO*
TrypLE Select	Cell Dissociation Reagent	*ThermoFisher 12563011*
Vascular Endothelial Growth Factor (VEGF-A)	Recombinant human (Sf21-derived); Medium isoform 165	*R&D Systems 293-VE*
Y-27632	ROCK inhibitor	*TOCRIS Bioscience 1254*
Accutase™	Cell Dissociation Reagent	*StemCell Technologies 07920*

2.1.2. Cell Culture Media Formulations

All liquid cell culture media was prepared in sterile conditions in laboratory-grade laminar flow hoods and filtered using 0.22 µm filters.

Table 2.2 Solutions and media formulations

Name	Composition
Flow-assisted cell sorting (FACS) Buffer[1]	Phosphate-buffered saline (PBS), 10% heat-inactivated fetal bovine serum (ΔFBS)†
FACS Buffer with DNAse[2]	FACS Buffer, 5 µg/mL DNAse (*Roche 1184932001*)
PBS with DNAse[2]	PBS, 5 µg/mL DNAse (*Roche; 1184932001*)
PBS/EDTA	PBS, 0.5 mM EDTA (*Corning 46-034-CI*); Kept at room temperature
Mouse ESC (mESC) Maintenance Medium[1]	Dulbecco's Modified Eagle Medium (DMEM *Life Technologies 11995-065*), 15% ΔFBS, CHO-LIF Conditioned Medium*, 1.5 x 10^{-4} M Monothioglycerol (MTG *Sigma M1753*)
mESC IMDM Maintenance Medium[1]	Iscove's Modified Dulbecco's Medium (IMDM *Life Technologies 12440-053*), 15% ΔFBS, CHO-LIF Conditioned Medium*
CHO-LIF Medium	IMDM, 10% ΔFBS
Serum Free Differentiation Medium (SFD)[2]	75% IMDM, 25% Ham's F12 (*Life Technologies 31765-035*), 0.5X N2 Supplement (*Life Technologies 17502-048*), 0.5X B27 Supplement (No Vitamin A, *Life Technologies 1258-010*), 1X Penicillin-Streptomycin-Glutamine (*Life Technologies 10378-016*), 0.05% BSA (*Life Technologies A10008-01*), 4.5 x 10^{-4} M MTG
Haematoendothelial Differentiation Medium (HED)[3]	SFD, 88 µg/mL Ascorbic Acid (*Sigma A4403*), 12.5 ng/mL bFGF, 20 ng/mL BMP4, 0.25 mM Br-cAMP, 4 µM SB, 20 ng/mL SCF, 20 ng/mL TPO, 10ng/mL Flt3-L
h-iPSC Maintenance Medium[4]	Essential 8™ Basal Medium (*Thermofisher A15169-01*), 1X Essential 8™ Supplement (*Thermofisher A15171-01*)
Human Hematopoietic Differentiation Medium A[4] (Hemato A)	STEMdiff™ Hematopoietic Basal Medium (*Stemcell Technologies 05311*), 1X STEMdiff™ Hematopoietic Supplement A (containing BMP4, bFGF, VEGF)
Human Hematopoietic Differentiation Medium B[4] (Hemato B)	STEMdiff™ Hematopoietic Basal Medium (*Stemcell Technologies 05311*), 1X STEMdiff™ Hematopoietic Supplement B (containing SCF, Flt3-L, TPO), 1X Penicillin-Streptomycin (*Thermofisher 15140-122*)
Matrigel Solution[2]	DMEM/F12 (*Life Technologies 10565-018*), 0.17 mg/mL Matrigel® (*Corning®, Growth Factor Reduced*)
0.1% Gelatin Solution[5]	PBS, 1 mg/mL Gelatin (*Sigma G1890*) autoclaved
Mouse CFU assays (Methylcellulose)	StemCell Tech 03444
Human CFU assays (Methylcellulose)	StemCell Tech 04445

(1) Prepared fresh and stored at 4°C for no more than a month's time
(2) Prepared fresh before each use
(3) Prepared fresh and stored at 4°C for no more than a week's time
(4) Aliquoted and stored at -20°C, then thawed before use and stored at 4°C for no more than a week's time
(5) Prepared and stored at 4°C indefinitely.
(†) FBS lot tested and heat-inactivated in-house
(*) See section 2.2.1. below for details.

2.1.3. Flow Cytometry Antibodies and Isotype Controls

Flow cytometry antibodies were stored at 4°C as per manufacturer's instructions. Amounts used per test corresponded to manufacturer's instructions. Where not specified, antibody amount was titrated to find best positive to negative signal ratio as defined by the equation: $\frac{\mathrm{MFIpos}-\mathrm{MFIneg}}{\mathrm{SDneg}}$ where MFI_{pos} corresponds to median fluorescence intensity (MFI) of the positive population, MFI_{neg} corresponds to MFI of the negative population, and SD_{neg} to the standard deviation of the negative population. Unless otherwise specified, a test corresponds to 5 x 10^5 to 1 x 10^6 cells in 100 ul of FACS buffer.

Table 2.3 Flow cytometry reagents

Antigen	Fluorochrome	Company/Catalogue	Species	µl per Test
CD150 (SLAM)	BV421	*Biolegend 115925*	Rat anti-mouse	1
CD16/32	PE	*Thermofisher 12-0161-81*	Rat anti-mouse	0.63
CD16/32 (FC Block)	Unconjugated	*Biolegend 101320*	Rat anti-mouse	2
CD201	PE	*Thermofisher 12-2012*	Rat anti-mouse	5
CD31	BV421	*BD Horizon 562939*	Rat anti-mouse	1
CD41	BV605	*Biolegend 133921*	Rat anti-mouse	2.5
CD43	BV421	*BD Horizon 562958*	Rat anti-mouse	1
CD45	FITC	*BD Bioscience 553080*	Rat anti-mouse	0.25
CD48	AF488	*Biolegend 103414*	Armenian hamster anti-mouse	1
cKit	APC	*Biolegend 105811*	Rat anti-mouse	0.13
Dll4	APC	*Biolegend 130813*	Armenian hamster anti-mouse	0.63
Flk-1 (VEGFR2)	PE	*Thermofisher 12-5821*	Rat anti-mouse	1
Jagged1	APC	*Biolegend 130913*	Armenian hamster anti-mouse	1
Lineage Stain	PE	*Biolegend 133303*	Rat and armenian hamster anti-mouse	20
Ly-6A/E (Sca-1)	BV650	*Biolegend 108143*	Rat anti-mouse	1
Notch1	APC	*Biolegend 130613*	Armenian hamster anti-mouse	1
PDGFRα (CD140a)	APC	*Thermofisher 17-1401*	Rat anti-mouse	1

VE-Cadherin (CD144)	PE-Cy7	*Biolegend 138015*	Rat anti-mouse	0.31
SCL	N/A	*Santa Cruz SC12984*	Goat polyclonal anti-mouse,rat,human	1.6*
Goat IgG Labeling Kit	AF488	*ThermoFisher Z25602*		5
Apelin Receptor	APC	*R&D Systems FAB856A*	Mouse anti-human	5
CD105	AF647	*BD Pharmingen 561439*	Mouse anti-human	5
CD235a	FITC	*Biolegend 349104*	Mouse anti-human	5
CD34	PE-Cy7	*BD Pharmingen 560710*	Mouse anti-human	10
CD34	PE	*BD Pharmingen 555822*	Mouse anti-human	20
CD38	APC	*BD Pharmingen 555462*	Mouse anti-human	20
CD43	BV711	*BD OptiBuild™ 743614*	Mouse anti-human	5
CD43	FITC	*BD Pharmingen 555475*	Mouse anti-human	20
CD45	V450	*BD Horizon 560367*	Mouse anti-human	5
CD45RA	APC-H7	*BD Pharmingen 560674*	Mouse anti-human	5
CD49f	PE-Cy5	*BD Pharmingen 551129*	Rat anti-human	20
CD73	PE	*BD Pharmingen 550257*	Mouse anti-human	20
CD73	FITC	*BD Pharmingen 561254*	Mouse anti-human	5
CD90	PE-Cy7	*BD Pharmingen 561558*	Mouse anti-human	5
CXCR4 (CD184)	PE-CF594	*BD Horizon 562389*	Mouse anti-human	5
Dll4	APC	*Biolegend 346508*	Mouse anti-human	5
VE-Cadherin (CD144)	BV605	*BD OptiBuild™ 743705*	Mouse anti-human	5
N/A	7-AAD Viability Dye	*Thermofisher 00-6993-50*		5
	Fixable Violet Live/Dead Stain	*ThermoFisher L34955*		1
Armenian Hamster IgG Rat IgG2b Rat IgG2a	PE	*Biolegend 133303*		20
Rat IgG2a	BV421	*Biolegend 400535*		1
Armenian Hamster IgG	AF488	*Biolegend 400923*		

BD™ CompBeads Plus	For anti-human antibodies	*BD Biosciences 51-9006274*		
BD™ CompBeads	For anti-mouse antibodies	*BD Biosciences 51-90-9001189*		

(*) See section 2.4.5 for intracellular staining protocol.

2.1.4. Taqman™ RT-qPCR primer and probe sets

All TaqMan® assays were purchased from ThermoFisher Scientific.

Table 2.4 Taqman™ primers and probes and Molecular Biology Reagents

Gene	Species	Assay	Probe
AA4.1 (CD93)	Mouse	*Mm00440239_g1*	FAM
ActB	Mouse	*Mm02619580_g1*	FAM
Aplnr (APJ)	Mouse	*Mm00442191_s1*	FAM
CD31	Mouse	*Mm01242576_m1*	FAM
CD43	Mouse	*Mm01164549_m1*	FAM
Cdh5 (VE-Cadherin)	Mouse	*Mm00486938_m1*	FAM
COUPTF-II	Mouse	*Mm00772789_m1*	FAM
Cxcr4	Mouse	*Mm01292123_m1*	FAM
Dll1	Mouse	*Mm01279269_m1*	FAM
Dll3	Mouse	*Mm00432854_m1*	FAM
Dll4	Mouse	*Mm00444619_m1*	FAM
Efnb2	Mouse	*Mm00438670_m1*	FAM
EphB4	Mouse	*Mm01201157_m1*	FAM
Erg	Mouse	*Mm01214246_m1*	FAM
Etv2	Mouse	*Mm00468389_m1*	FAM
Fli1	Mouse	*Mm00484410_m1*	FAM
Flk-1 (VEGFR2, KDR)	Mouse	*Mm00440109_g1*	FAM
Flt1	Mouse	*Mm00438980_m1*	FAM
Flt4	Mouse	*Mm01292604_m1*	FAM
GAPDH	Mouse	*Mm03302249_g1*	FAM
Gata2	Mouse	*Mm00492301_m1*	FAM
Gja4 (Cx37)	Mouse	*Mm01179783_m1*	FAM
Gja5 (Cx40)	Mouse	*Mm01265686_m1*	FAM
Hes1	Mouse	*Mm01342805_m1*	FAM
Hes5	Mouse	*Mm00439311_g1*	FAM
Hey1	Mouse	*Mm00468865_m1*	FAM
Hey2	Mouse	*Mm00469280_m1*	FAM
Hif1α	Mouse	*Mm00468869_m1*	FAM
Hif2α	Mouse	*Mm01236112_m1*	FAM
Itga2b (CD41)	Mouse	*Mm00439741_m1*	FAM
Jag1	Mouse	*Mm00496902_m1*	FAM
Jag2	Mouse	*Mm01325629_m1*	FAM
Lmo2	Mouse	*Mm01281680_m1*	FAM
Ly6a	Mouse	*Mm04337234_mH*	FAM

Lyl1	Mouse	*Mm00493219_m1*	FAM
Lyve1	Mouse	*Mm00475056_m1*	FAM
Meis1	Mouse	*Mm00487664_m1*	FAM
NFκB1	Mouse	*Mm00476361_m1*	FAM
Notch1	Mouse	*Mm00627185_m1*	FAM
Notch4	Mouse	*Mm00440525_m1*	FAM
Nrp1	Mouse	*Mm00435379_m1*	FAM
Nrp2	Mouse	*Mm00803099_m1*	FAM
PDGFRα	Mouse	*Mm00440701_m1*	FAM
Prom1	Mouse	*Mm00477115_m1*	FAM
Ptprc (CD45)	Mouse	*Mm01293577_m1*	FAM
Runx1	Mouse	*Mm01213404_m1*	FAM
Scl/Tal1	Mouse	*Mm01187033_m1*	FAM
Sox17	Mouse	*Mm00488363_m1*	FAM
Sox18	Mouse	*Mm00656049_gH*	FAM
Sox7	Mouse	*Mm00776876_m1*	FAM
Tek (Tie-2)	Mouse	*Mm00443243_m1*	FAM
18s	Human	*Hs99999901_s1*	VIC
ActB	Human	*Hs01060665_g1*	VIC
GAPDH	Human	*Hs03929097_g1*	VIC
HoxA10	Human	*Hs00172012_m1*	FAM
HoxA5	Human	*Hs00430330_m1*	FAM
HoxA6	Human	*Hs00430615_m1*	FAM
HoxA9	Human	*Hs00365956_m1*	FAM
Product	Company	Catalogue	
Phusion High-Fidelity PCR Kit	New England Biolabs	*M0530S*	
DNEasy Blood & Tissue Kit	Qiagen	*69506*	
RNAeasy Micro Kit	Qiagen	*74004*	
TaqMan™ RNA-to_Ct 1-Step Kit	AB	*439253*	

2.2. Cell Line Generation and Maintenance

Unless otherwise noted, all cells were cultured under sterile conditions in laboratory-grade tissue culture incubators at 37°C and controlled for 5% CO_2 at ambient O_2 levels. All cells were cultured on tissue-culture treated plasticware.

2.2.1. CHO-LIF Cells

Transgenic Chinese hamster ovarian cells (CHO-LIF) generated for in-house leukemia inhibitory factor (LIF) production were kindly donated by the Gordon Keller lab.

Cells were thawed from frozen stocks in a 75cm^2 tissue culture treated flask in CHO-LIF medium and allowed to reach ~80% confluency before medium was changed. Medium was then collected every two days and new medium was added. This was done 2 – 3 times until cells began dying and detaching into the supernatant.

Conditioned medium was stored at 4°C during collection time and then filtered using a 0.22 µm filter, aliquoted, and stored at -20°C.

Conditioned LIF medium was then tested on J1 cells at 1%, 1.5%, 2% and 4%. For different batches, the minimum concentration that kept mESC cells in an undifferentiated state was used in mESC maintenance medium formulation.

2.2.2. Mouse Embryonic Stem Cells (mESCs)

The mESC lines used in this thesis were the well-established and characterised J1 and Brachyury-GFP lines (Gadue et al. 2006). They have been used frequently in *in vitro* studies of mouse haematopoietic differentiation and development (Irion et al. 2010; Gadue et al. 2006).

2.2.2.1. Cell Passaging

mESCs were cultured on 6-well, tissue-culture treated plates and routinely passaged when cell clusters reached 60 – 75% confluency. A new well was treated

with 0.1% gelatin solution for at least 10 minutes at either room temperature or in the tissue culture incubator. Medium was removed from the well containing cells and cells were washed once with PBS. mESC clusters were then detached using 500 µl 0.25% Trypsin-EDTA (*ThermoFisher 25200-056*) for 3 minutes at 37°C.

Trypsin-EDTA was then quenched with 2.5 ml of mESC maintenance medium and cell suspension pipetted up and down to ensure single cell suspensions. 0.1% gelatin solution was removed from the new well, and 2.5 ml of mESC maintenance added to it. 500 µl of the single cell suspension was added to the new well for a 1 in 6 dilution and manually rocked to ensure even distribution of cells in well. Cells were split every other day.

2.2.2.2. Cell Freezing

Cells were frozen routinely in order to increase stocks of low-passage cells. This was done on days when regular passaging was done. The equivalent of one confluent well of a 6-well plate was frozen into one cryovial.

Cells were detached from well as if passaging, described in section 2.2.2.1. above. Cells were then centrifuged at 200 x G for five minutes. Supernatant was removed, and the resulting cell pellet resuspended in 500 µl of ΔFBS and added to cryovial. During this time, a 2X solution of freezing medium was prepared: 80% ΔFBS, 20% DMSO (Sigma). 500 µl of 2X freezing medium was added in dropwise fashion to cryovial while mixing with pipette.

Cryovials were then placed in CoolCell® LX (*biocision BCS-405*) containers and placed into -80°C storage overnight. Cryovials were then transferred into liquid nitrogen for long-term storage at -196°C.

2.2.2.3. Cell Thawing

A new well in a 6-well plate was prepared with gelatin as if passaging, described in section 2.2.2.1 above. 9 ml of mESC maintenance medium were added to a 14 ml Falcon tube. A frozen cryovial of cells was then quickly thawed in a 37°C water bath and added dropwise to mESC media in tube. Cells were centrifuged at 200 x G for five minutes. Supernatant was removed and cells resuspended in 3 ml mESC medium, then plated onto gelatin-coated 6-well plate. A media change was done early the following day, and cells allowed to grow to confluency before splitting. Cell batches were kept in culture for no longer than five weeks.

2.2.3. *Scl:mCherry* mESC

2.2.3.1. Guide RNA and Plasmid Design and Cloning

Single guide RNA (sgRNA) and homologous recombination template plasmid designs for creation of Scl/Tal1 mCherry reporter line (Figure 2.1a) were done through the WIMM Genome Engineering Service. Cloning of sgRNA oligos into pSpCas9(BB)-2A-GFP (PX458) cassette, as well as sequencing validation, minipreps, and surveyor assays also done by WIMM Genome Engineering Facility. Synthetic DNA donor cassette was purchased from GeneArt.

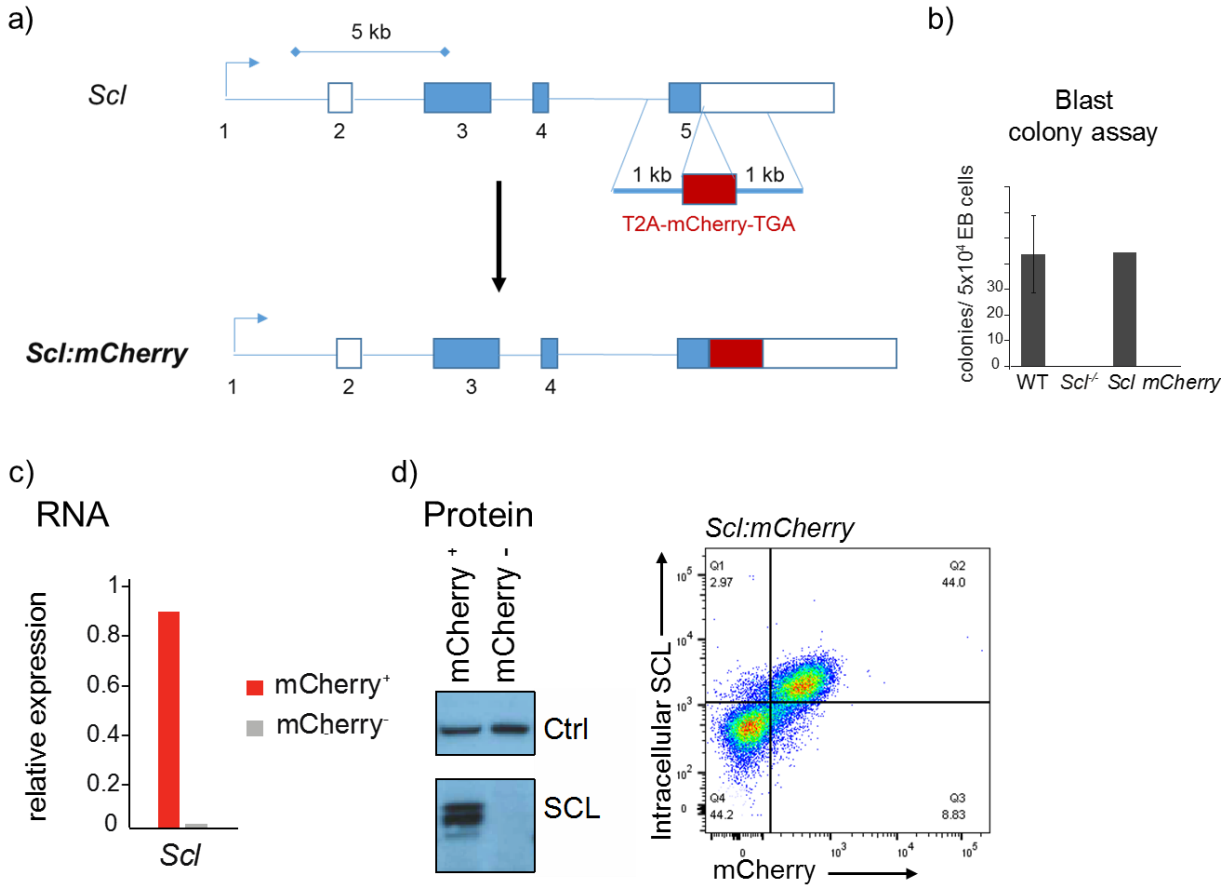

Figure 2.1. Generation and characterisation of Scl:mCherry reporter cell line
a) Schematic representation of the targeting strategy used to generate the *Scl:mCherry* reporter line. White boxes: UTR regions; blue boxes: exons; thin lines: introns; the T2A-mCherry-TGA sequences with 1kb homology arms with targeted insertion site are depicted at the top, and resulting *Scl:mCherry* product depicted below. b-d) Validation of the reporter line. Cells were differentiated in a serum containing medium and collected at day 3.5 for blast, RNA, and protein analyses (Chagraoui et al. 2018). b) Number of colonies per 5 x 10^4 cells from EBs of WT, *Scl*$^{-/-}$ and *Scl:mCherry* line, showing mCherry reporter line reproduces hematopoietic phenotype of its WT counterpart. c) *Scl* mRNA (by RT-qPCR) was exclusively detected in the mCherry$^+$ population following sorting. d) Left: SCL protein (Western Blot) was likewise also exclusively detected in mCherry$^+$ fraction post-sorting. Ctrl: loading control (mSIN3a); Right: Flow cytometry analysis at day 5.5 reveals that that all SCL-expressing cells co-express mCherry.

2.2.3.2. Transfection and Cell Cloning

Parental line J1s were thawed four days prior to transfection. Five hours prior to transfection, 1 µM SCR7 was added to medium. 2 x 10^6 cells were transfected with

a total of 12 µg of DNA at two different ratios of donor DNA to guide plasmid (10:1 and 5:1). Nucleofector™ (*Lonza*) was used to transfect cells.

Cells were replated onto gelatin post-transfection in mESC maintenance medium containing 1 µM SCR7 and allowed to recover for 3 days. Cells were then sorted using Flow Assisted Cell Sorting (FACS) as single cells based on GFP expression into 96-well plates and clones allowed to proliferate for 9 to 10 days before splitting into new 96-well plates. Four 96-well plates yielded 153 clones that proliferated at a rate comparable to the parent line and were subsequently expanded and transferred to four 48-well plates.

2.2.3.3. Clone Validation and Sequencing

DNA was isolated from the 153 clones with DNEasy Kit (Qiagen) and stored at -20ºC. However, as a preliminary screen to potentially identify correctly targeted clones out of a smaller pool of the 153 collected, 6 clones from each of the four 48-well plates were chosen at random (for a total of 24 clones), differentiated in serum-free conditions as described in Section 2.3.1, and cells collected at Day 5.5 of culture to assay for bulk mCherry expression by flow cytometry. Given low cell counts, it was necessary to pool Day 5.5 cells from all the clones originating from each individual plate (4 samples of 6 clones each) to have enough material for flow cytometry analysis. Three of the four samples (for a total of 18 potential clones) showed positive mCherry expression at this stage and it was the DNA of these 18 clones that was used to distinguish the individual clones with correct mCherry insertion. Primers spanning mCherry and homology sequence regions were designed in order to detect correct insertion of cassette into genomic locus through PCR:

Forward: CTGCCTCGTAGTTAGCAAAGG

Reverse: CACCTTGAAGCGCATGAACT

PCR reactions on these 18 clones were run using Phusion High-Fidelity PCR Kit (NE Biolabs). Five of the 18 clones were found to have positive bands at the expected size. These five clones were individually differentiated in serum-free conditions and cells collected at Day 5.5 to check for normal mCherry, Flk-1, PDGFRα, and intracellular SCL expression by Flow Cytometry. Three of these five samples, which in addition to mCherry expressed comparable levels of Flk-1 and PDGFRα to the WT parent line were sent for sequencing of the insertion site. Based on the results obtained from genomic PCR, *in vitro* differentiations, and sequencing results, one heterozygous clone was chosen for further analyses and validation was performed, as mentioned previously, by others in the lab. Figure 2.1b-d shows how *Scl:mCherry* cells produce comparable numbers to WT of BL-CFCs from Day 3.5 serum-containing differentiations, and how when sorted based on mCherry expression, it is the mCherry^{+} fraction that is positive for *Scl* at both the mRNA (tested by RT-qPCR) and protein levels (tested by western blot and flow cytometry) (Chagraoui et al. 2018). This clone was karyotyped by the WIMM mouse transgenic core facility. ~80% of the cells presented a normal karyotype. The PhD candidate did not screen the remaining DNA samples for the full set of 153 clones, and recognizes, in retrospect, this would have been beneficial in identifying other potential clones for further study.

2.2.3.4. Line Maintenance

The *Scl:mCherry* clone was cultured, maintained, expanded, and frozen as described for parental J1 lines in section 2.2.2.

2.2.4. Human Induced Pluripotent Stem Cells (h-iPSCs)

2.2.4.1. Human CD34+ haematopoietic stem and progenitor cells (HSPCs)

Human CD34+ HSPCs were obtained from healthy volunteers after informed consent in accordance with the Declaration of Helsinki, under an institutional review board-approved clinical protocol (NCT00001529). Patients underwent mobilization with a subcutaneous injection of 10 µg/kg G-CSF (filgrastim) for 5 days followed by leukapheresis using a Cobe Spectra Apheresis System (Terumo BCT). The mononuclear cell (MNC) concentrates were enriched in CD34+ HSPCs using a CliniMACS Plus instrument (Miltenyi Biotec) and cryopreserved prior to use for generation of iPSC lines.

2.2.4.2. Line Generation and Validation

h-iPSC lines used in this thesis were derived from human CD34+ HSPCs and developed in-house in collaboration with the NIH iPSC core facility. $CD34^+$ HSPCs were transfected with pluripotency transcription factors (TFs) *Sox2, cMyc, Oct4, Klf4* using Sendai virus vectors.

iPSC lines were then validated using alkaline-phosphatase (AK) staining. Clones with colonies exhibiting iPSC morphology were fixed and stained for AK using BCIP/NBT AK Phosphatase Substrate (*Vector SK-5400*). Similarly, cells were stained for Tra-1 and Nanog via flow cytometry by the NIH iPSC core facility. Finally, iPSCs were injected in Matrigel™ (Corning) plugs into NSG mice for the development of teratomas. Mice with observable tumours were sacrificed and histologically assayed for development of all three germ layers by the NHLBI Transgenic Core Facility.

Unless otherwise stated, all h-iPSC experiments in this thesis were done on the MCND-TENS2 h-iPSC line derived from normal $CD34^+$ cells.

2.2.4.3. Cell Passaging

6-well plates were coated with 1 ml Matrigel solution and either left overnight at 4°C or at room temperature for 1 hour before use. Unused coated plates were wrapped in sterile conditions with parafilm and stored at 4°C for up to ten days.

Cells were split when h-iPSC clusters reached ~60% confluency. Old medium was removed from the cells and well was washed once with PBS and once more with PBS/EDTA. Clusters were then lightly dissociated using 1 ml PBS/EDTA for 2.5 minutes at room temperature. PBS/EDTA was removed, and 1ml h-iPSC maintenance medium with 1.25 µM Y-27632 added to well. A 1000 µl pipette was used to break up cell clusters into smaller clusters by pipetting 3 – 4 times.

Matrigel solution was removed from new wells to be used and 2 ml h-iPSC medium with 1.25 µM Y-27632 added. Depending on experimental requirements 50 to 200 µl of cell clusters were transferred onto new wells. Usually, two to three wells at varying cluster amounts were plated for flexible passaging dates.

Media changes were done on cells daily. Cells were passaged every 3 to 4 days, and not kept in culture beyond passage 60.

2.2.4.4. Cell Freezing

Cells were frozen similarly to mESC cells, described in section 2.2.2.2. above, using h-iPSC maintenance medium with 10 µM Y-27632 instead of ΔFBS, taking care to not dissociate cell clusters with further pipetting.

2.2.4.5. Cell Thawing

Cell thawing was done in a similar manner to mESC thawing, described in section 2.2.2.3 above, using h-iPSC maintenance medium with 10 µM Y-27632 instead of mESC maintenance medium. Care was taken when resuspending pellet to ensure cell clusters were not dissociated further.

2.3. Pluripotent Stem Cell Differentiation

2.3.1. Mouse HSPC Differentiation

Protocol for differentiation of mouse HSPCs (Figure 2.2) was adapted from published protocols (Irion et al. 2010; Clarke et al. 2013; Chiang and Wong 2011). For all steps involving serum-free differentiation (SFD) and hematoendothelial differentiation (HED) media, AA, cytokines, and small molecules were thawed and added to media right before use.

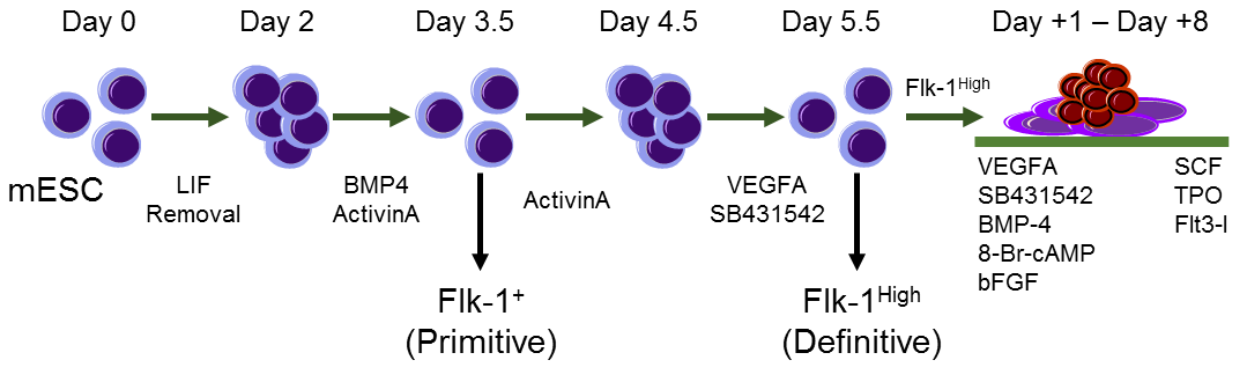

Figure 2.2. Differentiation scheme for mouse HSPC differentiation
Differentiation scheme for mouse HSPC differentiation. LIF : leukaemia inhibitory factor; BMP4: Bone morphogenic protein 4; VEGFA: Vascular Endothelial Growth Factor A; bFGF: Fibroblast growth factor, basic; SCF: Stem Cell Factor; TPO: Thrombopoietin; Flt3-l: Flt3 ligand. $FLK1^{High}$ cells are sorted and replated at Day 5.5 timepoint. Following this, timepoints are written as Day + X to depict days after sorting.

2.3.1.1. Days -1 – 3.5 EB Formation and Mesodermal Specification

24 hours prior to differentiation (D-1), mESCs were passaged as described in 2.2.2.1, using IMDM mESC maintenance medium instead of regular mESC maintenance medium in order to condition cells to IMDM.

On the day of differentiation (D0), mESC were detached from the well as described in section 2.2.2.1. 100,000 to 500,000 (cell line and batch dependent; titrated roughly every two years) mESC were seeded onto a 10-cm petri dish or equivalent 10-cm dish of non-adherent plastic in 10 ml of SFD 88 µg/ml AA.

Embryoid body (EB) formation was observed as early as D2, at which point cells express blastocyst marker gene *Fgf5* (data not shown). 48 hours following seeding, mesodermal differentiation was induced by addition of BMP4 (8 ng/ml) and ActA (2 ng/ml).

36 hours later (D3.5), EBs were collected into 50 ml Falcon tubes and spun down at 200 x G for 1 minute. Petri dishes were washed with PBS to collect remaining EBs and added to same Falcon tube for a PBS wash of EBs and spun down once more at 200 x G for 1 minute. EBs were then disaggregated using TrypLE Select (ThermoFisher) at 37°C for 3 to 4 minutes. TrypLE was quenched using FACS buffer. Cells were then either used for follow-up assays, or replated to continue differentiation.

Cells were replated in SFD with AA (88 µg/ml) and ActA (3 ng/ml) at a concentration of 500,000 cells per ml in 24-well, ultra-low attachment plates (*Corning 3473*).

2.3.1.2. Days 4.5 – 5.5 HE Specification

24 hours later (D4.5), $VEGFA_{165}$ (5 ng/ml [low] or 50ng/ml [high]) and SB (6 µM) were added to the culture as gently as possible to avoid disruption of re-aggregated clusters. For D4.5 follow-up assays, clusters were collected and dissociated as described above for D3.5 EBs.

24 hours later (D5.5), clusters were collected into Falcon tubes containing PBS/DNAse and spun at 200 x G for 1 minute. Cell clusters were then dissociated using TrypLE at 37°C for 3 – 4 minutes and quenched with FACS Buffer with DNAse. Cells were then stained for follow-up assays and sorting of Flk-1^{High}/PDGFRα^{-} HE as described in section 2.4.

2.3.1.3. Days 5.5 – 5.5+6 EHT Culture

On D5.5, prior to cluster collection, 24-well tissue-culture treated plates were coated with Matrigel solution and let sit at room temperature for 2 to 3 hours. Following cluster collection and dissociation, described above, and flow assisted cell sorting (FACS) of Flk-1^{High}/PDGFRα^{-} HE, cells were plated onto Matrigel-coated plates at 75,000 cells per well in 1 ml of HED medium with either VEGFA [low] (5 ng/ml) or VEGFA[high] (50 ng/ml).

Media changes were done every other day, at timepoints D+2, D+4, and D+6. HED medium was prepared fresh and added to wells after removal of old medium. For D+4 and D+6, supernatant was collected and spun down at 200 x G for 5 minutes and pellet resuspended in HED and replated onto well to avoid loss of floating hematopoietic progenitors.

For cell collection at these timepoints, supernatant was collected, and adherent cells detached using TrypLE at 37°C for 6 -7 minutes. TrypLE was quenched using FACS buffer, and cells counted and used for follow-up assays. If cells were cultured beyond six days of re-plating, media changes and cell collection continued to be done in the same fashion.

2.3.2. Human HSPC Differentiation

Protocol for h-iPSCs into HSPCs was originally developed in-house and patented under patent number WO2015050963 A1 (Figure 2.3). Patent license was purchased by StemCell™ Technologies Inc. and further developed into commercially available STEMdiff™ Hematopoietic Kit (StemCell Tech).

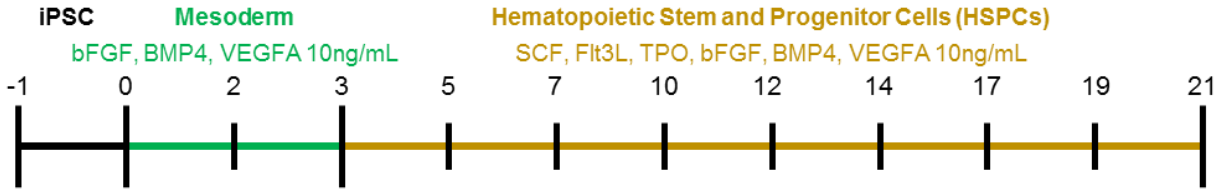

Figure 2.3. Differentiation scheme for h-iPSCs into HSPCs
Two separate phases for mesodermal and haematopoietic development, along with cytokines added to culture. bFGF: Fibroblast growth factor, basic; BMP4: Bone morphogenic protein 4; VEGFA: Vascular Endothelial Growth Factor A; SCF: Stem Cell Factor; Flt3L: Flt3 ligand; TPO: Thrombopoietin.

2.3.2.1. Days -1 – 3.5 Cluster Formation and Mesodermal Specification

24 hours prior to start of differentiation (D-1), cells were detached and passaged as described in section 2.2.4.3. However, because cluster number and confluence are critical for healthy differentiation of human iPSCs, 2 µl each of detached clusters were added to three wells of a 96-well, flat bottomed plate containing 50 µl of iPSC medium. Medium to large sized clusters (>20 cells) were then counted in each well to obtain a cluster count per µl.

~35 clusters each were then plated into wells of a 24-well plate with h-iPSC maintenance medium that had been previously prepared with Matrigel solution as described in section 2.2.4.3.

The following day (D0) and prior to differentiation, wells that were either underconfluent (<10 adherent clusters) or overconfluent (>50 adherent clusters) were discarded. h-iPSC maintenance medium was removed and 1 ml of Hemato A medium added to wells.

A half medium change was done 48 hours after Hemato A addition. For half media changes, fresh Hemato A was left in the tissue culture hood to reach room temperature. Old medium was then collected into a 50 ml Falcon Tube and pooled for all technical replicates. 500 µl of fresh Hemato A medium were added to the wells, followed by 500 µl of old medium. This assured an exact half medium change that accounted for evaporation of medium.

For mesodermal patterning experiments, CHIR and SB were added to fresh Hemato A medium prior to media change at a concentration of 6 µM (2X). Equal volumes of DMSO vehicle control were added to control Hemato A medium. Half medium change was then done as described above.

2.3.2.2. Days 3.5 – 21 Hematopoietic Specification and Culture

30 to 36 hours after D2 Hemato A half medium change (D3.5), Hemato A medium was removed and discarded. 1 ml of room temperature Hemato B was then added to wells.

Half medium changes, done in the same way as for D2 Hemato A medium change, were done with Hemato B at D5, D7, D10, D12, D14, D17, and D19, at which points cells were also collected. Cells were also collected at D21.

2.3.2.3. High VEGFA treatment

For high VEGFA treatment cultures, VEGFA was added to Hemato A and B before full and half media changes to bring concentration of VEGFA in medium to 200 ng/ml

2.3.2.4. Sample Collection and Preparation

On collection days mentioned above, supernatant for wells to be collected was removed and placed into 50 ml Falcon Tube. Wells were then washed once with 1 ml of PBS that was also transferred into the same 50 ml Falcon Tube. 500 µl of Accutase™ (StemCell Tech) were added to each well and incubated at 37°C for 10 minutes.

Wells were then pipetted up and down to ensure dissociation of all clusters from bottom of well. At later differentiation days, clusters will detach from bottom of the well but will not dissociate. Accutase solution was transferred to 50 ml tube containing sample supernatant, and wells washed with 1 ml of FACS buffer each to detach remaining cells.

50 ml solution in tube was once again pipetted up and down vigorously with a 1000 ml pipette in order to dissociate clusters as much as possible. 5 – 10 ml of FACS buffer were then added to solution to dilute out remaining active Accutase.

Cell solution was strained using 40 µm cell strainer (Corning). Cells were then spun down at 300 x G for 5 minutes and resuspended in 1 – 2 ml of FACS buffer for counting and processing for further assays.

2.4. Flow Cytometry and Flow Assisted Cell Sorting (FACS)

2.4.1. Analyzers and Sorters

All flow cytometry data were collected using BD LSRFortessa™ and BD LSRFortessa™ X-20 machines, calibrated on a daily basis. All flow assisted cell sorting (FACS) was done using BD FACSAria™ II or BD FACSAria™ Fusion machines, also calibrated on a daily basis. Differentiating mESC were sorted using 70 µm and 85 µm nozzles, while differentiating h-iPSCs were sorted using 100 µm nozzles.

All machines were controlled using BD FACSDiva™ software. Data was analysed using FlowJo software.

2.4.2. Sample Preparation and Staining

Single cell suspensions of 5 x 10^5 to 1 x 10^6 were resuspended in 100 µl of FACS buffer and stained using antibodies and test amounts listed in Table 2.3. Test volumes of antibodies were used even when fewer cells were available per sample. Cells were stained for 15 minutes at 4°C protected from light. Cells were then washed with 1 ml FACS buffer and centrifuged at 300 x G for 5 minutes.

Cells were then resuspended in 500 µl of FACS buffer and placed in appropriate 5 ml tubes for flow cytometry analysis. Where appropriate and needed, 5 µl of 7-AAD viability dye were added to the samples.

For stains with unclear gating populations and potential non-specific staining of haematopoietic progenitors expressing Fc Receptor (CD16/32), an Fc receptor blocking antibody was added to sample 10 minutes prior to staining.

2.4.3. Fluorescence Minus One, Isotype, and Single Stain Controls

When an experiment layout and stain were first being prepared, single stain controls were prepared using both cell samples as well as compensation beads: BD™ CompBeads Plus for mouse anti-human panels; BD™ CompBeads for rat anti-mouse panels. Single stain and unstained controls from cells were first used to adjust PMT voltages on channels. Single stain controls from beads were then used to fine-tune PMT voltages and avoid high spill-over and therefore, compensation needed. For subsequent experiments, either single stain controls from cells or beads were used to calculate compensations, depending on cell numbers available.

Compensation values calculated by FACSDiva software on analysis experiments were manually checked and adjusted using single stain controls post-hoc on FlowJo software.

Where gating of populations is not obvious given clear segregation of populations, different controls, such as fluorescence minus one (FMO), stained biologically negative controls, or isotype controls have been shown to be appropriate depending on experimental context (Maecker and Trotter 2006). For the purposes of this thesis, FMO controls were used throughout, except where biologically relevant negative controls were available. In one instance, two seemingly separate, but potentially negative populations with differing levels of autofluorescence prompted the use of FMO plus isotype controls to confirm negativity (Supplementary Figure 4.1). In one set of figures, a separate antibody (for which the population of interest was negative) conjugated to the same fluorophore as the antibody of interest was used as a substitute for an isotype or

biological negative control (Supplementary Figure 3.1). This technique for the use of an internal negative control to set gates was suggested by the Flow Cytometry expert that trained the PhD candidate in sorting techniques. In retrospect upon preparation of this thesis, it is clear that an isotype or FMO control would have served this same purpose in a way more commonly accepted by the Flow Cytometry community and in line with what is published by the haematology and developmental biology communities.

When stable signal value was required over the course of many days for comparable gate setting, Sphero™ Rainbow beads were used to track their MFI across experiment days to detect and correct potential laser drift.

2.4.4. Antibody Titration for Cell Sorting

Because a high number of cells was used for sorting experiments, a test was re-defined as 1 x 10^7 cells in 100 µl and antibody concentrations re-titrated to avoid over-staining as well as conserve antibody.

For mESC sorting experiments, Flk-1 PE, PDGFRα APC, and CD41 BV605 were all adjusted to an optimal concentration of 4 µl per test.

For h-iPSC sorting experiments, all antibodies were kept at same concentrations as listed in Table 2.3.

2.4.5. Intracellular staining

Cells were stained with fixable Live/Dead stain (ThermoFisher) at 4°C for 30 minutes following kit instructions. Cells were then washed with FACS buffer and centrifuged for 5 minutes at 300 X G.

Cell pellets were resuspended in 100 µl of FACS buffer and stained with cell surface markers as required, following protocol described in 2.4.2. Following this, stained cells were once more resuspended in 100 µl of FACS buffer. 100 µl of 4% paraformaldehyde (PAF) solution (EM Sciences) were added to the cells for a final solution of 2% PAF. Cells were fixed in PAF solution for 10 minutes at 4°C. Cells were washed and centrifuged as described previously.

Cells were resuspended in 100 µl of 0.1% triton X100 (Sigma) for ten minutes at 4°C to permeabilize cells.

SCL antibody was conjugated to AF488 fluorochrome using Zenon™ Alexa Fluor™ 488 Goat IgG Labeling Kit (ThermoFisher) following kit instructions. Briefly, 5 µl of antibody were added to 10 µl of conjugating component A for 5 minutes at room temperature, protected from light. This was followed by an additional 10 µl of blocking component B, incubated for 5 minutes at room temperature protected from light.

Following permeabilization, cells were washed and centrifuged as described above. Cells were then resuspended in 100 µl FACS buffer and incubated for 30 minutes at room temperature and protected from light. Cells were then washed, resuspended, and analysed in the same manner of standard flow cytometry samples.

2.5. Colony Forming Unit (CFU) Assay

2.5.1. Mouse CFU Assays

Mouse CFU assays (StemCell Tech) were run as per manufacturer's instructions. Briefly, 3000 total cells collected were suspended in 300 uL of DMEM with 2% FBS,

which was then added to the methocult tube and vortexed. Following 5 minutes to allow for bubble dissipation, 1.1 ml of the medium was plated onto 35 x 10 mm style tissue-culture dishes (Corning) for 1000 cells. Colonies were scored 9 to 11 days following plating.

2.5.2. Human CFU Assays

Human CFU assays (StemCell Tech) were run as per manufacturer's instructions, briefly described above. However, 9000 total sorted HSPCs were plated for 3000 cells per plate in control conditions, and 4500 total HSPCs plated for 1500 cells per plate in CHIR/SB treated samples.

2.6. Mouse Transplantation Assays

2.6.1. Mouse Strains

NOD-*Scid*-IL2rγ^{null} (NSG) immune-compromised mice were purchased from JAX® mouse laboratories and transported directly to NIH Animal Care Facility. Animals were housed and handled by trained facility personnel in accordance with the guidelines set by the Committee on Care and Use of Laboratory Animals of the Institute of Laboratory Animal Resources, National Research Council (DHHS publication No. NIH 85-23), and the protocol was approved by the Animal Care and Use Committee of the National Heart, Lung, and Blood Institute.

2.6.2. Irradiation and Transplantation

Mice (6- to 12-week old females) were sub-lethally irradiated with 270 rads early in the morning on the day of transplantation. Mice were transplanted by tail-vein

injections with sorted HSPCs ($CD45^+$, $CD43^+$, and $CD43^+CD45^+$) derived from D10 and D12 h-iPSC differentiation cultures. Two technical replicates per timepoint per differentiation were transplanted with total numbers of HSPCs collected at timepoint.

For mice transplanted with cells treated with high VEGFA, $CD34^{High}CD43^-CD45^-$ vascular endothelium was transplanted along with HSPCs.

2.6.3. Animal Euthanasia and Sample Collection

Animals were euthanized by CO_2 inhalation followed by cervical dislocation.

At least 12 weeks post-transplantation, bone marrow cells were collected by flushing mouse femurs, tibias and pelvic bones using X-Vivo Hematopoietic Medium (Lonza) containing PenStrep (1X). Cells were collected into appropriate tubes and pipetted up and down using P1000 pipettes in order to achieve full resuspension.

Cells were then filtered using 40 µM filter and centrifuged at 300 x G for 10 minutes. Pelleted cells were resuspended in ACK lysis buffer (Quality Biological) for 10 minutes at room temperature. Buffer was diluted using X-Vivo/Penstrep medium and once more centrifuged at 300 x G for 10 minutes.

Cells were resuspended in FACS buffer and counted. Cells were stained with human CD45 antibody as described in section 2.4.2. and analyzed for human cell engraftment.

2.7. RNA Preparation and Analysis

2.7.1. Standard RNA Collection and Processing

RNA for cells of interest was collected using the directions of RNAeasy Micro Kit (Qiagen). Carrier poly-A RNA was added to lysed samples of 100,000 cells or fewer.

2.7.2. Reverse Transcription and RT-qPCR

Reverse transcription (RT) and real-time, quantitative PCR (RT-qPCR) were done using TaqMan™ RNA-to_Ct 1-Step kit (AB) on AB Real-time 7500 or BioRad CFX 96 Real-time systems with probes and primers listed in Table 2.5. Reactions were duplexed to include primers and probes for the gene of interest and a housekeeping gene. Unless otherwise noted, the reference gene used for all experiments, both mouse and human, was *GAPDH*.

2.8. Data Analysis and Statistics

2.8.1. Flow Cytometry

Flow cytometry data were analysed and representative plots created using FlowJo software. Both mouse and human cells were first discriminated on basis of forward and side-scatter properties to remove debris and apoptotic cells, followed by forward scatter height and forward scatter width properties to discriminate doublets from the events analysed. Finally, if a live-dead stain and/or lineage stain were

included in the panel, live and lineage negative (where appropriate) cells were gated before moving on to further analysis.

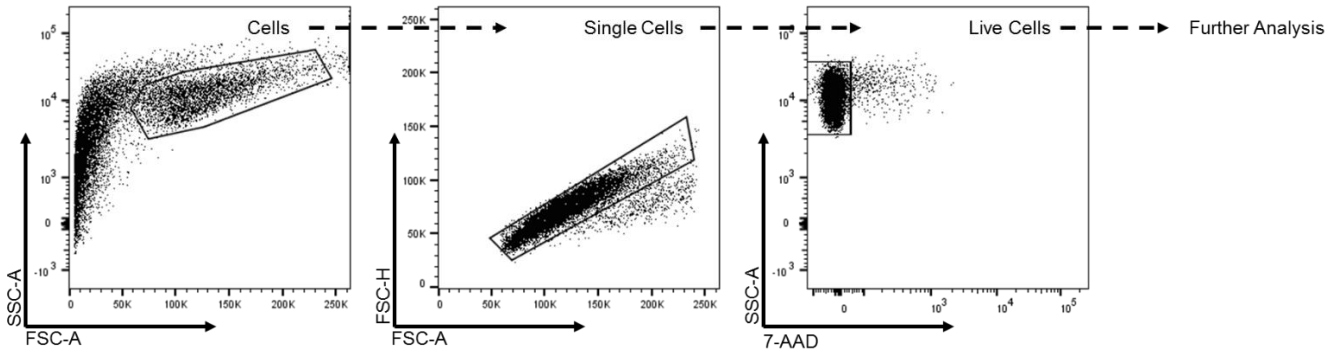

Figure 2.4 Representative plot of flow cytometry pre-gating for further analysis on all samples collected
Representative flow cytometry plots for h-iPSCs cells at Day 10 of differentiation are here used as an example of the pre-gating that took place for all samples (mouse and human) at all timepoints. Cells were first discriminated on the basis of forward and side scatter properties to capture cell populations. Cells were then further discriminated on the basis of height and area properties of the forward scatter signal to capture data on single cells and exclude doublets. Finally, cells were stained with either Hoechst viability dye or 7-AAD, or a fixable live/dead stain for intracellular flow cytometry protocols, to capture live cells and exclude dead cells from further analysis.

Percentages were calculated using FlowJo. Unless otherwise noted, populations are presented as percentage of total live cells analysed. Unless otherwise noted, percentages on representative figures and bar graphs are presented as averages of at least 3 biological replicates plus or minus standard deviation (SD).

Bar graphs were created and statistics calculated using Prism GraphPad software. Two-sided, unpaired t-tests were used to compare population means. Cut-off for statistical significance was a p value of < 0.05.

2.8.2. RT-qPCR

2.8.2.1. CT Thresholds and Values

Data was analysed using either AB 7500 software or Bio-Rad CFX maestro software for standard RT-qPCR and Biomark Real-time PCR Analysis for Biomark RT-qPCR data. Regardless of software, C_T thresholds were adjusted manually for individual genes and set equally across runs so that samples run on separate plates could be compared with minimal variability and error. For mouse samples, GAPDH probes with FAM for the same sample were run on a different well and used for all Gene of Interest (GOI) assays in that plate for that sample. Given sample quantity limitations for human samples, GAPDH probes with VIC fluorophore were multiplexed with GOI probes with FAM fluorophore.

Average C_T value from 2 technical replicates on plate from the same biological sample were used in calculations.

2.8.2.2. ΔC_T Calculations and 95% Confidence Interval

ΔC_T were calculated using the formula $\Delta C_{T\ GOI} - \Delta C_{T\ GAPDH}$. Average ΔC_T and SD values for at least three biological replicates were then calculated. Fold expression of gene was then calculated as $2^{\wedge-(\Delta CT)}$. Upper and lower boundaries of the 95% confidence interval were calculated as $2^{\wedge-(\Delta CT \pm SD)}$.

Bar graphs were created and statistics calculated using Prism GraphPad software. Two-sided, unpaired t-tests were used to compare linear ΔC_T values. Cut-off for statistical significance was a p value of < 0.05.

2.8.3. Multiple Sample Comparsion

Where multiple samples (whether linear ΔC_T values or percentages of populations from Flow Cytometry data) were all compared to each other, one-way ANOVA with Tukey's posthoc comparison test (Tukey 1949) was performed. In cases where it was appropriate to compare multiple samples to the control only, one-way ANOVA with Dunnett's posthoc comparison test (Dunnett 1964) was performed. Both of these tests were performed on using Prism GraphPad software. Cut-off for statistical significance was a p value of < 0.05.

2.8.4. CFU

Average of technical duplicates was used as CFU number for each of three biological replicates. Total CFU number per 100,000 cells was calculated $\frac{CFU\ Count}{Total\ Cells\ Plated} \times 100{,}000$. Bar graphs were created and statistics calculated using Prism GraphPad software.

2.8.5. Significance

Differences are considered to be statistically significant for p-values below 0.05. Following the Graph Pad p value style, p values are denoted as follows:

*	$p \leq 0.05$
**	$p \leq 0.01$
***	$p \leq 0.001$
****	$p \leq 0.0001$

3. Modelling Wave Two of Murine Haematopoiesis

3.1. Introduction

Numerous serum-free differentiation protocols supporting the production of HSPCs from mouse embryonic stem cells (mESCs) and their cellular and molecular characterisation have been previously reported (Clarke et al. 2013; Irion et al. 2010; Pearson et al. 2008; Mills et al. 2014; Chiang and Wong 2011; Pearson et al. 2015; Ng et al. 2005; Nostro et al. 2008). These protocols, to varying degrees, mimic many of the signals that cells in the embryo require to differentiate towards a mesodermal lineage, followed by commitment to a haematoendothelial and, finally, haematopoietic programme. These studies have reported the critical role that BMP4, VEGFA, and ActivinA signalling play in instructing cells towards mesodermal differentiations (Pearson et al. 2008; Irion et al. 2010; Chiang and Wong 2011; Ng et al. 2005; Nostro et al. 2008) and have titrated different combinations and timings of provision of these cytokines for optimal haematopoietic output.

Commitment of differentiating mESCs to a mesodermal fate *in vitro* is driven by BMP4 signalling (Park et al. 2004; Nostro et al. 2008; Pearson et al. 2008), and tracked through the expression of primitive streak marker gene *Brachyury* (*T*) (Gadue et al. 2006; Fehling et al. 2003). Shortly afterwards, at Day 3.25 – 3.5 in serum-free cultures, co-expression of *T* and FLK1 marks mesoderm containing BL-CFCs (Kennedy et al. 2007; Irion et al. 2010; Nostro et al. 2008). Some T^{+}FLK1^{-} cells at Day 3.25 – 3.5 express FLK1 a day later, and have vascular smooth muscle, endothelial, and cardiomyocyte differentiation potential (Kattman, Huber, and Keller 2006), suggesting heterogeneity within mesodermal populations expressing FLK1.

After Day 5.25, FLK1$^+$ cells no longer expressing mesodermal *T* can produce both definitive haematopoietic cells as well as endothelial cells (Kennedy et al. 2007; Irion et al. 2010; Nostro et al. 2008). The haematoendothelial commitment of FLK1$^+$ cells is driven mainly by VEGFA signalling (Park et al. 2004; Pearson et al. 2008), which activates downstream transcription factor *Etv2*, in turn activating the expression of haematoendothelial genes, *Fli1* and *Scl/Tal1*(Kataoka et al. 2011). SCL/TAL1 has been shown to employ both activating and repressive transcriptional mechanisms to drive cells towards a haematoendothelial fate while preventing commitment towards alternative mesodermal fates, such as cardiac (Org et al. 2015; Porcher, Chagraoui, and Kristiansen 2017; Chagraoui et al. 2018).

Following this haematoendothelial commitment step, FLK1$^+$ cells are usually sorted and plated in media with cytokines and small molecules (including BMP4, SCF,VEGFA, and TGF-β inhibitor SB431524) (Irion et al. 2010; Chiang and Wong 2011; Clarke et al. 2013) to promote HE differentiation and EHT, so that cells can give rise to HSPCs harbouring colony forming unit (CFU) potential.

Despite recent advances in the fields of developmental and stem cell biology, however, protocols have yet to be developed for the differentiation of mouse HSCs capable of reconstituting sub-lethally irradiated hosts in competitive transplantation assays. At best, studies have shown that use of VEGFA, BMP4, and ActivinA can lead to early FLK1$^+$ progenitors with long-term, but no secondary transplant, engraftment capacity (Pearson et al. 2015). Along with this lack of engraftment potential, studies have found similarities in the gene expression and immunophenotype of HSPCs arising in serum-containing systems and YS EMPs (McKinney-Freeman et al. 2012; McGrath et al. 2015; Keller et al. 1993). This

suggests improvements are needed to more closely monitor and produce the correct haematopoietic wave for producing engrafting HSCs *in vitro*.

Because of these studies, we further characterised a previously published serum-free mESC differentiation system reported to give rise to two independent waves of $FLK1^{+}$ progenitors with the capacity to differentiate into primitive and definitive haematopoietic progenitors (Irion et al. 2010) (Figure 3.1a). Given that the objectives of this thesis were to design protocols for the recapitulation of third-wave haematopoiesis, we reasoned that further characterisation of an existing two-wave protocol would allow for modifications to generate third-wave HSPCs.

3.2. Late-stage FLK1$^+$ haematoendothelial precursors lack *Brachyury* and PDGFRα expression

A previously published *Brachyury-GFP* (T-GFP) transgenic ESC line (Fehling et al. 2003) was used to trace the development of mesodermal cells during differentiation. *Brachyury* is expressed in developing primitive streak cells (Arnold and Robertson 2009), and is commonly used to track mesodermal specification of differentiating cells (Irion et al. 2010; Gadue et al. 2006; Fehling et al. 2003). Unlike previous serum-free *in vitro* studies however, cells were further characterised based on expression of cell-surface marker platelet derived growth factor receptor alpha (PDGFRα), another well characterised mesodermal marker that originally labels all FLK1$^+$ cells and later distinguishes PDGFRα$^+$ paraxial and cardiac mesoderm from FLK1$^+$PDGFRα$^-$ haematoendothelial mesoderm (Kataoka et al. 1997).

At early Day 3.5 of culture, all FLK1$^+$ cells are positive for PDGFRα, confirming what has been described both *in vivo* (Kataoka et al. 1997) as well as *in vitro* serum-based systems (Sakurai et al. 2006). FLK1$^+$PDGFRα$^+$ cells comprise 23.3 ± 5.2% of differentiating cells at this stage of culture (Figure 3.1b, panel one). As early mesodermal progenitors, these cells have also been shown in serum differentiation conditions to have the potential to differentiate into FLK1$^-$PDGFRα$^+$ paraxial mesodermal cells or FLK1$^+$PDGFRα$^-$ haematoendothelial cells (Sakurai et al. 2006). All FLK1$^+$ cells at this stage were also observed to be T-GFP$^+$ (Figure 3.1c, panel one), confirming previously published results (Irion et al. 2010; Nostro et al. 2008) as well as the cells' early mesodermal identity. In previous studies, this population has been reported as containing BL-CFCs that give rise to erythroid cells expressing mostly embryonic globins, marking them as progenitors with

primitive haematopoietic potential (Irion et al. 2010; Nostro et al. 2008; Kennedy et al. 2007).

At Day 4.5, a higher percentage of cells (40.4 ± 8.6%) expresses FLK1 and PDGFRα, though at lower levels than at Day 3.5 (Figure 3.1b, panel two). By this stage, cells have begun to downregulate GFP expression, as is expected from cells differentiating beyond a mesodermal progenitor stage. At this timepoint, only 13.5 ± 2.7% of the total culture is co-expressing FLK1 and GFP (Figure 3.1c, panel two). It bears noting that at this stage, this FLK1 fraction is very likely heterogeneous and contains $FLK1^{+}$ cells which were $FLK1^{+}$ at Day 3.5 and therefore contain primitive haematopoietic potential (Irion et al. 2010; Kattman, Huber, and Keller 2006), as well as $FLK1^{+}$ cells arising from $FLK1^{-}$ cells at Day 3.5, which have been described as having cardiomyocyte, endothelial, and vascular smooth muscle potential (Kattman, Huber, and Keller 2006).

At Day 5.5, the appearance of a $FLK1^{+}PDGFR\alpha^{-}$ population was observed. This downregulation of PDGFRα has been previously reported to correspond to commitment to a haematoendothelial lineage (Sakurai et al. 2006; Kataoka et al. 2011). Interestingly, this population also expresses higher FLK1 levels than a remaining $FLK1^{+}PDGFR\alpha^{+}$ population (Figure 3.1b, panel three). Given this, the population was labelled as $FLK1^{High}$ and will be referred to as such for the remainder of the text. These cells, which comprised 5.4 ± 1.4% of the total culture, were also GFP^{-}, as were most cells at this timepoint (Figure 3.1c, panel three). Previous studies have shown these Day 5.5 $T^{-}FLK1^{+}$ cells, when differentiated from purified Day 3.5 $FLK1^{-}$ cells, give rise to HSPCs that resemble *in vivo* definitive progenitors (Irion et al. 2010; Clarke et al. 2013; Clarke et al. 2015)(Figure 3.1a). Because $FLK1^{High}$ cells are $PDGFR\alpha^{-}$, it is unlikely that this population contains the

FLK1^{+} cardiomyocyte and vascular smooth muscle progenitors arising in culture at Day 4.5. However, given that Day 3.5 FLK1^{+} cells were not sorted out of the culture, this Day 5.5 FLK1^{High} population may also contain primitive BL-CFCs.

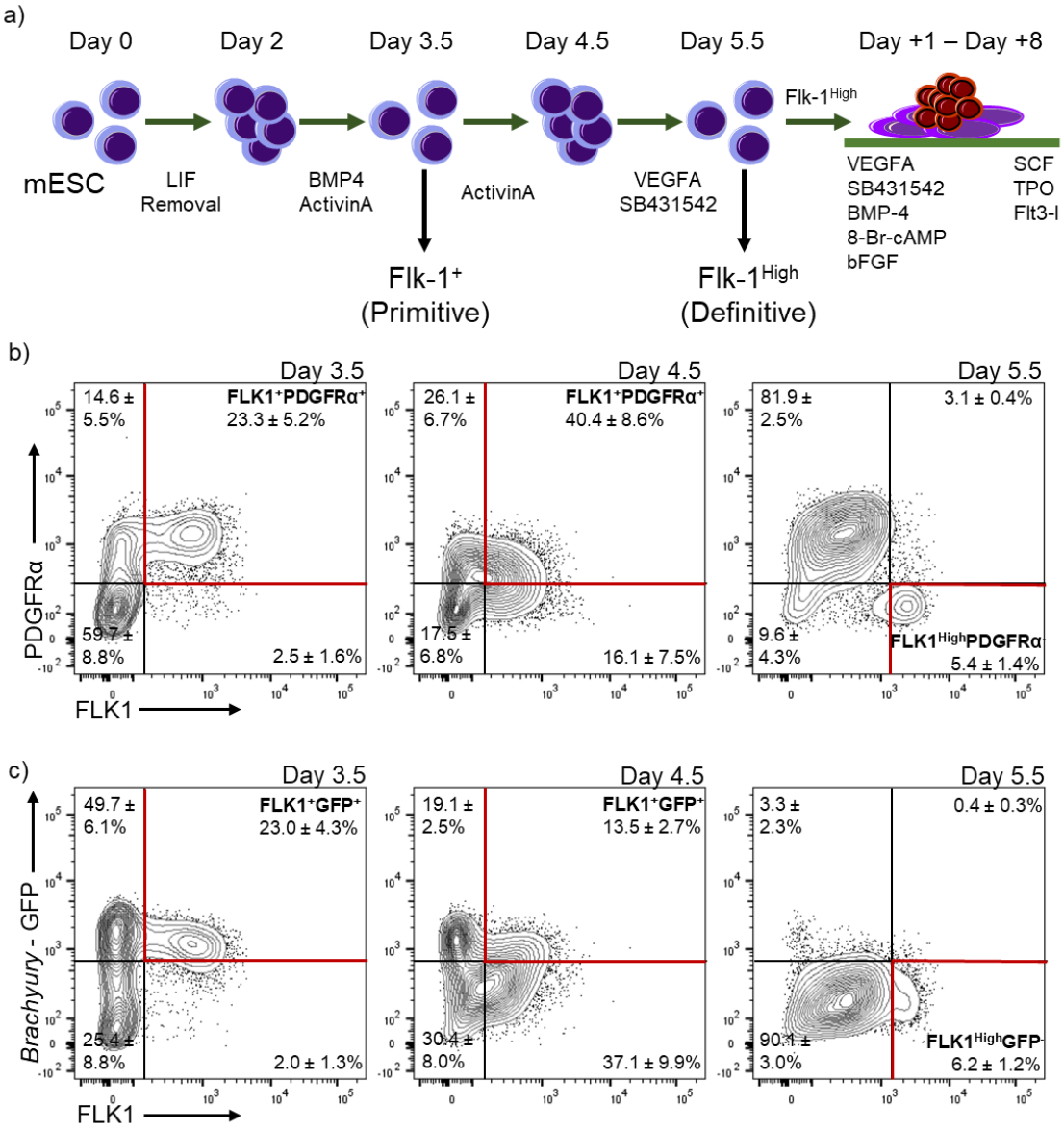

Figure 3.1 Characterisation of Two-Wave System
a) Differentiation scheme for mouse embryonic cells. b-c) Flow cytometry plots gated on single, live cells, depicting expression of PDGFRα, FLK1, and GFP expression in transgenic T-GFP mESCs at days 3.5, 4.5, and 5.5 of differentiation. n = 3 biological replicates (independent differentiations using same mESC line). Averages +/- SD are depicted. Red quadrants represent populations of interest for the purpose of this thesis. For general information regarding flow cytometry controls and gating used in this thesis, see sections 2.4.3 and 2.8.1, respectively.

3.3. FLK1^{High} cells express a Haematoendothelial Phenotype

It has been previously reported that Day 3.5 FLK1^{+} cells give rise to primitive, first-wave haematopoiesis (Irion et al. 2010), Day 4.5 FLK1^{+} cells to cardiac progenitors (Kattman, Huber, and Keller 2006), and Day 5.5 FLK1^{+} cells to definitive HSPCs resembling Wave 2 HSPCs (Irion et al. 2010; Clarke et al. 2013; Clarke et al. 2015). Because of their potential for definitive haematopoiesis, FLK1^{High} cells were further characterised using the J1 wild-type mESC line (Materials and Methods section 2.2.2).

At Day 5.5, cells of this mESC line gave rise to higher percentages of FLK1^{High} cells: 17.1 ± 9.8% (Figure 3.2a, panel one) compared to 5.4 ± 1.4% in T-GFP mESCs (Figure 3.1b, panel three). This suggests a heterogeneity among lines that continued to be observed throughout the course of this thesis. Preliminary data early in the course of this thesis showed that initial cell plating numbers affected both percentage of Day 3.5 FLK1^{+} cells and Day 5.5 FLK1^{High} cells (data not shown due to n = 1 biological replicate for each of four mESC lines). Because of this, it is recommended that replicate studies with different cell lines titrate starting cell numbers to achieve optimal FLK1 cell percentages for desired assays (For more detailed protocols see Materials and Methods section 2.3.1.1).

While the population corresponding to our Day 5.5 FLK1^{High} cells has been described as mesodermal progenitors in need of two to three days of further *in vitro* specification in haematopoietic and endothelial cytokines, such as BMP4, SCF, and FLT3-L, to specify into HE (Irion et al. 2010), flow cytometry analysis of cell surface markers showed that FLK1^{High} cells nearly homogeneously express VE-Cad and cKIT, and lack CD41 expression (Figure 3.2.a), an immunophenotype that has been previously been used, alongside functional studies, to characterise HE

in vitro (Eilken, Nishikawa, and Schroeder 2009; Frame et al. 2016; Lancrin et al. 2009; Lie-A-Ling et al. 2018).

Day 5.5 FLK1^{High} cells also express significantly higher levels, when compared to Day 3.5 FLK1^{+} cells, of *Sox17* and *Notch1*, endothelial genes previously reported to be associated with definitive haematopoiesis (Kumano et al. 2003; Hadland et al. 2004; Clarke et al. 2013) (Figure 3.2b). They also express haematoendothelial TFs *Scl/Tal1* and *Gata2,* and HE TF *Runx1* (Figure 3.2c), further characterizing the population as potentially containing functional HE, as opposed to mesodermal precursors in further need of specification. The fact that FLK1^{High} cells express *Sox17* at such high levels compared to Day 3.5 FLK1^{+} cells is in line with previous studies which used a *Sox17* reporter line to describe the subpopulation of Day 5.5 FLK1^{+} cells giving rise to definitive HSPCs as FLK1^{+}*Sox17*$^{+}$, and as expressing endothelial VE-Cad and CD31 but not haematopoietic CD41 (Irion et al. 2010; Clarke et al. 2013).

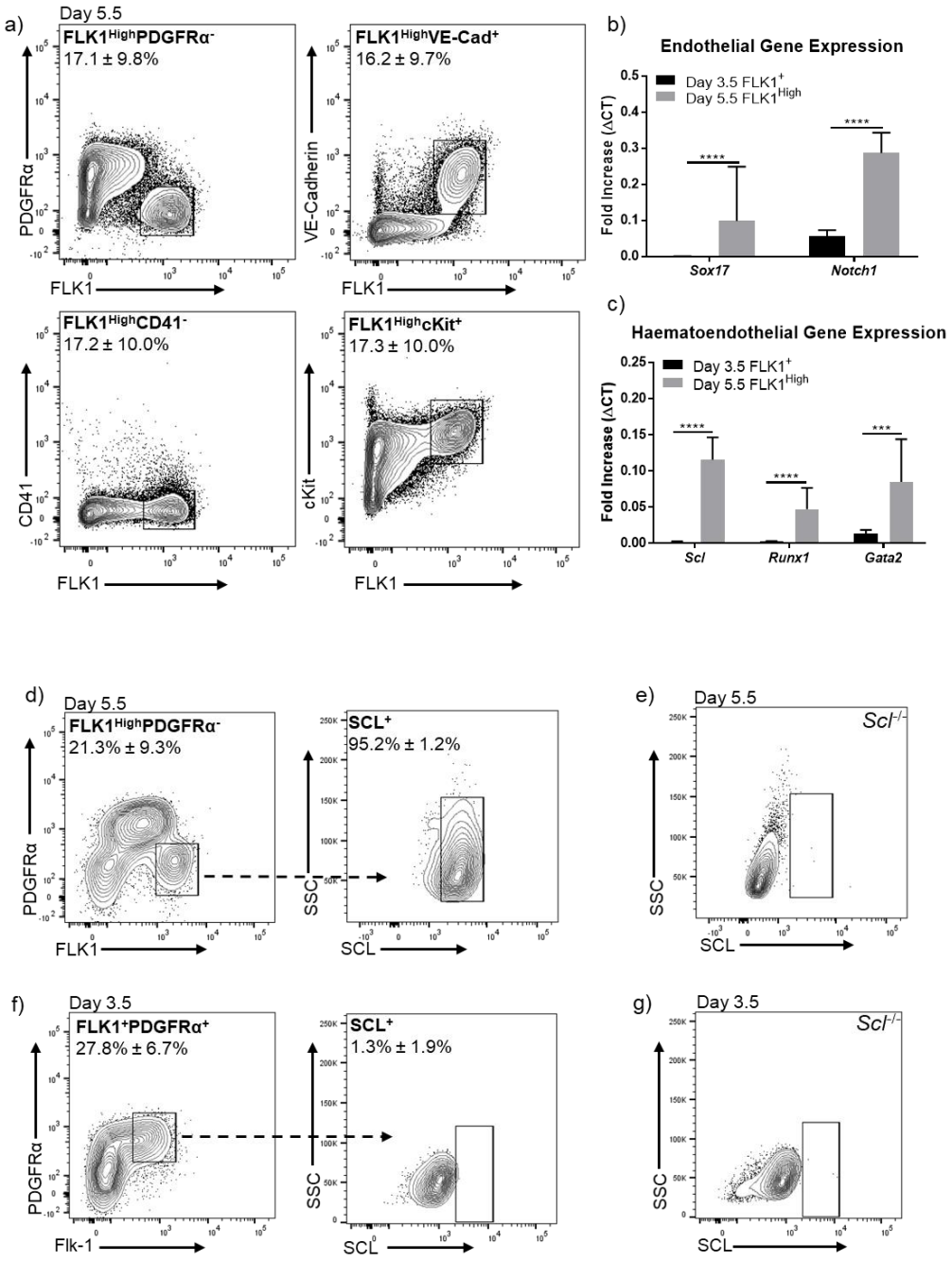

Figure 3.2. Day 5.5 FLK1^{High} cells present a Hematoendothelial Phenotype
a) Representative flow cytometry plots for J1 expression of FLK1, PDGFRα, VE-Cad, CD41, cKIT at Day 5.5. n = 3 biological replicates. Averages ± SD depicted. b-c) Gene expression of endothelial and haematoendothelial genes in sorted Day 3.5 FLK1^{+} and Day 5.5 FLK1^{High} cells by RT-qPCR. n = 4 biological replicates. Two-tailed, unpaired t-test on untransformed ΔCT values. d) Representative flow cytometry plot for intracellular expression of SCL/TAL1 in Day 5.5 FLK1^{High}PDGFRα^{-} cells. n = 4 biological replicates. Averages ± SD depicted. e) Representative intracellular flow cytometry plot of SCL/TAL1 expression in mESC-derived Day 5.5 *Scl*$^{-/-}$ cells, used as a control, in lieu of an isotype control, to set the gate in (d, right panel). f) Representative flow cytometry plot for intracellular expression of SCL/TAL1 in Day 3.5 FLK1^{+}PDGFRα^{+} cells. n = 3 biological replicates. Averages ± SD depicted. g) As in e) representative flow cytometry plot of SCL/TAL1 expression of Day 3.5 mESC-derived Day 3.5 *Scl*$^{-/-}$ cells, used to set the gate in (f, right panel).

Intracellular flow cytometry analysis confirmed near homogeneous expression of the haematoendothelial TF SCL/TAL1 in Day 5.5 FLK1^{High} cells at the protein level (Figure 3.2d-e) and lack of expression in Day 3.5 FLK1^{+} cells (Figure 3.2f-g). In this context, and given the interest of the Porcher lab in the function of SCL in haematopoietic development, we reasoned that (i) expression of SCL could serve as a marker to lineage-trace the origin of the Day 5.5 FLK1^{High} cells (see below Section 3.4) and (ii) an SCL reporter line would be useful to be able to isolate SCL-expressing cells and perform molecular studies in future experiments. For these reasons, an *Scl:mCherry* reporter line was developed in collaboration with other members of the lab by inserting *mCherry* into the 3'UTR of one of the *Scl* alleles, downstream of a self-cleaving T2A sequence, thus generating a heterozygous *Scl:mCherry* mESC line (Materials and Methods, Figure 2.1a, Chagraoui et al. 2018). The initial validation of the *Scl:mCherry* cell line was performed in serum-containing differentiation systems. This showed an *in vitro* differentiation capacity very similar to that of the WT parent ES line and expression of *Scl* mRNA and SCL protein exclusively in the mCherry+ fraction (Chagraoui et al. 2018). Characterisation of this line using the serum-free system described above also showed that the *Scl:mCherry* cells differentiated in a fashion similar to the WT parental line, with 13.3 ± 9.5% FLK1^{+}PDGFRα^{+} cells present at Day 3.5 (Figure 3.3b, top row, left plot), compared to 14.7 ± 9.8% in WT cells (Figure 3.3a, top row, left plot). At Day 4.5, these percentages ranged from 29.0% to 37.1% in *Scl:mCherry* cells (Figure 3.3b, middle row, left plot), compared to 36.1 ± 6.4% (Figure 3.3a, middle row, left plot). Higher percentages of FLK1^{High}PDGFRα^{-} cells were observed in *Scl:mCherry* cultures (42.2 ± 9.7% compared to 17.5 ± 1.4% in WT; Figure 3.3 a-b, bottom row, left plot). Given that

no differences were observed in further differentiations at this same timepoint (See below Section 3.4), this difference was likely due to variability and was therefore not explored further. Characterisation with this cell line also confirmed expression of *Scl* (94.3 ± 1.4%) in FLK1^{High} cells (Figure 3.3b, bottom row, right plot), and verified that *Scl* is not expressed in FLK1^{+} cells at Day 3.5. While no mCherry expression was detected at Day 4.5, RT-qPCR analysis of *Scl* or intracellular SCL staining is required to definitively confirm lack of *Scl* expression in FLK1^{+} cells at this timepoint.

Characterising a cellular population purely immunophenotypically has its limits, particularly given the fact that many of these haematoendothelial markers and TFs are expressed in endothelial, HE, and early haematopoietic populations in the developing embryo at varying developmental timepoints. To further study this population of haematoendothelial cells within a developmental context, further characterisation was required to test HE functionality as well as to determine which *in vivo* haematopoietic wave it most closely resembled.

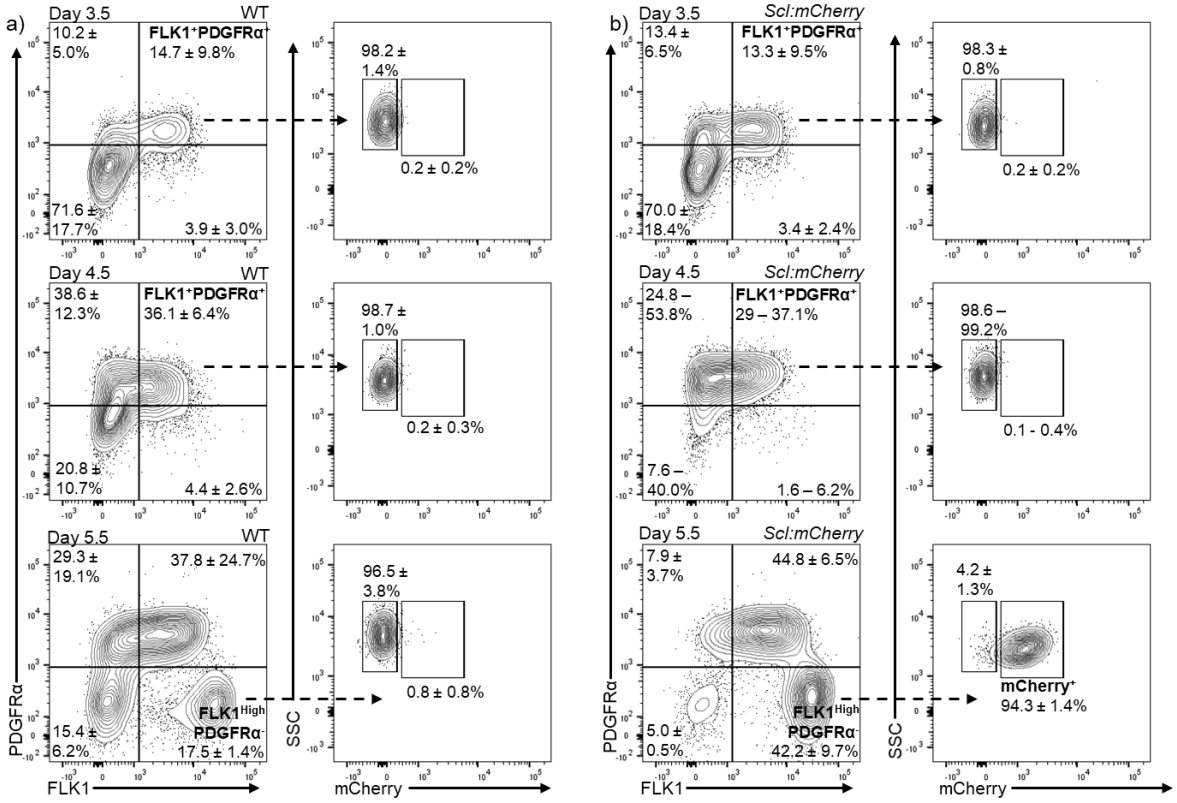

Figure 3.3 *Scl* expression using *Scl:mCherry* mESCs
a) Representative flow cytometry plots showing expression of FLK1 and PDGFRα in Day 3.5, 4.5, and 5.5 WT EBs (left panels), as well as autofluorescence in the mCherry channel of FLK1$^+$ populations of interest (right panels) used to set gates in the right panels of b. n = 3 biological replicates. Averages ± SD depicted. b) Representative flow cytometry plots showing expression of FLK1 and PDGFRα in Day 3.5, 4.5, and 5.5 *Scl:mCherry* EBs (left panels), as well as mCherry expression in the FLK1$^+$ populations of interest at these same days (right). n = 3 biological replicates for Days 3.5 and 5.5, and n = 2 biological replicates for Day 4.5. Averages ± SD depicted for Days 3.5 and 5.5 and ranges of values for Day 4.5 due to an n of 2.

3.4. Day 3.5 FLK1^{+} and FLK1^{-} Cells Equally Contribute to Day 5.5 FLK1^{High} Population

In vivo, early mesoderm spatially separates into YS and intraembryonic tissues during primitive streak formation; in *Xenopus*, the independent progenitors that will give rise to these distinct tissues can be traced as early as prior to gastrulation (Ciau-Uitz, Walmsley, and Patient 2000). Similarly, mesodermal progenitors of mouse YS Waves 1 and 2 specify prior to primitive streak formation (Padrón-Barthe et al. 2014). Unfortunately, missing spatial cues and architecture *in vitro* make mapping of these distinct tissues, and therefore, distinct haematopoietic waves, difficult.

Despite this, previous studies have shown that, when Day 3.5 FLK1^{+} cells are sorted and replated, they preferentially give rise to primitive, first-wave haematopoietic cells (Irion et al. 2010). Day 3.5 FLK1^{-} cells on the other hand, when purified and re-aggregated, generate FLK1^{+} cells *de novo* at Days 4.5 and 5.5, which give rise to cardiomyocyte, vascular smooth muscle, and endothelial progenitors (Kattman, Huber, and Keller 2006), and definitive haematopoietic progenitors (Irion et al. 2010; Clarke et al. 2013; Clarke et al. 2015), respectively. However, later studies showed that, while Day 3.5 FLK1^{+} cells do not originally express *Sox17*, similar to our own findings, they do express it 24 hours following re-aggregation, and can produce erythroid colonies whose globin expression marks them as EMP-like (Clarke et al. 2015). While haematopoietic progenitors derived from Day 5.5 FLK1^{+} cells give rise to definitive HPCs in a Notch-dependent manner, similar to Wave 3 haematopoiesis, studies with a *Sox-17*$^{-/-}$ mESC line revealed the persistence of Notch-independent, EMP-like progenitors arising from Day 5.5 FLK1^{+} cells as well (Clarke et al. 2015). This study suggests that while Day

3.5 FLK1^{+} and Day 5.5 FLK1^{+} cells might have the potential to produce HPCs resembling Waves 1 and 3 respectively, they also both share the potential to produce HPCs resembling Wave 2 EMPs.

In order to more closely study the relationship of Day 3.5 FLK1^{+} and FLK1^{-} cells with Day 5.5 FLK1^{High} cells, population-tracing experiments were designed to track the cellular origin of FLK1^{High} cells in Day 5.5 EBs: do these cells derive from Day 3.5 FLK1^{+} or FLK1^{-} cells? Given that Day 5.5 FLK1^{High} express SCL nearly ubiquitously (Figures 3.2d and 3.3b, bottom row), we made use of the *Scl:mCherry* and its WT parental line as a way to label FLK1^{High} cellular origin following re-aggregation experiments. FLK1^{+} and FLK1^{-} cells were sorted at Day 3.5 from both cell lines (Figure 3.4a). FLK1^{+} and FLK1^{-} cells from distinct genetic backgrounds were mixed and reaggregated to form EBs containing either FLK1^{-}(WT)/FLK1^{+}(*Scl:mCherry*) or FLK1^{-}(*Scl:mCherry*)/FLK1^{+}(WT) cells (Figure 3.4b, left and right panels, respectively). These EBs were then differentiated according to the standard differentiation protocol. At Day 5.5, FLK1^{High} cells were assayed for mCherry expression as a way to trace their population of origin, i.e. Day 3.5 FLK1^{-} or FLK1^{+} cells (Figure 3.4c). It should be noted that ~95% of Day 5.5 FLK1^{High} cells express SCL at the protein level (Figures 3.2d and 3.3b, bottom row), and that the absence or presence of mCherry protein is here used as a lineage-tracing marker strictly, and not as a way to measure *Scl* expression.

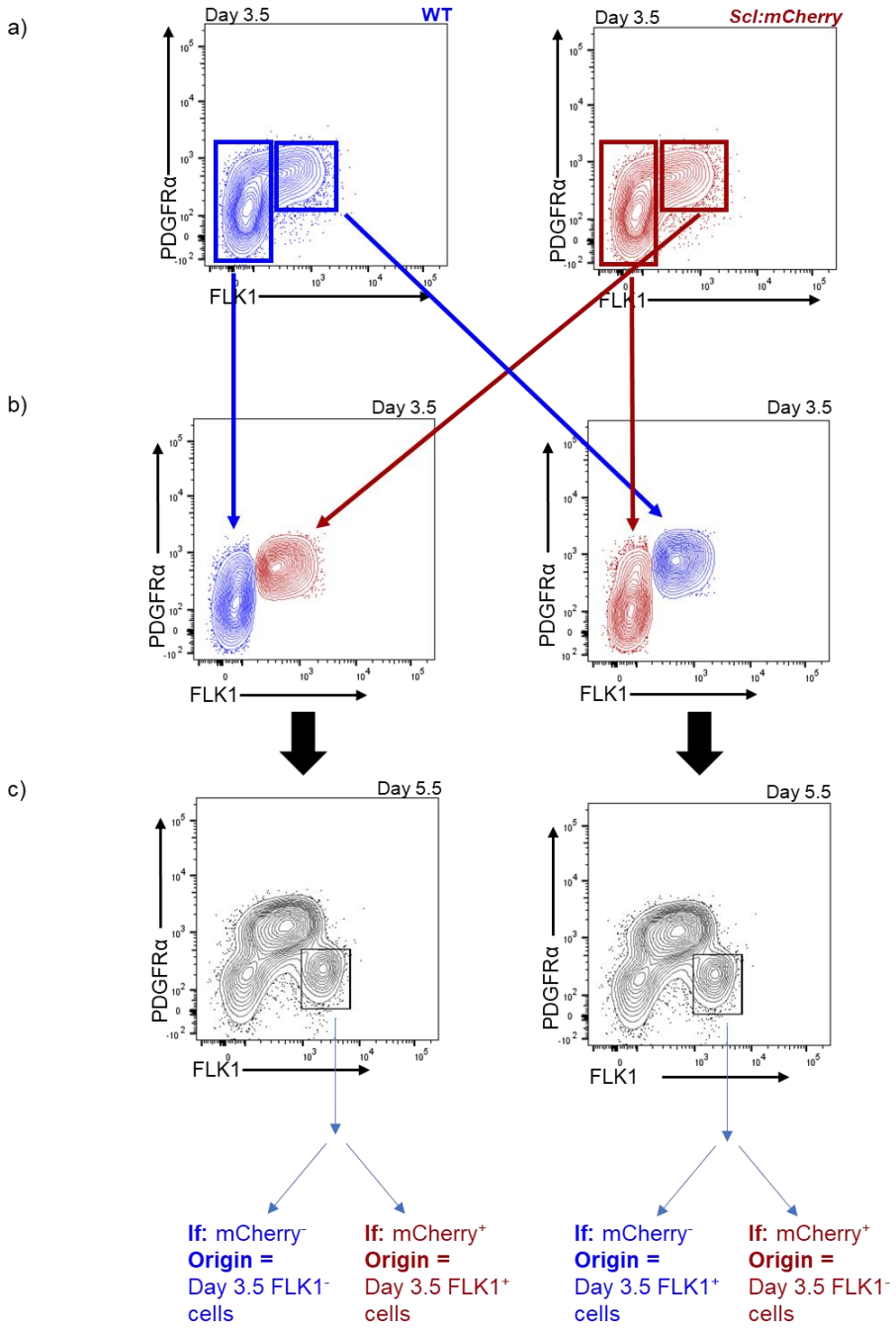

Figure 3.4. Population Tracing Experimental Design
a) Overview of gating strategy for FLK1^{+} and FLK1^{-} cells on a representative flow cytometry plot used to represent both WT and *Scl:mCherry* ES cells at Day 3.5 of differentiation b) Overlay flow cytometry plots simulating sorted FLK1^{+} and FLK1^{-} cells from each cell line reaggregated in appropriate ratios and differentiated for two more days. c) Diagram demonstrating how, in mixed cultures at Day 5.5, mCherry expression of FLK1^{High}PDGFRα^{-} cells, which express *Scl* almost ubiquitously, can be used to trace the Day 3.5 origin population of Day 5.5 FLK1^{High}PDGFRα^{-} cells.

At Day 3.5, both lines contained comparable FLK1^{+}PDGFRα^{+} percentages, with WT cells exhibiting an average of 25.9 ± 12.3% and *Scl:mCherry* cells an

average of 22.7 ± 9.3% across the three biological replicates (Figure 3.5a). In line with earlier data (Figure 3.3b), we also observed no mCherry expression in *Scl:mCherry* cells at this timepoint (Figure 3.5b). Sort gates were set using a FLK FMO sample (Figure 3.5c). The first biological replicate had the highest percentages of post-sort impurities across samples (from 3.4% to 7.7%, Figure 3.5d first row), with the following two showing significant improvements (less or equal to 0.5%, Figure 3.5d second and third row). For the first and second replicates, cells were reaggregated based on percentages of $FLK1^{+}PDGR\alpha^{+}$ cells at the time of sorting, roughly 1:4 (Figure 3.5a). Prior to the third replicate, it was suggested that given sorting was being done based on $FLK1^{+}$ gates only, without taking PDGFRα into account, $FLK1^{+}$ to $FLK1^{-}$ ratios were more appropriate for reaggregation. Reaggregation ratios were therefore adjusted to 1:1 for the third and final replicate (58.0% and 42.7% $FLK1^{+}$ cells in WT and *Scl:mCherry*, respectively, for this particular replicate).

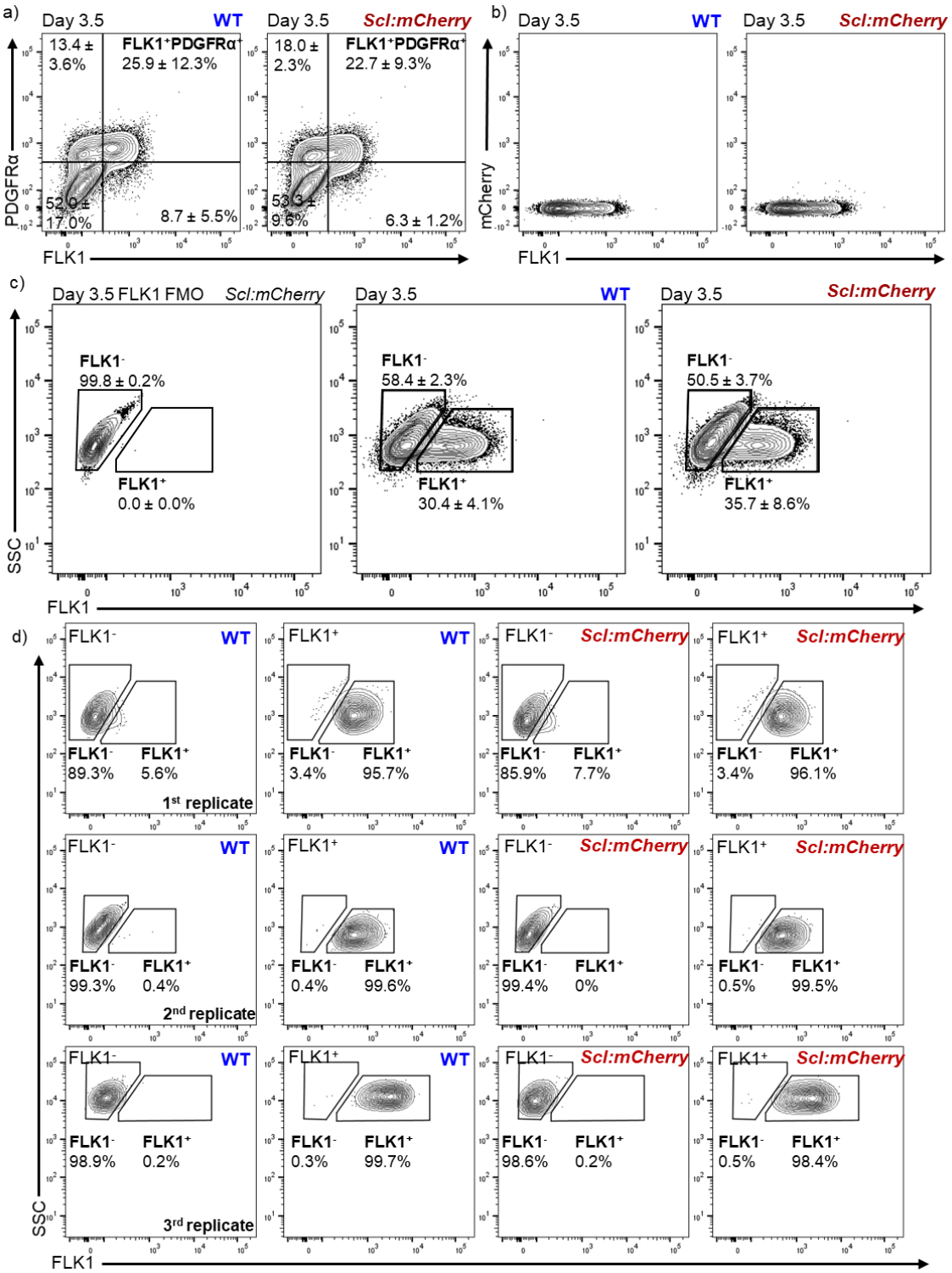

Figure 3.5 Sorting Strategy for Population Tracing Experiment

a) Representative flow cytometry plots of FLK1 and PDGFRα expression of WT and *Scl:mCherry* ESCs prior to sorting at Day 3.5. n = 3 biological replicates. Average ± SD depicted. b) Representative flow cytometry plots of three biological replicates showing no mCherry expression in either population at Day 3.5 prior to sorting. c) FLK1 FMO control at Day 3.5 showing sorting gate strategy alongside representative plots for WT and *Scl:mCherry* samples. n = 3 biological replicates. Average ± SD depicted. d) Flow cytometry plots of post-sorting purity checks for all samples across the three replicates.

Despite the differences in post-sort purities and re-aggregation ratios across the three biological replicates, results across the replicates were comparable. Day 5.5 control cultures derived from unsorted Day 3.5 WT cells (Figure 3.6a, left plot) were used as a negative control to help set the gates in the mCherry channel (Figure 3.6b, left plot). Day 5.5 cultures derived from Day 3.5 WT $FLK1^-$ only cells (Figure 3.6a, middle plot) confirmed previous studies which show *de novo* $FLK1^+$ expression from Day 3.5 $FLK1^-$ cells (Irion et al. 2010), and also served as a negative control for mCherry expression (Figure 3.6b, middle plot). In Day 5.5 cultures derived from a mix of Day 3.5 WT $FLK1^-$ and *Scl:mCherry* $FLK1^+$ cells (Figure 3.6a, right plot), 44.6 ± 5.4% of the $FLK1^{High}$ population was positive for mCherry expression (Figure 3.6b, right plot), showing Day 3.5 $FLK1^+$ cells have the potential to differentiate into and actually contribute to the pool of $FLK1^{High}$ cells at Day 5.5 in EB cultures where Day 3.5 $FLK1^+$ cells are not sorted out of the system.

Mirror experiments showed similar results. Day 5.5 control cultures derived from unsorted Day 3.5 *Scl:mCherry* cells (Figure 3.6c, left plot), served as a positive control that aided in gate setting for the mCherry channel (Figure 3.6d, left plot). Day 5.5 cultures derived from Day 3.5 *Scl:mCherry* $FLK1^-$ cells (Figure 3.6c, middle plot) also confirmed *de novo* $FLK1^+$ expression from Day 3.5 $FLK1^-$ cells and served as a positive control for mCherry expression (Figure 3.6d, middle plot). In Day 5.5 cultures derived from a mix of Day 3.5 *Scl:mCherry* $FLK1^-$ cells and WT $FLK1^+$ cells (Figure 3.6c, right plot), $FLK1^{High}$ cells also contained, on average, a 1:1 ratio of cells derived from Day 3.5 $FLK1^+$ and $FLK1^-$ cells (40.3 to 43.2% $mCherry^-$; Figure 3.6d, right plot). Notably, the experimental set-up is not perfectly precise, as demonstrated by the 1.1 ± 0.5% and 1.2 ± 0.7% percent of $mCherry^-$

cells in the FLK1^{High} fractions of *Scl:mCherry* control samples (Figure 3.6d, left and middle plots), representing cells which do not express SCL in this population. Likewise, there exists the error introduced by sort impurities, particularly salient in the first biological replicate, which is likely affecting results.

These experiments suggest that Day 3.5 FLK1^{+} cells have the potential to produce Day 5.5 FLK1^{High} cells that, when assayed immunophenotypically (FLK1^{High}PDGFRα^{-}SCL^{+}), are indistinguishable to those produced by Day 3.5 FLK1^{-} cells. While *Scl* expression was not directly assayed, and mCherry expression used rather as a population tracer, it can be assumed that in conditions where FLK1^{-} are not sorted out of the system at Day 3.5, some of the FLK1^{High} cells, which are nearly all SCL^{+} (Figure 3.2d, Figure 3.3b, Figure 3.6d left plot), were derived from Day 3.5 FLK1^{+} cells, though the exact percentages of these is unknown given our own artificial mixing ratios in the population tracing experiments.

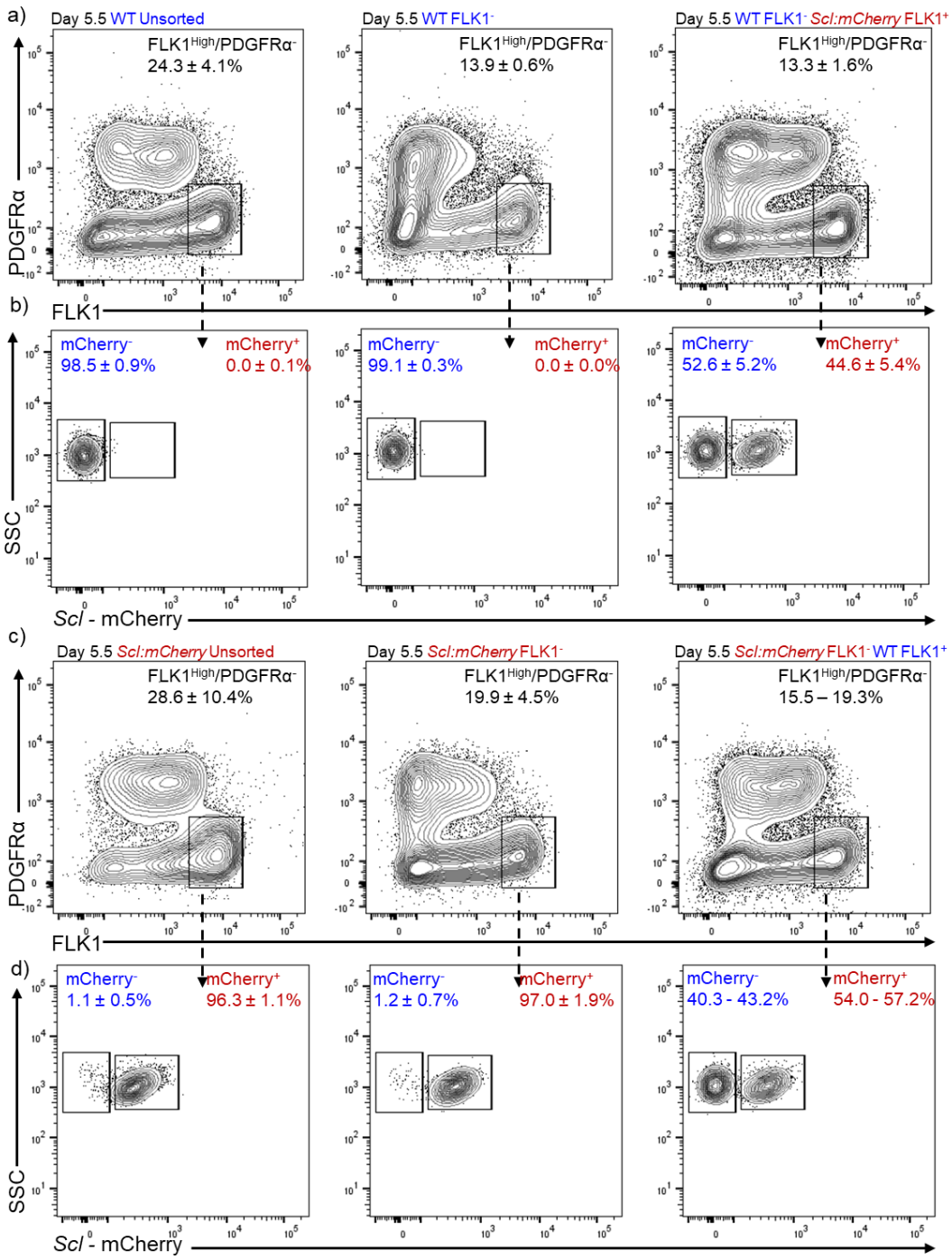

Figure 3.6 Population-Tracing Reveals Mixed Origin of Day 5.5 FLK1^{High} cells
a) Representative flow cytometry plots of FLK1 and PDGFRα expression in Day 5.5 cultures originating from Day 3.5 unsorted WT, FLK1$^-$ WT, and mixed WT FLK1$^-$ and *Scl:mCherry* FLK1$^+$ cultures. n = 3 biological replicates. Average ± SD depicted. b) Representative flow cytometry plots of mCherry expression in FLK1^{High} cells from cells in (a). n = 3 biological replicates. Average ± SD depicted. c) As in (a), but originating from Day 3.5 unsorted *Scl:mCherry, Scl:mCherry* FLK1$^-$ only, and *Scl:mCherry* FLK1$^-$ WT FLK1$^+$ mixed differentiation cultures. n = 3 biological replicates for unsorted and FLK1$^-$ (first and second column), and n = 2 biological replicates for mixed culture (third column) due to an accidentally unrecorded sample. Average ± SD depicted for first two columns and value ranges for third column due to n of 2. d) Plots as described in (b), but for FLK1^{High} populations from (c). n = 3 biological replicates for first two columns, and n = 2 for last column. Averages ± SD depicted for columns 1 and 2, and value ranges for last column.

3.5. FLK1^{High} Cells Arise in Response to VEGFA without an Arterial Niche or Identity

Previous reports have shown that FLK1^{+} cells respond to VEGFA by differentiating into cells with haematoendothelial potential in mouse *in vitro* cultures (Choi et al. 1998; Nostro et al. 2008; Pearson et al. 2008; Park et al. 2004) and that VEGFA is necessary *in vivo* for differentiation of FLK1^{+} mesoderm to endothelial and HE cells in developing zebrafish and *Xenopus* (Cleaver and Krieg 1998; Gering and Patient 2005; Ciau-Uitz et al. 2010; Ciau-Uitz et al. 2013; Leung et al. 2013). The development of the haematoendothelial FLK1^{High} population at Day 5.5 also likely occurs in response to the addition of VEGFA to cultures at Day 4.5. Our own preliminary data showed the FLK1^{High} population is present at Day 5.0, as early as twelve hours following the addition of VEGFA (Figure 3.7a).

In developing *Xenopus*, Vegfa isoforms have been shown to play distinct roles in the maturation and migration of mesodermal progenitors and in the production of HSPCs: the short and non ECM-bound isoform of Vegfa secreted from the hypochord is necessary for FLK1^{+} cell migration towards the midline, DA formation, and arterial programme specification, while the ECM-bound medium and long isoforms of Vegfa, found in the developing somites, are required for HSC formation but play no role in DA formation (Leung et al. 2013). While it is unknown whether these isoform-specific functions of Vegfa are conserved in mammals, mouse models of angiogenesis have shown that the binding of long and medium VEGFA isoforms to the ECM aids in localized VEGFA distribution, concentration, and release (Park, Keller, and Ferrara 1993; Chen et al. 2010; Goerges and Nugent 2004; Ruhrberg et al. 2002). *In vitro* studies in mouse cells have also shown that downstream signalling from VEGFA can differ among isoforms when

endothelial NRP1 acts as a coreceptor for $VEGFA_{165}$ and $VEGFA_{189}$, prolonging the time to degradation of the internalized VEGFA (Kofler and Simons 2015; Zhang, Lanahan, and Simons 2013). Given that *Nrp1* is not expressed in endothelial cells until after DA formation and establishment of an arterial programme (Chong et al. 2011) at E8.5 in mice however, it is unlikely that migrating cells encountering long and medium VEGFA isoforms are able to signal in this same manner, though this has yet to be formally demonstrated.

To test whether different VEGFA isoforms had any effect on the generation of $FLK1^{High}$ cells at Day 5.5 in our own system, equal concentrations (5 ng/ml) of soluble $VEGFA_{121}$, $VEGFA_{165}$, and $VEGFA_{189}$ were added to separate samples at Day 4.5, alongside a control to which no exogenous VEGFA was added. All samples showed similar distribution of FLK1 and PDGFRα populations (Figure 3.7b). However, one-way ANOVA with Tukey's posthoc test for multiple sample comparison showed addition of $VEGFA_{165}$ and $VEGFA_{189}$ led to significantly higher percentages of $FLK1^{High}$ cells at Day 5.5 compared to samples with no VEGFA added, and, in the case of $VEGFA_{165}$ also compared to $VEGFA_{121}$ samples (Figure 3.7c). This shows VEGFA plays some role in the differentiation or proliferation of the $FLK1^{High}$ cells. Whether the small percentages of $FLK1^{High}$ cells in the no VEGFA control samples were due to endogenous expression of VEGFA or other growth factors released by the cultured cells was not explored and requires further study. RT-qPCR was also used to assay the expression of haematoendothelial genes in sorted Day 5.5 $FLK1^{High}$ treated with different VEGFA isoforms. We found no statistically significant differences in *Dll4, Runx1, Scl,* and *Notch1* expression in $FLK1^{High}$ cells treated with no VEGFA and any of the VEGFA isoforms, suggesting that, while different isoforms might affect the percentage of cells differentiating into

FLK1^{High} cells, they do not affect gene expression (Figure 3.7d). These conclusions are of course limited to the genes assayed. Likewise, high inter-replicate variability in RT-qPCR data could be potentially masking biologically relevant differences. Though further study could potentially shed light on the lack of apparent differences, it was decided that such studies were beyond the scope of this thesis. Given the highest percentages of FLK1^{High} resulted from using VEGFA$_{165}$, the most commonly commercially available and used isoform *in vitro*, we continued to use this isoform for all future experiments.

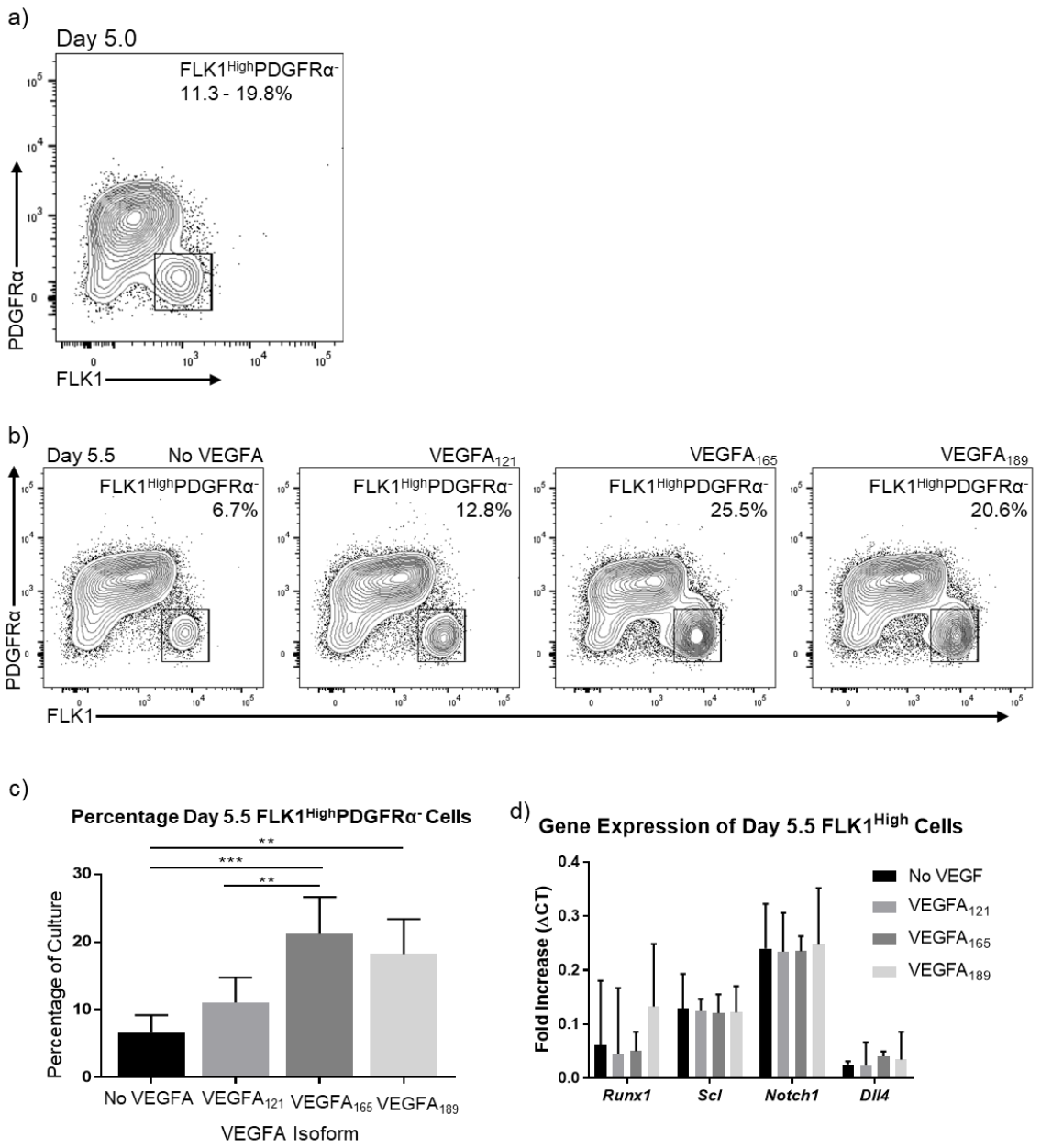

Figure 3.7 Day 5.5 FLK1^{High} cell response to VEGFA addition at Day 4.5

a) Representative flow cytometry plot depicting FLK1 and PDGFRα expression at Day 5.0, twelve hours after addition of VEGFA at Day 4.5. n = 2 biological replicates. Range of values is depicted due to n of 2. b) Representative flow cytometry plots depicting FLK1 and PDGFRα expression at Day 5.5 in cultures treated with no exogenous VEGFA or soluble short, medium, and long VEGFA isoforms at Day 4.5 of culture. c) Percentages of FLK1^{High}PDGFRα^{-} cells at Day 5.5 in varying culture conditions as depicted in (b). n = 4 biological replicates for No VEGFA, and n = 6 biological replicates for isoform treatments. Averages ± SD depicted. Ordinary one-way ANOVA with Tukey's posthoc multiple comparison test used. d) Gene expression from RT-qPCR of FLK1^{High} cells sorted from various cultures as depicted in (b). n = 4 biological replicates. No significant differences found among samples for ΔCT values of same gene compared using ordinary, one-way ANOVA with Tukey's posthoc multiple comparison test.

To assess whether the expression of a haematoendothelial phenotype occurred exclusively at time of appearance of the FLK1^{High} population, cells collected from day 3.5, 4.5, and 5.5 EBs were all stained for VE-Cad and cKIT. Cells do not robustly express either marker until day 5.5 (Figure 3.8a), when PDGFRα expression levels are down-regulated and FLK1 levels up-regulated (Figure 3.1b). At Day 4.5, only 0.5 ± 0.1% of cells are VE-Cad^{+}cKIT^{+}, compared to 13.9 ± 10.8% at Day 5.5.

Given the fact that HE cells in the third wave of haematopoiesis arise within an arterial niche that expresses Notch ligands and receptors (Chong et al. 2011; de Bruijn et al. 2002; de Bruijn et al. 2000; Robert-Moreno et al. 2005), and as expression of *Notch1* is detected in Day 5.5 FLK1^{High} cells (Figure 3.2b), we further assayed differentiating cells for expression of Notch receptor NOTCH1 by flow cytometry. Expression of the arterial Notch signalling ligand DLL4 was also assayed to see whether HE cells had been exposed to arterial-specific Notch signalling prior to HE specification. Data showed that 11.8 ± 10.0% of cells in culture were VE-Cad^{+}NOTCH1^{+} at Day 5.5 (Figure 3.8b). Similar to cKIT expression, VE-Cad cells are homogenous in their NOTCH1 expression. In contrast, only 2.5 ± 1.4% of cells in culture expressed a VE-Cad^{+}DLL4^{+} arterial progenitor phenotype (Figure 3.8c). Differentiating cells expressed neither NOTCH1 receptor nor DLL4 ligand before Day 5.5 (Figure 3.8 b-c).

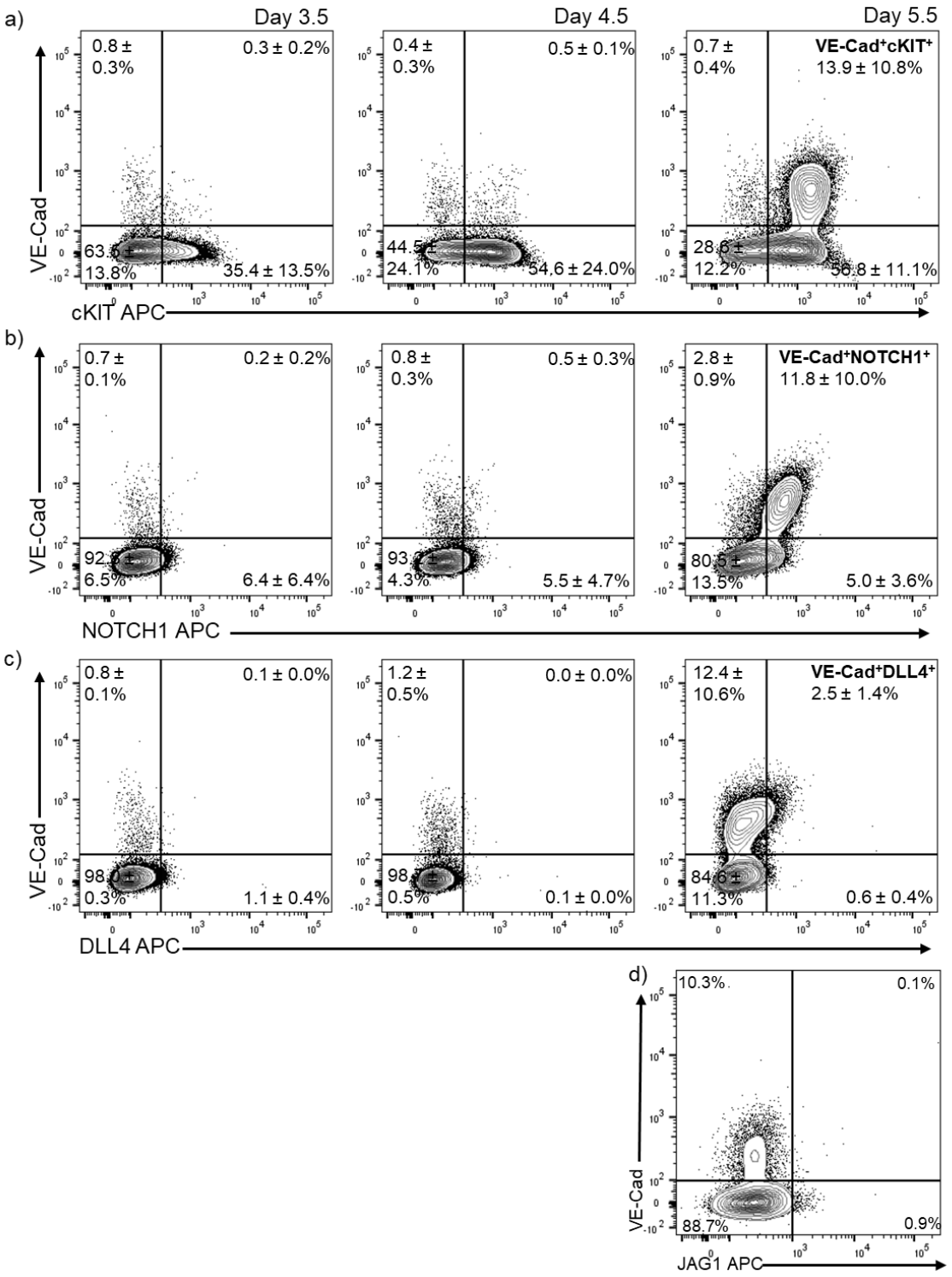

Figure 3.8. HE specifies after day 4.5 outside of an arterial Notch context
Representative flow cytometry plots for VE-Cad and either a) cKIT, b) NOTCH1, or c) DLL4 at differentiation days 3.5, 4.5, and 5.5 from the same sample stained independently for each panel. n = 3 biological replicates. Average ± SD depicted. Gates set as in Supplementary Figure 3.1a d) Flow cytometry plot for preliminary n of 1 staining of Day 5.5 VE-Cad and JAG1. Gates set as in Supplementary Figure 3.1b.

While other Notch signalling receptors, such as NOTCH4, and ligands, such as JAG1, are also expressed in murine arterial endothelium *in vivo* (Villa et al. 2001), they are developmentally expressed at the gene expression level after *Dll4* (Chong et al. 2011), and unlikely to be present in the absence of this ligand which initiates differentiation towards an arterial fate (Fish and Wythe 2015). The same is true for other markers of arterial identity, such as CXCR4 and EFNB2 (Chong et al. 2011). Preliminary n of 1 data revealed that, while a small percentage of VE-Cad^{-} cells expressed JAG1 at Day 5.5 (0.9%), no VE-Cad^{+} cells did so (Figure 3.8d). Therefore, HE specification of FLK1^{High} cells in this system likely occurs outside of an arterial Notch signalling context, though we cannot definitively exclude Notch signalling through ligands and receptors not tested. This is similar to what has been reported for second wave haematopoiesis, which occurs prior to arterio/venous specification in the YS vascular labyrinth (Frame et al. 2016) and in both fish and mammals is independent of Notch signalling (Hadland et al. 2004; Kumano et al. 2003; Bertrand et al. 2010a).

3.6. FLK1^{High} cells produce HSPCs immunophenotypically resembling second wave haematopoiesis.

To test the haematopoietic potential of FLK1^{High} cells, FLK1^{High}PDGFRα^{-}CD41^{-} cells were sorted at Day 5.5 (Figure 3.9b, Supplementary Figure 3.2a) and replated on Matrigel in serum-free media with cytokines and small molecules that have been reported to be critical for the survival of FLK1^{+} HE cells undergoing EHT (Chiang and Wong 2011) (Figure 3.9a-b). These include BMP4, VEGFA, and SB431542 in addition to basic fibroblast growth factor (bFGF) and a cyclic AMP mimic that is readily taken up by cells in culture (8-Br-cAMP). Media was also supplemented with Stem Cell Factor (SCF), FLT3 ligand (FLT3-L), and Thrombopoietin (TPO), all growth factors which have been reported to maintain HSPCs in a more multipotent, undifferentiated state (Sitnicka et al. 1996) (Figure 3.9a). Serum-free medium with this combination of cytokines will be referred to as hematoendothelial differentiation (HED) medium for the remainder of this text. Similar to what has been reported in other *in vitro* systems in which developing endothelial cells undergo EHT (Yvernogeau et al. 2016; Bos, Hawkins, and Zovein 2015), budding, rounded cells were observed in culture. While single budding cells can be observed as early as two days post replating in some differentiations, most rounded groups of cells are clearly and reproducibly visible by Day +4 of culture (Figure 3.9d).

Cells also progressively up- and then down-regulate expression of CD41, much like what has been reported previously for developing HSPCs *in vivo* (Rybtsov et al. 2014), as well as continue to express variable levels of cKIT. Two days after replating these CD41^{-} cells, at culture Day +2, 35.6 ± 8.4% of cells express CD41 mostly at medium levels. This percentage peaks four days after replating (Day +4) with 73.6 ± 10.6% of the cultured cells expressing CD41 at

medium and high levels, then decreases to 50.3 ± 19.2% of cells expressing CD41 mainly at high levels by Day +6 of culture (Figure 3.10a). Likewise, expression of pan-haematopoietic CD45 becomes upregulated in cells as culture progresses, though not to the degree that CD41 does, suggesting perhaps the HSPCs in the culture are in further need of maturation: at Day +6, only 22.1 ± 5.0% of cultured cells express CD45 (Figure 3.10b). Finally, cultured cells downregulate endothelial VE-Cad. Nearly all $FLK1^{High}$ cells at Day 5.5 express VE-Cad (Figure 3.2a). Two days after plating, the percentage of VE-Cad^{+} cells in culture has decreased to 70.7 ± 3.4%, a percentage which by Day +6 of culture is only 7.3 ± 2.2% of cultured cells (Figure 3.10c). The appearance of rounded cells, expression of CD41 and CD45, and downregulation of VE-Cad of sorted Day 5.5 $FLK1^{High}$ cells all demonstrate that $FLK1^{High}$ cells are not only immunophenotypically haematoendothelial in nature, but also contain, at the population level, cells that can produce budding haematopoietic cells. Given the clear differences in the cKIT expression of CD41, CD45, and VE-Cad expressing cells at different timepoints, we further characterised the immunophenotype of various cell populations.

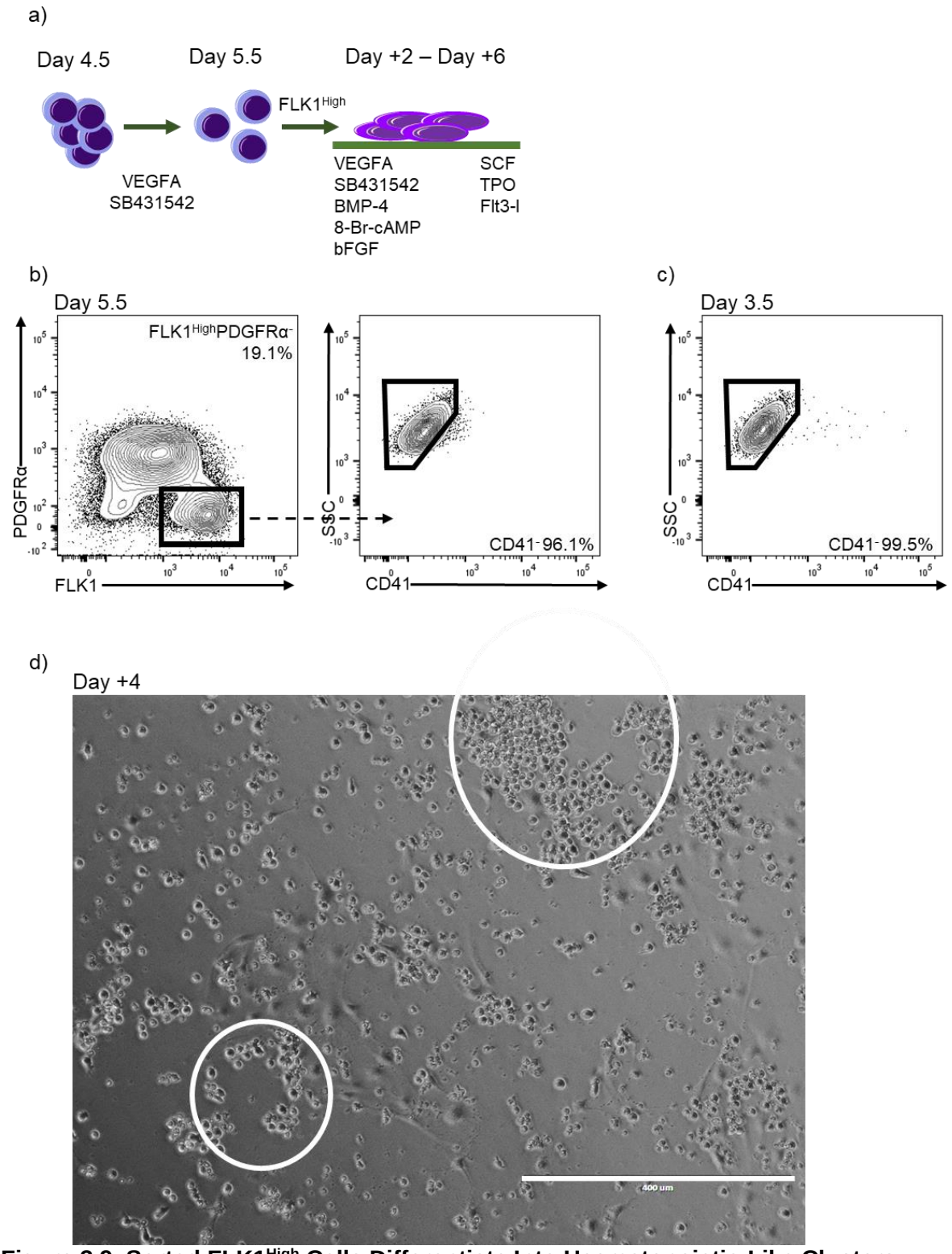

Figure 3.9. Sorted FLK1^{High} Cells Differentiate Into Haematopoietic-Like Clusters
a) Differentiation scheme in which FLK1^{High} cells are replated in Matrigel and haematoendothelial differentiation (HED) cytokines. b) Representative flow cytometry plots with gating strategy for sorting FLK1^{High}PDGRα^{-}CD41^{-} cells c) Representative flow cytometry plot of Day 3.5 cells from staggered differentiation to b, sampled on the same day and used as a negative control for setting the CD41 gate in b. d) Brightfield images of cultured cells at four days after replating. White circles point to rounded cell clusters. Scale bar = 400 µm.

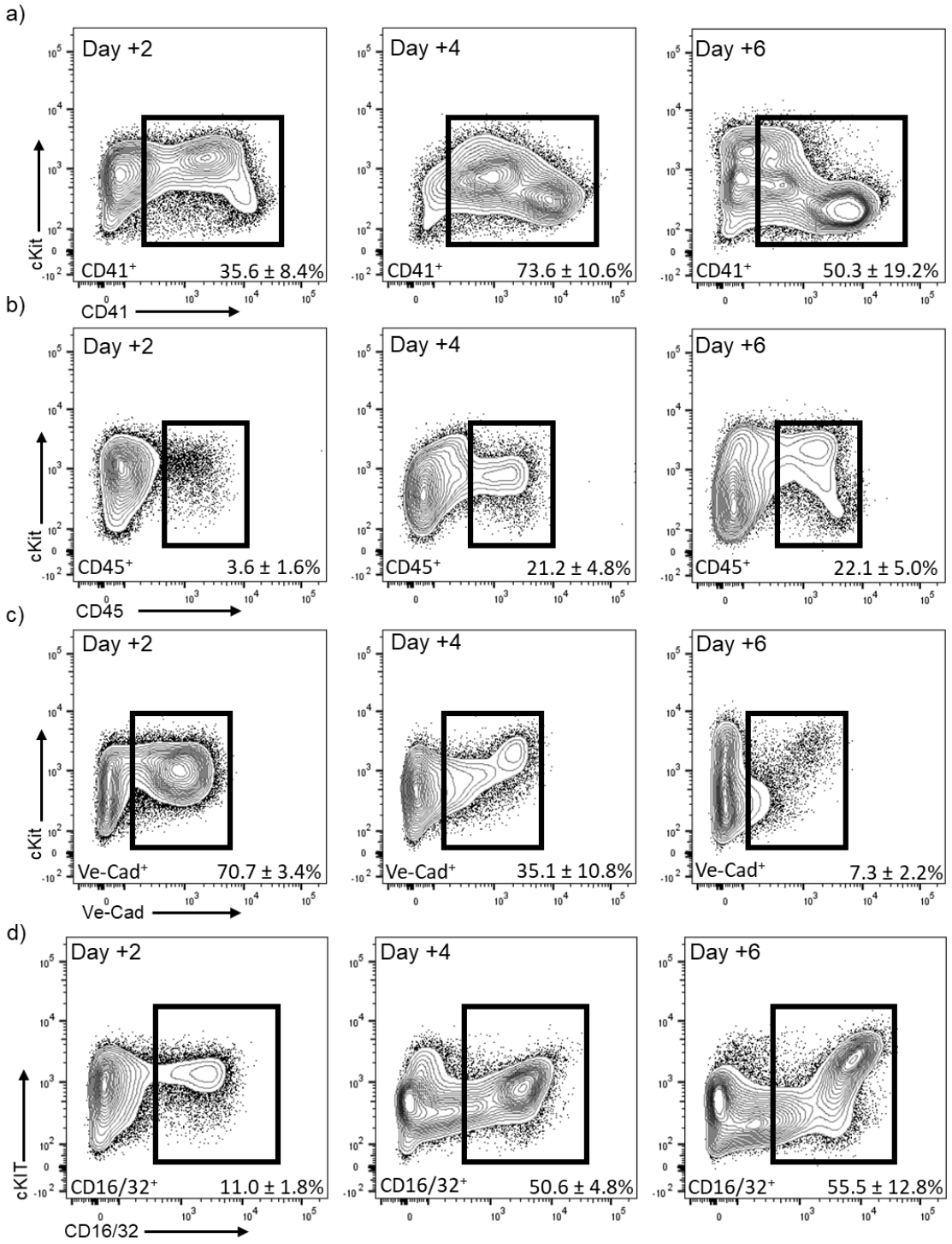

Figure 3.10 Replated FLK1^{High} Cells Develop Haematopoietic Immunophenotype
a-d) Representative flow cytometry plots of cKIT expression alongside CD41, CD45, VE-Cad, or CD16/32 expression in cultured cells at Day +2, +4, and +6 of replating. Gates were set using FMO controls shown in Supplementary Figure 3.2c. n = 4 biological replicates. Averages ± SD depicted.

One of the difficulties the field has faced in determining whether *in vitro* cells more closely resemble second- or third-wave HSPCs is the shared immunophenotype among these differentiating progenitors (McGrath et al. 2015). Recently however, definitive, second-wave HSPCs arising in the YS and *in vitro* were described as expressing Fc receptors CD16 and CD32 (McGrath et al. 2015). Beyond that, a follow-up study found that cKIT expression in developing YS cells can be used to distinguish definitive erythromyeloid progenitors (EMPs) from more differentiated macrophage and megakaryocyte progenitors arising from first-wave haematopoiesis (McGrath et al. 2015; Frame et al. 2016). EMPs were described as having a $cKIT^{+}CD16/32^{+}CD41^{+}$ immunophenotype and erythroid, macrophage, and granulocytic potential. Differentiating megakaryocyte progenitors were described as having a $cKIT^{-}CD41^{High}$ phenotype, while a population of $cKIT^{-}CD45^{+}CD16/32^{+}$ cells was shown to have exclusively macrophage potential (Frame et al. 2016).

Given these published data, haematopoietic differentiation of sorted $FLK1^{High}$ cells was characterised for expression of these markers as cells differentiated and underwent EHT. Cells begin to express CD16/32 as early as two days after replating (11.0 ± 1.8% of cells in culture, Figure 3.10d) and continue to either upregulate the marker, proliferate, or both, leading to more than half (55.5 ± 12.8%) of the culture being $CD16/32^{+}$ by Day +6. While some cells retain a $cKIT^{+}VE\text{-}Cad^{High}$ endothelial immunophenotype at Day +4 (20.6 ± 8.3%, Figure 3.11a/e), this percentage decreases over time to reach 2.1 ± 0.8% of the culture at Day +6 (Figure 3.11e).

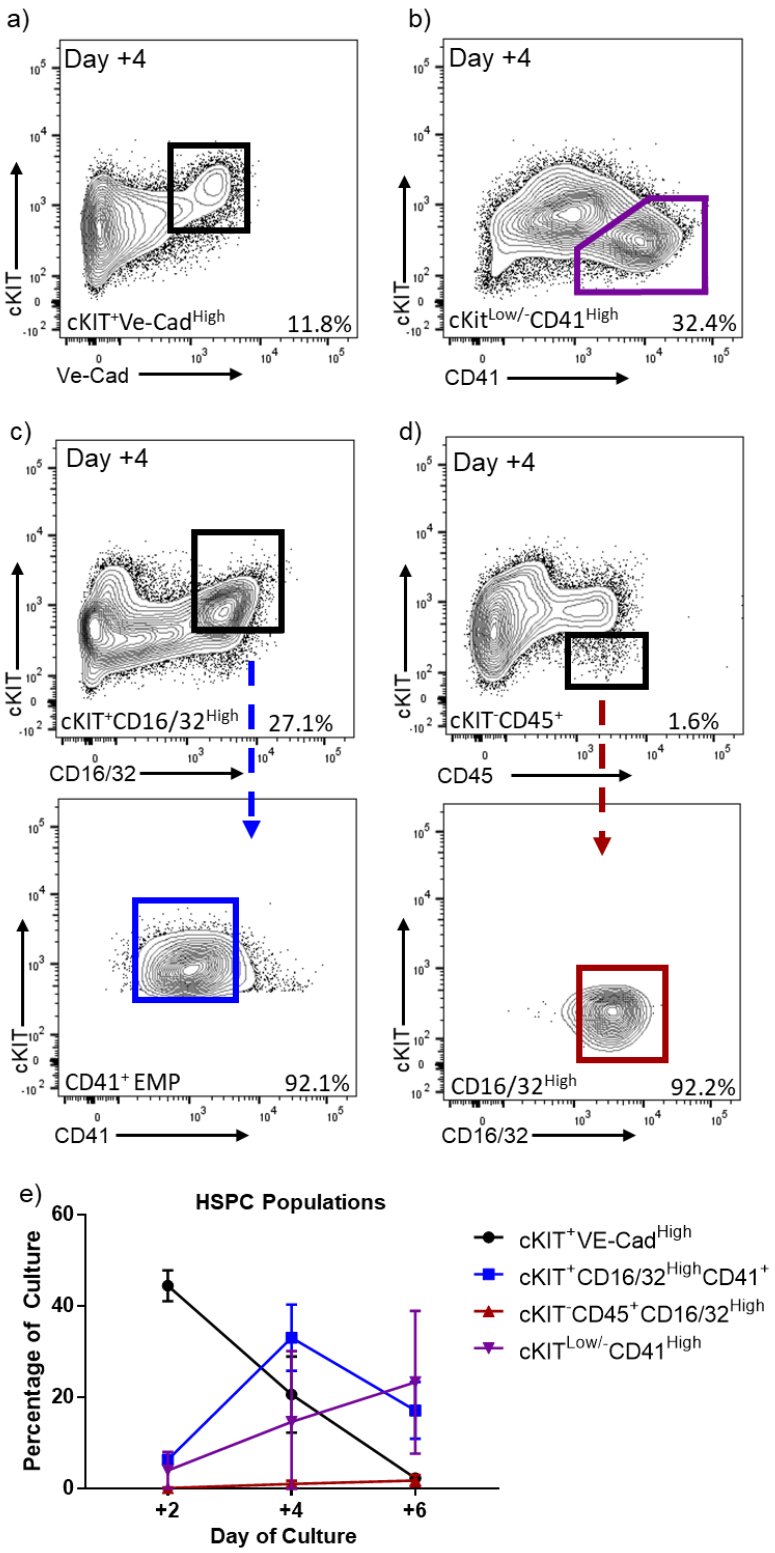

Figure 3.11 FLK1^{High} HE differentiates into second wave-like HSPCs

a) Representative flow cytometry plot of Day +4 expression of cKIT and VE-Cad. Gate for cKIT in this, c, and d set using FMO control (Supplementary Figure 3.2d) b) Representative flow cytometry plot of Day +4 expression of cKIT and CD41. c) Representative flow cytometry plots of Day +4 expression of cKIT, CD16/32, and CD41. d) Representative flow cytometry plots of Day +4 expression of cKIT, CD45, and CD16/32. e) Percentages of different HSPC-like populations at culture Day +2, +4, and +6 after replating. n = 4 biological replicates. Averages ± SD depicted.

Likewise, HSPCs in culture immunophenotypically resemble those arising in second-wave haematopoiesis *in vivo*. A population of $CD41^{High}cKIT^{low}$ cells, similar to previously described YS megakaryocyte progenitors, was observed at low percentages of culture at early days, but increasing in percentage until Day +6 (Figure 3.11b,e), at which point they comprised the largest population of HSPCs in culture at 23.3 ± 15.6%. This could, in part, be due to the levels of TPO (20 ng/ml) added to the culture media. A population of $cKIT^{-}CD45^{+}$ cells that is exclusively $CD16/32^{+}$ (Figure 3.11d), like previously described macrophage progenitors, was observed in culture, albeit at low percentages, comprising only 1.8 ± 1.2% of the cells in culture by Day +6. Finally, an EMP-like $cKIT^{+}CD16/32^{+}$ population present in the culture also expressed $CD41^{+}$ (Figure 3.11c), consistent with previously published literature (Frame et al. 2016). By Day +6, $CD41^{+}cKIT^{+}$ cells have mutually exclusive expression of VE-Cad and CD16/32 (Figure 3.12). Whether this suggests two separate populations of *in vitro* HSPCs expressing $cKIT^{+}CD41^{+}$VE-Cad^{+} and EMP-like $cKIT^{+}CD41^{+}CD16/32^{+}$, or a transition from VE-Cad expressing HE (Lie-A-Ling et al. 2018) to CD16/32 expressing EMP-like cells can only be tested by further sorting, replating, and functional differentiation assays, including cytospins to assay the morphology of the cells' progeny. Altogether, the presence of these HSPC populations shows $FLK1^{High}$ cells, as a population, contain cells that can functionally undergo EHT to produce HSPCs that, at the immunophenotypic level, resemble second-wave haematopoietic cells. Given that the immunophenotypes of EMPs and other progenitors were described from *in vivo* YS cultures, however, further functional studies on the potential of these progenitors would be required to definitively identify the cells as second-wave like.

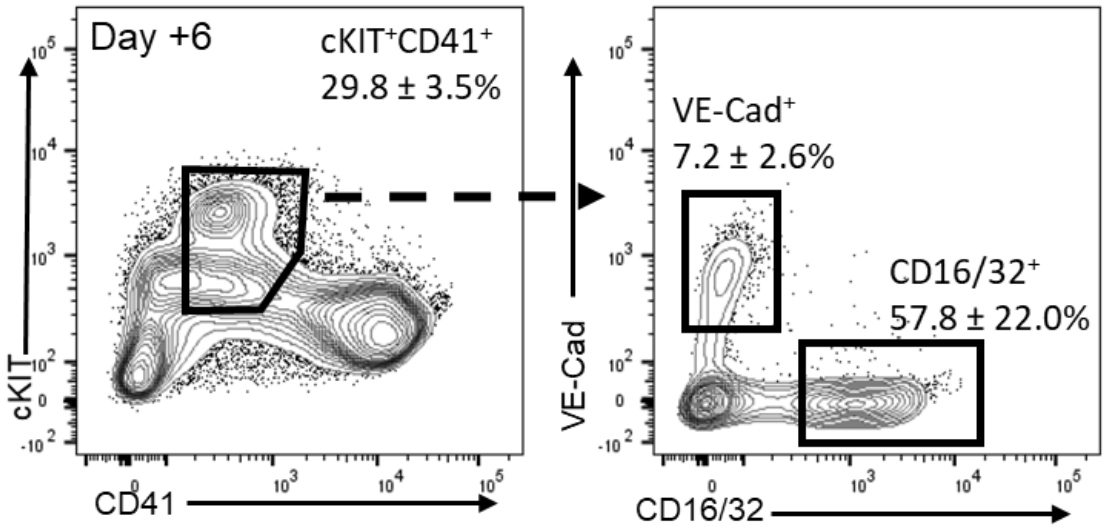

Figure 3.12 Mutually Exclusive Expression of VE-Cad and CD16/32 in cKIT$^+$CD41$^+$ cells at Day +6

Representative flow cytometry plots at Day +6 expression of CD41, cKIT, VE-Cad, and CD16/32. Gates set as in 3.10 and 3.11. n = 4 biological replicates. Averages ± SD depicted.

3.7. Discussion

Taken together, these data show that the previously reported wave of FLK1^{+} definitive progenitors (Irion et al. 2010; Clarke et al. 2013) is a population with a FLK1^{High}PDGFRα^{-} immunophenotype also homogeneous in its expression of a VE-Cad^{+}cKIT^{+}CD41^{-}NOTCH1^{+}SCL^{+} haematoendothelial phenotype, and containing functional HE. Population tracing experiments with an *Scl:mCherry* line however, showed that in an unsorted EB context, this FLK1^{High} population arises from both Day 3.5 FLK1^{+} cells, which have been reported to give rise to primitive haematopoiesis, and Day 3.5 FLK1^{-} cells (Irion et al. 2010). While characterisation based on immunophenotype alone is limited, these results are in line with studies that have shown reaggregated Day 3.5 FLK1^{+} cells can express Sox17 and also produce EMP-like cells (Clarke et al. 2015), as well as give rise to HPCs with limited engraftment capacity (Pearson et al. 2015). It is also worth noting that the variable and continuous nature of the system makes the Day 3.5 timepoint somewhat arbitrary. In other words, there will be cells at this stage that, regardless of FLK1 expression, may be developmentally more or less differentiated than others in the same EB or culture: a FLK1^{-} cell might be expressing *Flk1* at the mRNA level, and express FLK1 at the cell surface level shortly after sorting at Day 3.5. Beyond that, while cell purities for two of three replicates were above 98%, only single-cell studies can truly reveal the bi- or unipotent nature of the cells found in this population. Neither our experiments nor those in previously published work (Irion et al. 2010; Clarke et al. 2013; Clarke et al. 2015) can distinguish between the possibility that the Day 3.5 FLK1^{+} population is heterogeneous, containing progenitors that independently give rise to primitive erythropoiesis and Day 5.5 FLK1^{High} cells, or that the Day 3.5 FLK1^{+} cell is a bipotent progenitor to both of

these waves. For these reasons, sorting experiments such as these are much more precise and informative when done at the clonal level.

Despite experimental limitations, the potentially inter-related nature of the FLK1 waves in the system is an important distinction, as *in vivo* haematopoietic waves have been shown to arise independently of each other: in mouse, lineage tracing experiments have shown that the progenitors giving rise to YS first (primitive) and second (definitive) waves are distinct and specified prior to primitive streak formation (Padrón-Barthe et al. 2014); in *Xenopus*, primitive and definitive haematopoiesis can be traced to distinct progenitors prior to gastrulation (Ciau-Uitz, Walmsley, and Patient 2000). The fact that the Day 3.5 $FLK1^{+}$ wave *in vitro* can give rise to the $FLK1^{High}$ wave, however, is perhaps not so surprising. The BL-CFC, a population of cells with the capacity to clonally give rise to both haematopoietic as well as endothelial cells *in vitro*, was first described in the context of an EB system in medium containing serum (Choi et al. 1998; Keller 2001; Faloon et al. 2000). This was then expanded to the *in vivo* finding of a cell population in the early primitive streak which contained the same haemangioblast potential (Huber et al. 2004) when placed in an *in vitro* blast colony assay. Later studies revealed that while cells in the primitive streak might have haemangiogenic potential, they are fated to become either haematopoietic or endothelial (and later HE) populations, but never both, in the *in vivo* context (Ueno and Weissman 2006; Padrón-Barthe et al. 2014). Importantly, these experiments do show that strictly using Day 3.5 $FLK1^{+}$ and Day 5.5 $FLK1^{High}$ populations in experiments to compare or make conclusions regarding *in vitro* primitive and definitive populations is imprecise. Given their potential for primitive haematopoietic differentiation (Irion et al. 2010), as well as Day 5.5 $FLK1^{High}$ definitive HE potential, Day 3.5 $FLK1^{+}$ cells

at the population level are either heterogeneous and contain progenitors for both primitive and definitive waves, or contain bipotent progenitors, similar to the described BL-CFC of serum containing systems (Choi et al. 1998; Faloon et al. 2000).

This of course, begs the question as to the importance of using FLK1^{High} progenitors that developed only independently of Day 3.5 FLK1^{+} cells for engrafting HSPC differentiation experiments. Using this population tracing system, it is technically feasible to separate the FLK1^{High} cells at Day 5.5 in mixed cultures based on mCherry expression for further functional and molecular assays. It would be interesting to assay whether cell origin at Day 3.5 explains the mix of Notch-independent, EMP-like, and Notch-dependent populations reported to arise from these cells (Clarke et al. 2015), or whether the population truly is functionally homogeneous. Preliminary n = 1 experiments of FLK1^{High} cells sorted based on mCherry expression day Day 5.5 revealed no apparent difference in cKIT and VE-Cad expression, nor in *Notch1*, *Sox17*, *Gata2*, *Scl*, *Runx1*, and *Dll4* expression, though biological replicates and functional data are needed to make any definitive conclusions regarding this. As mentioned above, it is also unclear if Day 3.5 is the only and most efficient cut-off point for these developing FLK1 populations.

It is also important to note that Day 5.5 FLK1^{High} cells, though expressing NOTCH1 at this stage, do not express NOTCH1 prior to this, and are therefore likely not exposed to arterial notch signalling prior to haematoendothelial specification. This is also due to lack of DLL4 expression in the system save for small percentages in FLK1^{High} cells at Day 5.5. Preliminary data revealed fewer than 1% of cells expressed JAG1 at this timepoint, though again, replicates are required to confirm this. While other potential arterial markers, such as CXCR4 and

EFNB2, as well as arterial Notch ligands and receptors, such as NOTCH4, could have been assayed, these are all activated downstream of DLL4 in developing endothelium *in vivo*. Whether or not the same is true of our system *in vitro* remains to be tested. The lack of DLL4 expression in the system is reminiscent of second-wave HE *in vivo*, which arises in the YS prior to the specification of vessels into arterial or venous lineages (Frame et al. 2016).

When plated in serum-free medium with HED cytokines, FLK1^{High} cells upregulate haematopoietic CD41 and subsequently, CD45, while downregulating VE-Cad expression. Likewise, cells differentiate into cKIT^{+}CD16/32^{+}CD41^{+} cells, which have been previously described in both the YS and serum-containing differentiation systems (Frame et al. 2016; McGrath et al. 2015) as EMPs, part of second-wave haematopoiesis. We also found populations with the same immunophenotypes as previously described megakaryocyte (CD41^{High}cKIT^{-}) and macrophage progenitors (CD45^{+}cKIT^{-}CD16/32^{+}). Sorting experiments to validate the potential of these various immunophenotypic progenitors arising in a serum-free system, along with morphological studies of their haematopoietic progeny are still required. *In vivo*, the more differentiated megakaryocyte and macrophage progenitors detected by these immunophenotypes in the YS at E9.5 are thought to arise from earlier, first-wave haematopoietic progenitors present at E7.5 and E8.5, and not from EMPs. Whether the same is true in this *in vitro* system would also have to be validated, and again raises the question of heterogeneity in the FLK1^{High} population, which can give rise to differently biased progenitors without passing through a multi-potent EMP stage. Though tested by others (Irion et al. 2010; Clarke et al. 2013), our group did not validate or test the lymphoid potential of these FLK1^{High} haematoendothelial progenitors. In agreement with what has been

published previously regarding serum-containing mESC to HSPC differentiation systems then (Keller et al. 1993; McKinney-Freeman et al. 2012; McGrath et al. 2015), these data show that FLK1^{High} and downstream HSPCs in this serum-free system resemble second-wave haematopoiesis at an immunophenotypic level.

4. Modelling Arterial Murine Haematopoiesis

4.1. Introduction

One of the main differences between second- and third-wave haematopoiesis is that third-wave HSCs develop in arterial regions of the embryo (de Bruijn et al. 2002; de Bruijn et al. 2000; Frame et al. 2016). This has been shown in sites such as the AGM (de Bruijn et al. 2002; de Bruijn et al. 2000) and vitelline and umbilical arteries (Gordon-Keylock et al. 2013). In contrast, second-wave haematopoiesis occurs in sites prior to arterial and venous specification (Frame et al. 2016).

As discussed earlier (Section 1.4.1), VEGFA plays an important role in the specification of arterial endothelium. In *Xenopus*, studies have shown that LP mesoderm FLK1^{+} endothelial progenitors are exposed to high concentrations of the non-ECM bound isoform of VEGFA, VEGFA$_{120}$, originating from the hypochord, which acts as a chemokine during their migration towards the midline of the embryo to form the DA (Cleaver and Krieg 1998), and is necessary for the activation of an arterial programme (Leung et al. 2013). During migration, cells are exposed to the medium and long isoforms of VEGFA, VEGFA$_{164}$ and VEGFA$_{188}$. These VEGFA isoforms are ECM-bound (Park, Keller, and Ferrara 1993) and expressed by the developing somites (Ciau-Uitz et al. 2013), and have been shown to be necessary for *Runx1* activation and subsequent EHT in the DA, but not for global arterial specification, like VEGFA$_{120}$ is (Leung et al. 2013).

Endothelial activation of arterial DLL4 (Duarte et al. 2004) and a subsequent arterial programme has been shown both *in vitro* and *in vivo* to be downstream of VEGFA signalling (Lanner, Sohl, and Farnebo 2007; Leung et al. 2013; Sriram et al. 2015; Zhang et al. 2008a). At day E8.0 of mouse embryonic development, prior to their migration to the midline, cells in the lumenised paired dorsal aortae already express arterial *Dll4*, followed by *Efnb2, Cx40, Cx37, Hey1, Nrp1, Notch1,* and

Notch4 at E8.25 (Chong et al. 2011). At around this same time, the developing heart tube also begins beating (McGrath et al. 2003), which leads to flow and shear stress in arterial vessels. This is critical for maintaining *Efnb2* expression and committing to an arterial identity beyond initial VEGFA activation (Masumura et al. 2009), as quail and chicken chimaera experiments have shown that arterial cells grafted to venous regions of low shear stress downregulate an arterial programme in favour of a venous one (Othman-Hassan et al. 2001; Moyon et al. 2001).

While it is still unknown if HE in the DA needs to activate a cell-intrinsic arterial programme prior to EHT in order to give rise to HSCs, studies in mouse have found that arterial EFNB2 labels *in vitro* definitive haematopoietic progenitors (Chen et al. 2016) and that $DLL4^{+}$ HE gives rise to HSCs (Hadland et al. 2017). Conversely, human *in vitro* studies suggest early bifurcation of arterial progenitors and HE cells, finding that $DLL4^{-}$ cells give rise to definitive haematopoietic populations (Ayllón et al. 2015; Ditadi et al. 2015). Despite these discrepancies, there is clear evidence both *in vivo* and *in vitro* that Notch signalling from neighbouring arterial cells is critical for HSC emergence, function, and expansion (Hadland et al. 2015; Gori et al. 2015; Ayllón et al. 2015; Gama-Norton et al. 2015; Monteiro et al. 2016). *Runx1* expression and subsequent HSC emergence are dependent on timing and dosage of Notch signalling (Kim et al. 2014; Zhang et al. 2015), with maturing HSCs later becoming Notch-independent (Souilhol et al. 2016). Global over-expression of NOTCH1 receptor, but not NOTCH4 in endothelial cells leads to a block of HSC emergence (Tang et al. 2013), while NOTCH1 attenuation leads to decreased HSPCs in the FL (Gerhardt et al. 2014). Notch ligands have also been shown to be important, as AGM HE cells at E11.5

can activate an arterial programme when exposed to extrinsic DLL4 and a haematopoietic one when exposed to JAG1 (Gama-Norton et al. 2015).

Given the ability of Day 5.5 FLK1^{High} cells to generate third wave-like Notch-dependent, HPCs (Clarke et al. 2013; Clarke et al. 2015), we hypothesized that increasing arterial differentiation through VEGFA and Notch signalling in our system might provide some of the cues necessary to confer engrafting, HSC-like properties to the haematopoietic cells developing from our cultures.

4.2. Treatment of FLK1^{+} cells with high VEGFA concentrations leads to activation of Notch signalling and initiation of an arterial programme

Given various publications showing that *in vitro* exposure to high levels of VEGFA leads to DLL4 expression and arterial differentiation (Joo et al. 2012; Zhang et al. 2008a; Lanner, Sohl, and Farnebo 2007), we tested the effect of increasing the level of VEGFA exposure at Day 4.5. Cells were treated with either control 5 ng/ml (the concentration used in all previous experiments in this thesis) or high 50 ng/ml concentrations (Figure 4.1a), a concentration which has been previously reported in protocols to differentiate arterial endothelial cells from FLK1^{+} progenitors (Joo et al. 2012; Lanner, Sohl, and Farnebo 2007).

Higher VEGFA concentrations led to a significant increase in percentage of FLK1^{High} HE cells at Day 5.5 (33.6 ± 8.5% compared to 22.9 ± 8.6%, Figure 4.1b-c) , further pointing to the role that VEGFA plays in the transition from FLK1^{+} cells at Day 4.5 to FLK1^{High}PDGFRα^{-} cells at Day 5.5 and in their proliferation. Likewise, treating with 50 ng/ml of VEGFA led to a slight but significant decrease in FLK1 expression in FLK1^{High} cells at Day 5.5, as evidenced by a decrease in median fluorescence intensity (MFI) of signal by flow cytometry in FLK1^{High} HE cells (Figure 4.1c-d). This is likely due to increased internalization of activated FLK1 (Basagiannis et al. 2016), as opposed to an internal negative regulatory feedback mechanism, which has been reported for the soluble form of VEGFR-1 (Saito et al. 2013), but not membrane bound VEGFR-1 or VEGFR-2 (FLK1).

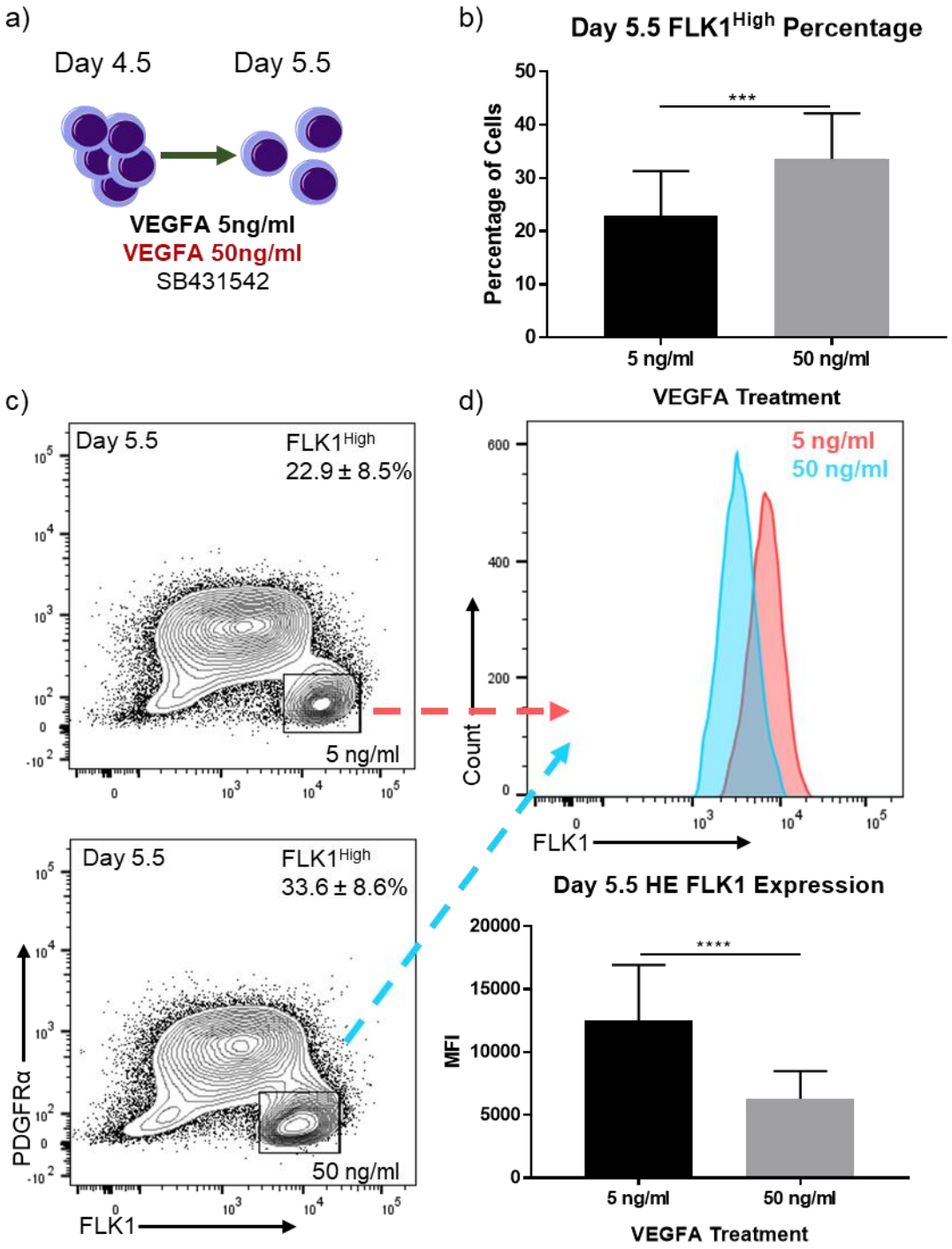

Figure 4.1. High Concentration of VEGFA leads to an increase in FLK1^{High} percentages and decreased FLK1 expression

a) Differentiation experimental design. Cells are treated with SB and either 5 ng/ml or 50 ng/ml VEGFA at Day 4.5. b) Percentage of FLK1^{High}PDGFRα^{-} cells at Day 5.5; n = 17 biological replicates. Averages ± SD depicted. Two-tailed, unpaired t-test. c) Representative flow cytometry plots of FLK1 and PDGFRα expression at Day 5.5 for 5 ng/ml and 50 ng/ml treated cells. d) Representative histogram and values of median fluorescence intensity (MFI) of Day 5.5 FLK1^{High} cells treated with 5 ng/ml or 50 ng/ml VEGFA; n = 17 biological replicates. Averages ± SD depicted. Two-tailed, unpaired t-test.

More importantly, treating with 50 ng/ml of VEGFA led to significant increases in the percentage of VE-Cad^{+}DLL4^{+} cells at Day 5.5 (Figure 4.2a-b). While only 4.9 ± 1.1% of cells at Day 5.5 express a VE-Cad^{+}DLL4^{+} immunophenotype when treated with 5 ng/ml at Day 4.5, 23.6 ± 13.2% of cells do so, with higher levels of DLL4 expression, when treated with 50 ng/ml. Changes were also seen at the gene expression level, with higher levels of *Dll4* expression in FLK1^{High} cells at Day 5.5 (Figure 4.2c) as well as downstream Notch genes *Hes1* and *Hey1*. This data is in agreement with published data which show VEGFA as an upstream agonist of *Dll4* and Notch signalling (Hayashi and Kume 2008). Interestingly, there was also a decrease in *Runx1* expression in high VEGFA-treated FLK1^{High} cells (Figure 4.2c), though this was not statistically significant. This is reminiscent of data which has shown the endothelial and arterial programmes to be mutually repressive of the haematopoietic programme (Lizama et al. 2015), as well as of data that shows that *Runx1* activation in the AGM is both time- and dosage-dependent on Notch (Kim et al. 2014; Zhang et al. 2015; Gama-Norton et al. 2015).

To further elucidate whether Notch played a role in *Runx1* regulation in these cells, a small molecule inhibitor, DAPT, which blocks γ-secretase, a critical cleavage enzyme in the Notch signalling process (Kopan and Ilagan 2009), was added to the cells alongside 50 ng/ml VEGFA at Day 4.5. The ability of DAPT to supress Notch signalling in FLK1^{High} cells was observed through *Hes1* signal in the 50 ng/ml + DAPT being equal to that of 5 ng/ml control, and *Hey1* being significantly lower (Figure 4.2d). In both 50 ng/ml treated samples with or without DAPT, *Runx1* levels were significantly lower than in control conditions. This could potentially suggest that in these cells, regulation of *Runx1* at this specific timepoint is Notch-

independent, similar to what has been described for second-wave HE in the YS (Hadland et al. 2004; Kumano et al. 2003). Interestingly however, significantly higher levels of arterial genes *Dll4*, *Efnb2*, and *Cxcr4* were observed in 50 ng/ml treated cells, levels which decreased to or below control levels when 50 ng/ml treated cells were also treated with DAPT (Figure 4.2d). This suggests that treating cells with high concentrations of VEGFA leads to a concomitant Notch-dependent activation of an arterial programme. Given that this is bulk RT-qPCR data obtained from sorting the $FLK1^{High}$ population, we cannot rule out the alternative explanation that high levels of VEGFA are driving more cells in the population towards an arterial endothelial fate instead of a haematoendothelial one, and therefore decreasing the overall *Runx1* levels expressed at the population level. The decreased levels of *Runx1* in the DAPT-treated sample could also be due to the significantly lower Notch signalling levels in this sample compared to both the 5 ng/ml and 50 ng/ml samples, evidenced by significantly lower *Hey1* expression. This would be in line with studies showing Notch-dependence of *Runx1* activation in HE populations (Zhang et al. 2015; Gama-Norton et al. 2015), and also shows some baseline level of Notch signalling in 5 ng/ml samples (indirectly evidenced by significantly lower levels of *Hey1* when DAPT is added to 50 ng/ml culture). To test whether endothelial TF levels were also affected at the population level due to high VEGFA and downstream Notch signalling, and were potentially responsible for *Runx1* regulation as has been previously described (Lizama et al. 2015), expression of HE *Sox17* as well as closely related endothelial TFs, *Sox7* and *Sox18* were measured (Figure 4.2e). No significant differences in expression of any of these genes was observed among 5 ng/ml, 50 ng/ml, and 50 ng/ml + DAPT treated cells, suggesting that, at the population level, high levels of VEGFA and

Notch signalling do not affect the expression levels of these endothelial transcription factors.

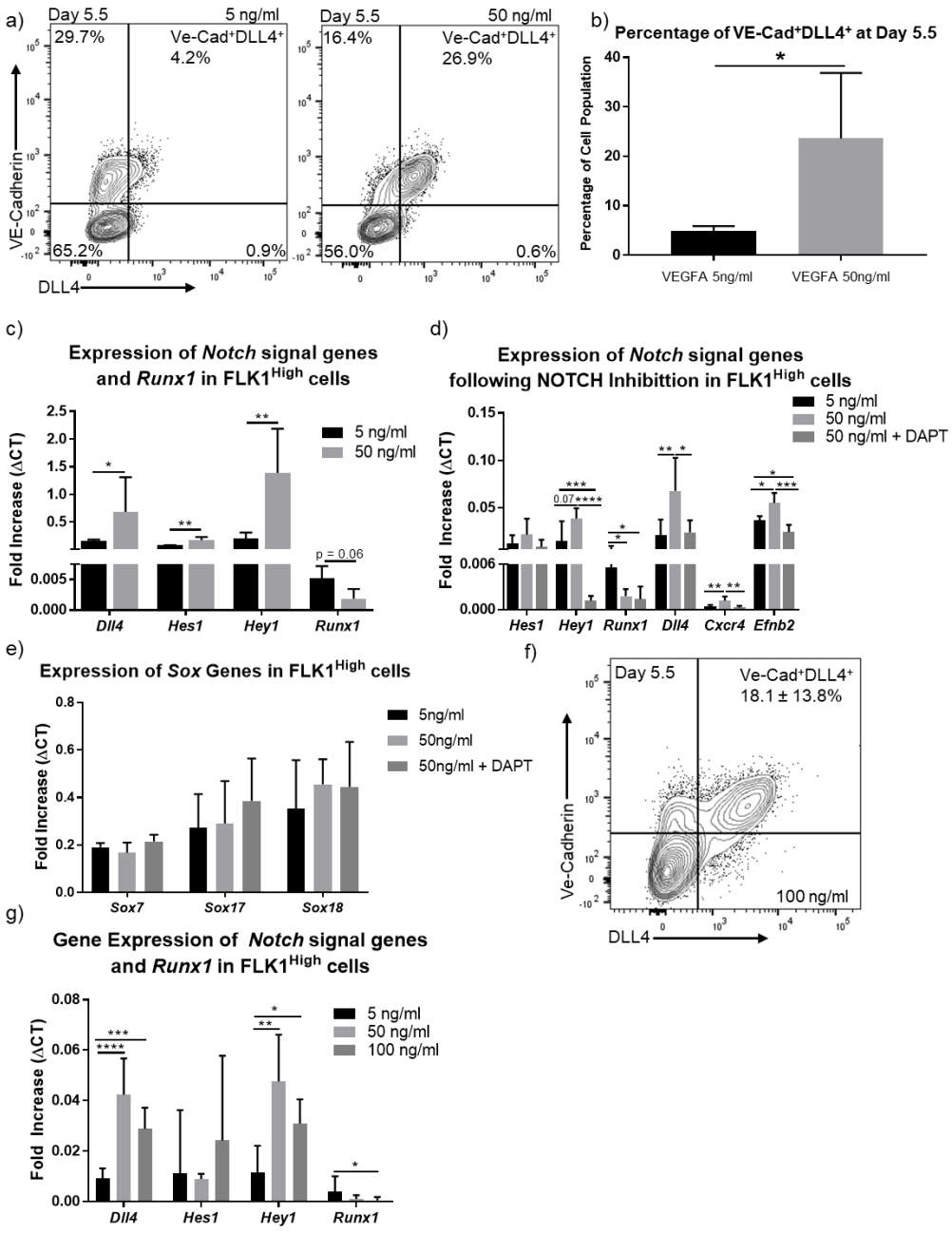

Figure 4.2 High Concentration of VEGFA leads to an Increase in DLL4 Expression and downstream Notch signalling

a) Representative flow cytometry plots of VE-Cadherin and DLL4 expression in Day 5.5 EBs treated with either 5 ng/ml or 50 ng/ml VEGFA at Day 4.5. b) Percentages of VE-Cad^{+}DLL4^{+} cells in EBs at Day 5.5. n = 5 biological replicates. Average ± SD depicted. Two-tailed, unpaired t-test. c) Gene expression by RT-qPCR of sorted FLK1^{High} cells from different treatment conditions. n = 3 biological replicates d) Gene expression of *Runx1*, notch, and arterial genes of FLK1^{High} cells at Day 5.5, including sample treated with γ-secretase inhibitor, DAPT; n = 3 biological replicates. One-way, ordinary ANOVA with Tukey's posthoc test for multiple comparisons used. e) *Sox* gene expression in FLK1^{High} cells at Day 5.5. n = 3, biological replicates separate from those in d f) Representative flow cytometry plot of VE-Cadherin and DLL4 in Day 5.5 cells treated with 100 ng/ml VEGFA at Day 4.5. n = 3 biological replicates. Average ± SD depicted g) Gene expression of Day 5.5 FLK1^{High} cells treated with 5, 50, and 100 ng/ml at Day 4.5; n =3 biological replicates One-way, ordinary ANOVA with Tukey's posthoc test for multiple comparisons used.

To test whether the effects of arterial activation and *Runx1* suppression were affected by dosages beyond 50 ng/ml, cells were treated with 100 ng/ml VEGFA (Zhang et al. 2008a) at Day 4.5 and $FLK1^{High}$ cells assayed for DLL4 expression as well as expression of *Dll4, Hey-1*, *Hes-1*, and *Runx1*. There were no significant differences ($p = 0.3$) between the percentages of $VE\text{-}Cad^{+}DLL4^{+}$ cells at 100 ng/ml and 50 ng/ml. Cells treated with 100 ng/ml had an average of 18.1 ± 13.9% cells expressing VE-Cad and DLL4 (Figure 4.2f), compared to 23.6 ± 13.2% in 50 ng/ml treated cultures (Figure 4.2a). Likewise, there were no differences in the expression of any genes tested in $FLK1^{High}$ cells among 50 ng/ml and 100 ng/ml conditions (Figure 4.2g). Given these data, 50 ng/ml was chosen as the treatment condition for further studies.

4.3. Short-term exposure to high VEGFA levels leads to activation and maintenance of key arterial genes in culture

To determine whether Notch signalling and activation of arterial genes affected downstream HE potential and function of FLK1^{High} cells, FLK1^{High} cells from both conditions were sorted at Day 5.5 and replated in serum-free media with HED cytokines, as previously described. However, here, VEGFA concentration in HED conditions was either 5 ng/ml or 50 ng/ml, corresponding to the VEGFA treatment received by the cells at Day 4.5 (Figure 4.3a).

While the presence of CD45^{+} cells was observed in cultures treated with control 5 ng/ml VEGFA, there were few CD45^{+} cells in cultures treated with 50 ng/ml (Figure 4.3b-c). Likewise, high levels of VEGFA seemed to have a detrimental effect on the cells' viability (Figure 4.3d) and ability to proliferate (Figure 4.3e), with cell counts and cell viabilities being significantly lower than control 5 ng/ml treated cells. While this effect of high VEGFA concentrations on viabilities and proliferation has not been reported for differentiating FLK1^{+} mouse endothelial cells, it has been documented in human serum-free systems (Sriram et al. 2015).

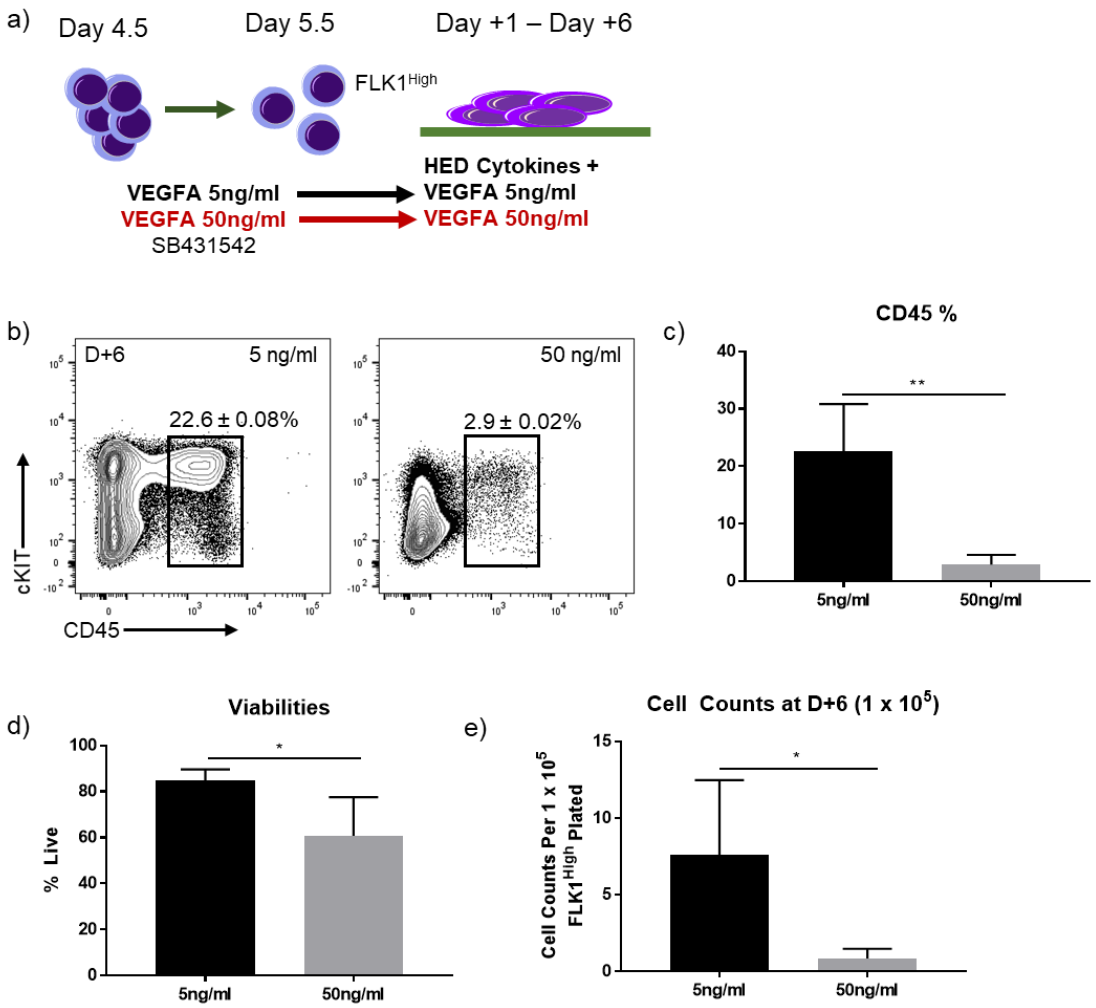

Figure 4.3 Long-term exposure to high VEGFA levels is detrimental to FLK1^{High} cells
a) Experimental strategy in which FACS-purified FLK1^{High} cells from either condition are plated into serum-free medium with either 5 ng/ml or 50 ng/ml VEGFA, according to original treatment at Day 4.5. Sorting gate strategy set as in 3.9 b) Representative flow cytometry plots for cKIT and CD45 expression 6 days after replating; n = 4 biological replicates. c) Percentage of CD45^{+} cells at Day +6. Average ± SD depicted; Two-tailed, unpaired t-test d) Total culture viabilities at Day +6; n = 4 biological replicates. Average ± SD depicted. Two-tailed, unpaired t-test e) Cell counts at day +6 per 1 x 10^5 FLK1^{High} plated at Day 5.5. n = 4 biological replicates. Average ± SD depicted. Two-tailed, unpaired t-test.

Given these lower viabilities and cell counts, culture conditions were adjusted so that cells were only transiently exposed to high VEGFA levels and Notch signalling at Day 4.5, and then returned to control levels of 5 ng/ml (Figure 4.4a). Increases in cell viability were observed in these conditions, though these were not statistically different to either control cultures or those in continued 50

ng/ml VEGFA (Figure 4.4b). Though no differences in viabilities (Figure 4.4b) and total cell counts (Figure 4.4c) were observed for cells in any of culture conditions for 2 and 4 days following plating, control conditions continued to have statistically higher cell counts than both conditions in which cells were treated with 50 ng/ml at Day 4.5, regardless of VEGFA treatment following sorting (Figure 4.4c). Though cells treated with only transient levels of VEGFA trended towards higher cell counts than cells in continued high VEGFA treatment at Day +6, these changes were not significant, and suggest restoring VEGFA levels to 5 ng/ml after cell sorting does not lead to significant improvements in cell proliferation. Returning the cells from 50 ng/ml to 5 ng/ml of VEGFA after plating also led to an increase in the percentage of $CD45^+$ cells in culture, though these percentages continue to be significantly lower than control conditions at 5 ng/ml 2 and 4 days after sorting, and are neither statistically higher than 50 ng/ml cultures nor lower than 5 ng/ml cultures 6 days after sorting (Figure 4.4d/f). Like cells in continued high VEGFA culture, cells in 50 to 5 ng/ml VEGFA cultures had significantly higher percentages of $cKIT^+VE\text{-}Cad^+$ cells than 5ng/ml cultures 4 and 6 days after replating (Figure 4.4e/g), data which is consistent with VEGFA as a driver of endothelial differentiation and identity. It is interesting that despite decreased levels of VEGFA after replating, the same or slightly higher percentages of endothelial cells are present in the culture than in cultures with maintained levels of high VEGFA, suggesting some measure of positive regulation which maintains these percentages of endothelial cells following the transient treatment with high VEGFA.

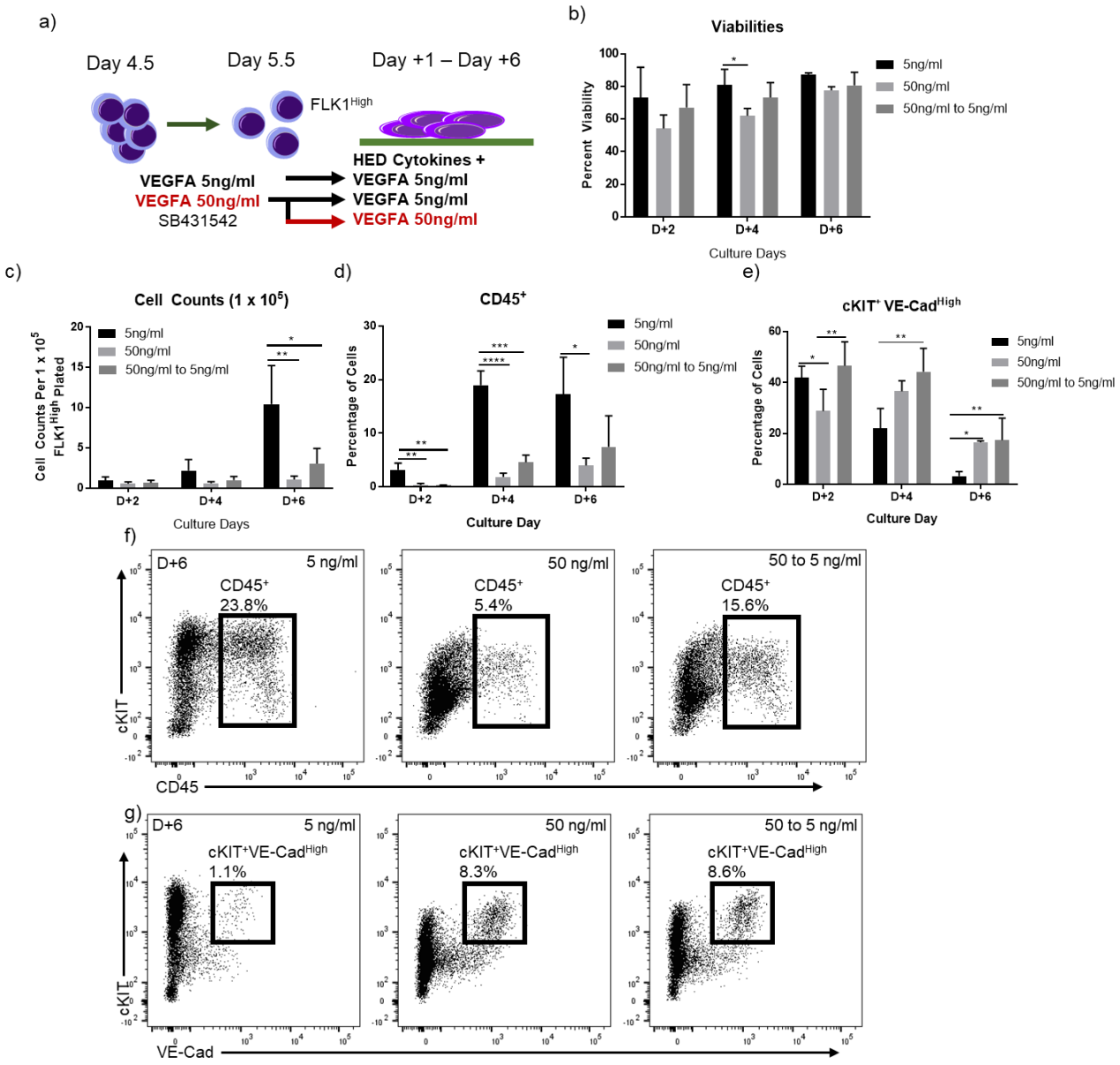

Figure 4.4. Decreasing levels of VEGFA partially rescues haematopoiesis
a) Experimental strategy: Day 5.5 FLK1^{High} cells treated with 50 ng/ml were sorted into wells containing either 50 ng/ml VEGFA or 5 ng/ml VEGFA, like control cells. b) Cell viabilities as measured by AO/PI staining at Day +2, +4, and +6. n = 4 biological replicates. Average ± SD depicted. Ordinary, one-way ANOVA with Tukey's posthoc test for multiple comparisons. c) Cell counts per 1 x 10^5 FLK1^{High} cells sorted and plated at Day 5.5 of culture. Average ± SD depicted. Ordinary, one-way ANOVA with Tukey's posthoc test for multiple comparisons. d) Percentage of CD45$^+$ cells, assayed by flow cytometry, in the culture at Day +2, +4, and +6. n = 4 biological replicates. Average ± SD depicted. Ordinary, one-way ANOVA with Tukey's posthoc test for multiple comparisons. e) Percentage of cKIT$^+$VE-Cad^{High} cells, assayed by flow cytometry, in the culture at Day +2, +4, and +6. n = 4 biological replicates. Average ± SD depicted. Ordinary, one-way ANOVA with Tukey's posthoc test for multiple comparisons. f) Representative flow cytometry plots associated with d, showing cKIT and CD45 expression at Day +6 across samples. g) Representative flow cytometry plots associated with e, showing cKIT and VE-Cad expression at Day +6 across samples.

Interestingly however, cells cultured in both 50 ng/ml and 50 to 5 ng/ml activated and maintained Notch signalling at the population level, as measured by *Hes1* and *Hey1* expression. Cells in these two conditions had higher levels of *Hey1* expression 4 and 6 days after replating when compared to cells grown in 5 ng/ml VEGFA, despite no significant differences 2 days after replating (Figure 4.5a). The same was true of *Hes1* expression, though in this case cells had significantly higher levels of *Hes1* at 4 days after replating, with no significance 6 days after plating (Figure 4.5a). Despite the fact that cells in 50 to 5 ng/ml VEGFA treatment trend towards lower expressions of these genes, these are still significantly higher than control (5 ng/ml) cultures, suggesting that, like the percentage of endothelial cells present in the cultures, the Notch programme is maintained to some degree after removal of high VEGFA levels.

Similar to this, expression of arterial genes *Dll4, Efnb2,* and *Nrp1* are significantly higher in 50 ng/ml than in 5 ng/ml control cultures at Day +4 and Day +6 (Figure 4.5b). For these three genes, this statistical significance is maintained as late as 6 days after replating, again suggesting that burst treatment of cells with high levels of VEGFA is sufficient to initiate a global arterial programme that is maintained for at least 6 days. Expression of *Itga2b* (CD41), on the other hand, is only significantly different to control at Day 5.5 and Day +4 in cells treated with 50 ng/ml VEGFA (Figure 4.5c).

Of note however, while venous transcription factor *COUP-TFII* is downregulated in 50ng/ml FLK1^{High} cells at day 5.5, both 50 ng/ml cells as well as 50 ng/ml to 5ng/ml cells express it at higher levels at Day +4 and +6. This could be due to the higher percentage of endothelial cells present in culture (Figure 4.4e), or to cells not expressing Notch at Day 5.5 that later proliferate. Additionally, this

could be due to the fact that, while a venous programme is originally repressed in favour of an arterial one by VEGFA signalling in endothelial cells, continued repression of venous *COUP-TFII* in differentiating endothelium depends on shear stress from blood flow in the dorsal aorta (Masumura et al. 2009; Othman-Hassan et al. 2001; Moyon et al. 2001), something missing from most *in vitro* culture systems, including this one.

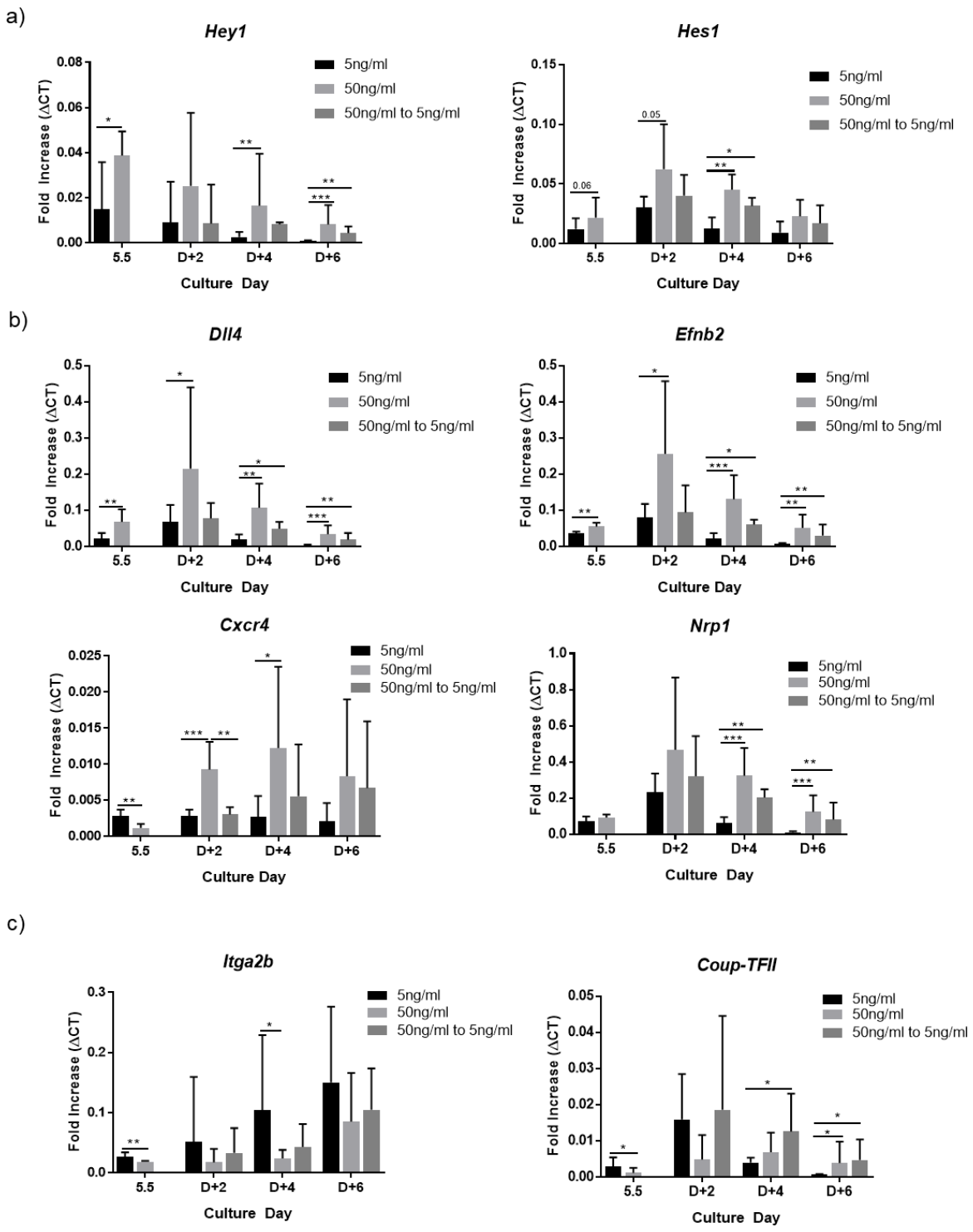

Figure 4.5 High levels of VEGFA lead to sustained global arterial programme
a) Expression of downstream Notch genes by RT-qPCR of sorted FLK1^{High} cells at Day 5.5, and unsorted cells at days +2, +4, and +6 of culture. n = 5 biological replicates; ± SD, One-sided ANOVA with Tukey's post-hoc test for multiple population comparison. b) As in a, except expression of arterial genes c) As in a, except expression of haematopoietic *Itga2b* and venous *Coup-TFII*.

To determine whether there was a dosage effect when treating cells with VEGFA at Day 4.5, various concentrations were tested, ranging from control 5 ng/ml to 75 ng/ml (Figure 4.6a). Preliminary data of n = 1 biological replicate suggested plateaus in *Dll4* and *Runx1* expression at Day 5.5 beyond the 50 ng/ml dose (Figure 4.6b-c), similar to what was seen when 100 ng/ml was compared to 5 and 50 (Figure 4.2g). More replicates however, as well as higher dosages would have to be tested in order to provide a proper titration curve. Data of n = 2 biological replicates also showed a plateau beyond 50 ng/ml in the percentage of cells expressing CD45 at Day +6 (Figure 4.6d-e), as well as in the percentage of $cKIT^{+}CD41^{+}VE\text{-}Cad^{-}$ HPCs (Figure 4.6 f and h). No apparent differences were observed in $cKIT^{-}CD41^{High}$ or $cKIT^{+}CD41^{+}VE\text{-}Cad^{High}$ populations at Day +6 (Figure 4.6 g and i). Given this lack of discernable differences beyond the 50 ng/ml dosage, this dosage was maintained for further experiments.

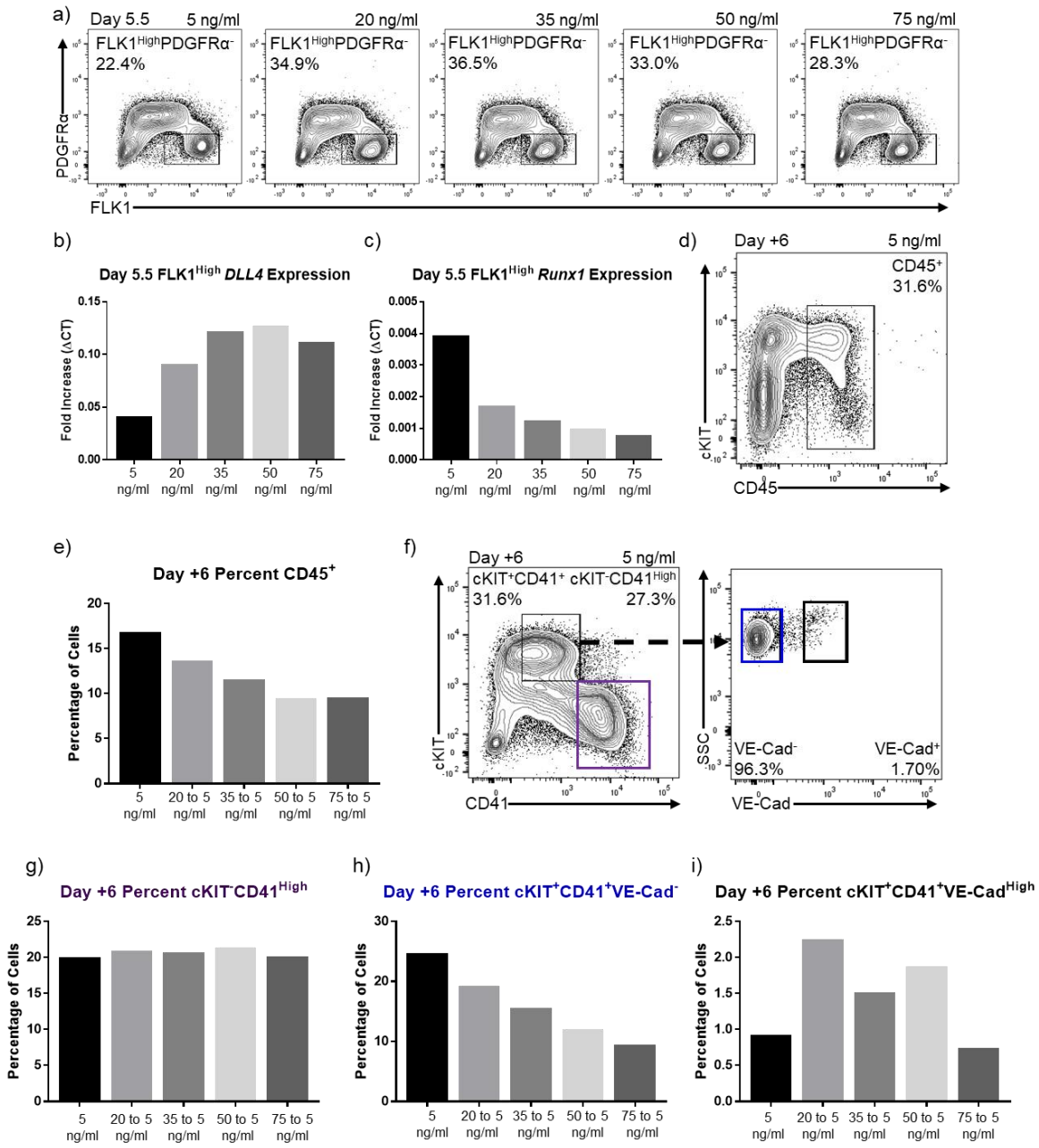

Figure 4.6 Downstream Effects of VEGFA Titration at Day 4.5

a) Representative flow cytometry plots of FLK1 and PDGFRα expression at Day 5.5 following addition of different VEGFA concentrations at Day 5.5. b) *Dll4* expression by RT-qPCR of sorted FLK1^{High} cells at Day 5.5. Average of two technical replicates from one biological replicate are depicted. c) As in b, except depicting *Runx1* expression d) Representative flow cytometry plot depicting cKIT and CD45 expression of replated FLK1^{High} cells at Day +6. e) Average percentage of CD45^{+} cells at Day +6 in cultures from different VEGFA concentrations at Day 4.5 replated in 5 ng/ml after sorting. n = 2 biological replicates. f) Representative flow cytometry plots depicting cKIT, CD41, and VE-Cad expression of replated FLK1^{High} cells at Day +6. g-i) Average percentage of gated cells as in f, from different VEGFA concentrations at Day 4.5. n = 2 biological replicates.

4.4. Global arterial programme leads to no differences in HSPC phenotype and function

To determine the effect of a transiently activated arterial and Notch programme on the downstream phenotype and function of HSPCs, as well as to assay for the presence of AGM-like progenitors, cells were differentiated in low (5 ng/ml) and high (50 ng/ml) VEGFA concentrations and sorted as in previous sections, but replated only in 5 ng/ml VEGFA, regardless of VEGFA treatment at Day 4.5 (Figure 4.7a). Given the presence of an arterial program and HSPCs in the culture, cells at Day +6 were then stained for a recently described immunophenotype of Type I and Type II Pre-HSCs. These cells have been described as being present in the developing DA and able to differentiate into engrafting HSCs when plated on supportive stromal cells (Zhou et al. 2016; Gordon-Keylock et al. 2013).

While slightly higher percentages and cell counts of cells expressing the Type I $CD31^{+}CD41^{Low}CD45^{-}cKit^{+}CD201^{High}$ phenotype (Figure 4.7b) were present at Day +6 in the 50 ng/ml to 5 ng/ml condition when compared to 5 ng/ml control, this was not statistically different (Figure 4.7b-d). This trend was not observed for the Type II phenotype of $CD31^{+}CD45^{+}cKit^{+}CD201^{High}$ (Figure 4.7e) on the same samples, where both conditions contained Type II Pre-HSC cells at nearly negligible percentages and counts in culture (Figure 4.7e-g). This shows that, at least at an immunophenotypic level, increasing VEGFA levels and activating Notch signalling has little effect on these cells. Of course, the possibility that at Day +6 cells have moved past the Pre-HSC stage in culture is possible. Preliminary data of n =1, however, showed no apparent differences in Pre-HSC percentages at Day +4 either (data not shown).

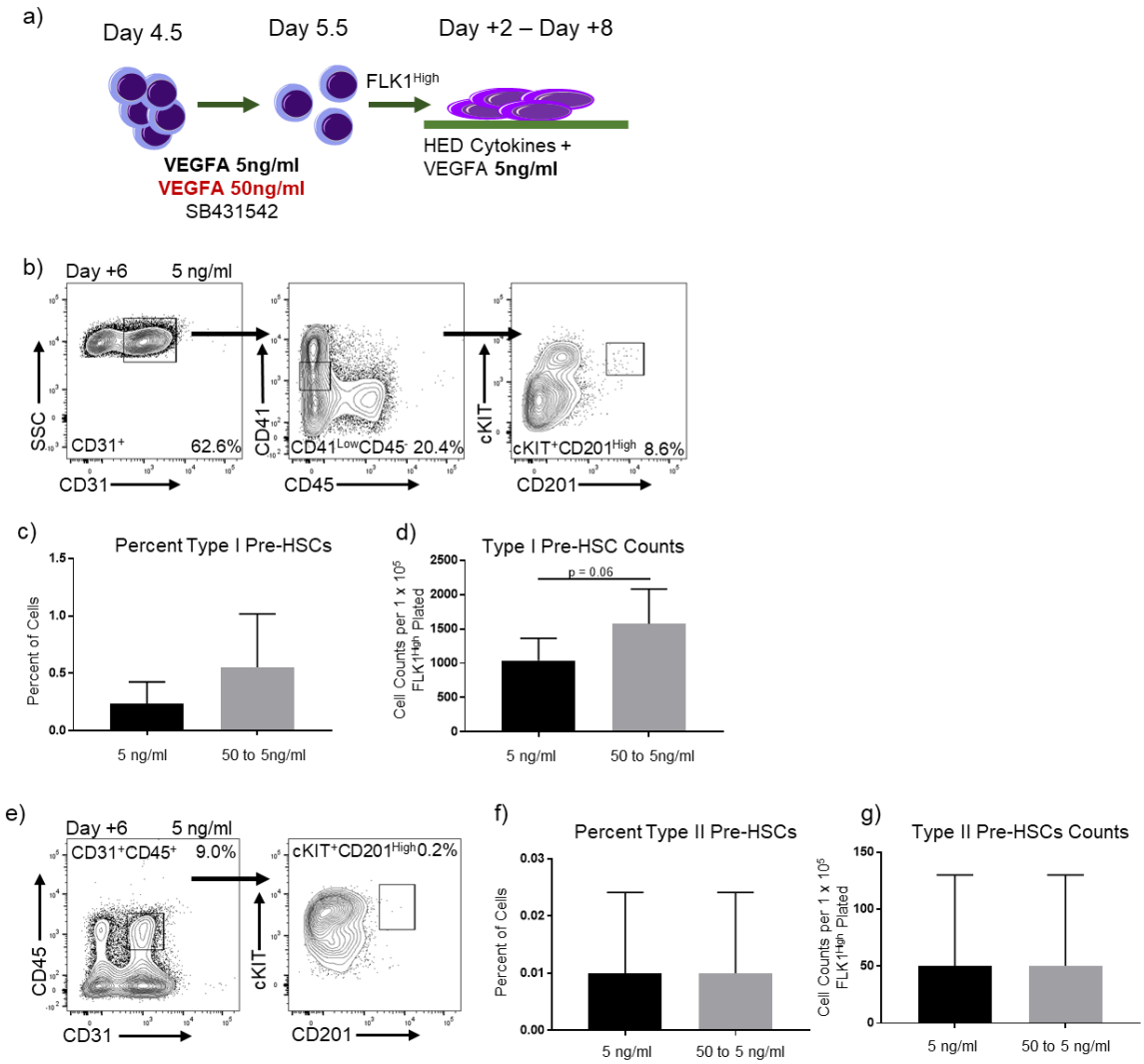

Figure 4.7. Type I and Type II Pre-HSCs in culture

a) Experimental procedure: Cells were differentiated as in previous experiments and Day 5.5 FLK1^{High} cells sorted into HED medium with 5 ng/ml VEGFA, regardless of VEGFA conditions at Day 4.5. b) Representative flow cytometry plots of control conditions at Day +6 showing gating strategy for Type I Pre-HSC (CD31^{+}CD41^{Low}CD45^{-}cKIT^{+}CD201^{High}) c) Percentage of cells in culture expressing a Pre-HSC Type I phenotype at Day +6. No significance using two-tailed, unpaired t-test; Average ± SD depicted, n = 4 biological replicates. d) Type I pre-HSC cell counts at Day +6 per 1 x 10^{5} FLK1^{High} cells plated at Day 5.5. Two-tailed, unpaired t-test; Average ± SD depicted, same n = 4 biological replicates from (b – c). e) Representative flow cytometry plot and gating strategy for Pre-HSC Type II phenotype (CD31^{+}CD45^{+}cKIT^{+}CD201^{High}) on same samples as (b – d). f) Percentage of cells in culture expressing a Pre-HSC Type II phenotype. No significant differences using two-tailed, unpaired t-test; Average ± SD depicted, n = 4. g) Type II pre-HSC cell counts at Day +6 per 1 x 10^{5} FLK1^{High} cells plated at Day 5.5. Two-tailed, unpaired t-test; Average ± SD depicted, same n = 4 biological replicates as (b – f).

To determine whether cells had differentiated towards more mature HSCs during culture time, cells at Day +6 and Day +8 were also stained for the adult HSC markers Lineage^{-}Sca1^{+}cKit^{+} (LSK) and CD48^{-}CD150^{+} (SLAM) (Figure 4.8a). Gates

for Lineage stain, CD48, and CD150 were all set using fluorescence minus one (FMO) with isotype controls (Supplementary Figure 4.1). As with Pre-HSC stains, no differences were observed in the percentage nor counts of LSK (Figure 4.8b-c) or LSK SLAM (Figure 4.8d-e) cells between treatment conditions at either Day +6 or Day +8, though statistics were performed only on Day +6 LSK samples, given n = 2 biological replicates for LSK samples at Day +8 and LSK SLAM samples for both Day +6 and Day +8. The presence of immunophenotypic LSK cells in 5 ng/ml treated samples, suggests that even progenitors arising in a second-wave-like *in vitro* environment (Chapter 3), can present an LSK immunophenotype. The expression of Sca1 had been previously been reported for this system (Irion et al. 2010), despite clear *in vivo* evidence that places it as a marker of intraembryonic haematopoietic tissue only at early developmental stages (McGrath et al. 2015; Chen et al. 2011). Though a small percentage of cells at this time also express an LSK SLAM immunophenotype, it does so with high variabilities. Given this system hasn't been previously reported to produce engrafting HSPCs (Irion et al. 2010; Clarke et al. 2013), it is unlikely that this small percentage of cells contains engrafting potential. While slight increases in $Lin^{-}cKit^{-}Sca1^{+}$ were observed in cells treated with 50 ng/ml (data not shown), further inquiry into this population fell outside the scope of this thesis.

To assess progenitor function, bulk cultures from Day +6 were taken and replated in methylcellulose with haematopoietic cytokines for colony forming unit (CFU) assays (Figure 4.8f). All colony types save GEMM were observed, with lower total colony counts in the 50 to 5 ng/ml conditions (Figure 4.8g), mirroring LSK progenitor percentages and counts (Figure 4.8b), and confirming the lower percentages of $CD45^{+}$ cells observed in these conditions (Figure 4.4d). The

majority of the colonies formed were of GM origin for both conditions, followed by G colonies, similar to previously published observations in this differentiation system (Irion et al. 2010). The presence of E and M colonies in both samples shows that progenitors of all common myeloid lineages are produced from the replated $FLK1^{High}$ cells in this system, including GM progenitors of multilineage potential. Except for differences in colony count, no other apparent differences are observed when cells are treated with high VEGFA concentrations at Day 4.5.

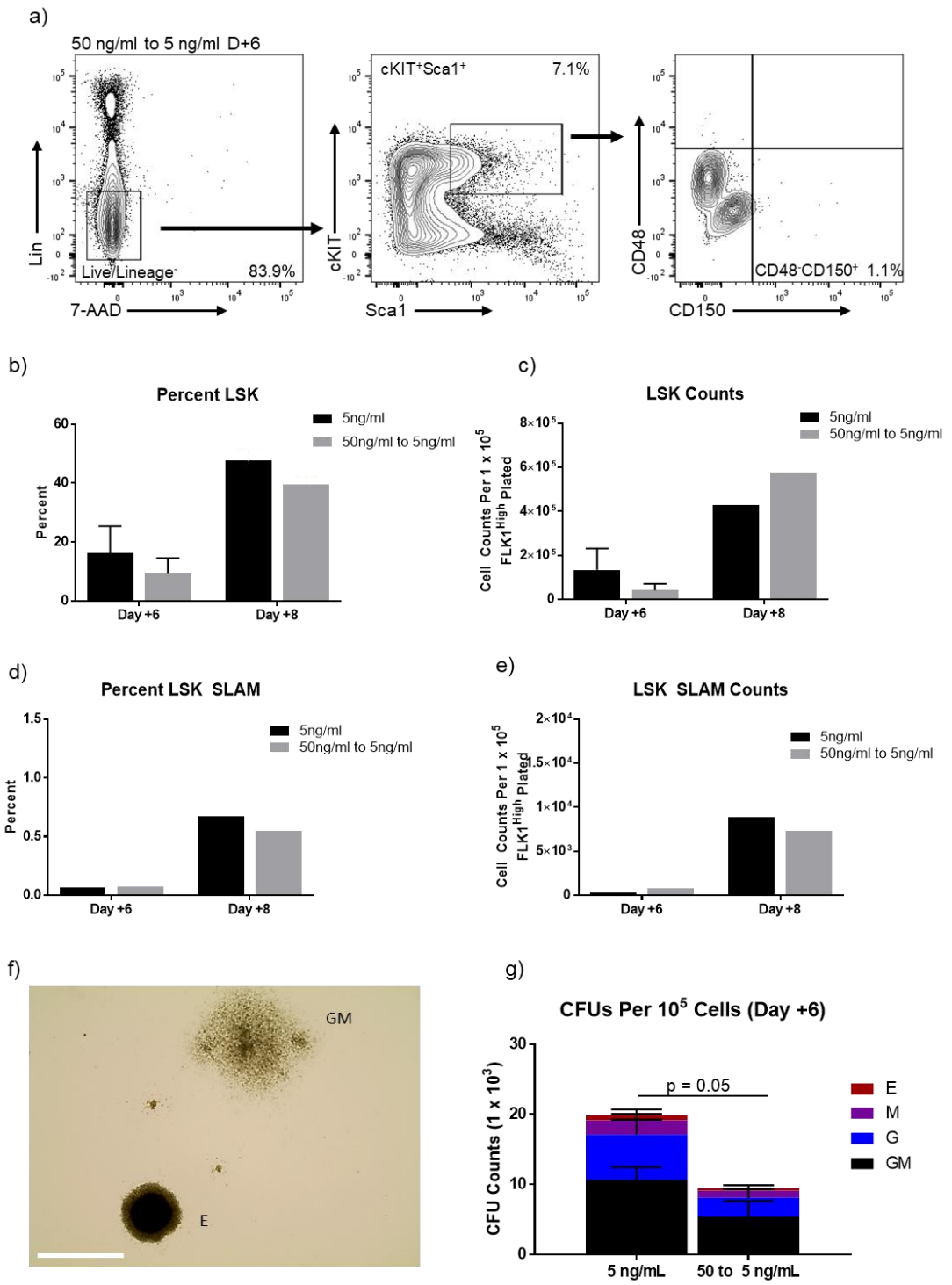

Figure 4.8 LSK SLAM Immunophenotype and CFU

a) Representative flow cytometry plots and gating strategy for LSK and LSK SLAM populations. b) LSK percentages of culture at Day + 6 (n = 3 biological replicates) and Day +8 (n = 2 biological replicates). c) LSK counts at Days +6 and +8 per 1 x 10^5 FLK^{High} cells plated at Day 5.5. Same replicates as in b. d) LSK SLAM percentages of culture at Day +6 and Day +8; n = 2 biological replicates for both timepoints. e) LSK SLAM counts at Days +6 and +8 per 1 x 10^5 FLK^{High} cells plated at Day 5.5. Same replicates as in d f) Representative image of Erythroid (E) and GM (Granulocyte/Macrophage) colonies; scale bar = 1mm. e) CFU counts per total 1 x 10^5 cells in culture at Day +6: M = macrophage; G = granulocyte. n = 3 biological replicates. Averages ± SD depicted. Two-tailed, unpaired t-test.

4.5. An *in vitro* DLL4+ HE with haematopoietic progenitor potential

Given contradicting data in the literature regarding the haemogenic potential of $DLL4^+$ endothelium (Ditadi et al. 2015; Hadland et al. 2017; Park et al. 2018; Uenishi et al. 2018), as well as to further characterise the differentiation system in more detail, VE-Cad^+ cells at Day 5.5 from both 5ng/ml VEGFA and 50ng/ml VEGFA systems were sorted based on $DLL4^+$ expression into HED medium containing 5ng/ml VEGFA and differentiated for 6 days after replating (Figure 4.9a, Supplementary Figure 4.2a).

Cells were then stained at Day +6 for CD41, cKIT, and VE-Cad expression to characterise the presence of $CD41^{High}cKIT^-$, $CD41^+cKIT^+$VE-Cad^- and $CD41^+cKIT^+$VE-Cad^{High} progenitors (Figure 4.9b) described in previously published literature (Frame et al. 2016; McGrath et al. 2015), and in Section 3.6 of this thesis. $DLL4^-$ cells in both conditions gave rise to mostly $CD41^{High}cKIT^-$ megakaryocyte-like progenitors (Figure 4.9b, left column, rows 1 and 3; Figure 4.9c, top plot). Conversely, $DLL4^+$ cells in both conditions gave rise to mostly immunophenotypic $cKIT^+CD41^+$VE-Cad^{High} cells (Figure 4.9b, right column; Figure 4.9c, middle plot). This confirmed past data that showed that cells treated with high levels of VEGFA (in which most VE-Cad^+ cells were also $DLL4^+$) maintained higher percentages of $cKIT^+$VE-Cad^{High} cells at Day +6 (Figure 4.4e).

Interestingly, $DLL4^-$ cells differentiating from cells treated with 50 ng/ml gave rise to some residual VE-Cad^{High} cells by Day +6, similar to the $DLL4^+$ cells, though these percentages were significantly lower than in cultures deriving from $DLL4^+$ cells (Figure 4.9c, middle plot). This could be due to cells exposed to high levels of VEGFA which do not yet express DLL4 at time of sorting and are therefore sorted

with the DLL4^{-} negative fraction. Single-cell sorting strategies would have to be undertaken to test this explanation. Likewise, further sorting and gene expression studies are required to ascertain whether immunophenotypic cKIT^{+}CD41^{+}VE-Cad^{High} cells arising from these cultures at Day +6 contain haematopoietic potential, and whether or not they express an arterial, venous, haematopoietic programme, or any combination of those.

Importantly however, cKIT^{+}CD41^{+}VE-Cad^{-}, cells immunophenotypically resembling EMPs, only arise in low percentages from the DLL4^{-} population in cultures treated with 5 ng/ml, while the DLL4^{+} sorted cells do not give rise to them (Figure 4.9b, top two rows; Figure 4.9c, bottom plot). In cells treated with 50 ng/ml however, both DLL4^{-} and DLL4^{+} cells give rise to these cells (Figure 4.9b, bottom two rows; Figure 4.9 c, bottom plot), albeit at high variabilities, showing a potential DLL4^{+} functional HE population in our own system, as has been recently described in differentiating human system (D'Souza, Kumar, and Slukvin 2018; Park et al. 2018).

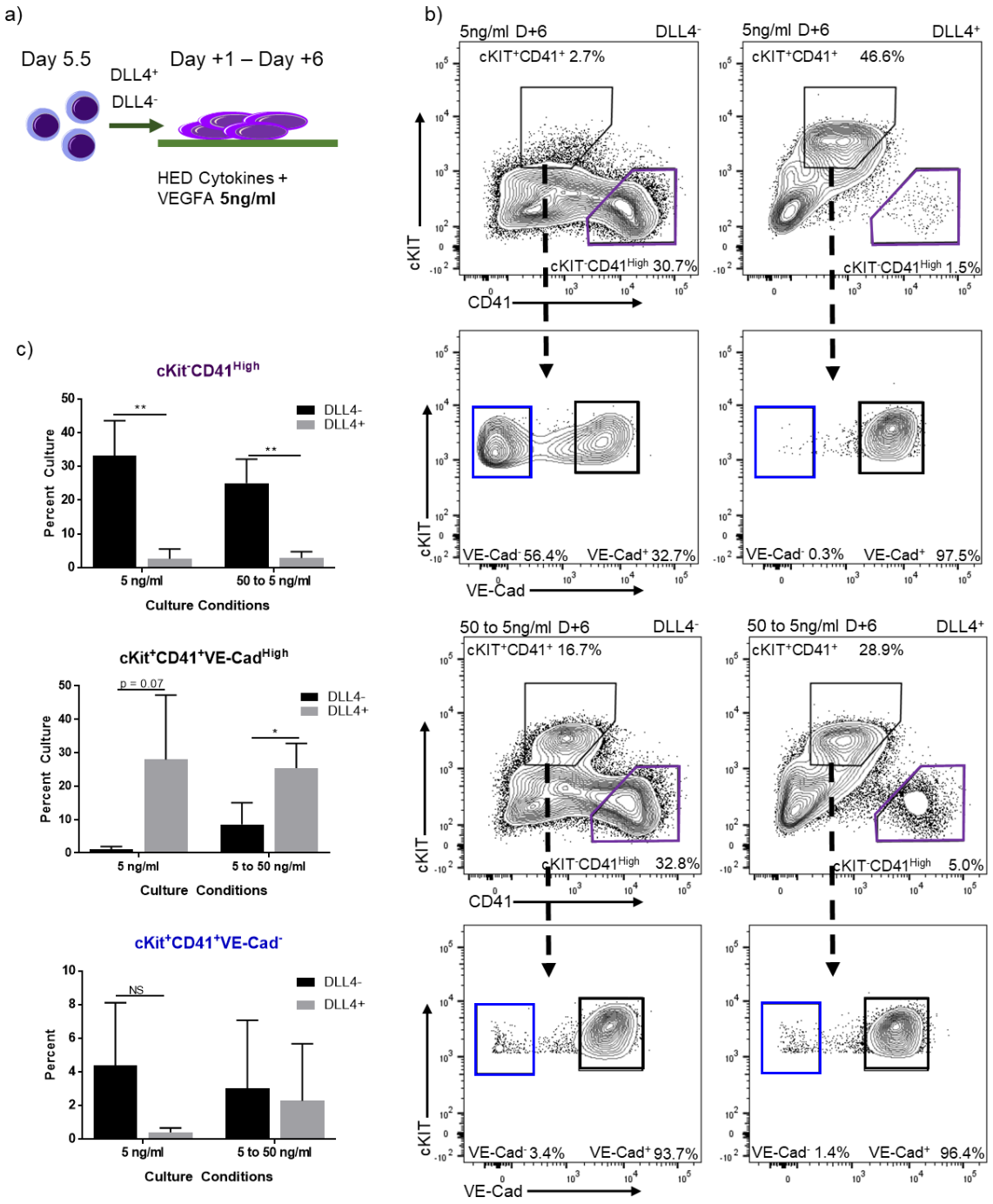

Figure 4.9 Haematopoietic Potential of DLL4$^-$ and DLL4$^+$ HE

a) Differentiation scheme. Cells were differentiated as per previous experiments, in 5 or 50 ng/ml VEGFA from Day 4.5 to 5.5, and then sorted at Day 5.5 based on VE-Cad$^+$ and either DLL4$^+$ or DLL4$^-$ expression. Gating strategy for sorting and purity checks in Supplementary Figure 4.2 b) Representative flow cytometry plots of cKIT, CD41, and VE-Cad expression of cells from each sample at Day +6 after replating. c) Percentages of cKIT$^-$CD41^{High} progenitors, cKIT$^+$CD41$^+$VE-Cad^{High}, and cKIT$^+$CD41$^+$VE-Cad$^-$ cells in culture at Day +6. n = 3 biological replicates. Averages ± SD depicted. Two-tailed, unpaired t-test between DLL4$^-$ and DLL4$^+$ from same VEGFA treated sample.

To test the haematopoietic potential of progenitors arising from this population in an unbiased way, bulk cultures at Day +6 from all samples were replated in CFU assays (Figure 4.10a). Confirming the lack of EMP-like or Meg-like progenitors detected immunophenotypically by flow cytometry, cells arising from 5 ng/ml DLL4^{+} cells showed no CFU potential, with an occasional small single E or G colony appearing per plate. This shows that, at least in these conditions, the cKIT^{+}CD41^{+}VE-Cad^{High+} populations contain no haematopoietic potential without further differentiation. Therefore, as far as was tested, all haematopoietic potential for 5 ng/ml treated cells resides in the DLL4^{-} endothelium, similar to what has been reported in some human systems (Ditadi et al. 2015).

On the other hand, while DLL4^{-} cells from 50 to 5 ng/ml showed most haematopoietic potential, some potential from colonies resembling GM colonies was also observed in the DLL4^{+} cells from this sample. In fact, haematopoietic potential from these cells was almost exclusively restricted to small numbers in high variabilities (an average of 0, 1.5, 10, and 34 per plate across biological replicates) of these colonies larger, and therefore more highly proliferative, than those arising from DLL4^{-} cells in either 5 ng/ml or 50 to 5 ng/ml treated cells (Figure 4.10b). Given low colony counts and high variabilities, CFU counts from these 50 to 5 ng/ml DLL4^{+} cells were not statistically higher than 5 ng/ml DLL4^{+} colony counts, though differences were apparent. It needs to be noted that further assays to determine the nature of the colonies (flow cytometry for immunophenotype and cytospins for morphology) are lacking. Likewise, though no impurities from the CD41^{-}VE-Cad^{+}DLL4^{-} were present in the DLL4^{+} sample, as evidenced by post-sort purity checks at Day 5.5, there were impurities from the CD41^{-}VE-Cad^{-} fraction (Supplementary Figure 4.2b), and could account for the small number of

progenitors at Day +6. Of course, if impurities were the cause for the appearance of these colonies, one would expect an equal number, in the DLL4^{+} fraction from 5 ng/ml samples, which were sorted on the same machines on the same day. Regardless, more replicates and assays, including single cell sorting at Day 5.5, are required to characterise this population more precisely.

Should these results be confirmed by future studies, they would resemble what has recently been reported in human and mouse studies (D'Souza, Kumar, and Slukvin 2018; Park et al. 2018; Hadland et al. 2017), and confirm the presence of a DLL4^{+} HE population in mice that can give rise, at the population level, to multilineage haematopoietic progenitors. More importantly however, this could also suggest that early exposure to VEGFA and Notch signal activation affects downstream haematopoietic potential of DLL4^{+} endothelium.

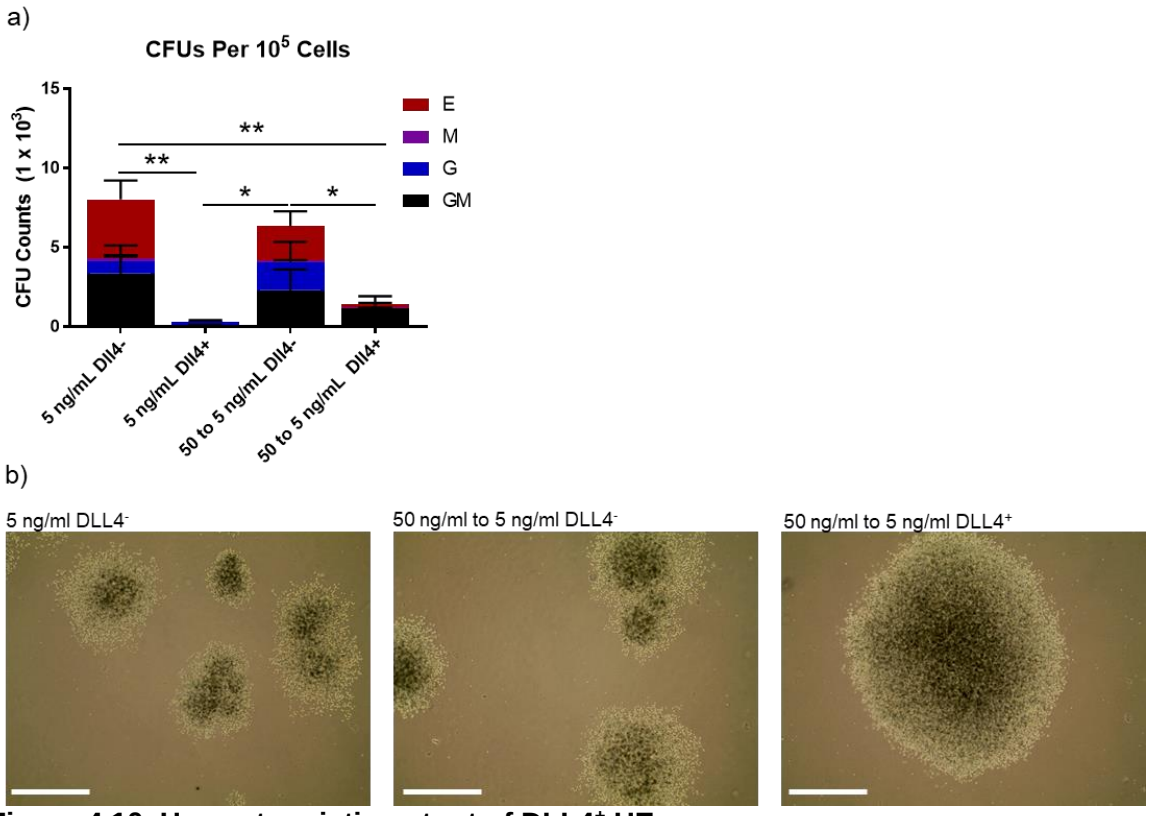

Figure 4.10. Haematopoietic output of DLL4^{+} HE
a) CFU assays for bulk cells at Day +6. n = 4 biological replicates; Two-sided ANOVA with post-hoc Tukey's correction for multiple comparisons. b) Representative images of large colonies in samples. Scale bar = 1 mm.

4.6. Discussion

Previous studies have shown the importance of VEGFA signalling on both arterial as well as haematopoietic programmes in the developing DA in *Xenopus* and zebrafish (Cleaver and Krieg 1998; Gering and Patient 2005; Ciau-Uitz et al. 2010; Ciau-Uitz et al. 2013; Leung et al. 2013). Our *in vitro* data showed that Day 4.5 $FLK1^+$ cells can be induced to activate Notch signalling and an arterial programme in high levels of VEGFA (50 ng/ml) when compared to control conditions (5 ng/ml), in line with what has been previously reported (Joo et al. 2012; Zhang et al. 2008a; Lanner, Sohl, and Farnebo 2007).

This increase in VEGFA does not only lead to arterial differentiation, but also prevents the cells from activating *Runx1*. In order to compare these results to *in vivo* studies, which have found Notch timing and dosage to be critical for *Runx1* activation in the DA (Richard et al. 2013; Huang et al. 2013; Zhang et al. 2015; Gama-Norton et al. 2015), further exploration of the Notch ligands and receptors present at both Day 4.5 and Day 5.5 are required. This would help to determine whether or not some of the HE produced in this system is similar to second-wave haematopoiesis, which is Notch independent, or third-wave, which is Notch dependent (Hadland et al. 2004; Kumano et al. 2003). Though endothelial TFs *Sox7, Sox17,* and *Sox18* have been shown *in vivo* to be repressive of *Runx1* and a haematopoietic programme (Lizama et al. 2015), VEGFA is, in our cultures, not affecting the expression of these genes, as differences in levels of these TFs were not noted in different conditions. Further studies, particularly at the single-cell level, are required to fully understand this regulation of *Runx1* and could lead to interesting insights on the role, if any, that VEGFA plays in *Runx1* regulation, whether through or independent of, Notch signalling pathways. These studies

were, quite unfortunately, outside the scope and timing of this thesis. They will ultimately help elucidate the different ways in which VEGFA regulates HE differentiation, both in second-wave and third-wave haematopoiesis, and potentially lead to insights that allow better design of differentiation protocols.

While plating FLK1^{High} cells in high levels of VEGFA negatively impacts cell viability and counts, as well as haematopoietic output and cluster formation, returning cells to low levels of VEGFA allows for haematopoietic development alongside the differentiation of a global arterial niche. Studies which explore the ways in which VEGFA affects the cycling and proliferation of endothelial, HE, and haematopoietic cells are needed to elucidate whether or not this decrease in proliferation is of importance to HSPC function in this system, as HSCs *in vivo* have been shown to be mostly in quiescent G_0 phase (Nakamura-Ishizu, Takizawa, and Suda 2014; Batsivari et al. 2017).

Transient treatment with high levels of VEGFA and Notch activation does not lead to differences in the percentages of Type I or Type II pre-HSCs in culture, nor to the presence of SLAM LSK cells. One possibility for this is that, given that the HE that develops is second-wave like, it lacks the required mesodermal programming as well as the ability to respond to Notch signalling in a way that leads to engrafting HSCs, and is in line with the literature that shows Notch signalling and an arterial niche on their own are not sufficient for HSC differentiation. Very recently, human iPSC studies have shown the existence of definitive HE which expresses arterial markers and genes and also gives rise to lymphoid cells and cells which express foetal and adult globin at higher frequencies than non-arterial HE (Park et al. 2018; Uenishi et al. 2018). Importantly, this population of cells is dependent on Notch signalling to activate EHT, similar to AGM

HE. Similarly in the developing mouse, DLL4^{+} cells have been shown to be precursors to engrafting HSCs, while DLL4^{-} HE differentiates into non-engrafting progenitors (Hadland et al. 2017). Treating cells with high levels of VEGFA in our system also leads to the presence, albeit at very low frequencies, of DLL4^{+} cells with haematopoietic potential restricted mostly to colonies resembling GM colonies, though further characterization is required to test their actual phenotype. This is in stark contrast to DLL4^{+} cells sorted from cultures treated with 5 ng/ml, which do not have any haematopoietic potential when replated in CFU assays, similar to what has been previously reported in other human systems (Ditadi et al. 2015). Indeed, contradicting studies in human differentiation systems use different concentrations of VEGFA in their cultures, which, like in our system, could explain contrasting results. Studies which report Notch-dependent DLL4^{+} HE use 50 ng/ml of VEGFA throughout culture (D'Souza, Kumar, and Slukvin 2018), while studies which report no haematopoietic potential in DLL4^{+} endothelium and all definitive HE potential in the DLL4^{-} endothelium initially use 15 ng/ml and decrease to 5 ng/ml for EHT conditions (Ditadi et al. 2015). Of course, it should also be noted that the timing at which these cells are collected in these studies is different, with the DLL4^{+} HE being described at Day 5 of an EB culture while the DLL4^{-} HE study looks at DLL4 expression at Day 8 of culture, making it difficult compare and rule out the possibility that in these studies, definitive HE also passed through a DLL4^{+} HE intermediate.

One difference that our system had to other studies reporting DLL4^{+} HE is that the haematopoietic output of DLL4^{+} cells is restricted to very few and large, seemingly multilineage myeloid colonies, while in human studies CFU potential from DLL4^{+} cells is both varied as well as higher in numbers than for DLL4^{-} cells

(Uenishi et al. 2018). In contrast to our own studies however, DLL4^{+} cells were plated on OP9-DLL4 supportive stroma, as opposed to Matrigel, which could explain these discrepancies. The level of DLL4 expression, or impurities in the population arising from sorting could also be responsible for this. Single-cell index-sorting strategies, such as those used by (Hadland et al. 2017), in which the DLL4 level of every single cell sorted is recorded, are required to address both of these concerns.

Single cell differentiation assays with both these *in vitro* populations, as well as those found in the yolk sac and AGM, are also required to more fully understand how VEGFA dosing regulates *Runx1* and EHT through both Notch-dependent and Notch-independent pathways, and leads to HE potential of DLL4^{+} cells. Despite study caveats, these data show that the context in which arterial progenitors are produced (in this report, specific to VEGFA signalling) can influence their downstream haematopoietic potential and provides a well-characterised system in which mouse DLL4^{-} and DLL4^{+} cells can be used for further mechanistic and molecular studies.

5. Modelling Human Arterial Haematopoiesis

5.1. Introduction

While differentiating mESC systems are a powerful tool with which to explore mammalian haematopoiesis, the development of iPSC technology has allowed the field to undertake similar experiments with human PSC sources. This not only circumvents the ethical concerns with using human ESCs, but also allows for disease modelling and genetic correction of human cells *ex vivo*. As mentioned in section 1.1, many obstacles remain before clinically-safe engrafting HSCs differentiated from h-iPSCs can be brought to the clinic.

Only one pre-print protocol has reported the production of engraftable HSCs from h-iPSC sources without the use of ectopic expression of potentially oncogenic TF (Guyonneau-Harmand et al. 2017). Unfortunately, this serum-free system has not yet been properly characterised or optimized, and continues to await peer review. It is still unknown which of all the growth factors used in this study are required for HSC differentiation and at which times.

Other *in vitro* studies published during the course of this thesis however, have made great strides at providing insights into the mechanisms that drive human mesodermal cells towards first- or second-wave haematopoiesis. Of particular note, one group has shown that mesodermal patterning through small molecule repression and activation of Activin/Nodal and Wnt/β-catenin pathways, respectively, is required to downregulate primitive (first-wave) and enrich for definitive (second-wave) haematopoietic programmes (Kennedy et al. 2012; Sturgeon et al. 2014; Ditadi et al. 2015). Shortly before gastrulation in the developing mouse embryo (E5.5), spatial axes are established based on growth factor gradients. Specifically, the proximal/distal axis, which determines cell commitment to extra-embryonic or embryonic tissue, is determined by a Nodal

signalling gradient; higher levels of Nodal correspond to the proximal, extra-embryonic tissue (Arnold and Robertson 2009). In a similar manner, canonical Wnt/β-catenin gradients determine the posterior/anterior axis, higher levels of Wnt corresponding to the posterior of the embryo (Arnold and Robertson 2009). Using small molecules to block and activate these pathways *in vitro*, where spatial cues are missing, is meant to drive the differentiation of the correct mesodermal populations, and enriches for definitive haematopoietic progenitors (Kennedy et al. 2012; Sturgeon et al. 2014; Ditadi et al. 2015). A follow-up study found this patterning also activates *HOXA* cluster genes (Ng et al. 2016), critical for adult HSC and progenitor function (Alharbi et al. 2012). The study also reported activation of some arterial genes in endothelial populations, albeit at low levels, together with expression of venous genes. Despite this, mesodermal patterning alone is insufficient to drive the *in vitro* generation of HSPC populations.

As has been mentioned in previous chapters, whether HE needs to activate an arterial programme to give rise to HSCs is unknown (Chapter 1, Figure 1.7). Most of the seemingly contradictory literature on the topic has been very recently published describing human *in vitro* systems. On one hand, studies show $DLL4^-$ HE gives rise to definitive HSPCs, at least in second-wave haematopoiesis (Ditadi et al. 2015; Ayllón et al. 2015), while others show that $DLL4^+$ HE does exist *in vitro* and leads to definitive HSPC differentiation (Park et al. 2018; Uenishi et al. 2018). In the previous chapter, we discussed how our own data from differentiating mESC cells shows this discrepancy could potentially be explained by the different VEGFA concentrations used in different protocols, though the issue of timing can also not be discarded. It should also be noted that all of these studies address the *potential* and not the *requirement* of $DLL4^+$ HE in HSC ontogeny.

Regardless of whether a cell-intrinsic or niche arterial programme is required, it is clear from these and other studies (Gori et al. 2015; Hadland et al. 2015) that a global arterial context is necessary, though perhaps not sufficient (Ng et al. 2016; Park et al. 2018) for HSC development. Arterial *Dll4* is an important Notch ligand and is expressed in the developing dorsal aorta (DA) at the population level prior to EHT, along with arterial *Nrp1* (Chong et al. 2011), a VEGFA co-receptor. Both the Notch and VEGF pathways have been reported as critical to the developing arterial (Lawson et al. 2001; Yamamizu et al. 2010; Duarte et al. 2004; Quillien et al. 2014; Lanner, Sohl, and Farnebo 2007; Sriram et al. 2015; Zhang et al. 2008a) and HSC (Hadland et al. 2004; Leung et al. 2013) programmes, prompting our decisions to explore VEGFA concentrations and their effect on differentiating HSPCs in previous chapters.

Given these reports and our previous data, we sought to translate some of our findings on VEGFA from a mESC system to a human iPSC system as well as fully characterise said system at both the HSPC and monolayer niche level. For this purpose, an h-iPSC to HSPC differentiation protocol previously developed in the lab, commercially available as STEMdiff™ Hematopoietic Kit by StemCell™ Technologies was chosen. This monolayer system provides a clinically-safe, as well as modifiable and scalable platform for producing HSPCs. The fact that it is commercially available and used by labs worldwide for other HSPC experiments and disease modelling makes full characterisation of the system important.

5.2. *In vitro* system produces HSPCs

A monolayer-based protocol that was previously developed in-house, commercially available as STEMCell™ Technologies STEMDiff™ Haematopoietic Differentiation Kit, was used to differentiate h-iPSCs into HSPCs. Prior to differentiation, h-iPSCs are plated as small clusters of cells. Twenty-four hours later, cell clusters are treated with haematopoietic differentiation medium A, which contains bFGF, BMP4, and VEGFA to induce mesodermal and haemangiogenic fates in the differentiating cells (Figure 5.1a). Following three days of culture, haematopoietic differentiation medium B is added, which in addition to haematopoietic medium A cytokines, also contains SCF, TPO, and FLT3-L to support arising HSPCs. During early culture days, differentiating mesodermal cells display a fibroblast-like morphology, with budding clusters appearing at later stages, along with freely floating cells (Figure 5.1b).

To more fully characterise cells arising from this system, both adherent and non-adherent cells were taken from culture at days 5 – 21 (Figure 5.1a). Due to the technical inability to truly separate all the adherent monolayer from cluster and freely floating cells, a first pass of post-hoc gating was applied to all Flow Cytometry data to distinguish developing HSPCs from adherent monolayer cells. Any cell expressing haematopoietic CD43, CD45, or both, was classified as an HSPC, while double negative cells were characterised as non-haematopoietic monolayer (Figure 5.1c,d).

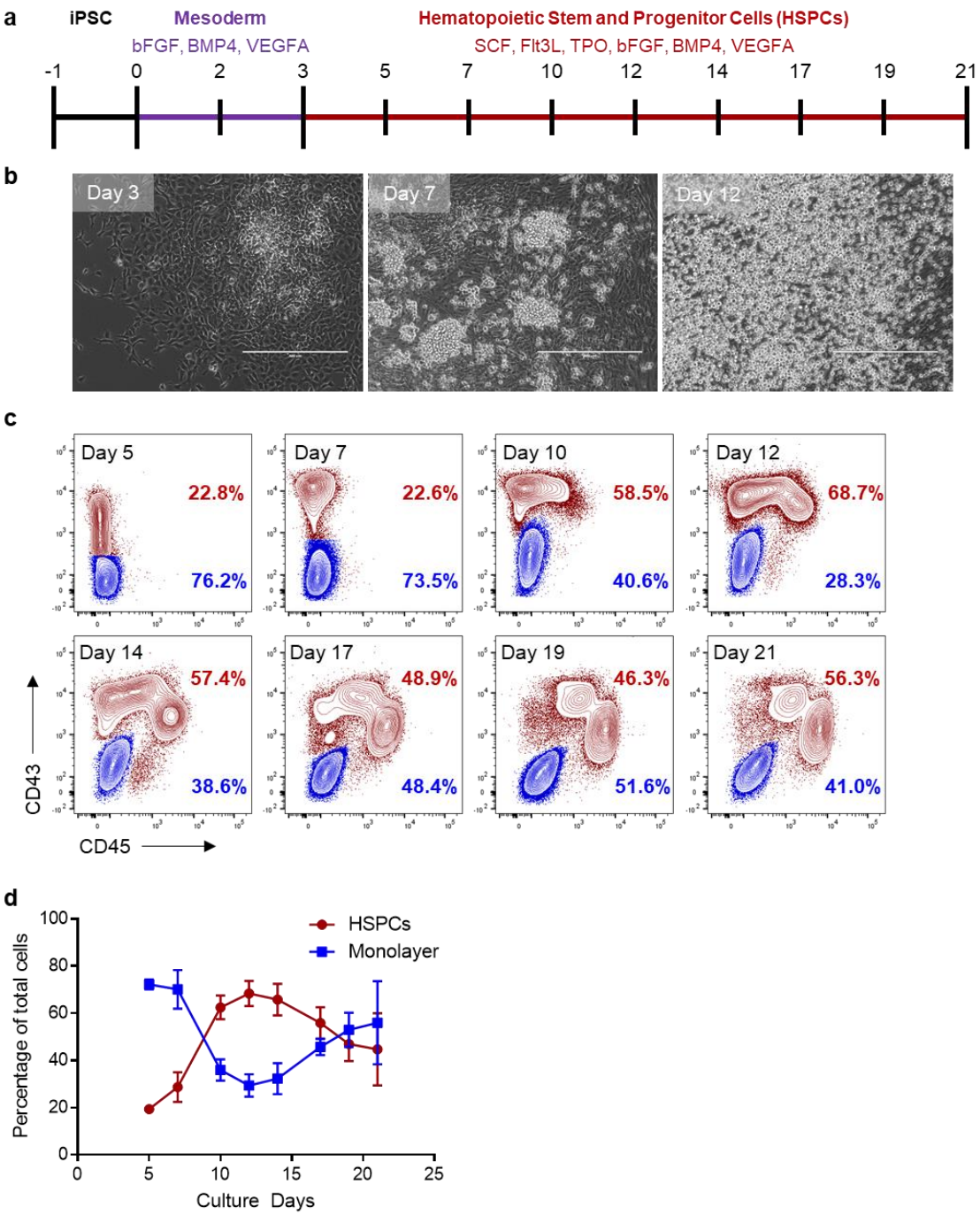

Figure 5.1 HSPC Differentiation from h-iPSCs

a) Differentiation scheme for h-iPSC to HSPC differentiation, using commercially available STEMDiff™ Kit. Day 0 – Day 3, mesodermal specification stage. Day 3 – Day 21, HSPC differentiation and expansion stage. Large bars represent full media changes or stop of culture. Small bars represent half media changes. Data is collected for all timepoints starting at Day 5. b) Representative phase-contrast microscopy images taken at various timepoints; Day 3: Fibroblast-like mesodermal colony; Day 7: Arising HSPC clusters; Day 12: Free-floating cells. Scale bar = 400 µM c) Representative flow cytometry overlays of HSPC and Monolayer populations gated on CD43 and CD45 expression at timepoints collected; Red = HSPCs; Blue = Monolayer. FMO controls and gating strategy in Supplementary Figure 5.1 d) Percentages of HSPCs and Monolayer cells throughout culture. n = 3 biological replicates on same iPSC line. Averages ± SD depicted.

In line with morphological observations of the appearance of clusters and an increase in cells found in the supernatant, an increase in culture percentages of immunophenotypic HSPCs, concomitant with a decrease in percentage of monolayer cells, was initially observed (Figure 5.1d). HPC percentages peaked at day 12, comprising 68.4 ± 5.4% of the culture, followed by a slow decrease at later stages of culture (Figure 5.1c-d). This data shows the differentiating h-iPSC system produces CD43- and CD45-expressing immunophenotypic HSPCs. It is likely that this increase in HSPCs is due to both cells arising from the monolayer at early (and potentially later stages), as well as the proliferation of $CD43^{+}$ HSPCs present as early as Day 5, which later express CD45 (Figure 5.1c). It is likely that, similar to what has been reported *in vitro* for various other systems across model organisms (Yvernogeau et al. 2016; Lancrin et al. 2009; Bos, Hawkins, and Zovein 2015; Ditadi et al. 2015), the differentiating endothelial cells in the system undergo EHT to produce the HSPCs. However, while live imaging studies were undertaken by others in the lab to observe instances of EHT at the single-cell level, data gathered from the images were inconclusive.

5.3. HSPCs arise in two waves of erythromyeloid potential

HSPCs developing in the system were then further characterised by analysing expression of CD235a, CD34, CD43, CD45, and CXCR4, all markers shown to be important in the characterisation and function of differentiating HSPCs (Kucia et al. 2003; Rybtsov et al. 2014; Sturgeon et al. 2014). Early culture days showed the development and then disappearance of an early $CD235a^{+}CD45^{-}$ wave of cells, the majority of which are also $CD34^{-}$ (Figure 5.2a). This first, early wave, in line with primitive erythroid waves observed *in vitro* (Kennedy et al. 2012), peaks at culture day 7, comprising 19.6 ± 1.4% of the total HSPC fraction (Figure 5.2c).

This was followed by a wave of haematopoietic progenitors expressing low levels of CD45 and high levels of CD34 (Figure 5.2b, blue gates). This wave of cells peaks at day 12, comprising 20.3 ± 1.6% of the total HSPC fraction (Figure 5.2b-c). When left in culture, these cells begin to lose CD34 expression and upregulate CD45, increasing in percentage of total HSPCs through day 21 (Figure 5.2b, orange gates). At later culture days, a majority of these cells also express erythroid CD235a and homing ligand CXCR4 (CD184) (Figure 5.2b). Because erythroid cells lose CD45 expression as they mature and in order to ensure that no erythroid cells were excluded from the first-pass HSPC gate because of this, CD235a expression of the $CD43^{-}CD45^{-}$ monolayer fraction at all timepoints was checked. On average, fewer than 1% of monolayer cells were $CD235a^{+}$ at any given timepoint (Supplementary Figure 5.2c), save for Days 10 and 12 (1.1 ± 0.8% and 1.2 ± 1.0%, respectively), suggesting the 21 days in culture do not allow enough time for maturing erythroid progenitors to lose CD45 expression. When HSPCs were sorted (based on CD43 and 45 expression, as gated in Supplementary Figure 5.1a) into colony-forming unit (CFU) assays, a shift from

CFU-G, CFU-M, and CFU-GM progenitors towards almost exclusively CFU-E and BFU-E progenitors (Figure 5.2d-e) was observed as differentiation culture progressed. These results suggest a specification, at the population level, from a multilineage myeloid potential to a more specified erythroid potential as culture time progresses. Overall, the differentiation system allows for tracking of two independent haematopoietic waves, a first erythroid wave followed by a second wave of progenitors with erythro-myeloid potential that, when left in culture, preferentially differentiate towards an erythroid lineage.

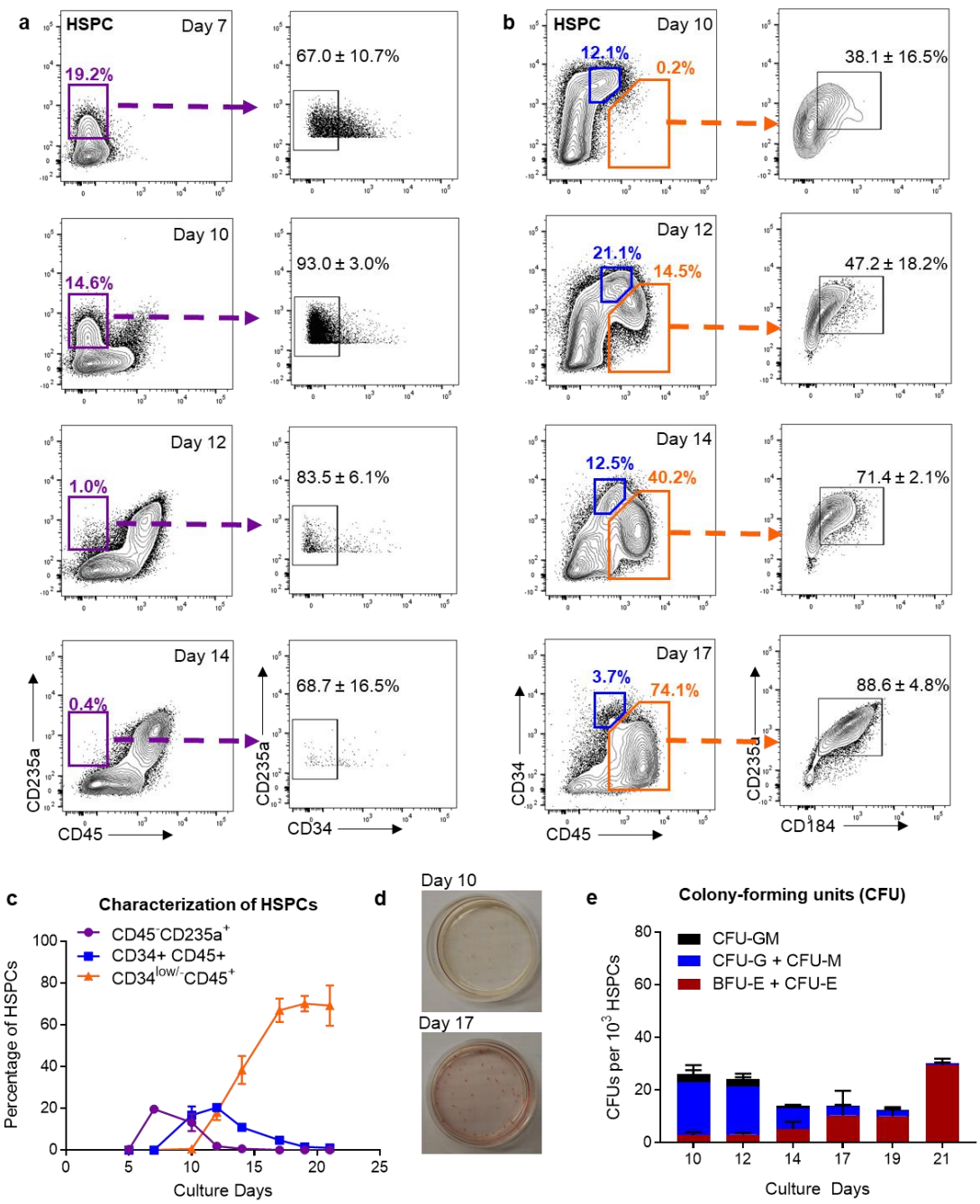

Figure 5.2 HSPCs arise in two waves of erythromyeloid potential

a) Representative flow cytometry plots of HSPCs at different timepoints for CD235a and CD45, and CD34 expression. Purple gates represent early erythroid population. CD235 and CD34 FMO control found in Supplementary Figure 5.1b-c. b) Representative flow cytometry plots of HSPCs at different timepoints for CD34, CD45, CD235a and CD184 expression. Blue gates represent early $34^{+}CD45^{+}$ progenitor and orange gates represent later $34^{Low/-}CD45^{+}$ progenitor. FMO controls found in Supplementary Figure 5.2a-b. c) Percentage of HSPCs with immunophenotypes observed in (a-b). n = 3 biological replicates. Averages ± SD are depicted. d) Representative CFU plates from HSPCs sorted on CD43 and CD45 expression (as depicted in Supplementary Figure 5.1a) at Day 10 or Day 17. e) Total CFU counts per 10^3 HSPCs at different timepoints. n = 3 biological replicates. Averages ± SD depicted.

Given the presence of $CD34^{+}CD45^{+}$ progenitors with GM potential at the population level in the differentiation system, HSPCs were characterised using the five-colour stain known to most specifically identify engrafting adult hematopoietic stem cells (HSCs) (Notta et al. 2011). Cells were stained for a $CD45^{+}CD34^{+}CD38^{-}CD90^{+}CD45RA^{-}CD49f^{+}$ immunophenotype (Figure 5.3a). Despite high numbers ($2.7 \pm 1.0 \times 10^{3}$) of immunophenotypic HSC-like cells at day 12 of differentiation (Figure 5.3b), sorted HSPCs at days 10 and 12 of differentiation culture failed to engraft in irradiated NSG mouse transplantation assays (Figure 5.3c-d).

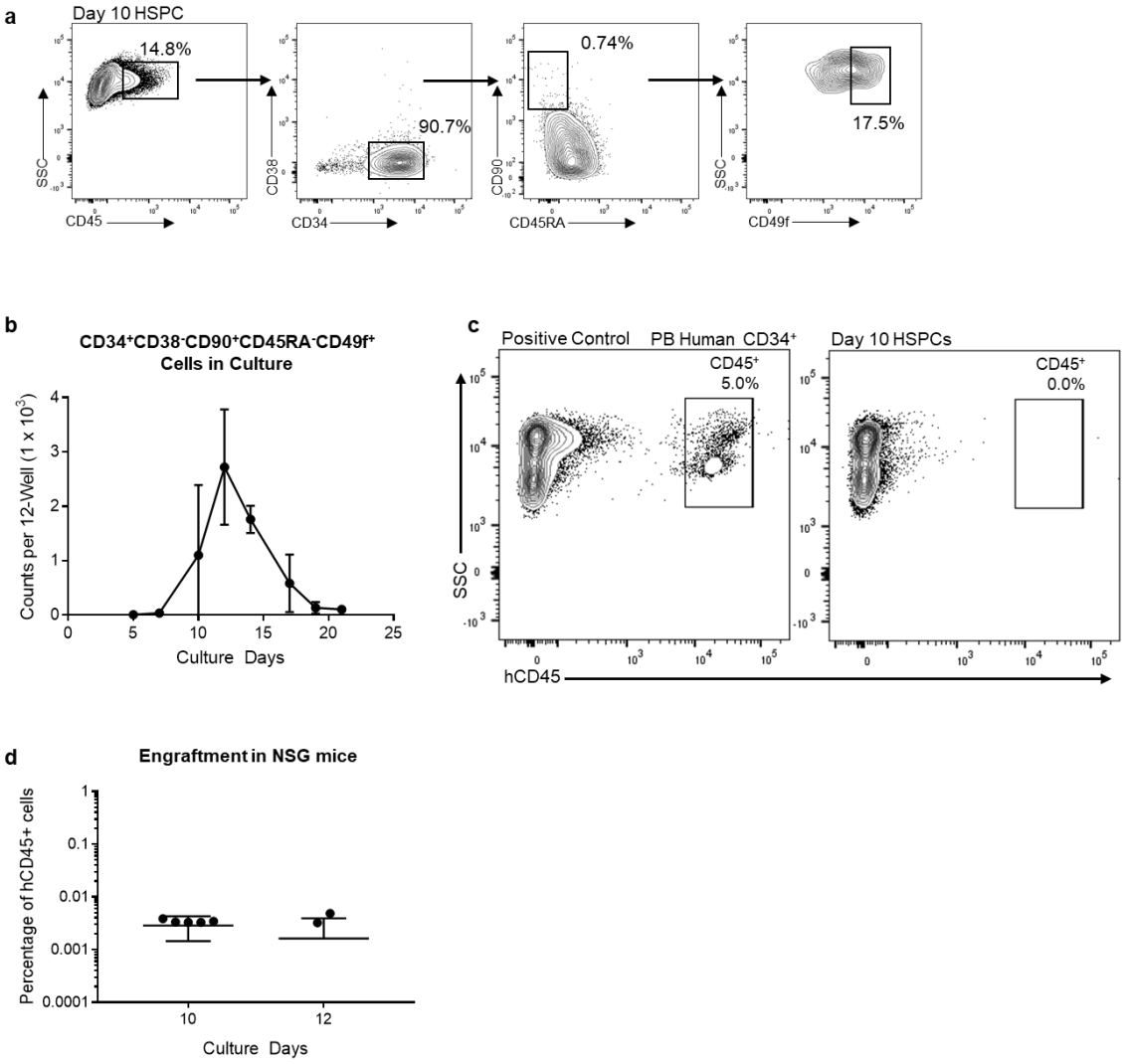

Figure 5.3 Adult HSC Immunophenotype Does Not Distinguish Engrafting HSPCs arising in h-iPSC System

a) Representative flow cytometry plots and gating strategy at Day 10 for $CD45^+CD34^+CD38^-CD90^+CD45RA^-CD49f^+$ HSPCs. b) Total counts for $CD45^+CD34^+CD38^-CD90^+CD45RA^-CD49f^+$ cells per well in a 12-well dish; n = 3 biological replicates. Averages ± SD are depicted. c) Representative flow cytometry plots of h-CD45 expression in NSG mice 4 months following irradiation and transplantation with sorted HSPCs at Day 10 or 12 timepoints. Experimental positive control from mouse transplanted with human PB $CD34^+$ cells for a colleague's experiment; harvested on the same day. d) Percent of h-$CD45^+$ cells in NSG mice as depicted in (c). n = 6 mice per timepoint: 2 technical replicates for each of 3 independent differentiations (biological replicates). Bars represent averages ± SD. Values of 0 not represented given log scale of graph.

5.4. Differentiation leads to low percentages of endothelial niche in monolayer

Multiple studies have shown the importance of the arterial niche on differentiating HE and HSCs (Hadland et al. 2015; Lu et al. 2016; Gori et al. 2015). Given the HSC-like cells' inability to engraft, the $CD43^{-}CD45^{-}$ adherent monolayer throughout culture days was assessed for the presence of a differentiating arterial niche. In *in vitro* human systems, expression of endothelial CD34 and CD144 (VE-Cad) can be used to distinguish vascular endothelium (VE) from mesenchyme-like stroma which lacks expression of these markers (Guibentif et al. 2017) (Figure 5.4a). While HSPCs arise and develop in endothelial niches throughout development across species (de Bruijn et al. 2000; Frame et al. 2016; Tamplin et al. 2015), $CD34^{+}CD144^{+}$ VE (Figure 5.4a) cells were found to comprise only a small percentage of monolayer cells, peaking at Day 5 with 7.8 ± 3.5% and slowly decreasing in percentage as time progressed (Figure 5.4b). VE populations were further characterised based on previously reported expression of arterial CD184, DLL4, and endothelial CD73 (Ditadi et al. 2015) (Figure 5.4c): $CD34^{+}CD144^{+}CD73^{Mid}CD184^{+}$ cells have been reported to express arterial endothelium genes, while $CD34^{+}CD144^{+}CD73^{+}CD184^{-}$ cells have been reported to express venous endothelial transcription factor COUP-TFII. Given the recent description of $CD73^{-}DLL4^{+}$ arterial definitive HE (Uenishi et al. 2018), VE cells were also characterised based on DLL4 and CD73 expression (Figure 5.4d). In this system, the small amount of VE present is mainly comprised of venous endothelium, with nearly no arterial endothelium (Figure 5.4e). Immunophenotypic arterial endothelium peaked in percentage of total monolayer cells at 3.6 ± 2.4% on Day 7 and rapidly decreased following this. Likewise, nearly no

immunophenotypic arterial HE arises in this system, with the majority of $CD73^-$ $DLL4^+$ cells present at culture Day 5 and comprising only 1.3 ± 1.7% of the total monolayer. The majority of cells comprising the *in vitro* monolayer are stroma with no expression of endothelial markers CD34 or CD144 throughout culture days, peaking at Day 21 with over 90% of monolayer cells (Figure 5.4b). When further assayed for mesenchymal markers, these cells were found to progressively upregulate MSC-like CD90, CD73, and CD105 (Figure 5.5a-b). When assayed for MSC functionality at Day 21, sorted $CD43^-CD45^-$ monolayer cells successfully differentiated into chondrocyte and osteoblast lineages similar to control MSCs. Cells failed to differentiate into adipocytes however, suggesting a more limited potential than true MSC cells derived from patient samples (Figure 5.5c). Due to this lack of an arterial endothelium niche and overabundance of mesenchymal-like stroma in the monolayer, we sought to enhance arterial niche differentiation throughout culture to further instruct differentiating HSPCs towards functionality and engraftment.

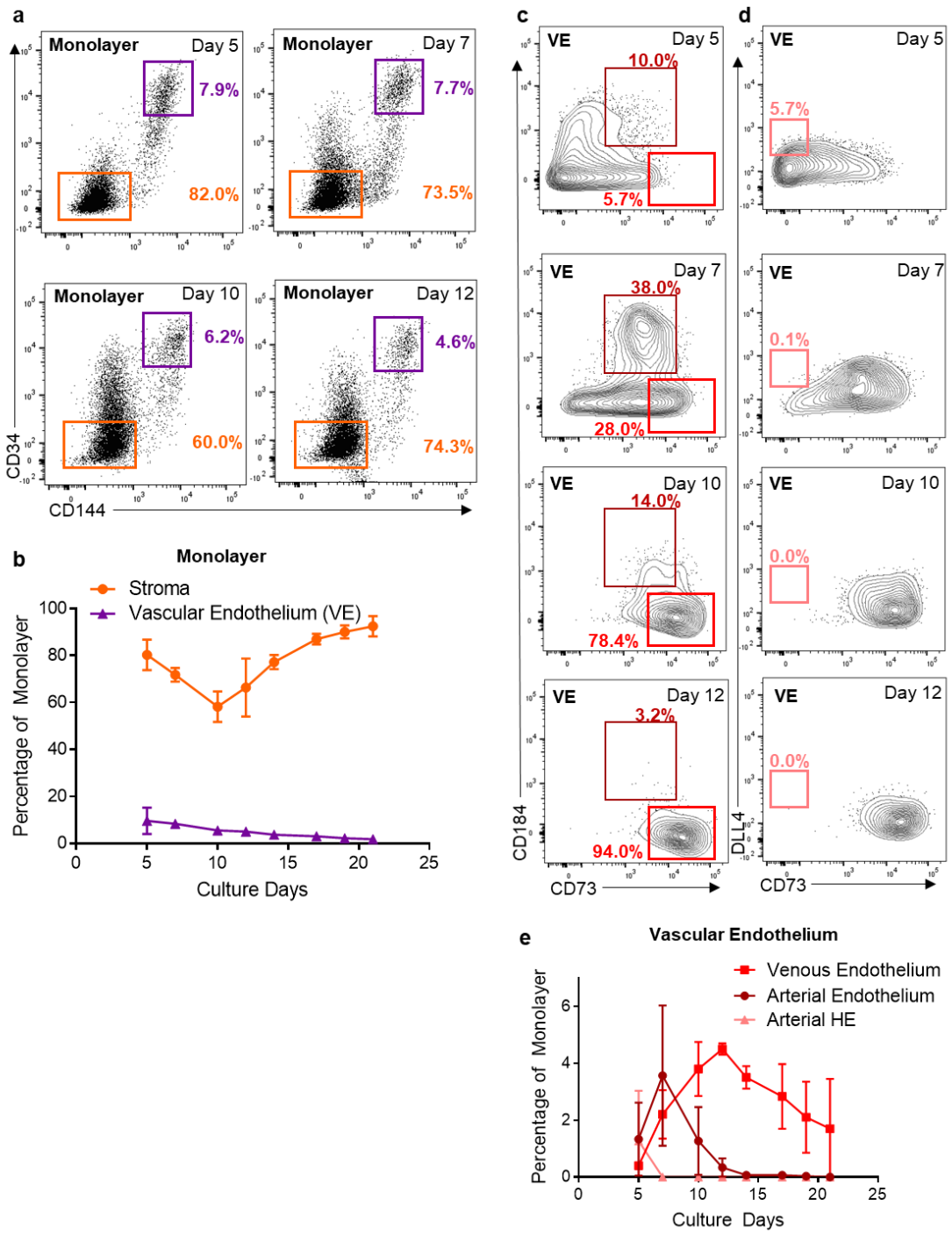

Figure 5.4 Monolayer Characterisation

a) Representative flow cytometry plots gated on monolayer populations and depicting endothelial CD34 and CD144 (VE-Cad) expression. Purple gates = Vascular Endothelium (VE); Orange gates = double negative Stroma. Gates set as in Supplementary Figure 5.3a. b) Percentage of monolayer with a stromal or VE immunophenotype at different timepoints. n = 3 biological replicates; averages ± SD depicted c) Representative flow cytometry plots gated on VE populations depicting endothelial CD73 and arterial CD184 (CXCR4) expression. Dark red gates = Arterial endothelium; red gates = Venous endothelium. Gates set as in Supplementary Figure 5.3b. d) Representative flow cytometry plots gated on VE populations depicting endothelial CD73 and arterial DLL4. Pink gates = Arterial HE. Gates set as in Supplementary Figure 5.4 e) Percentage of monolayer with a Venous, Arterial, or Arterial HE phenotype. n = 3 biological replicates; averages ± SD depicted.

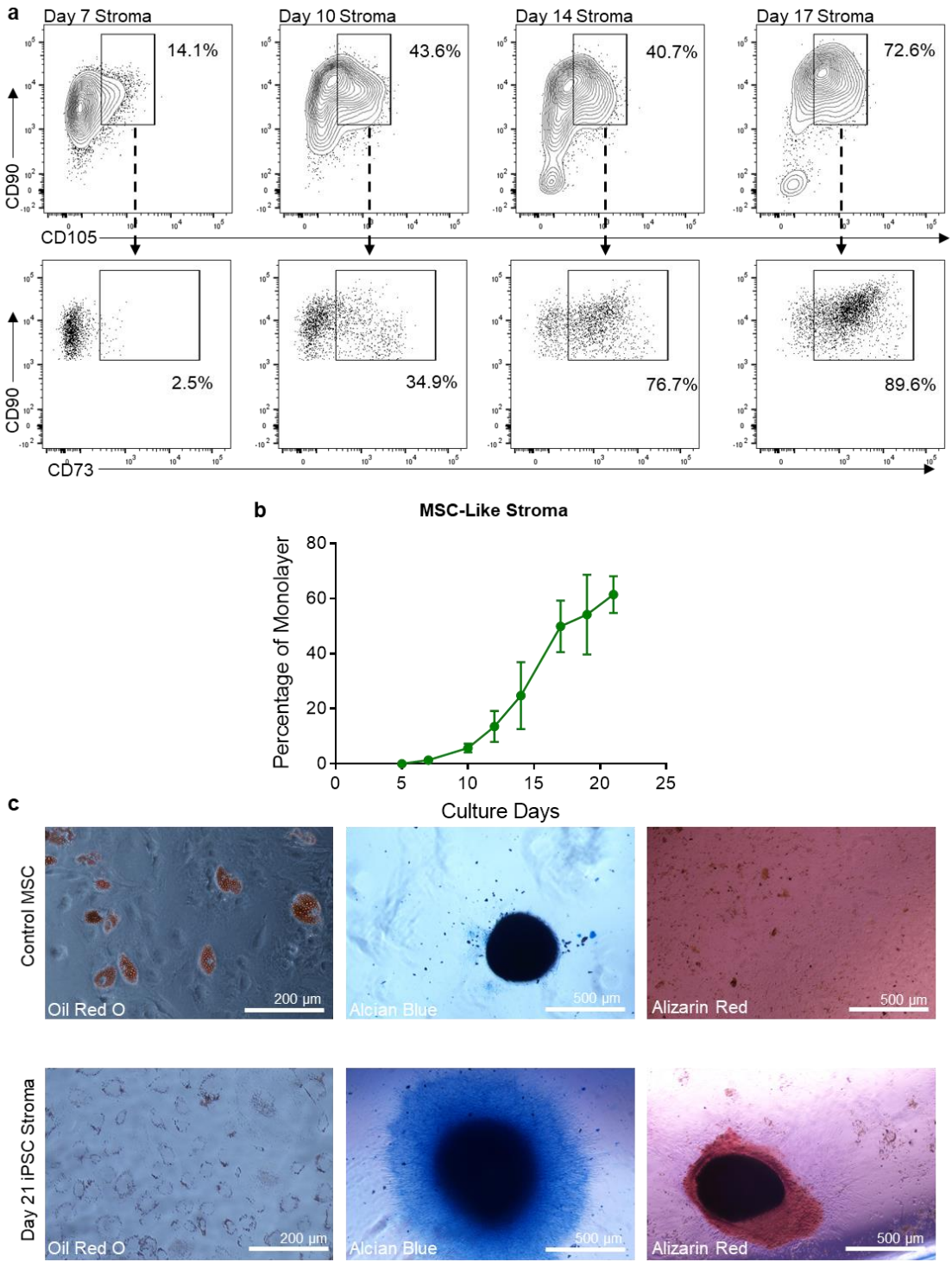

Figure 5.5 Characterisation of Mesenchymal-like Stroma
a) Representative flow cytometry plots of CD90, CD105, and CD73 expression in $CD34^-$ $CD144^-$ stroma at various timepoints. b) Average percentage of the monolayer comprised of $CD90^+CD105^+CD73^+$ MSC-like cells. n = 3 biological replicates. Averages ± SD depicted. c) Sample images depicting Oil Red O, Alcian Blue, and Alizarin Red lineage staining for adipocyte, chondrocyte, and osteoblast differentiation of sorted $CD43^-CD45^-$ monolayer cells at Day 21 of differentiation followed by appropriate lineage differentiation protocols. Control from healthy donor volunteer bone marrow, passage 4. n = 2 biological replicates.

5.5. Mesodermal patterning activates *HOX* code in VE and HSPC populations but is insufficient for engraftment

During early stages of development, signalling gradients provide spatial and temporal cues to the germ layers to specify into correct tissues (Arnold and Robertson 2009). Because these gradients can be missing *in vitro,* previous studies have sought to modulate these pathways using small molecule agonists and antagonists. Previous studies have shown that blocking Activin/Nodal and activating Wnt/β-catenin during the mesodermal stage of differentiation nearly abrogates primitive haematopoiesis and leads to higher percentages of definitive haematopoiesis (Kennedy et al. 2012; Sturgeon et al. 2014). This treatment has also been shown to activate the HOXA code alongside arterial genes in differentiating cells to yield AGM-like tissue and HSPCs in EB differentiation systems (Ng et al. 2016).

HOXA genes have been reported in multiple studies to be critical for the regulation of HSC function and maintenance (Dickson et al. 2009; Lawrence et al. 2005), and have been shown to be originally activated during spatial patterning of mesodermal development (Pindyurin and van Steensel 2012). To activate HOXA cluster genes and improve the monolayer system towards definitive, if not engrafting, HSPC differentiation, differentiating cells were treated similarly to previous studies. Wnt agonist CHIR99021 (3 μM) and Nodal antagonist SB431542 (3 μM) small molecules were added to the culture for 30 – 36 hours between Days 2 and 3 of differentiation. Differences in the colony potential of differentiating HSPCs, as well as activation of HOXA cluster genes were assayed.

Both Day 7 $CD34^{High}CD43^{-}$ VE and Day 12 $CD34^{+}CD45^{+}$ HSPCs were assayed for expression of a panel of *HOXA* genes (Figure 5.6a,b). We found that,

like what has been previously published (Ng et al. 2016), early short-term treatment with small molecules leads to activation of *HOXA* cluster gene expression that is maintained in both populations and up to ten days later (Figure 5.6a,b). In VE populations, *HOXA* cluster gene levels tested were higher than those in peripheral blood (PB) $CD34^+$ cells used as a reference, while sorted $CD34^+CD45^+$ HPSCs developed *in vitro* showed levels lower to PB $CD34^+$ cells. Interestingly, we also saw a decrease in *HOXA6* expression, a gene that has been associated with stem and progenitor as well as leukaemogenic activity (Dickson et al. 2009), in treated $CD34^+CD45^+$ HSPCs. This was the only gene of the ones assayed that showed a decrease in expression in treated cells, and only in HSPC populations.

Likewise, HSPC immunophenotype and function were assayed in treated cells. CFU assays showed decreases in total CFU counts at Day 12, as well as increases in CFU counts at Days 19 and 21, which are also almost entirely erythroid in nature (Figure 5.6c). Globin expression of erythroid cells differentiated from sorted HPSCs at different timepoints showed the primitive nature of the erythroid wave that arises at Day 7, which is composed mostly of embryonic ε-globin and completely lacks β-globin expression at the protein level (Figure 5.6d). Erythroid cells derived from Day 17 HSPCs in both control and CHIR/SB cultures had some β-globin expression and increase in fetal γ-globin expression at the expense of ε-globin, demonstrating their definitive nature. While it appears that CHIR/SB treatment led to Day 17 HSPCs that produced erythroid cells with slightly higher β-globin expression and lower ε-globin expression, not enough biological replicates were tested to assess this difference statistically.

Despite the presence of cells that produce erythroid cells with β and γ-globin, however, $CD34^+CD38^-CD90^+CD45RA^-CD49f^+$ (Figure 5.7a) counts per well

in CHIR/SB cultures were decreased from control cultures at Day 12 and Day 14 of differentiation (Figure 5.7b) with no differences reaching statistical significance. Functionally, HSPCs sorted at days 10 and 12 failed to engraft in NSG mouse models (Figure 5.7c,d). Therefore, despite activation of *HOXA* cluster genes in cells, these protocol modifications did not lead to engrafting, functional HSCs, confirming findings in similarly treated EB systems (Ng et al. 2016). Due to the high numbers of definitive BFU-E and CFU-E activity present at later stages of culture however, these modifications to the system could make it an attractive protocol for the differentiation of therapeutically relevant definitive erythroid cells.

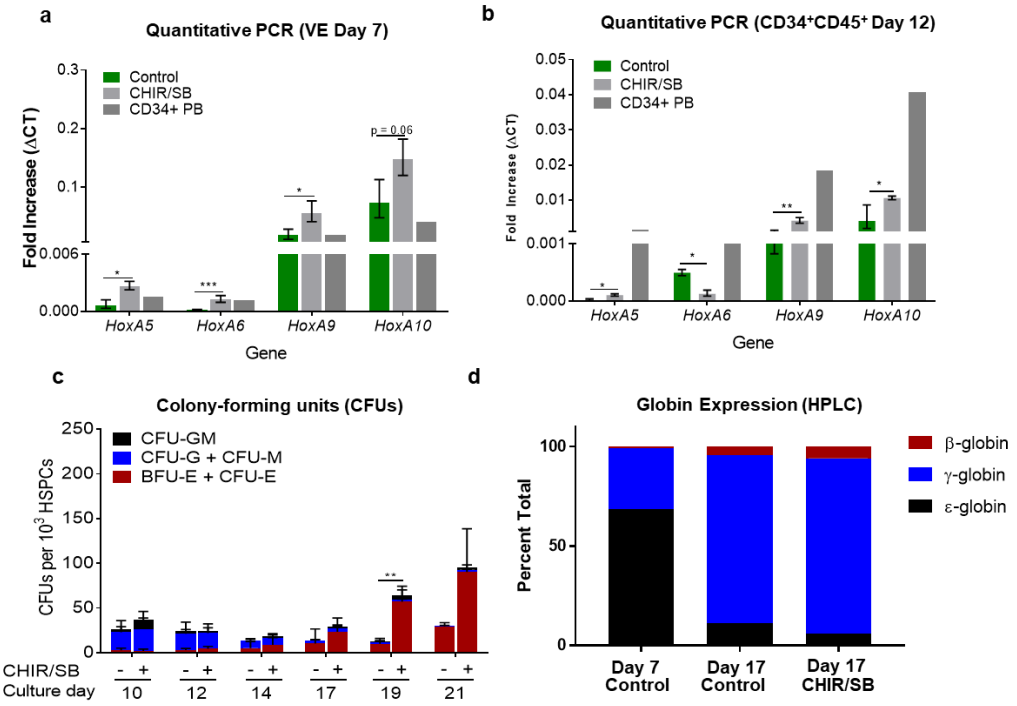

Figure 5.6 Mesodermal patterning activates Hox code
a) Hox gene expression of sorted VE cells, as gated in Supplementary Figure 5.3a, at Day 7 of culture; n =3 biological replicates. Single n of 1 from human PB CD34$^+$ cells used as positive control and reference. b) Hox gene expression of CD34$^+$CD45$^+$ cells, as gated in Supplementary Figure 5.2a. n = 3. c) Total CFU counts per 10^3 HSPCs (sorted on CD43 and CD45 expression as depicted in Supplementary Figure 5.1a) at different timepoints in cultures with and without small molecule treatment at mesodermal stage. n = 3 biological replicates. Averages ± SD depicted. d) Globin protein expression in erythroid cells differentiated from sorted HSPCs at different timepoints. n = 3 technical replicates pooled from 2 biological replicates for control and 2 technical replicates from 1 biological replicate for CHIR/SB.

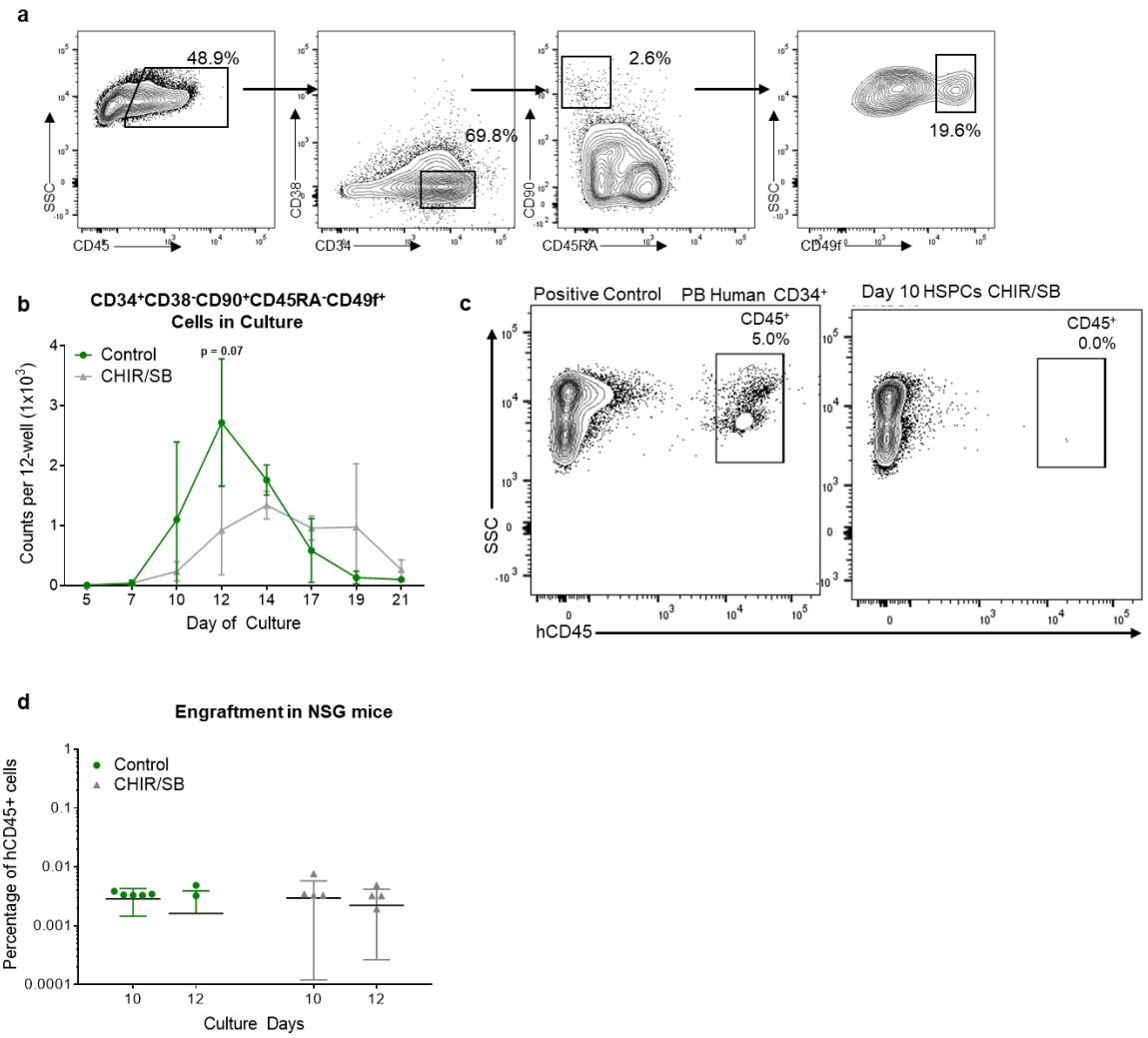

Figure 5.7 Mesodermal Patterning is Insufficient for iPSC-derived HSPC engraftment a) Representative flow cytometry plots and gating strategy at Day 10 for $CD45^+CD34^+CD38^-CD90^+CD45RA^-CD49f^+$ HSPCs, as in Figure 5.3. b) Total counts for $CD45^+CD34^+CD38^-CD90^+CD45RA^-CD49f^+$ per well in a 12-well dish; n = 3 biological replicates. Averages ± SD are depicted. Unpaired, two-sided t-test comparing treated and control samples from each timepoint c) Representative flow cytometry plots of h-CD45 expression in NSG mice 4 months following irradiation and transplantation with sorted HSPCs at Day 10 or 12 timepoints. Same experimental positive control plot as in Figure 5.3: mouse transplanted with human PB $CD34^+$ cells d) Percent of h-$CD45^+$ cells in NSG mice as depicted in c. n = 6 mice per timepoint: 2 technical replicates for each of 3 independent differentiations (biological replicates). Bars represent averages ± SD. Values of 0 not represented given log scale of graph.

5.6. High VEGFA in culture leads to sustainable arterial niche and arterial HE

Because VEGFA signalling lies upstream of arterial genes and Notch signalling (Hayashi and Kume 2008; Lanner, Sohl, and Farnebo 2007), and given insights gained from the mouse differentiation model, we hypothesized that increasing the levels of VEGFA throughout the days of culture would yield a more robust arterial niche to potentially give rise to and support differentiating HSCs. VEGFA concentrations were increased from control levels (10 ng/ml) to 200 ng/ml, as used in the latest system reported to produce engrafting HSCs from differentiating iPSC embryoid bodies (Guyonneau-Harmand et al. 2017). High VEGFA levels were introduced at Day 0 of culture and maintained throughout the differentiation. High concentrations of VEGFA were also used together with mesodermal patterning with small molecules from culture Day 2 – 3 to investigate possible combinatorial effects on differentiating cells, studying the effect that an arterial niche would have on cells arising from definitive mesodermal progenitors.

Similar to control conditions, all three treatment conditions underwent EHT with incremental increases in percentages of HSPCs expressing CD43, CD45, or both, concomitant with decrease in double negative monolayer cells at early culture timepoints before levelling out (Figure 5.8a). While treatment with high levels of VEGFA alone did not seem to have a significant impact in the distribution of monolayer and HSPCs save for the first day, treatment with either small molecules alone or in combination with high levels of VEGFA led to significantly higher percentages of monolayer cells at the expense of HSPCs (Figure 5.8b-c). The treatments showed a combination effect, as changes were more pronounced in combination conditions.

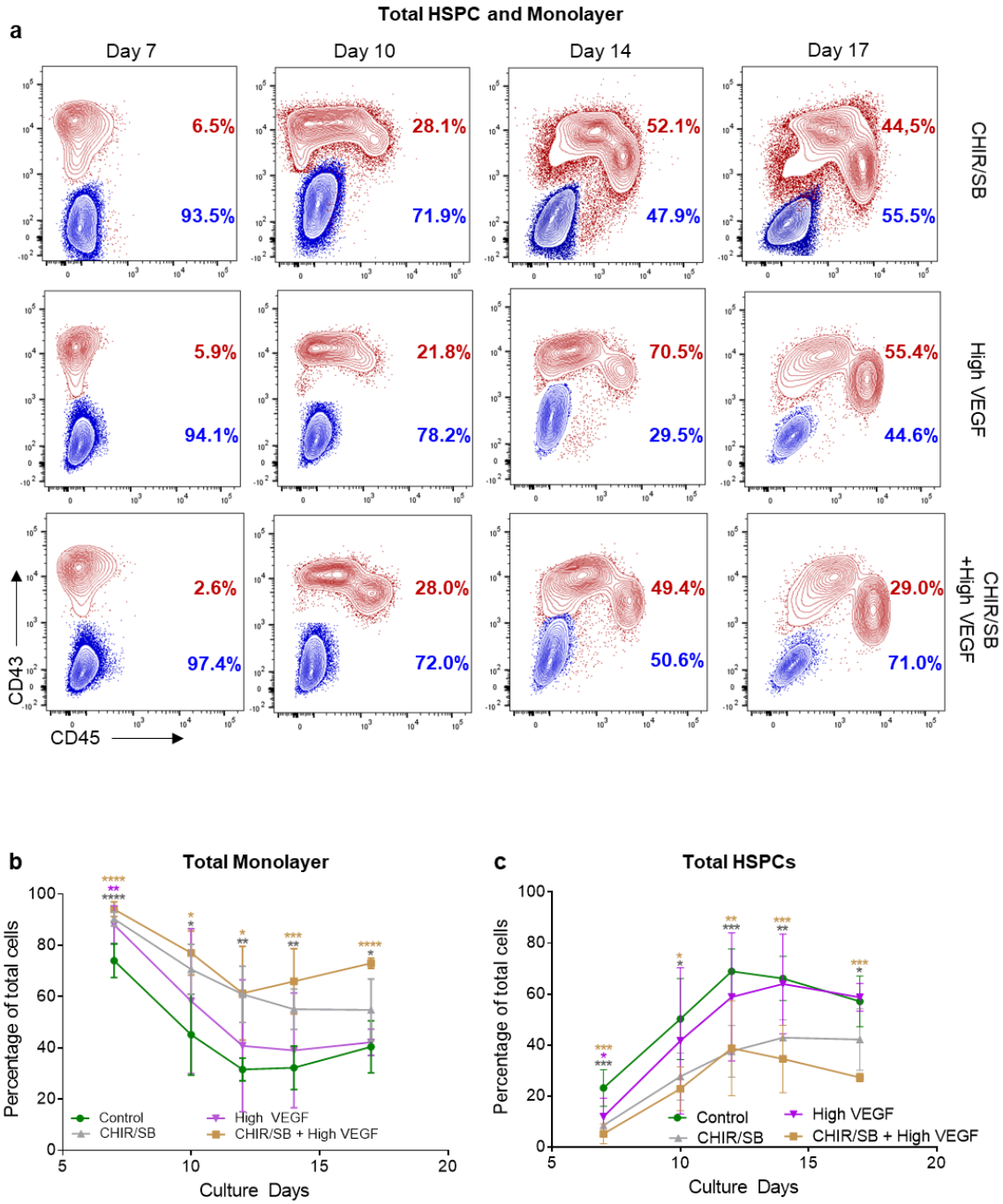

Figure 5.8 HSPC and Monolayer in h-iPSC Treatment Conditions
a) Representative overlay of flow cytometry plots of $CD43^{-}CD45^{-}$ monolayer populations and $CD43^{+}CD45^{+}$ HSPCs for treatment conditions; Blue = monolayer, Red = HSPCs. Gates set as in Supplementary Figure 5.1a b) Percentage monolayer cells, as gated in a, of total cultures at various timepoints; n = 5 for control, CHIR/SB, n = 4 for High VEGF, CHIR/SB + High VEGF. Average ± SD depicted. Ordinary, two-Way ANOVA with Dunnett's posthoc test for multiple sample comparison to control only. c) Percentage of HSPCs, as gated in a, of total cultures at various timepoints. Statistics and replicates as in b.

Treatment with both small molecules and high VEGFA concentrations led to few differences in the composition of HSPCs throughout culture (Figure 5.9a). The biggest differences in the $CD34^{+}CD45^{+}$ population were observed early at Day 7, as all treatments showed a significant increase in these cell's percentages, at a time when these populations haven't yet arisen in control conditions (Figure 5.9b). Beyond this timepoint, only the samples treated with small molecules showed a significant increase in $CD34^{+}CD45^{+}$ populations over controls at Days 10 and 17, with no significant differences at Day 12. Likewise, all treatment conditions showed a trend of differentiating towards the $CD34^{low/-}CD45^{+}$ erythroid progenitor population (Figure 5.9c). Small molecule treatment of cells increases the percentage of this population at Days 10 and 12 of culture, while High VEGFA treatment leads to lower percentages than control at later Days 14 and 17. Combinatorial treatment only leads to significantly higher percentages of this population at Day 10 of culture.

The presence of the $CD45^{-}CD34^{-}$ primitive erythroid wave, present at early stages in control conditions, was also assayed. In agreement with previous studies (Kennedy et al. 2012; Sturgeon et al. 2014), we found that treating with small molecules to pattern the mesoderm leads to lower percentages of primitive haematopoietic progenitor cells in early culture days, though this trend is only significant at Day 10 and doesn't lead to complete abrogation of these populations, suggesting inefficient dosages, at least compared to published results. Treatment with high VEGFA levels also results in lower percentages (though significant only at Day 7) of primitive erythroid progenitors, as does combination treatment, significant at both Day 7 and Day 10 (Figure 5.10).

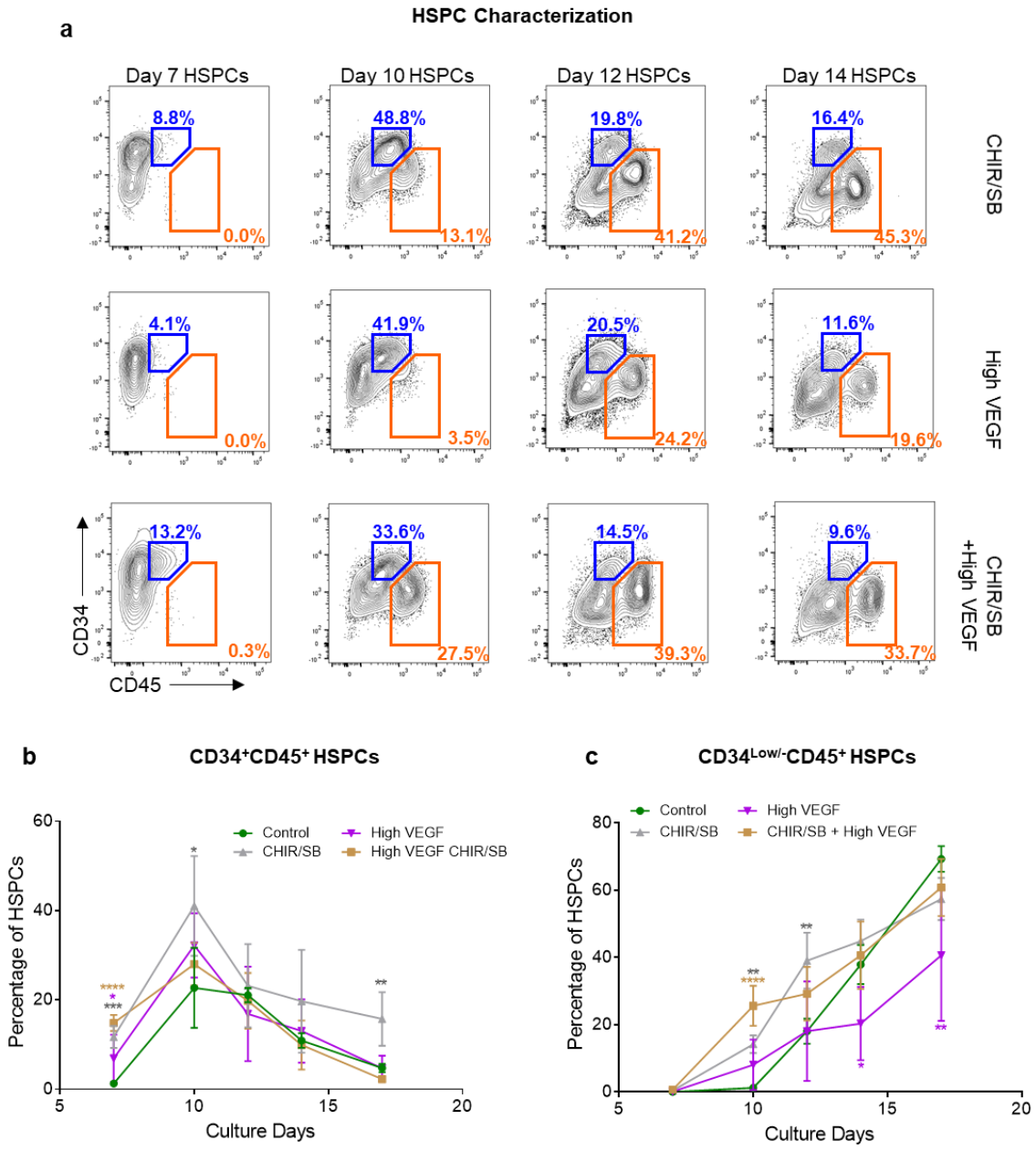

Figure 5.9 HSPC Characterisation in h-iPSC Treatment Conditions
a) Representative flow cytometry plots of CD34 and CD45 expression in HSPC populations; Blue Gates = $CD34^{+}CD45^{+}$, Orange Gates = $CD34^{Low/-}CD45^{+}$. Gates set as in Supplementary Figure 5.2a b) Percentage $CD34^{+}CD45^{+}$, as gated in a, of HSPCs at various timepoints; n = 5 for control, CHIR/SB; n = 4 for High VEGF, CHIR/SB + High VEGF, Averages ± SD depicted; Ordinary, two-Way ANOVA with Dunnett's posthoc test for multiple sample comparison to control only. c) Percentage of $CD34^{Low/-}CD45^{+}$, as gated in a, of HSPCs at various timepoints. Statistics and replicates as in b.

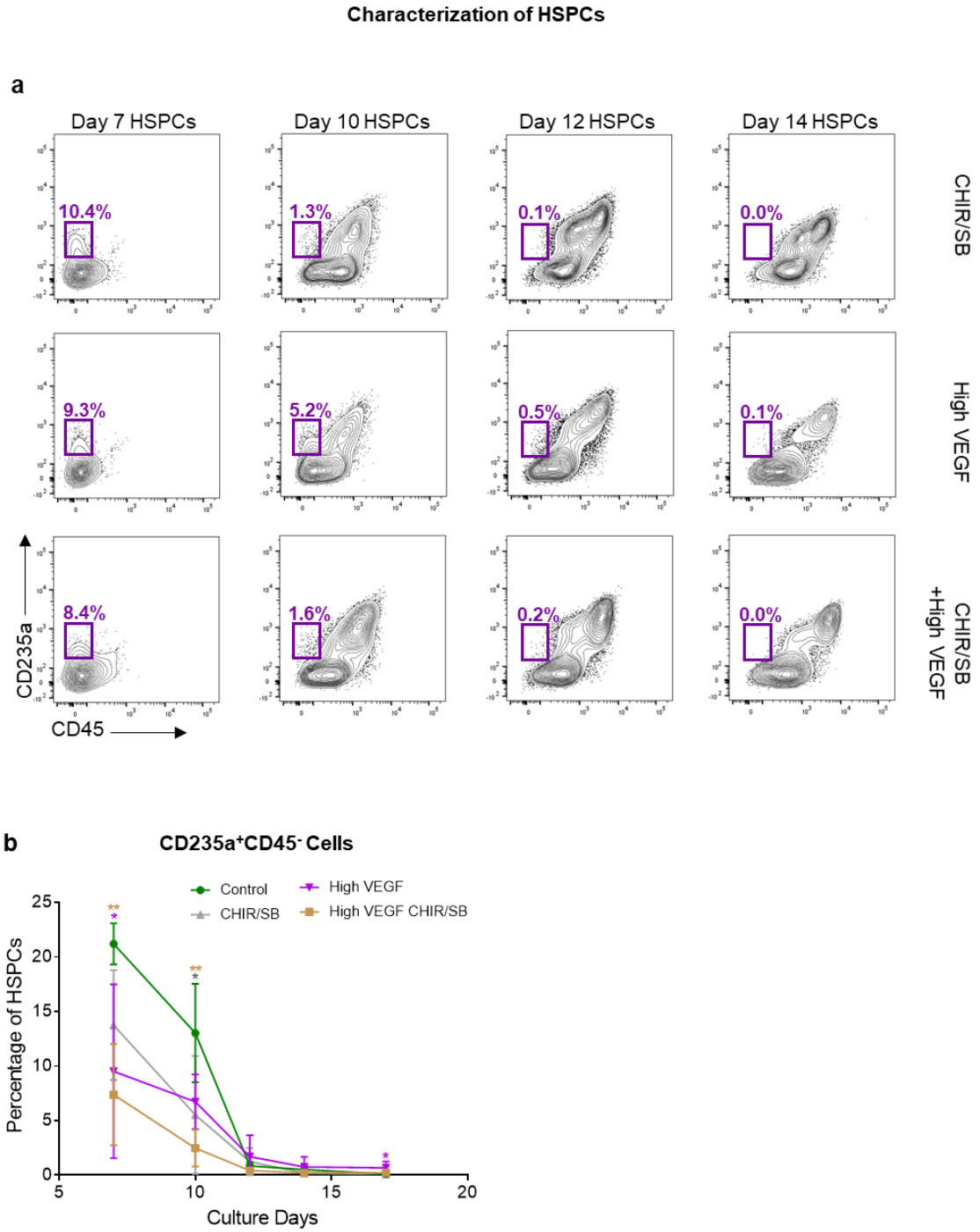

Figure 5.10 HSPC Characterisation in h-iPSC Treatment Conditions (Continued)
a) Representative flow cytometry plots of CD45 and CD235a expression in HSPC populations; purple gates = $CD235a^{+}CD45^{-}$ cells. Gates set as in Supplementary Figure 5.1b b) Percentage of HSPCs composed of primitive erythroid cells, as gated in a, at various timepoints; n = 5 for control, CHIR/SB; n = 4 for High VEGF, CHIR/SB + High VEGF. Averages ± SD depicted. Ordinary, two-Way ANOVA with Dunnett's post-hoc test for multiple sample comparison to a control only.

At the monolayer level (Figure 5.11a), the treatments had differing effects. Treatment with CHIR/SB alone led to significantly higher percentages of the monolayer composed of $CD34^{-}CD144^{-}$ stroma at Day 10 and Day 12 of culture, while treatment with high levels of VEGFA alone led to a significant decrease in stromal percentages at all timepoints (Figure 5.11b). Combination treatment showed a less pronounced decrease in stromal composition of monolayer, potentially due to the opposing effects of the two treatments.

On the other hand, combination treatment led to higher percentages than control of VE percentages in the monolayer at Day 7 of culture, as did treatment with VEGFA alone, to a lesser degree (Figure 5.11c). On its own, treatment with small molecules led to no significant differences in VE percentages at early timepoints compared to control, suggesting, as expected, VEGFA is the main driver of VE development and proliferation at these stages. SB/CHIR treated cells also trended towards lower VE percentages at later culture stages, though these differences were not significant. This effect also occurs in combination-treated cells, as there is no significant difference between VE percentages to control cells at these timepoints, while cells treated with high VEGFA alone maintain significantly higher VE percentages, despite high variabilities (Figure 5.11c). Preliminary data suggests that the drastic decrease in VE populations at Day 10 across conditions has to do with kit specifications of half media changes at Day 7 and then Day 10, as opposed to every other day. At Day 7, VE cells from samples treated with CHIR/SB and VEGFA also have significantly higher levels of *HoxA5*, *HoxA9*, and *HoxA10* expression (Figure 5.11d) than cells treated with VEGA only, suggesting that addition of high VEGFA does not negate the effect of the small molecules on HOXA gene expression. Bad sample quality in HSPC populations

from which RNA was extracted prevented us from testing whether this significance remained in HSPC populations at later timepoints in high VEGFA treated samples, and requires further testing.

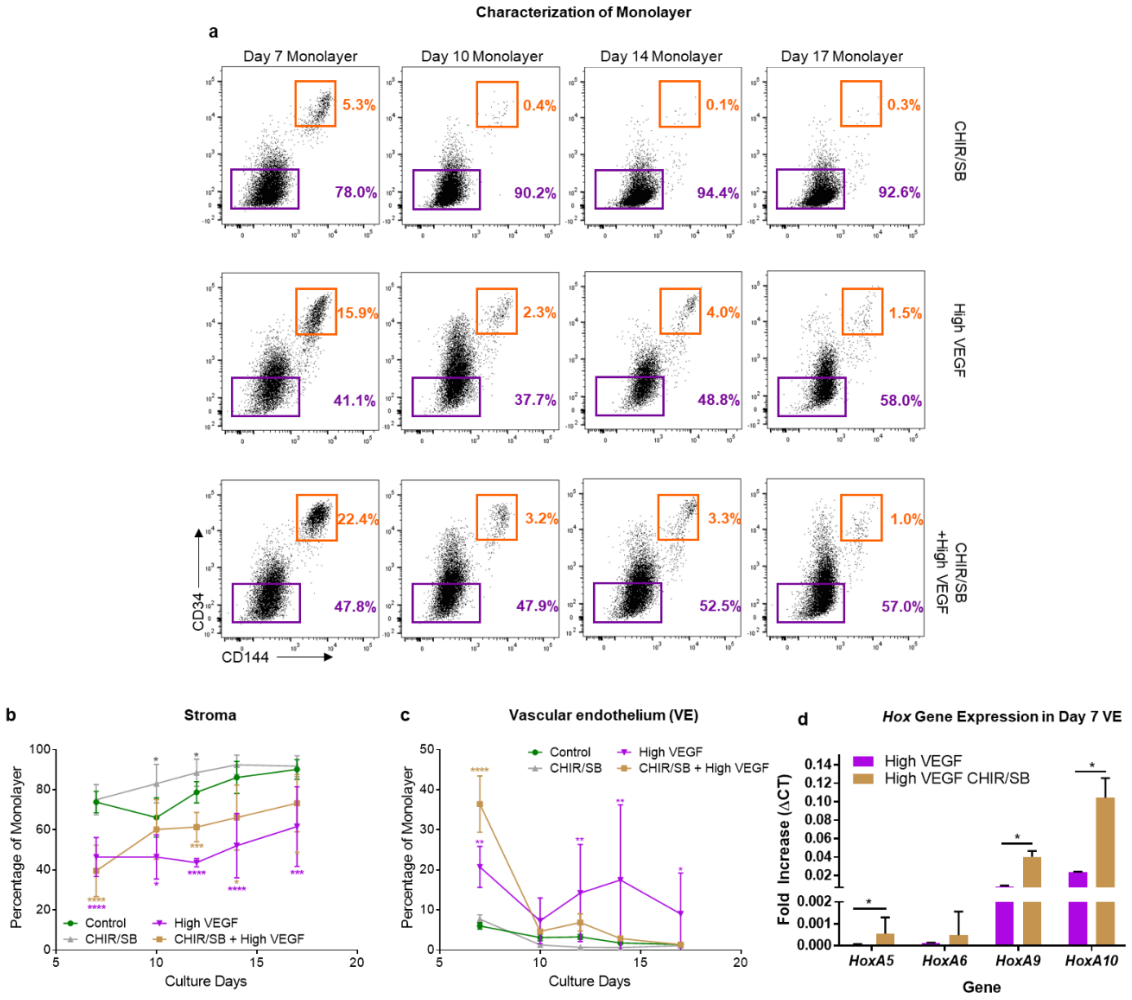

Figure 5.11 Monolayer Characterisation in h-iPSC Treatment Conditions
a) Representative flow cytometry plots of $CD34^{-}CD144^{-}$ stromal populations and $CD34^{+}CD$ $CD144^{+}$ VE; Purple Gates = stroma, Orange Gates = VE. Gates set as in Supplementary Figure 5.3a b) Percentage stromal cells, as gated in a, of monolayer at various timepoints; n = 5 for control, CHIR/SB; n = 4 for High VEGF, CHIR/SB + High VEGF. Averages ± SD Depicted; Ordinary, two-Way ANOVA with Dunnett's post-hoc population comparisons to control. c) Percentage of VE, as gated in a, of monolayer at various timepoints. Statistics and replicates as in b. d) RT-qPCR data of *Hox* gene expression in sorted Day 7 VE populations, as gated in a, of samples treated with either High VEGFA or High VEGFA and CHIR/SB; n = 3 experimental replicates; 95% confidence intervals depicted; unpaired, two-sided t-test on linear ΔCT values as in rest of RT-qPCR data in thesis and described in more detail in Materials and Methods section.

Analysis of the composition of the VE itself revealed that in conditions treated with high levels of VEGFA, both alone and in combination with small

molecules, the majority of VE is comprised of arterial endothelium as late as Day 14 of culture, a time at which no arterial endothelium is left in control cultures or cultures treated with small molecules alone (Figure 5.12a). When visualised as a percentage of the entire monolayer (Figure 5.12b), the trends observed follow those of total VE (Figure 5.11c), albeit with higher variabilities. Combination treatment leads to significantly higher percentages of the arterial endothelial composition of the monolayer at Day 7 that are not sustained beyond Day 10, while treating with higher levels of VEGFA alone leads to a recovery of higher arterial endothelium percentages at culture Days 12 and 17 (Figure 5.12b).

Given these increases in cells expressing an arterial phenotype, data collected was also analysed for the presence of $DLL4^{+}CD73^{-}$ cells, the immunophenotype recently reported for arterial HE (Uenishi et al. 2018). Cells in the VE gate from combination treatments expressing a $CD73^{-}DLL4^{+}$ immunophenotype (Figure 5.12c) were found to comprise a significantly higher percentage of the monolayer than in control cultures at early Day 7 (Figure 5.12d). Though the same trend is observed at Day 5, lack of replicates at this time point did not allow for statistical analysis. While treatment with high levels of VEGFA alone also led to apparently higher percentages of arterial HE at Day 5, these were not as high as those produced in combination treatment, again suggesting a combinatorial effect from treatment with both small molecules and high VEGFA levels. This combinatorial effect could in part, be due to the combination of proper mesodermal patterning alongside activation of an arterial niche.

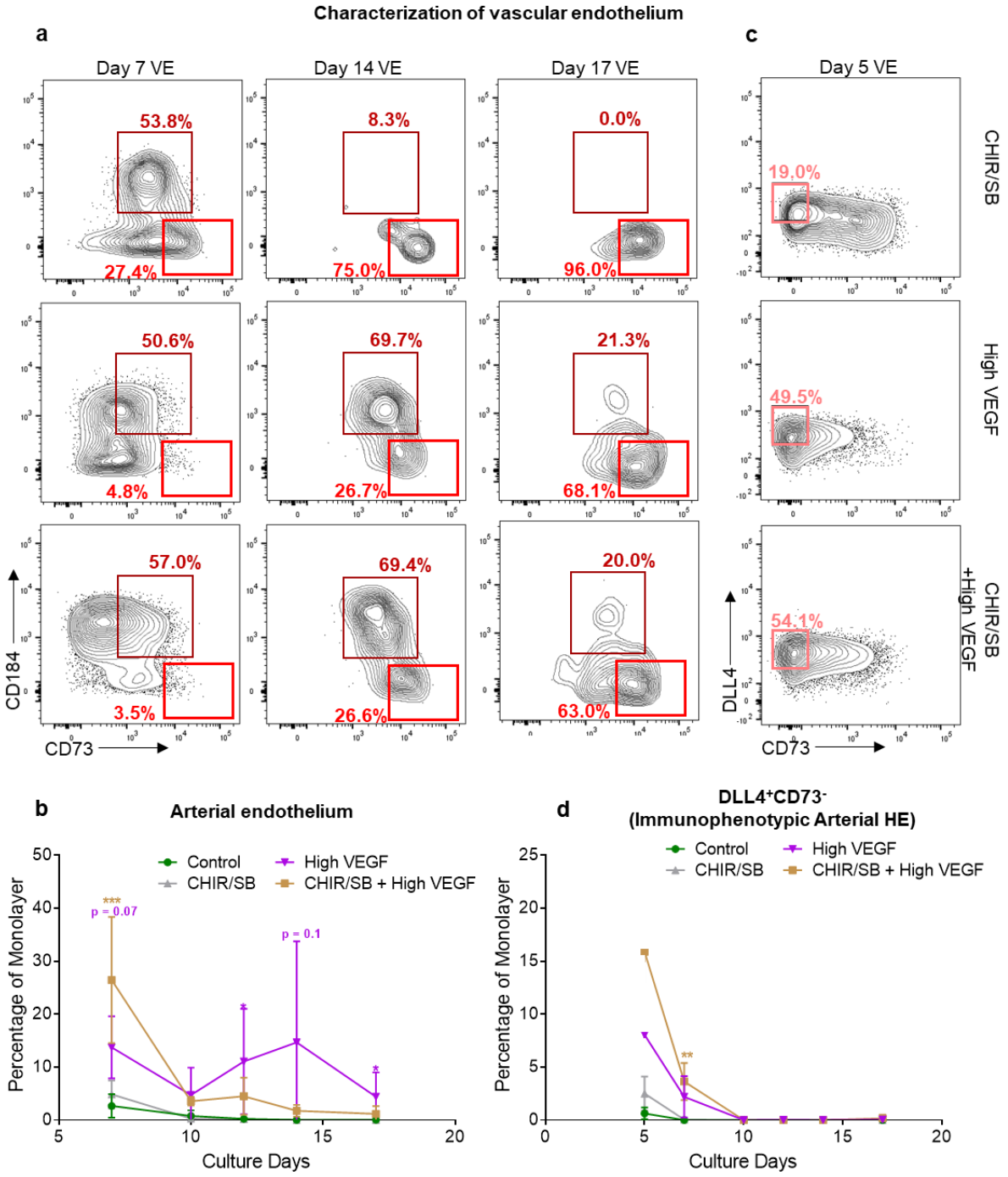

Figure 5.12. VE Characterisation in h-iPSC Treatment Conditions

a) Representative flow cytometry plots of CD73 and CD184 expression in VE populations; dark red Gates = $CD184^{+}CD73^{Mid}$ arterial endothelium, red gates = $CD184^{-}CD73^{High}$ venous endothelium. Gates set as in Supplementary Figure 5.3b b) Percentage of monolayer composed of arterial endothelial cells, as gated in a, at various timepoints; n = 5 for control, CHIR/SB; n = 4 for High VEGF, CHIR/SB + High VEGF, Averages ± SD Depicted; Ordinary, two-Way ANOVA with Dunnett's post-hoc population comparisons to control. c) Representative flow cytometry plots of CD73 and DLL4 expression in VE populations; pink gates = $DLL4^{+}CD73^{-}$ endothelium. Gates set as In Supplementary Figure 5.4 d) Percentage of $DLL4^{+}CD73^{-}$ cells, as gated in c, of monolayer at various timepoints. Statistics and replicates as in b*. (*) n = 2 for d) Day 5 timepoint for High VEGF and CHIR/SB + High VEGF. No statistics were run for this timepoint given n of 2.

5.7. Discussion

Our data suggest that modulating the concentration of VEGFA is an important aspect of PSC to HSPC differentiation systems. In the same way that the presence of $DLL4^+$ cells with haematopoietic potential are detected in the mESC differentiation system when cells are treated with high concentrations of VEGFA (Chapter 4.5), high VEGFA concentrations in this h-iPSC monolayer system led to the development of immunophenotypic $DLL4^+CD73^-$ VE cells, which have recently been described *in vitro* as arterial HE (Uenishi et al. 2018). Of course, further sorting and single-cell experiments are required to verify that, in this system, $DLL4^+CD73^-$ cells also have the potential to undergo EHT and produce HSPCs.

VEGFA concentrations in both mouse and human differentiation systems for VE or HE are often overlooked, ranging from 5 ng/ml through 200 ng/ml (Irion et al. 2010; Guyonneau-Harmand et al. 2017). While high concentrations of VEGFA (at 50 ng/ml) have been reported to adversely affect proliferation and viability of human $FLK1^+$ endothelial progenitors (Sriram et al. 2015), we observed this in the mESC differentiation system, but not in this h-iPSC differentiation system, which used four times as much VEGFA (200 ng/ml) as Sriram et al. One working hypothesis is that this discrepancy is due to purification of FLK1 cells before or shortly after exposure to high VEGFA levels in the mESC system reported in this thesis as well as the h-iPSC system which reported these adverse effects (Sriram et al. 2015); other h-iPSC studies, such as the one in this chapter, use either unsorted monolayer strategies or EB systems, where other cells could be acting as VEGFA sinks or creating concentration gradients across the EB. It should be noted however, that the recent report which described arterial HE also sorts endothelial progenitors, albeit with $CD31^+$ magnetic assisted cell sorting

(MACS), and uses 50 ng/ml of VEGFA, reporting no detrimental effects to the viability or proliferation of cells (Uenishi et al. 2018).

As our data in both mouse and human systems has shown, VEGFA concentrations can be used to increase the percentage of both arterial HE as well as a supportive arterial niche present in the system, which can be maintained throughout culture. Further studies will have to determine whether or not these high VEGFA concentrations have a direct effect on differentiating HSPCs, as opposed to merely indirectly through Notch signalling in arterial progenitors. For this, consistent maintenance of the arterial niche throughout culture days is required. As mentioned earlier, the decrease in VE and arterial endothelial cells at Day 10 of culture, a critical timepoint right before the highest HSC-like cells are detected, is likely due to the differentiation kit's protocol, which calls for half media changes every other day save for Days 10 and 17, at which point two days have passed before half media changes are done. Future studies are planned to test the effect that consistent half media changes done daily or every other day will have on the VE populations found in culture. Bioreactors which simulate the shear stress from blood flow could ideally provide both a constant supply of renewed cytokines as well as the shear stress signalling that maintains arterial identity *in vivo*.

Activation of *Hox* genes in differentiating HSPCs through ectopic TF activation has been previously shown to affect differentiating HSPC function and even lead to engraftment (Kyba, Perlingeiro, and Daley 2002). Beyond this, Notch signalling from the arterial niche has been shown to be independently regulated and missing in these cells (McKinney-Freeman et al. 2012), and to confer full lymphoid potential (Lu et al. 2016). While a previous study has observed the effects that small molecule activation of *HOXA* genes in the presence of relatively high

VEGFA levels (50 ng/ml) has on differentiating HPSC populations, the study found low activation of arterial genes alongside venous genes in developing endothelial cells (Ng et al. 2016).

While it remains to be seen how different VEGFA levels in this h-iPSC system lead to varying commitment levels of an arterial lineage, our study is, to our knowledge, the first to observe the effects that definitive mesodermal patterning and subsequent *HOXA* gene activation can have in combination or independently of concomitant arterial niche activation without ectopic TF activation of potentially oncogenic *Hox* genes as in Lu et al (Lu et al. 2016). Preliminary data of n = 1 suggests HSPCs arising from high VEGFA and combination treatment protocols fail to engraft NSG mouse models. Replicate engraftment studies, recently completed following this thesis' *viva* examination, also showed no engraftment. Further replicate experiments are also needed to see if treating cells with high VEGFA leads to statistically higher percentages of adult β-globin production in downstream erythroid cells. As mentioned in the introduction, protocols which recapitulate second-wave, definitive haematopoiesis are not necessarily approaching HSC production, as second- and third-wave haematopoiesis occur at different and independent times and locations in the embryo.

Follow up studies to those that reported arterial HE showed that activation of ectopic ETS1 or MAPK/ERK signalling through small molecules leads to the described arterial niche effect of giving greater lymphoid potential to differentiating HSPCs (Park et al. 2018). ETS1 signalling has been reported to signal in conjunction with VEGFA in endothelial cells (Chen et al. 2017). VEGFA is also known to signal through MAPK/ERK pathways in angiogenesis (Shin et al. 2016). It therefore remains to be seen whether high VEGFA levels in differentiating

cultures are activating the same or different genetic programmes than ectopic ETS1 activation. Whether through small molecule activation of MAPK/ERK or high VEGFA levels (or both), as well as *HOXA* activation through the use of small molecules, protocols for the differentiation of functionally engrafting HSPCs will require activation of both a differentiating arterial niche as well as of *HOX* cluster genes. These studies in a monolayer h-iPSC to HSPC model not only provide a modifiable and clinically-safe model for the production of therapeutic HSPCs, but also point to VEGFA as an important factor to be considered when designing protocols for this purpose. They add to the recent and important literature on the topic, and similar to studies in this thesis in a mouse model, point towards VEGFA concentrations as a potential explanation for seemingly contradictory results regarding the haematopoietic potential of developing arterial cells (Ditadi et al. 2015; Hadland et al. 2017; Ayllón et al. 2015; Uenishi et al. 2018).

6. Conclusion

Autologous, gene-corrected, haematopoietic stem cell transplant (HCT) can provide better treatment alternatives for patients with a variety of bone marrow failures and malignant haematopoietic disorders. Given the loss of the majority of HSCs in patients with inherited bone marrow failures, it is likely that *in vitro*-derived HSCs will first be tested in these groups. Despite advances in our understanding of HSC development and two recent publications detailing protocols for the *in vitro* differentiation of HSCs upon overexpression of TFs (Sugimura et al. 2017; Lis et al. 2017), much work remains to characterise the *in vivo* signals necessary and sufficient for the differentiation of functional, engrafting HSPCs. Recapitulating these signals *in vitro* will allow for the development of scalable, transgene-free, clinically safe protocols that can be used to differentiate HSCs as a suitable replacement for allogeneic HCT. In the following sections, I aim to provide some general concluding thoughts gained from reviewing the literature, writing this thesis, and the conversations during its *viva voce* examination, on what I see as two essential but unanswered questions in the field, as well as suggest potential avenues for future experimentation in attempts to further inform production of HSPCs *in vitro*.

6.1. The Mesodermal Conundrum: Driving Wave 3 Haematopoiesis

As was explored throughout this thesis, it is clear from *in vivo* models in *Xenopus* that the mesodermal precursors which give rise to YS haematopoiesis (Wave 1 and 2 equivalents) and those that give rise to intraembryonic haematopoiesis (Wave 3) are distinct and specified early in development (Ciau-Uitz, Walmsley, and Patient 2000). *In vivo* studies in mice have also shown that early mesodermal precursors to both Wave 1 and Wave 2 haematopoiesis in the YS BI are specified prior to gastrulation, and that these cells rarely give rise, at the clonal level, to both Wave 1 primitive red blood cells and endothelium (including Wave 2 HE), if at all (Ueno and Weissman 2006; Padrón-Barthe et al. 2014). While these *in vivo* models demonstrate uni-lineage *fate* (with respect to primitive erythroid and endothelial fates) of these YS mesodermal progenitors, their bi-lineage *potential*, and what led them to be described as haemangioblasts, becomes evident only as an artefact of *in vitro* assays (Huber et al. 2004). The haemangioblast equivalent that arises from mouse pluripotent cultures *in vitro*, the $FLK1^{+}$ BL-CFC (Choi et al. 1998; Faloon et al. 2000) is similarly multipotent: *in vitro*, this population has also been shown to give rise to vascular smooth muscle populations in addition to endothelium and blood (D'Souza, Elefanty, and Keller 2005).

In the serum-free culture system explored and characterized in this thesis, we also found that early-stage $FLK1^{+}$ cells, described in the literature as mainly giving rise to primitive haematopoiesis (Irion et al. 2010), could in fact also give rise to late-stage $FLK1^{High}$ cells of a Wave 2-like nature (Clarke et al. 2013; Clarke et al. 2015). Likewise, preliminary data showed that the $FLK1^{High}$ cells arising from early $FLK1^{-}$ and $FLK1^{+}$ cells were seemingly the same, at least at the

immunophenotypic level tested. In order to confirm this, functional and RNA-sequencing experiments in our population-tracing system would have to be undertaken. Day 5.5 FLK1^{High} cells can be sorted based on their mCherry expression (and therefore, origin from Day 3.5 FLK1^{+} or FLK1^{-} cells), and used in downstream RNA-sequencing experiments in which differences in global gene expression can be assayed, or in functional experiments where, through replating on OP-9 and OP9-DLL1/DLL4 cells, downstream haematopoietic potential can be assessed. These experiments however, are limited by the assumption that the Day 3.5 FLK1^{+} (also PDGFRα^{+}) population is, in and of itself homogenous. This is unlikely, as the cells are purified based expression of only one marker, FLK1. Indeed, a recent single cell RNA sequencing study of mouse embryos from E6.5 to E8.5 showed the heterogeneity (at the gene expression level) found within *Flk1* expressing populations (Pijuan-Sala et al. 2019). Follow-up clonal studies would be useful in addressing this limiting assumption. Day 3.5 FLK1^{-} and, more importantly, FLK1^{+} cells, from a line which ubiquitously expresses any of the fluorescent proteins, can be clonally sorted and reaggregated with WT cells to assess downstream lineage at Day 5.5 and beyond. For a more complete picture, this experiment could also be repeated with FLK1^{+} and FLK1^{-} cells from earlier and later time timepoints.

The topic of different mesodermal populations and their downstream lineages becomes particularly salient in the context of the human iPSC systems. Through manipulation of the WNT and Activin signalling pathways, one can abrogate the primitive haematopoietic wave in favour of a definitive one, and therefore “pattern,” the mesoderm to produce definitive haematopoietic waves (Kennedy et al. 2012; Sturgeon et al. 2014; Ditadi et al. 2015). However, as has

been discussed throughout this thesis, if these waves more closely resemble YS haematopoiesis, then conclusions drawn from these *in vitro* studies are limited to this context. Conditions favouring Wave 2 haematopoiesis, definitive though it may be, will still come up short of HSC production. It is likely that *in vitro* as in *in vivo,* the bifurcation of Wave 2 and Wave 3 haematopoiesis occurs at the mesodermal stage, where instruction of the mesoderm at the genetic and epigenetic level is required early on to respond to appropriate signals at later differentiation stages.

Different approaches can be used to attempt to differentiate mesoderm that can produce Wave 3 haematopoietic cells. High-throughput, automated cell culture techniques can be used to screen thousands of cell culture conditions at once in an unbiased fashion. Alternatively, one could also carefully and precisely design a differentiation protocol, favouring (and purifying) specific lineages while blocking others through the use of small molecules. Such an approach was used by Loh and colleagues to differentiate a variety of highly purified mesodermal lineages (Loh et al. 2016). Whether using either of these approaches or some combination of both, there needs to be markers, either at the immunophenotypic or gene expression level, used to “flag,” the intraembryonic mesoderm and other downstream lineages once they are produced.

Attempts have been made, and in the context of those specific studies, succeeded, in finding differences between intraembryonic and extraembryonic mesodermal or downstream populations in the YS and AGM. While YS haematopoiesis is not dependent on Notch activity in the way that intraembryonic haematopoiesis is (Hadland et al. 2004; Kumano et al. 2003), this is not so much a marker as it is a post-hoc test for producing intraembryonic haematopoiesis, and is not entirely precise. Beyond complete abrogation of AGM haematopoiesis, the

two studies mentioned above also showed slight decreases in YS haematopoietic output upon lack of Notch signalling, making the functionality of this assay imprecise in the *in vitro* context, where lack of spatial cues do not allow for ad-hoc separation of populations. Similarly, though YS HE has been shown to be independent of and not express the Ly6a gene at the time of YS haematopoiesis, unlike its AGM HE counterpart, Ly6a is later expressed in the YS (Chen et al. 2011), making this again, an imprecise marker for AGM HE *in vitro*, where timing and spatial references used by investigators to define populations are missing. Recently a study found that expression of the *Hlf* gene distinguishes HE that produces HSCs from that which produces EMPs (Yokomizo et al. 2019). Some *Hlf*-expressing HE that lead to the differentiation of lymphoid progenitors were also detected in the YS, albeit at low frequencies. Though this marker could potentially be useful at the HE differentiation stages, it is not expressed early on at the mesodermal level, and so would not be useful for determining specification of the mesoderm.

RNA sequencing experiments comparing YS and Intraembryonic mesoderm, or downstream YS HE and AGM HE might likewise yield some answers in this arena. However, given that the timing of YS HE and AGM HE ontogeny is different, even designing experiments in which developmentally-matched HE populations from both sites are compared would prove technically difficult. Using a slightly different approach, one recent study aimed at mapping early lineage decisions in the developing embryo, from the primitive streak to early somite stages of development (E6.5 – 8.5) (Pijuan-Sala et al. 2019). This study produced a wealth of data, housed in an online repository, that can be mined for some of these potential genes of interest. For example, various clusters of endothelial

populations, including those expressing haematopoietic genes, were detected. In follow-up experiments, investigators spatially separated cells from the allantois, YS, and intraembryonic regions before sorting on FLK1^{+} and single cell RNA-sequencing once more. The data was mapped back to their original data-set and interestingly enough, some of the endothelial clusters were also separated based on spatial distribution in the embryo. Though limited to only one developmental timepoint, data such as these can be mined for genes differentially expressed between extra- and intra-embryonic populations, with follow-up studies assessing not just the biological relevance, but the practicality of using such markers to trace mesodermal specification *in vitro*.

6.2. The Arterial Conundrum: Arterial Programming of HE

If most pluripotent systems to date are limited by driving mesoderm and downstream lineages that resemble YS endothelium and haematopoietic cells, then the same is likely true of the systems used in this thesis. Indeed, some of our data in both the mouse and human systems assayed seemed to suggest this. The fact that FLK1^{High} cells arise with no supportive arterial niche indirectly suggests this second wave-like identity, among other immunophenotypic data (Frame et al. 2016)(Chapter 3). While transiently treating FLK1^{High} HE cells with higher levels of VEGFA led to a global upregulation of arterial and Notch signalling genes in culture, we found no differences in the immunophenotype of differentiating HSPCs, nor their CFU potential. By adding higher levels of VEGFA to either the human or mouse systems, it is possible that we were driving differentiation towards short-lived YS arterial endothelial cells, and not intraembryonic-like arterial endothelium.

Therefore, the observations in this system that suggest the haematopoietic potential of DLL4^{+} endothelium could be dependent on varying exposures to VEGFA (Chapter 4, Figure 6.1), are limited to an *in vitro* context, and may not have significance or relevance to *in vivo* intraembryonic conditions. Further testing, particularly at the clonal and functional level, is required to rule out the possibility that contamination at the population level from DLL4^{-} cells in sorted DLL4^{+} samples are what are leading to the low levels of observed haematopoietic output from DLL4^{+} cells. If confirmed however, these findings could lead to the consolidation of recent and seemingly contradictory data on the haematopoietic potential of DLL4^{+} cells during HSPC ontogeny *in vitro* (Ditadi et al. 2015; Ayllón et al. 2015; Park et al. 2018; Uenishi et al. 2018). While it is likely possible to have some level of haematopoietic output from YS cells expressing DLL4^{+} (Uenishi et al.

2018)(Chapter 4, Figure 6.1b), it is more probable that *in vivo* YS conditions and similarly, *in vitro* conditions, favour the early lineage separation of HE from endothelium that will differentiate into venous and arterial cells (Ditadi et al. 2015; Frame et al. 2016)(Chapter 4, Figure 6.1a). In our human system, the mesoderm was patterned with small molecules in combination with high VEGFA, which lead to an increase in both arterial endothelium (Ditadi et al. 2015) and immunophenotypic HE (Uenishi et al. 2018) at early culture days. However, the fact that the model is one of YS-like haematopoiesis limits not just our conclusions about the role that VEGFA might play in haematopoiesis to *in vitro* conditions, but also the potential for HSC production of the system. In other words, the presence of DLL4^{+} endothelial cells that can produce HSPCs signals the presence of intraembryonic HE and improvements towards HSC production no more than does the presence of a definitive wave *in vitro*.

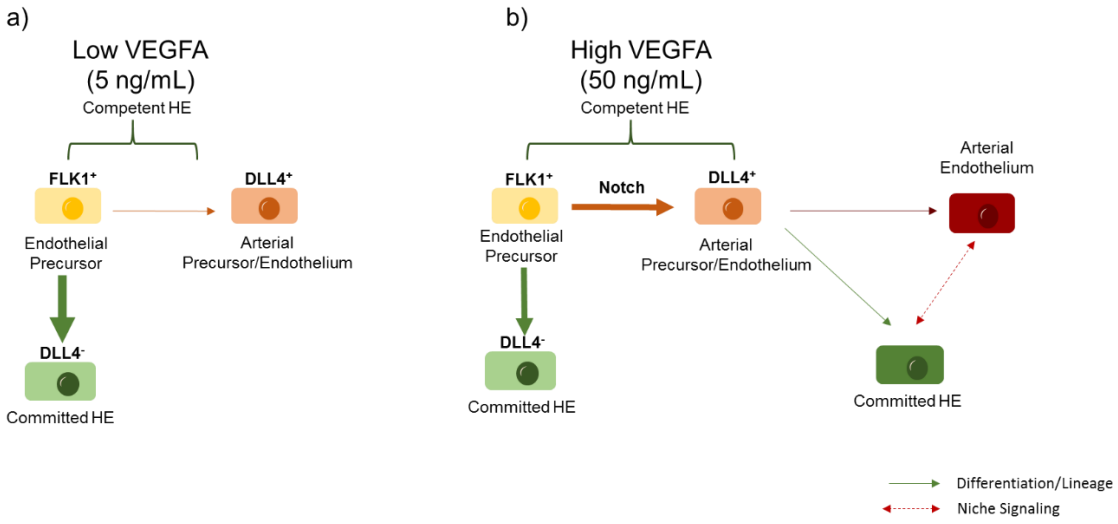

Figure 6.1 Chapter 4: VEGFA regulation of DLL4^{+}/DLL4^{-} HE
a) In culture conditions with low VEGFA concentrations, few DLL4^{+} cells with no HSPC potential were present at the time of HE specification. DLL4^{-} cells contained second wave-like HSPC potential. b) In culture conditions with high VEGFA concentrations, both DLL4^{+} and DLL4^{-} cells had some level of HSPC potential, concomitant with an upregulation of arterial identity and Notch signalling genes.

Because of the limitations of the *in vitro* systems listed above, it is unlikely that experiments done *in vitro* will solve the question of whether a cell-intrinsic arterial programme is required in HE to produce HSCs. Future *in vivo* conditional lineage-tracing studies in *Efnb2, Nrp1, Dll4,* and *Cxcr4* reporter mouse lines could answer the question of whether HSCs passed through an intermediate HE population that expressed any of these individual arterial markers, but still doesn't get at the question of whether any of these are intrinsically required to produce HSCs. Potential experiments to answer this question would be to use chimeric mice, in which traceable *Efnb2*$^{-/-}$, *Dll4*$^{-/-}$, or *Nrp1*$^{-/-}$ mESCs are injected into WT embryos, to trace the contribution of these cells to adult blood lineages. Of course, any other number of arterial markers (save for *Cxcr4*, a critical HSPC homing ligand, whose role would therefore only be able to be assayed up to EHT) could be tested in this way. Still, these studies would address only one of the many questions surrounding the pathways critical to HSC ontogeny. While I was interested in exploring the role that hypoxia, inflammatory signalling, and shear stress, among other conditions and stimuli, affected and potentially improved *in vitro* HSPC protocols, this was beyond the scope of the thesis and would have further diffused rather than focused the work.

Throughout the process for producing this thesis, through experiments, readings, and conversations, it has become clear to me that the process for producing HSCs *in vitro* still has some way to go, and will require exploration of not just the mesodermal origin of the HSC lineage and its developmental relationship with the arterial lineage, as discussed in this chapter, but also exploration of the pathways described above. The data presented here provides two controlled and

characterised systems that can be used for future studies of YS-like *in vitro* HSPC development. If not the characterizations and modifications to existing systems that led to the data presented here, then hopefully some of the conversations spurred by colleagues, critics, and collaborators captured herein will provide insights into the recapitulation of *in vivo* conditions for the production of HSCs. These, alongside new *in vivo* discoveries in what is a fast-moving field can pave the way towards a better understanding of HSC differentiation and the development of scalable differentiation systems for their production as personalized therapies for patients with various congenital blood disorders.

Appendix I: Supplementary Figures

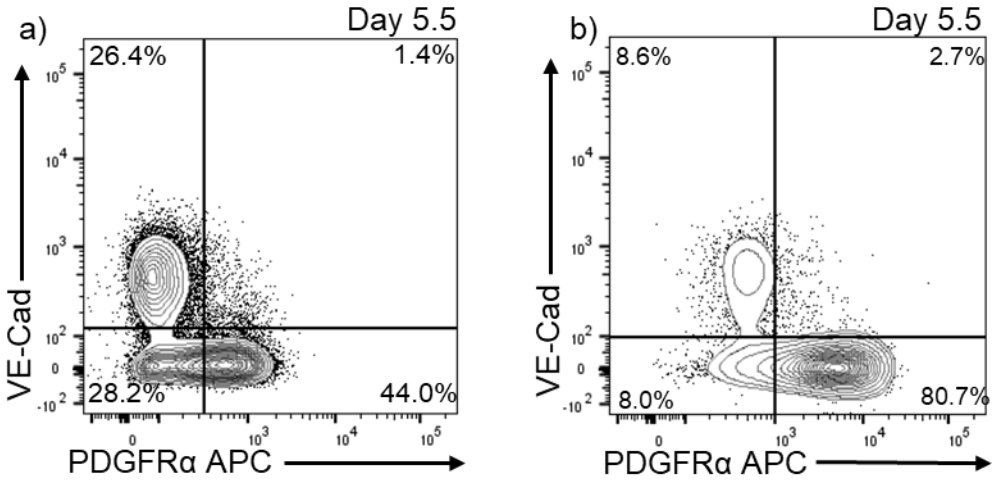

Supplementary Figure 3.1. Associated with Figure 3.8
a) Flow cytometry plot of Day 5.5 VE-Cad and PDGFRα (APC) staining from the same sample as 3.8a-c, independently stained. Given that the NOTCH1, cKIT, DLL4 antibodies were all APC conjugated, and that FLK1^{High}VE-Cad^{+} cells at Day 5.5 are PDGFRα^{-} (Figure 3.2), this sample was used as an internal negative control to set the gates. See Materials and Methods section 2.4.3 for further comment. b) Flow cytometry plot of Day 5.5 VE-Cad and PDGFRα (APC) staining from the same sample as 3.8d. Given JAG1 is also APC-conjugated and VE-Cad and PDGFRα mutually exclusive, as above, this was used as an internal negative control to set the gate in 3.8d. As is discussed in the materials and methods section 2.4.3, either an isotype or FMO would have served as a more appropriate control.

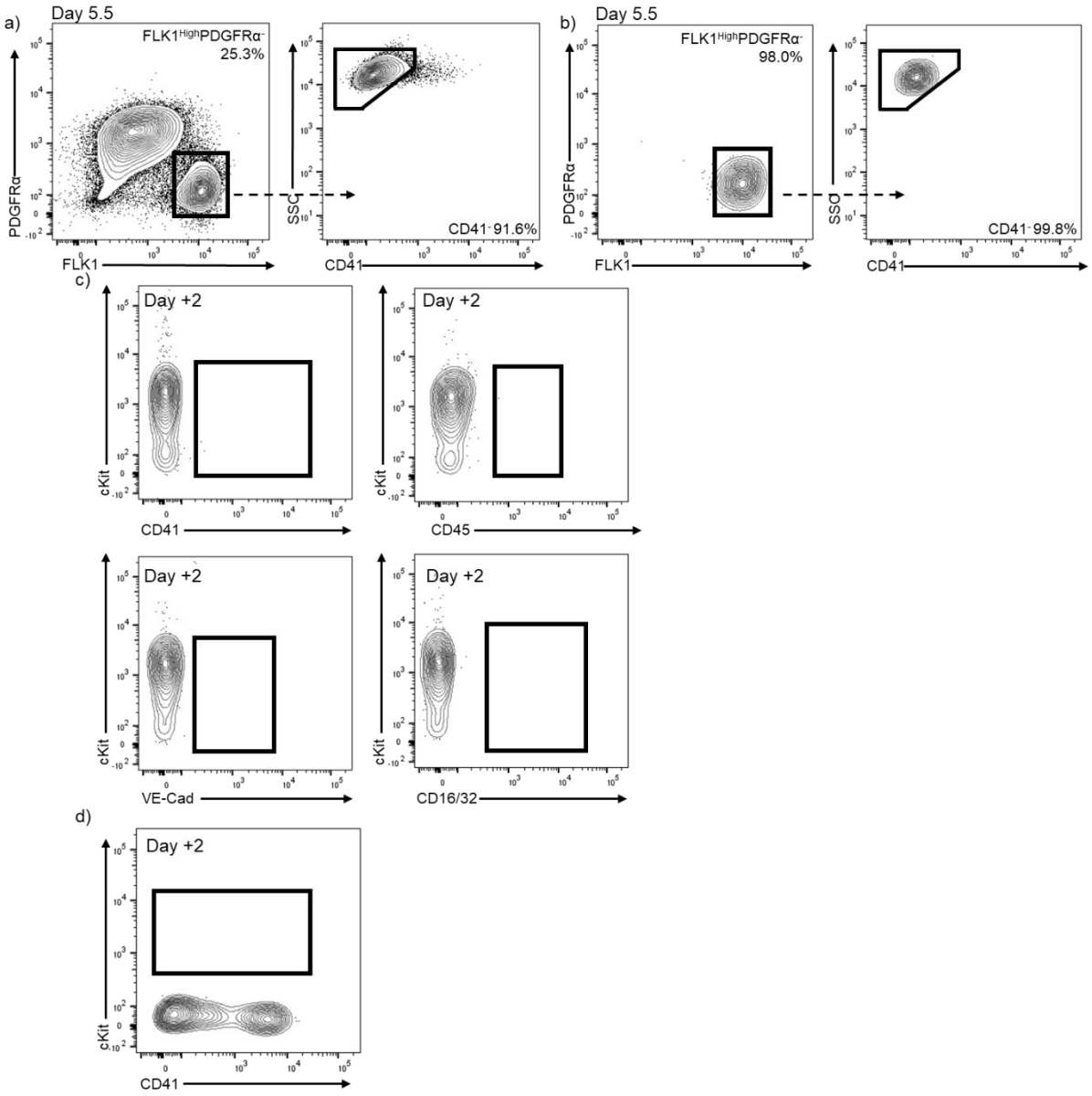

Supplementary Figure 3.2 Associated with Figures 3.9, 3.10, and 3.11
a) Representative flow cytometry plots of a separate differentiation to 3.9b, with gating strategy for sorting FLK1^{High}PDGFRα^{-}CD41^{-} cells b) Representative flow cytometry plots showing purity checks for FLK1^{High}PDGFRα^{-}CD41^{-} sample sorted in a. c) Representative flow cytometry plots of CD41, CD45, VE-Cad, and CD16/32 FMO controls for setting gates in Figure 3.10. d) Representative flow cytometry plot of cKIT FMO control for setting gates in Figure 3.11.

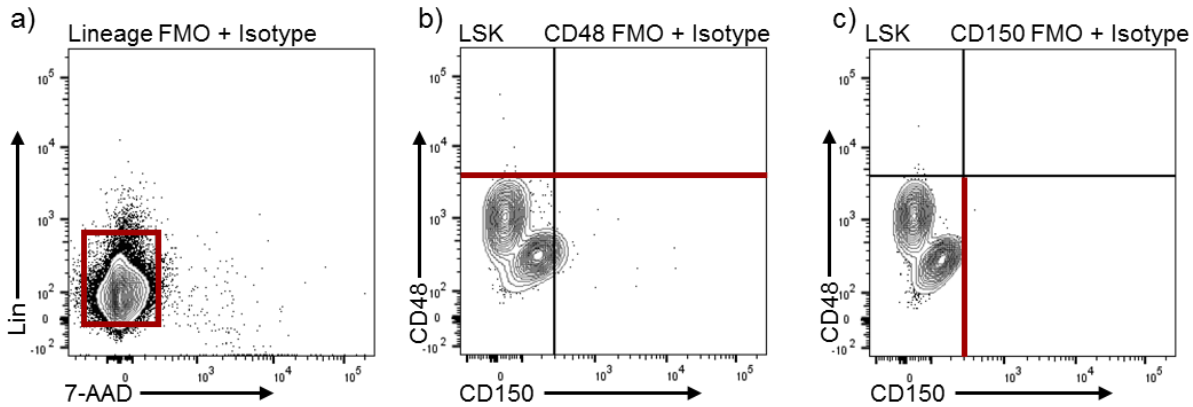

Supplementary Figure 4.1 HSPC characterisation associated with Figure 4.7
a) Representative flow cytometry plot for lineage (FMO + Isotype) control. b) Representative flow cytometry plot gated on LSK for CD48 (FMO + Isotype) control. c) Representative flow cytometry plot gated on LSK for CD150 (FMO + Isotype) control. Red gates for b-c represent gate set using control.

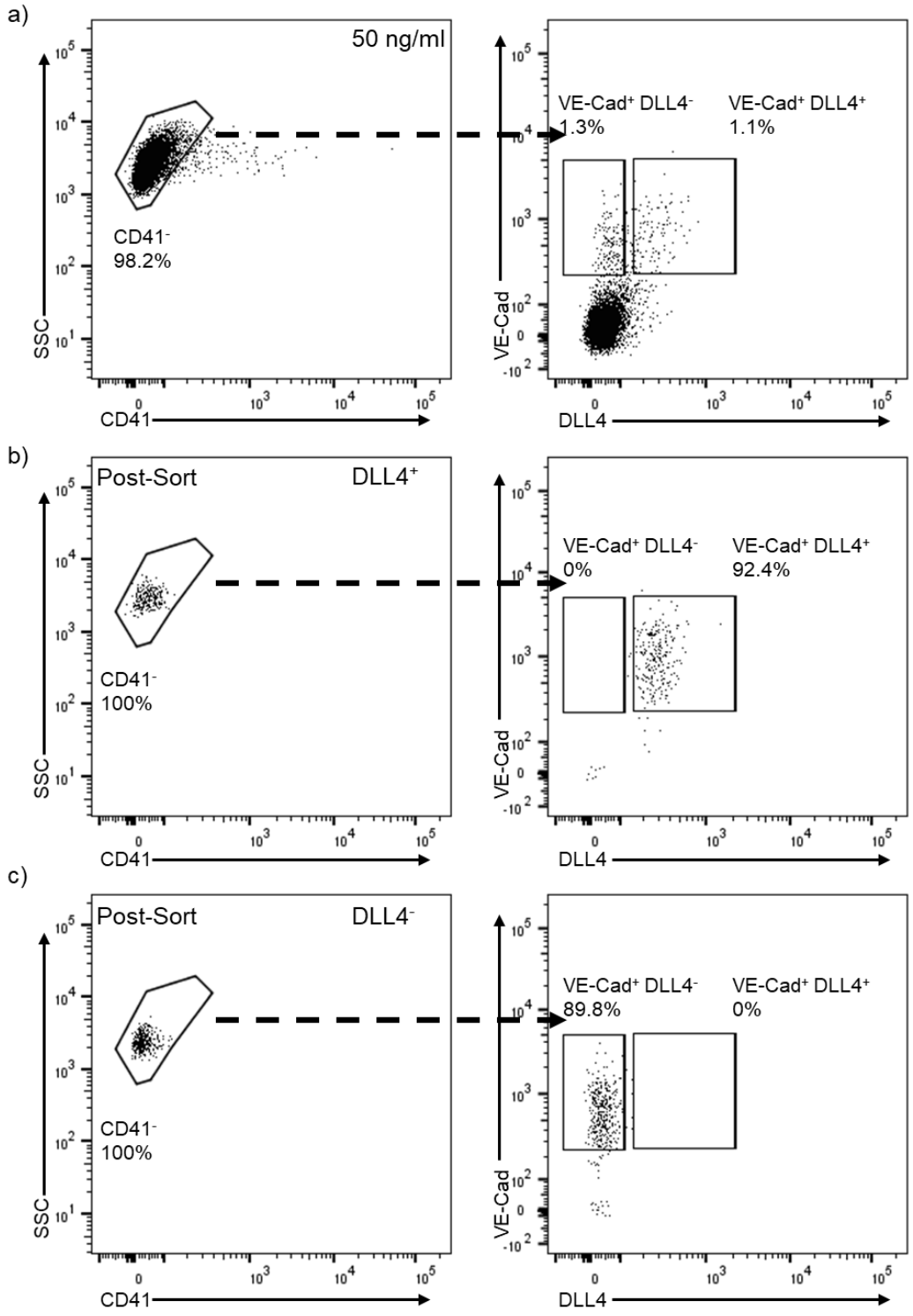

Supplementary Figure 4.2 Gating Strategy and Purity Checks associated with Figure 4.9

a) Flow cytometry plot depicting CD41, VE-Cad, and DLL4 expression at Day 5.5 on cells treated with 50 ng/ml at Day 4.5 and gates depicting $CD41^{-}VE\text{-}Cad^{+}DLL4^{-}$ and $CD41^{-}VE\text{-}Cad^{+}DLL4^{-}$ sorting strategy. b) Flow cytometry plot depicting representative $DLL4^{+}$ post-sort purity check. c) Flow cytometry plot depicting $DLL4^{-}$ post-sort purity check.

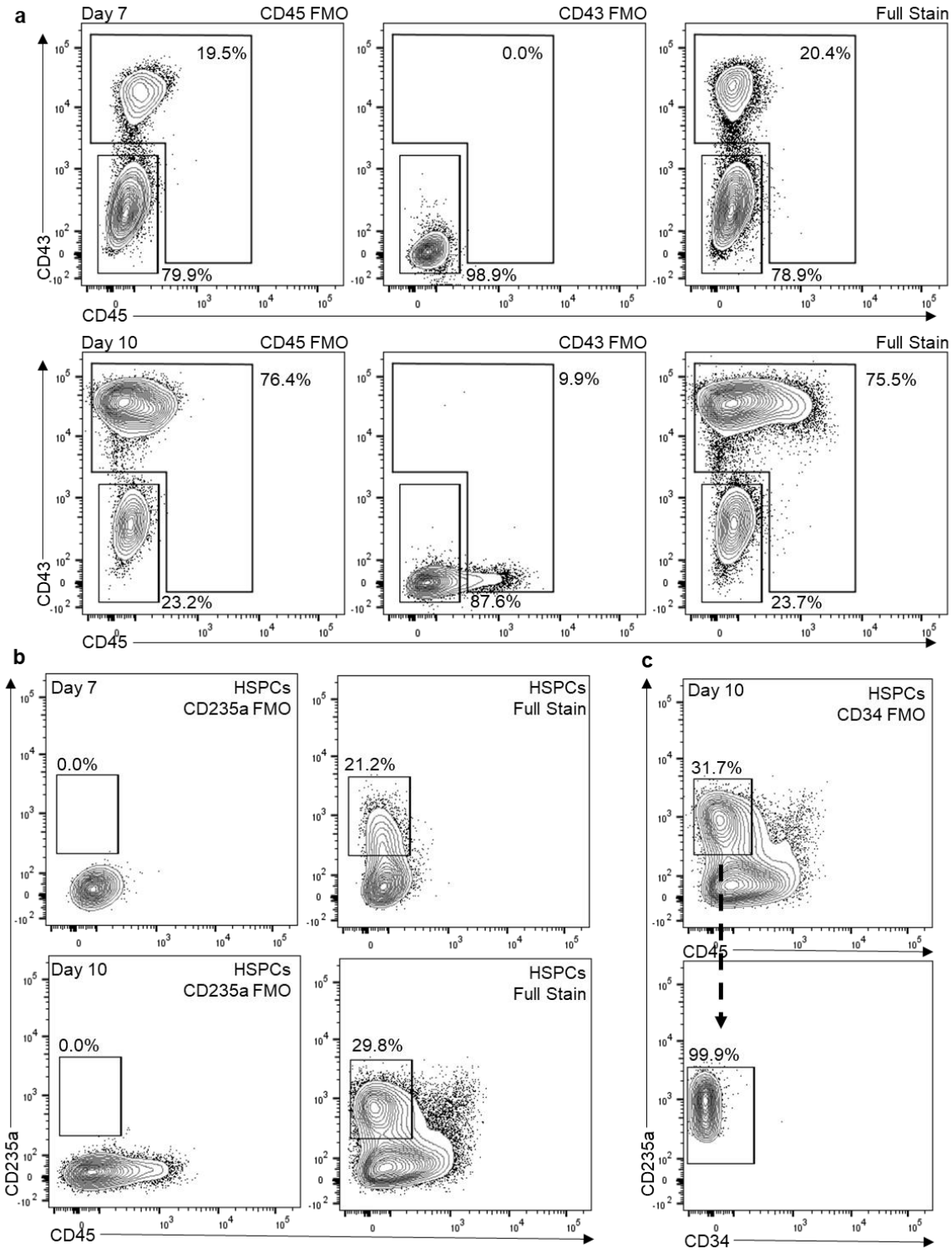

Supplementary Figure 5.1 FMO Controls Associated with Figures 5.1 and 5.2
a) Representative flow cytometry plots of samples at Day 7 and Day 10 with FMO controls for CD43 and CD45, as well as fully stained sample with gating strategy. b) Representative flow cytometry plots of CD45 and CD235a expression in gated HSPC populations at Days 7 and 10. CD235a FMO plot as well as fully stained sample with gating strategy depicted. c) Representative flow cytometry plots of CD235a, CD45, and CD34 expression in gated HSPC populations at Day 10 of culture. CD34 FMO plot within $CD235a^{+}CD45^{-}$ population depicted.

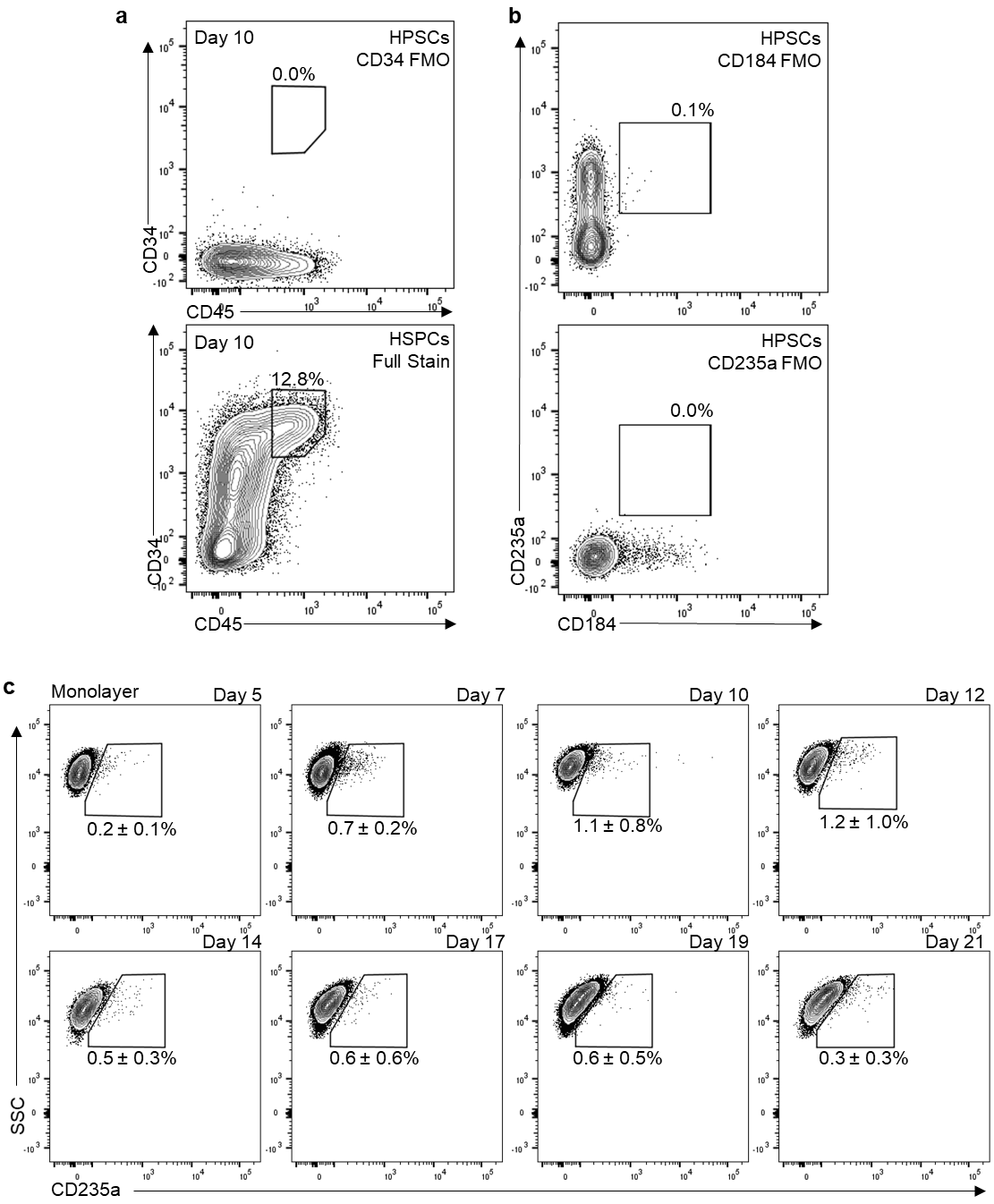

Supplementary Figure 5.2 FMO Controls Associated with Figure 5.2 and Monolayer CD235a Expression

a) Representative flow cytometry plots of CD45 and CD34 expression in gated HSPC populations at Day 10 of culture. CD34 FMO plot as well as fully stained sample with gating strategy depicted. b) Representative flow cytometry plots of CD235a and CD184 expression in gated HSPC populations at Day 10 of culture. CD235a and CD184 FMOs with gating strategy depicted. c) Representative flow cytometry plots of CD235a expression in gated $CD43^{-}CD45^{-}$ monolayer cells for all timepoints collected. n = 3 biological replicates. Averages ± SD depicted.

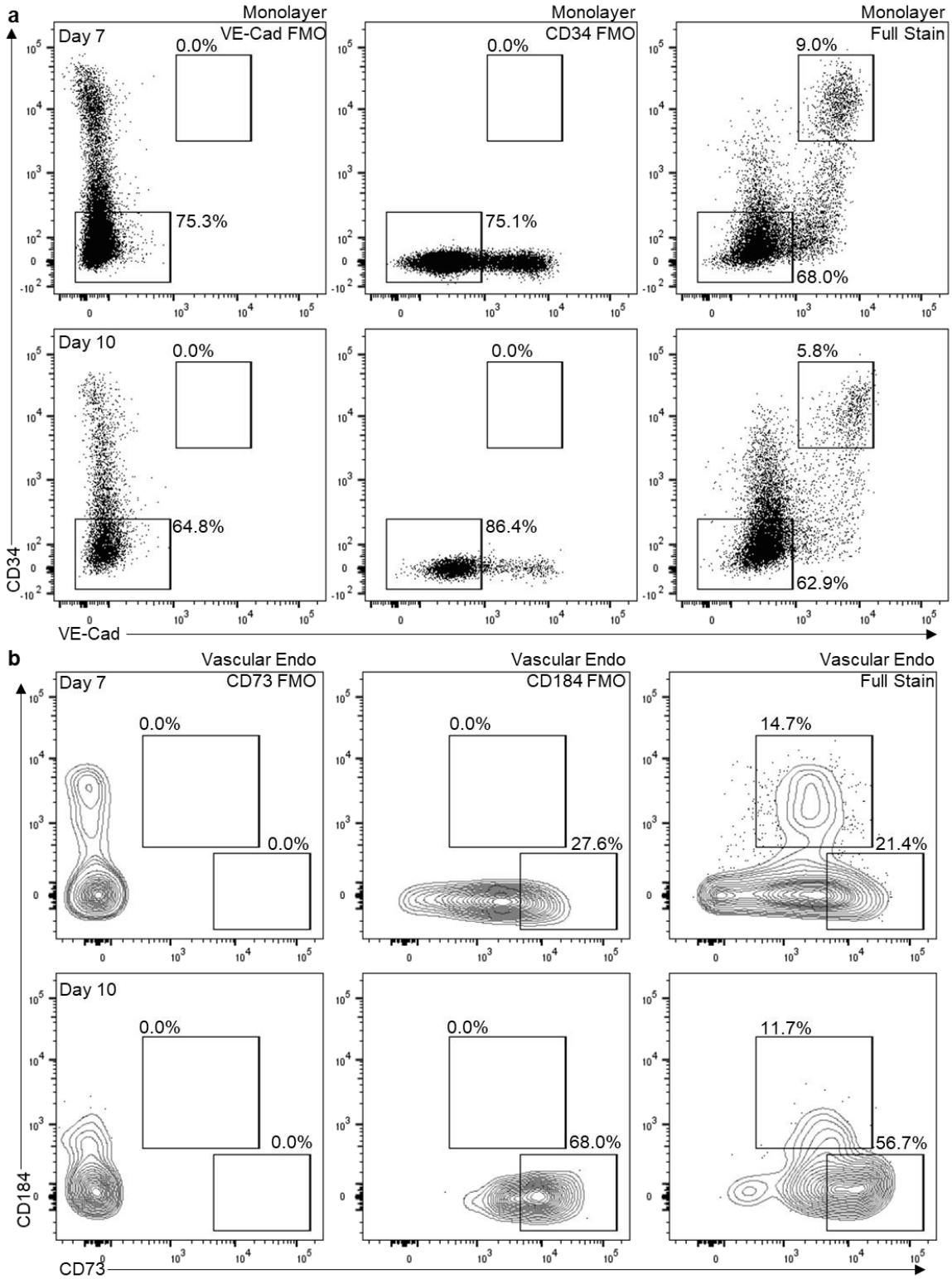

Supplementary Figure 5.3 FMO Controls Associated with Figure 5.3
a) Representative flow cytometry plots of CD34 and CD144 (VE-Cad) expression in gated $CD43^{-}CD45^{-}$ monolayer populations at Day 7 and 10 of culture. CD34 and VE-Cad FMO plots as well as fully stained sample with gating strategy depicted. b) Representative flow cytometry plots of CD184 and CD73 expression of gated $CD34^{High}VE\text{-}Cad^{+}$ Vascular Endothelial populations at Day 7 and 10 of culture. CD73 and CD184 FMO plots as well as fully stained sample with gating strategy depicted.

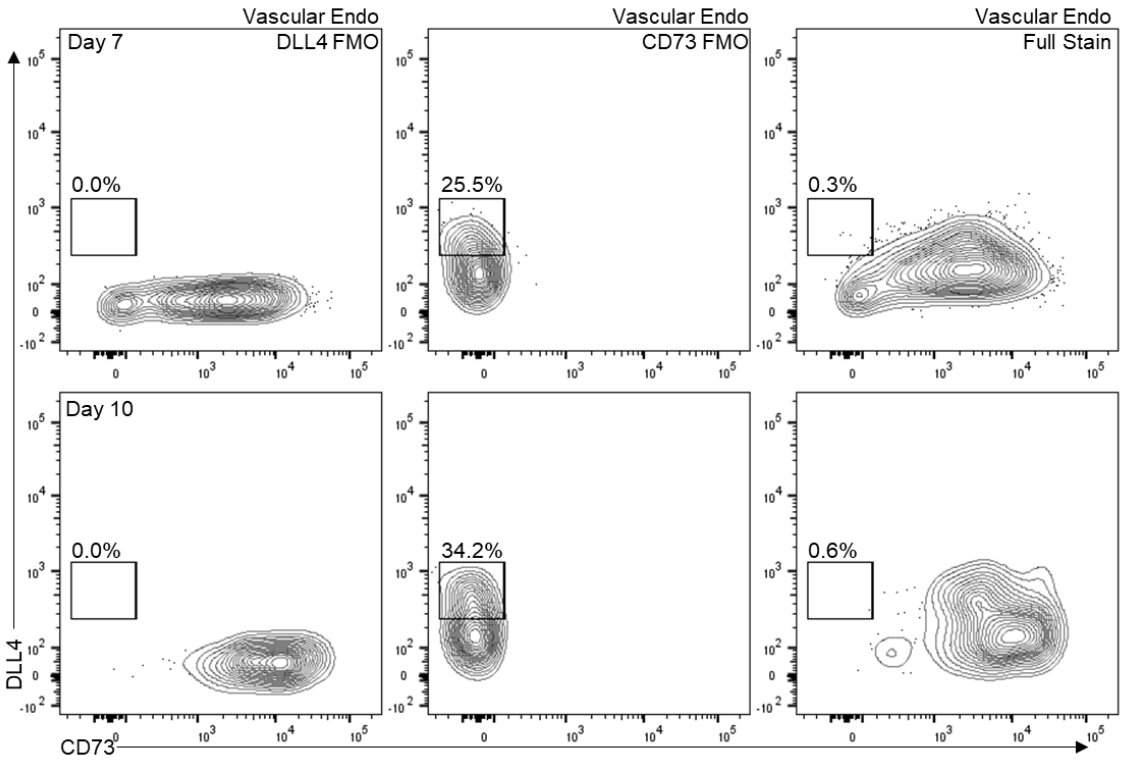

Supplementary Figure 5.4 Additional FMO Controls Associated with Figure 5.3
Representative flow cytometry plots of CD73 and DLL4 expression in the same gated $CD34^{High}VE\text{-}Cad^{+}$ populations as Supplementary Figure 5.3 at Day 7 and 10. DLL4 and CD73 plots as well as fully stained sample with gating strategy depicted.

References

Alharbi, R. A., R. Pettengell, H. S. Pandha, and R. Morgan. 2012. 'The role of HOX genes in normal hematopoiesis and acute leukemia', *Leukemia*, 27.

Amabile, G., R. S. Welner, C. Nombela-Arrieta, A. M. D'Alise, A. Di Ruscio, A. K. Ebralidze, Y. Kraytsberg, M. Ye, O. Kocher, D. S. Neuberg, K. Khrapko, L. E. Silberstein, and D. G. Tenen. 2013. 'In vivo generation of transplantable human hematopoietic cells from induced pluripotent stem cells', *Blood*, 121: 1255-64.

Arnold, Sebastian J., and Elizabeth J. Robertson. 2009. 'Making a commitment: cell lineage allocation and axis patterning in the early mouse embryo', *Nature Reviews Molecular Cell Biology*, 10.

Aspalter, Irene, Emma Gordon, Alexandre Dubrac, Anan Ragab, Jarek Narloch, Pedro Vizán, Ilse Geudens, Russell Collins, Claudio Franco, Cristina Abrahams, Gavin Thurston, Marcus Fruttiger, Ian Rosewell, Anne Eichmann, and Holger Gerhardt. 2015. 'Alk1 and Alk5 inhibition by Nrp1 controls vascular sprouting downstream of Notch', *Nature Communications*, 6.

Ayllón, V., C. Bueno, V. Ramos-Mejía, O. Navarro-Montero, C. Prieto, P. J. Real, T. Romero, M. J. García-León, M. L. Toribio, A. Bigas, and P. Menendez. 2015. 'The Notch ligand DLL4 specifically marks human hematoendothelial progenitors and regulates their hematopoietic fate', *Leukemia*, 29: 1741-53.

Basagiannis, Dimitris, Sofia Zografou, Carol Murphy, Theodore Fotsis, Lucia Morbidelli, Marina Ziche, Christopher Bleck, Jason Mercer, and Savvas Christoforidis. 2016. 'VEGF induces signalling and angiogenesis by directing VEGFR2 internalisation through macropinocytosis', *Journal of cell science*, 129: 4091-104.

Batsivari, A., S. Rybtsov, C. Souilhol, A. Binagui-Casas, D. Hills, S. Zhao, P. Travers, and A. Medvinsky. 2017. 'Understanding Hematopoietic Stem Cell Development through Functional Correlation of Their Proliferative Status with the Intra-aortic Cluster Architecture', *Stem Cell Reports*, 8: 1549-62.

Bertrand, J. Y., J. L. Cisson, D. L. Stachura, and D. Traver. 2010a. 'Notch signaling distinguishes 2 waves of definitive hematopoiesis in the zebrafish embryo', *Blood*, 115: 2777-83.

Bertrand, Julien Y., Neil C. Chi, Buyung Santoso, Shutian Teng, Didier Y. R. Stainier, and David Traver. 2010b. 'Haematopoietic stem cells derive directly from aortic endothelium during development', *Nature*, 464: 108-11.

Böiers, Charlotta, Joana Carrelha, Michael Lutteropp, Sidinh Luc, Joanna Green, Emanuele Azzoni, Petter S. Woll, Adam J. Mead, Anne Hultquist, Gemma Swiers, Elisa Perdiguero, Iain C. Macaulay, Luca Melchiori, Tiago C. Luis, Shabnam Kharazi, Tiphaine Bouriez-Jones, Qiaolin Deng, Annica Pontén, Deborah Atkinson, Christina T. Jensen, Ewa Sitnicka, Frederic Geissmann, Isabelle Godin, Rickard Sandberg, Marella de Bruijn, and Sten Jacobsen. 2013. 'Lymphomyeloid Contribution of an Immune-Restricted Progenitor Emerging Prior to Definitive Hematopoietic Stem Cells', *Cell Stem Cell*, 13: 535-48.

Boisset, Jean-Charles, Wiggert van Cappellen, Charlotte Andrieu-Soler, Niels Galjart, Elaine Dzierzak, and Catherine Robin. 2010. 'In vivo imaging of haematopoietic cells emerging from the mouse aortic endothelium', *Nature*, 464: 116-20.

Bos, Frank L., John S. Hawkins, and Ann C. Zovein. 2015. 'Single-cell resolution of morphological changes in hemogenic endothelium', *Development*, 142: 2719-24.

Brown, Louise A., Adam Rodaway, Thomas F. Schilling, Trevor Jowett, Philip W. Ingham, Roger K. Patient, and Andrew D. Sharrocks. 2000. 'Insights into early vasculogenesis revealed by expression of the ETS-domain transcription factor Fli-1 in wild-type and mutant zebrafish embryos', *Mechanisms of development*, 90: 237-52.

Butko, Emerald, Claire Pouget, and David Traver. 2016. 'Complex regulation of HSC emergence by the Notch signaling pathway', *Developmental Biology*, 409: 129-38.

C.H., Waddington. 1957. *The Strategy of the Genes*.

Cai, Z., M. de Bruijn, X. Ma, B. Dortland, T. Luteijn, R. J. Downing, and E. Dzierzak. 2000. 'Haploinsufficiency of AML1 affects the temporal and spatial generation of hematopoietic stem cells in the mouse embryo', *Immunity*, 13: 423-31.

Chagraoui, H., M. S. Kristiansen, J. P. Ruiz, A. Serra-Barros, J. Richter, E. Hall-Ponsele, N. Gray, D. Waithe, K. Clark, P. Hublitz, E. Repapi, G. Otto, P. Sopp, S. Taylor, S. Thongjuea, P. Vyas, and C. Porcher. 2018. 'SCL/TAL1 cooperates with Polycomb RYBP-PRC1 to suppress alternative lineages in blood-fated cells', *Nat Commun*, 9: 5375.

Chen, II, A. Caprioli, H. Ohnuki, H. Kwak, C. Porcher, and G. Tosato. 2016. 'EphrinB2 regulates the emergence of a hemogenic endothelium from the aorta', *Sci Rep*, 6: 27195.

Chen, J., Y. Fu, D. S. Day, Y. Sun, S. Wang, X. Liang, F. Gu, F. Zhang, S. M. Stevens, P. Zhou, K. Li, Y. Zhang, R. Z. Lin, L. E. H. Smith, J. Zhang, K. Sun, J. M. Melero-Martin, Z. Han, P. J. Park, B. Zhang, and W. T. Pu. 2017. 'VEGF amplifies transcription through ETS1 acetylation to enable angiogenesis', *Nat Commun*, 8: 383.

Chen, Michael J., Yan Li, Maria De Obaldia, Qi Yang, Amanda D. Yzaguirre, Tomoko Yamada-Inagawa, Chris S. Vink, Avinash Bhandoola, Elaine Dzierzak, and Nancy A. Speck. 2011. 'Erythroid/Myeloid Progenitors and Hematopoietic Stem Cells Originate from Distinct Populations of Endothelial Cells', *Cell Stem Cell*, 9: 541-52.

Chen, Tom T., Alfonso Luque, Sunyoung Lee, Sean M. Anderson, Tatiana Segura, and Luisa M. Iruela-Arispe. 2010. 'Anchorage of VEGF to the extracellular matrix conveys differential signaling responses to endothelial cells', *The Journal of Cell Biology*, 188: 595-609.

Chiang, Po-Min, and Philip C. Wong. 2011. 'Differentiation of an embryonic stem cell to hemogenic endothelium by defined factors: essential role of bone morphogenetic protein 4', *Development*, 138: 2833-43.

Choi, K., M. Kennedy, A. Kazarov, J. C. Papadimitriou, and G. Keller. 1998. 'A common precursor for hematopoietic and endothelial cells', *Development (Cambridge, England)*: 725-32.

Chong, Diana C., Yeon Koo, Ke Xu, Stephen Fu, and Ondine Cleaver. 2011. 'Stepwise arteriovenous fate acquisition during mammalian vasculogenesis', *Developmental Dynamics*, 240: 2153-65.

Ciau-Uitz, A., P. Pinheiro, R. Gupta, T. Enver, and R. Patient. 2010. 'Tel1/ETV6 specifies blood stem cells through the agency of VEGF signaling', *Dev Cell*, 18: 569-78.

Ciau-Uitz, Aldo, Philip Pinheiro, Arif Kirmizitas, Jie Zuo, and Roger Patient. 2013. 'VEGFA-dependent and -independent pathways synergise to drive Scl expression and initiate programming of the blood stem cell lineage in Xenopus', *Development*, 140: 2632-42.

Ciau-Uitz, Aldo, Maggie Walmsley, and Roger Patient. 2000. 'Distinct Origins of Adult and Embryonic Blood in Xenopus', *Cell*, 102: 787-96.

Clarke, R. L., A. M. Robitaille, R. T. Moon, and G. Keller. 2015. 'A Quantitative Proteomic Analysis of Hemogenic Endothelium Reveals Differential Regulation of Hematopoiesis by SOX17', *Stem Cell Reports*, 5: 291-304.

Clarke, Raedun L., Amanda D. Yzaguirre, Yumi Yashiro-Ohtani, Antoine Bondue, Cedric Blanpain, Warren S. Pear, Nancy A. Speck, and Gordon Keller. 2013. 'The expression of Sox17 identifies and regulates haemogenic endothelium', *Nature Cell Biology*, 15: 502-10.

Cleaver, O., and P. A. Krieg. 1998. 'VEGF mediates angioblast migration during development of the dorsal aorta in Xenopus', *Development (Cambridge, England)*, 125: 3905-14.

Clements, Wilson K., Albert D. Kim, Karen G. Ong, John C. Moore, Nathan D. Lawson, and David Traver. 2011. 'A somitic Wnt16/Notch pathway specifies haematopoietic stem cells', *Nature*, 474: 220.

Coffin, J. D., and T. J. Poole. 1988. 'Embryonic vascular development: immunohistochemical identification of the origin and subsequent morphogenesis of the major vessel primordia in quail embryos', *Development (Cambridge, England)*, 102: 735-48.

Cong, Le, Ann F. Ran, David Cox, Shuailiang Lin, Robert Barretto, Naomi Habib, Patrick D. Hsu, Xuebing Wu, Wenyan Jiang, Luciano A. Marraffini, and Feng Zhang. 2013. 'Multiplex Genome Engineering Using CRISPR/Cas Systems', *Science*, 339: 819-23.

Costa, Guilherme, Valerie Kouskoff, and Georges Lacaud. 2012. 'Origin of blood cells and HSC production in the embryo', *Trends in Immunology*, 33: 215-23.

Craig, Marcia L., and Elizabeth S. Russell. 1964. 'A developmental change in hemoglobins correlated with an embryonic red cell population in the mouse', *Developmental Biology*, 10: 191-201.

Crisan, Mihaela, and Elaine Dzierzak. 2016. 'The many faces of hematopoietic stem cell heterogeneity', *Development*, 143: 4571-81.

Crisan, Mihaela, Parham Kartalaei, Chris S. Vink, Chris Vink, Tomoko Yamada-Inagawa, Karine Bollerot, Wilfred van Ijcken, Reinier van der Linden, Susana M. de Lopes, Rui Monteiro, Christine Mummery, and Elaine Dzierzak. 2015. 'BMP signalling differentially regulates distinct haematopoietic stem cell types', *Nature Communications*, 6.

Cumano, A., C. Furlonger, and C. J. Paige. 1993. 'Differentiation and characterization of B-cell precursors detected in the yolk sac and embryo body of embryos beginning at the 10- to 12-somite stage', *Proc Natl Acad Sci U S A*, 90: 6429-33.

D'Souza, S. L., A. G. Elefanty, and G. Keller. 2005. 'SCL/Tal-1 is essential for hematopoietic commitment of the hemangioblast but not for its development', *Blood*, 105: 3862-70.

D'Souza, Saritha S., Akhilesh Kumar, and Igor Slukvin. 2018. 'Functional heterogeneity of endothelial cells derived from human pluripotent stem cells', *Stem Cells and Development*.

de Bruijn, Marella, and Elaine Dzierzak. 2017. 'Runx transcription factors in the development and function of the definitive hematopoietic system', *Blood*, 129: 2061-69.

de Bruijn, Marella, Xiaoqian Ma, Catherine Robin, Katrin Ottersbach, Maria-Jose Sanchez, and Elaine Dzierzak. 2002. 'Hematopoietic Stem Cells Localize to the Endothelial Cell Layer in the Midgestation Mouse Aorta', *Immunity*, 16: 673-83.

de Bruijn, Marella, Nancy A. Speck, Marian Peeters, and Elaine Dzierzak. 2000. 'Definitive hematopoietic stem cells first develop within the major arterial regions of the mouse embryo', *The EMBO Journal*, 19: 2465-74.

de la Morena, Teresa M., and Richard A. Gatti. 2011. 'A History of Bone Marrow Transplantation', *Hematology/Oncology Clinics of North America*, 25: 1-15.

Diaz, Miguel F., Nan Li, Hyun Lee, Luigi Adamo, Siobahn M. Evans, Hannah E. Willey, Natasha Arora, Yu-suke Torisawa, Dwayne A. Vickers, Samantha A. Morris, Olaia Naveiras, Shashi K. Murthy, Donald E. Ingber, George Q. Daley, Guillermo García-Cardeña, and Pamela L. Wenzel. 2015. 'Biomechanical forces promote blood development through prostaglandin E2 and the cAMP–PKA signaling axis', *The Journal of Experimental Medicine*, 212: 665-80.

Dickson, Glenda J., Alexandra Kwasniewska, Ken I. Mills, Terence Lappin, and Alexander Thompson. 2009. 'Hoxa6 potentiates short-term hemopoietic cell proliferation and extended self-renewal', *Experimental Hematology*, 37: 322-333000.

Dieterlen-Lievre, F., L. Pardanaud, K. Bollerot, and T. Jaffredo. 2002. 'Hemangioblasts and hemopoietic stem cells during ontogeny', *C R Biol*, 325: 1013-20.

Ditadi, Andrea, Christopher M. Sturgeon, and Gordon Keller. 2016. 'A view of human haematopoietic development from the Petri dish', *Nature Reviews Molecular Cell Biology*, 18: 56-67.

Ditadi, Andrea, Christopher M. Sturgeon, Joanna Tober, Geneve Awong, Marion Kennedy, Amanda D. Yzaguirre, Lisa Azzola, Elizabeth S. Ng, Edouard G. Stanley, Deborah L. French, Xin Cheng, Paul Gadue, Nancy A. Speck, Andrew G. Elefanty, and Gordon Keller. 2015. 'Human definitive haemogenic endothelium and arterial vascular endothelium represent distinct lineages', *Nature Cell Biology*, 17: 580-91.

Dorfman, D. M., D. B. Wilson, G. A. Bruns, and S. H. Orkin. 1992. 'Human transcription factor GATA-2. Evidence for regulation of preproendothelin-1 gene expression in endothelial cells', *The Journal of biological chemistry*, 267: 1279-85.

Dou, Diana R., Vincenzo Calvanese, Maria I. Sierra, Andrew T. Nguyen, Arazin Minasian, Pamela Saarikoski, Rajkumar Sasidharan, Christina M. Ramirez, Jerome A. Zack, Gay M. Crooks, Zoran Galic, and Hanna K. A. Mikkola. 2016. 'Medial HOXA genes demarcate haematopoietic stem cell fate during human development', *Nature Cell Biology*, 18: 595-606.

Douagi, I., P. Vieira, and A. Cumano. 2002. 'Lymphocyte commitment during embryonic development, in the mouse', *Semin Immunol*, 14: 361-9.

Drake, C. J., and P. A. Fleming. 2000. 'Vasculogenesis in the day 6.5 to 9.5 mouse embryo', *Blood*: 1671-79.

Duarte, António, Masanori Hirashima, Rui Benedito, Alexandre Trindade, Patrícia Diniz, Evguenia Bekman, Luís Costa, Domingos Henrique, and Janet Rossant. 2004. 'Dosage-sensitive requirement for mouse Dll4 in artery development', *Genes & Development*, 18: 2474-78.

Dunnett, CW. 1964. 'New tables for multiple comparisons with a control', *Biometrics*, 20: 482-91.

Dzierzak, Elaine, and Nancy A. Speck. 2008. 'Of lineage and legacy: the development of mammalian hematopoietic stem cells', *Nature Immunology*, 9: 129-36.

Eilken, Hanna M., Shin-Ichi Nishikawa, and Timm Schroeder. 2009. 'Continuous single-cell imaging of blood generation from haemogenic endothelium', *Nature*, 457: 896-900.

Eliades, A., S. Wareing, E. Marinopoulou, M. Z. H. Fadlullah, R. Patel, J. B. Grabarek, B. Plusa, G. Lacaud, and V. Kouskoff. 2016. 'The Hemogenic Competence of Endothelial Progenitors Is Restricted by Runx1 Silencing during Embryonic Development', *Cell Rep*, 15: 2185-99.

Ema, M., T. Yokomizo, A. Wakamatsu, T. Terunuma, M. Yamamoto, and S. Takahashi. 2006. 'Primitive erythropoiesis from mesodermal precursors expressing VE-cadherin, PECAM-1, Tie2, endoglin, and CD34 in the mouse embryo', *Blood*, 108: 4018-24.

Faloon, P., E. Arentson, A. Kazarov, C. X. Deng, C. Porcher, S. Orkin, and K. Choi. 2000. 'Basic fibroblast growth factor positively regulates hematopoietic development', *Development*, 127: 1931-41.

Fares, Iman, Jalila Chagraoui, Yves Gareau, Stéphane Gingras, Réjean Ruel, Nadine Mayotte, Elizabeth Csaszar, David J. H. F. Knapp, Paul Miller, Mor Ngom, Suzan Imren, Denis-Claude Roy, Kori L. Watts, Hans-Peter Kiem, Robert Herrington, Norman N. Iscove, Keith R. Humphries, Connie J. Eaves, Sandra Cohen, Anne Marinier, Peter W. Zandstra, and Guy Sauvageau. 2014. 'Pyrimidoindole derivatives are agonists of human hematopoietic stem cell self-renewal', *Science*, 345: 1509-12.

Fatima, S., S. Zhou, and B. P. Sorrentino. 2018. 'Marking of definitive HSC precursors in E7.5-E8.5 embryos using an Abcg2-CreER lineage-tracing mouse model', *Exp Hematol*, 65: 29-33.

Fehling, H. J., G. Lacaud, A. Kubo, M. Kennedy, S. Robertson, G. Keller, and V. Kouskoff. 2003. 'Tracking mesoderm induction and its specification to the hemangioblast during embryonic stem cell differentiation', *Development*, 130: 4217-27.

Fish, Jason E., and Joshua D. Wythe. 2015. 'The molecular regulation of arteriovenous specification and maintenance', *Developmental Dynamics*: 391-409.

Forlani, Sylvie, Kirstie A. Lawson, and Jacqueline Deschamps. 2003. 'Acquisition of Hox codes during gastrulation and axial elongation in the mouse embryo', *Development*, 130: 3807-19.

Frame, Jenna M., Katherine H. Fegan, Simon J. Conway, Kathleen E. McGrath, and James Palis. 2016. 'Definitive Hematopoiesis in the Yolk Sac Emerges from Wnt-Responsive Hemogenic Endothelium Independently of Circulation and Arterial Identity', *STEM CELLS*, 34: 431-44.

Fraser, S. T., M. Ogawa, T. Yokomizo, Y. Ito, S. Nishikawa, and S. Nishikawa. 2003. 'Putative intermediate precursor between hematogenic endothelial cells and blood cells in the developing embryo', *Dev Growth Differ*, 45: 63-75.

Gadue, Paul, Tara L. Huber, Patrick J. Paddison, and Gordon M. Keller. 2006. 'Wnt and TGF-β signaling are required for the induction of an in vitro model of primitive streak formation using embryonic stem cells', *Proceedings of the National Academy of Sciences*, 103: 16806-11.

Gama-Norton, Leonor, Eva Ferrando, Cristina Ruiz-Herguido, Zhenyi Liu, Zenhy Liu, Jordi Guiu, Abul Bmmk Islam, Sung-Uk Lee, Minhong Yan, Cynthia J. Guidos, Nuria López-Bigas, Takahiro Maeda, Lluis Espinosa, Raphael Kopan, and Anna Bigas. 2015. 'Notch signal strength controls cell fate in the haemogenic endothelium', *Nature Communications*, 6: 8510.

Ganuza, M., A. Chabot, X. Tang, W. Bi, S. Natarajan, R. Carter, C. Gawad, G. Kang, Y. Cheng, and S. McKinney-Freeman. 2018. 'Murine hematopoietic stem cell activity is derived from pre-circulation embryos but not yolk sacs', *Nat Commun*, 9: 5405.

Ganuza, M., T. Hall, D. Finkelstein, A. Chabot, G. Kang, and S. McKinney-Freeman. 2017. 'Lifelong haematopoiesis is established by hundreds of precursors throughout mammalian ontogeny', *Nat Cell Biol*, 19: 1153-63.

Genthe, Jamie R., and Wilson K. Clements. 2017. 'R-spondin-1 is required for specification of hematopoietic stem cells through Wnt16 and Vegfa signaling pathways', *Development*, 144.

Gerhardt, Dawson M., Kostandin V. Pajcini, Teresa D'altri, LiLi Tu, Rajan Jain, Lanwei Xu, Michael J. Chen, Stacey Rentschler, Olga Shestova, Gerald B. Wertheim, John W. Tobias, Michael Kluk, Antony W. Wood, Jon C. Aster, Phyllis A. Gimotty, Jonathan A. Epstein, Nancy Speck, Anna Bigas, and Warren S. Pear. 2014. 'The Notch1 transcriptional activation domain is required for development and reveals a novel role for Notch1 signaling in fetal hematopoietic stem cells', *Genes & Development*, 28: 576-93.

Gering, M., A. R. F. Rodaway, B. Göttgens, R. K. Patient, and A. R. Green. 1998. 'The SCL gene specifies haemangioblast development from early mesoderm', *The EMBO Journal*, 17: 4029-45.

Gering, Martin, and Roger Patient. 2005. 'Hedgehog Signaling Is Required for Adult Blood Stem Cell Formation in Zebrafish Embryos', *Developmental Cell*, 8: 389-400.

Gering, Martin, Yoshihiro Yamada, Terence H. Rabbitts, and Roger K. Patient. 2003. 'Lmo2 and Scl/Tal1 convert non-axial mesoderm into haemangioblasts which differentiate into endothelial cells in the absence of Gata1', *Development*, 130: 6187-99.

Goerges, Adrienne L., and Matthew A. Nugent. 2004. 'pH Regulates Vascular Endothelial Growth Factor Binding to Fibronectin A MECHANISM FOR CONTROL OF EXTRACELLULAR MATRIX STORAGE AND RELEASE', *Journal of Biological Chemistry*, 279: 2307-15.

Goessling, Wolfram, Robyn S. Allen, Xiao Guan, Ping Jin, Naoya Uchida, Michael Dovey, James M. Harris, Mark E. Metzger, Aylin C. Bonifacino, David Stroncek, Joseph Stegner, Myriam Armant, Thorsten Schlaeger, John F. Tisdale, Leonard I. Zon, Robert E. Donahue, and Trista E. North. 2011. 'Prostaglandin E2 Enhances Human Cord Blood Stem Cell Xenotransplants and Shows Long-Term Safety in Preclinical Nonhuman Primate Transplant Models', *Cell Stem Cell*, 8: 445-58.

Gomez Perdiguero, E., K. Klapproth, C. Schulz, K. Busch, E. Azzoni, L. Crozet, H. Garner, C. Trouillet, M. F. de Bruijn, F. Geissmann, and H. R. Rodewald. 2015. 'Tissue-resident macrophages originate from yolk-sac-derived erythro-myeloid progenitors', *Nature*, 518: 547-51.

Gordon-Keylock, Sabrina, Malgorzata Sobiesiak, Stanislav Rybtsov, Kate Moore, and Alexander Medvinsky. 2013. 'Mouse extraembryonic arterial vessels harbor precursors capable of maturing into definitive HSCs', *Blood*, 122: 2338-45.

Gori, Jennifer L., Jason M. Butler, Yan-Yi Chan, Devikha Chandrasekaran, Michael G. Poulos, Michael Ginsberg, Daniel J. Nolan, Olivier Elemento, Brent L. Wood, Jennifer E. Adair, Shahin Rafii, and Hans-Peter Kiem. 2015. 'Vascular niche promotes hematopoietic multipotent progenitor formation from pluripotent stem cells', *Journal of Clinical Investigation*, 125: 1243-54.

Guibentif, Carolina, Roger Rönn, Charlotta Böiers, Stefan Lang, Shobhit Saxena, Shamit Soneji, Tariq Enver, Göran Karlsson, and Niels-Bjarne Woods. 2017. 'Single-Cell Analysis Identifies Distinct Stages of Human Endothelial-to-Hematopoietic Transition', *Cell Reports*, 19: 10-19.

Guyonneau-Harmand, Laurence, Bruno L'Homme, Brigitte Birebent, Christophe Desterke, Nathalie Chevallier, Loic Garcon, Helene Lapillonne, Marc Benderitter, Francois Delhommeau, Thierry Jaffredo, Alain Chapel, and Luc Douay. 2017. 'Transgene-free hematopoietic stem and progenitor cells from human induced pluripotent stem cells', *bioRxiv*.

Hadland, Brandon K., Stacey S. Huppert, Jyotshnabala Kanungo, Yingzi Xue, Rulang Jiang, Thomas Gridley, Ronald A. Conlon, Alec M. Cheng, Raphael Kopan, and Gregory D. Longmore. 2004. 'A requirement for Notch1 distinguishes 2 phases of definitive hematopoiesis during development', *Blood*, 104: 3097-105.

Hadland, Brandon K., Barbara Varnum-Finney, Pankaj K. Mandal, Derrick J. Rossi, Michael G. Poulos, Jason M. Butler, Shahin Rafii, Mervin C. Yoder, Momoko Yoshimoto, and Irwin D. Bernstein. 2017. 'A Common Origin for B-1a and B-2 Lymphocytes in Clonal Pre-Hematopoietic Stem Cells', *Stem Cell Reports*, 8: 1563-72.

Hadland, Brandon K., Barbara Varnum-Finney, Michael G. Poulos, Randall T. Moon, Jason M. Butler, Shahin Rafii, and Irwin D. Bernstein. 2015. 'Endothelium and NOTCH specify and amplify aorta-gonad-mesonephros-derived hematopoietic stem cells', *The Journal of clinical investigation*, 125: 2032-45.

Hayashi, Hisaki, and Tsutomu Kume. 2008. 'Foxc Transcription Factors Directly Regulate Dll4 and Hey2 Expression by Interacting with the VEGF-Notch Signaling Pathways in Endothelial Cells', *PLoS ONE*, 3.

Hoeffel, G., J. Chen, Y. Lavin, D. Low, F. F. Almeida, P. See, A. E. Beaudin, J. Lum, I. Low, E. C. Forsberg, M. Poidinger, F. Zolezzi, A. Larbi, L. G. Ng, J. K. Chan, M. Greter, B. Becher, I. M. Samokhvalov, M. Merad, and F. Ginhoux. 2015. 'C-Myb(+) erythro-myeloid progenitor-derived fetal monocytes give rise to adult tissue-resident macrophages', *Immunity*, 42: 665-78.

Hoeffel, G., Y. Wang, M. Greter, P. See, P. Teo, B. Malleret, M. Leboeuf, D. Low, G. Oller, F. Almeida, S. H. Choy, M. Grisotto, L. Renia, S. J. Conway, E. R. Stanley, J. K. Chan, L. G. Ng, I. M. Samokhvalov, M. Merad, and F. Ginhoux. 2012. 'Adult Langerhans cells derive predominantly from embryonic fetal liver monocytes with a minor contribution of yolk sac-derived macrophages', *J Exp Med*, 209: 1167-81.

Huang, Caoxin, Melany Jackson, Kay Samuel, Helen A. Taylor, Sally Lowell, and Lesley M. Forrester. 2013. 'Haematopoietic differentiation is inhibited when Notch activity is enhanced in FLK1+ mesoderm progenitors', *Stem Cell Research*, 11: 1273-87.

Huber, T. L., V. Kouskoff, H. J. Fehling, J. Palis, and G. Keller. 2004. 'Haemangioblast commitment is initiated in the primitive streak of the mouse embryo', *Nature*, 432: 625-30.

Iacovino, M., D. Chong, I. Szatmari, L. Hartweck, D. Rux, A. Caprioli, O. Cleaver, and M. Kyba. 2011. 'HoxA3 is an apical regulator of haemogenic endothelium', *Nat Cell Biol*, 13: 72-8.

Inlay, Matthew A., Thomas Serwold, Adriane Mosley, John W. Fathman, Ivan K. Dimov, Jun Seita, and Irving L. Weissman. 2014. 'Identification of Multipotent Progenitors that Emerge Prior to Hematopoietic Stem Cells in Embryonic Development', *Stem Cell Reports*, 2: 457-72.

Irion, Stefan, Raedun L. Clarke, Hervé Luche, Injune Kim, Sean J. Morrison, Hans-Joerg Fehling, and Gordon M. Keller. 2010. 'Temporal specification of blood progenitors from mouse embryonic stem cells and induced pluripotent stem cells', *Development*, 137: 2829-39.

Ivanovs, Andrejs, Stanislav Rybtsov, Elizabeth S. Ng, Edouard G. Stanley, Andrew G. Elefanty, and Alexander Medvinsky. 2017. 'Human haematopoietic stem cell development: from the embryo to the dish', *Development*, 144: 2323-37.

Jaffredo, T., R. Gautier, V. Brajeul, and F. Dieterlen-Lievre. 2000. 'Tracing the progeny of the aortic hemangioblast in the avian embryo', *Dev Biol*, 224: 204-14.

Jaffredo, T., R. Gautier, A. Eichmann, and F. Dieterlen-Lievre. 1998. 'Intraaortic hemopoietic cells are derived from endothelial cells during ontogeny', *Development*, 125: 4575-83.

Jin, Suk-Won, Dimitris Beis, Tracy Mitchell, Jau-Nian Chen, and Didier Y. R. Stainier. 2005. 'Cellular and molecular analyses of vascular tube and lumen formation in zebrafish', *Development*, 132: 5199-209.

Johnson, Scott A., and Mervin C. Yoder. 2005. 'Reconstitution of hematopoiesis following transplantation into neonatal mice', *Methods in molecular medicine*, 105: 95-106.

Joo, Hyung, Dong-Kyu Choi, Joon Lim, Jin-Sung Park, Seung-Hun Lee, Sukhyun Song, Jennifer H. Shin, Do-Sun Lim, Injune Kim, Ki-Chul Hwang, and Gou Koh. 2012. 'ROCK suppression promotes differentiation and expansion of endothelial cells from embryonic stem cell–derived Flk1+ mesodermal precursor cells', *Blood*, 120: 2733-44.

Jordan, C. T., and I. R. Lemischka. 1990. 'Clonal and systemic analysis of long-term hematopoiesis in the mouse', *Genes & Development*, 4: 220-32.

Jordan, H. E. 1917. 'Aortic Cell Clusters in Vertebrate Embryos', *Proceedings of the National Academy of Sciences*, 3: 149-56.

Kartalaei, Parham, Tomoko Yamada-Inagawa, Chris S. Vink, Emma de Pater, Reinier van der Linden, Jonathon Marks-Bluth, Anthon van der Sloot, Mirjam van den Hout, Tomomasa Yokomizo, Lucila M. van Schaick-Solernó, Ruud Delwel, John E. Pimanda, Wilfred van Ijcken, and Elaine Dzierzak. 2015. 'Whole-transcriptome analysis of endothelial to hematopoietic stem cell transition reveals a requirement for Gpr56 in HSC generation', *The Journal of Experimental Medicine*, 212: 93-106.

Kataoka, H., N. Takakura, S. Nishikawa, K. Tsuchida, H. Kodama, T. Kunisada, W. Risau, T. Kita, and S. I. Nishikawa. 1997. 'Expressions of PDGF receptor alpha, c-Kit and Flk1 genes clustering in mouse chromosome 5 define distinct subsets of nascent mesodermal cells', *Dev Growth Differ*, 39: 729-40.

Kataoka, Hiroshi, Misato Hayashi, Reiko Nakagawa, Yosuke Tanaka, Naoki Izumi, Satomi Nishikawa, Martin Jakt, Hiroshi Tarui, and Shin-Ichi Nishikawa. 2011. 'Etv2/ER71 induces vascular mesoderm from Flk1+PDGFRα+ primitive mesoderm', *Blood*, 118: 6975-86.

Kattman, Steven J., Tara L. Huber, and Gordon M. Keller. 2006. 'Multipotent Flk-1+ Cardiovascular Progenitor Cells Give Rise to the Cardiomyocyte, Endothelial, and Vascular Smooth Muscle Lineages', *Developmental Cell*, 11: 723-32.

Keller, G. 2001. 'The Hemangioblast.' in, *Stem Cell Biology* (Cold Spring Harbor).

Keller, Gordon, Marion Kennedy, Thalia Papayannopoulou, and Michael V. Wiles. 1993. 'Hematopoietic commitment during embryonic stem cell differentiation in culture', *Molecular and cellular biology*, 13: 473-86.

Kennedy, Marion, Geneve Awong, Christopher M. Sturgeon, Andrea Ditadi, Ross LaMotte-Mohs, Juan Zúñiga-Pflücker, and Gordon Keller. 2012. 'T Lymphocyte Potential Marks the Emergence of Definitive Hematopoietic Progenitors in Human Pluripotent Stem Cell Differentiation Cultures', *Cell Reports*, 2: 1722-35.

Kennedy, Marion, Sunita L. D'Souza, Macarena Lynch-Kattman, Staci Schwantz, and Gordon Keller. 2007. 'Development of the hemangioblast defines the onset of hematopoiesis in human ES cell differentiation cultures', *Blood*, 109: 2679-87.

Kim, Albert D., Chase H. Melick, Wilson K. Clements, David L. Stachura, Martin Distel, Daniela Panáková, Calum MacRae, Lindsey A. Mork, Gage J. Crump, and David Traver. 2014. 'Discrete Notch signaling requirements in the specification of hematopoietic stem cells', *The EMBO Journal*, 33: 2363-73.

Kingsley, P. D., J. Malik, K. A. Fantauzzo, and J. Palis. 2004. 'Yolk sac-derived primitive erythroblasts enucleate during mammalian embryogenesis', *Blood*, 104: 19-25.

Kissa, Karima, and Philippe Herbomel. 2010. 'Blood stem cells emerge from aortic endothelium by a novel type of cell transition', *Nature*, 464: 112-15.

Kofler, N. M., and M. Simons. 2015. 'Angiogenesis versus arteriogenesis: neuropilin 1 modulation of VEGF signaling', *F1000Prime Rep*, 7: 26.

Kopan, R., and M. X. Ilagan. 2009. 'The canonical Notch signaling pathway: unfolding the activation mechanism', *Cell*, 137: 216-33.

Kovach, John S., Paul A. Marks, Elizabeth S. Russell, and Hazel Epler. 1967. 'Erythroid cell development in fetal mice: Ultrastructural characteristics and hemoglobin synthesis', *Journal of Molecular Biology*, 25: 131-42.

Kucia, Magda, Kacper Jankowski, Ryan Reca, Marcin Wysoczynski, Laura Bandura, Daniel J. Allendorf, Jin Zhang, Janina Ratajczak, and Mariusz Z. Ratajczak. 2003. 'CXCR4–SDF-1 Signalling, Locomotion, Chemotaxis and Adhesion', *Journal of Molecular Histology*, 35: 233-45.

Kumano, Keiki, Shigeru Chiba, Atsushi Kunisato, Masataka Sata, Toshiki Saito, Etsuko Nakagami-Yamaguchi, Tomoyuki Yamaguchi, Shigeo Masuda, Kiyoshi Shimizu, Tokiharu Takahashi, Seishi Ogawa, Yoshio Hamada, and Hisamaru Hirai. 2003. 'Notch1 but Not Notch2 Is Essential for Generating Hematopoietic Stem Cells from Endothelial Cells', *Immunity*, 18: 699-711.

Kumaravelu, Parasakthy, Lilian Hook, Aline M. Morrison, Jan Ure, Suling Zhao, Sergei Zuyev, John Ansell, and Alexander Medvinsky. 2002. 'Quantitative developmental anatomy of definitive haematopoietic stem cells/long-term repopulating units (HSC/RUs): role of the aorta-gonad-mesonephros (AGM) region and the yolk sac in colonisation of the mouse embryonic liver', *Development*, 129: 4891-99.

Kyba, Michael, Rita Perlingeiro, and George Q. Daley. 2002. 'HoxB4 Confers Definitive Lymphoid-Myeloid Engraftment Potential on Embryonic Stem Cell and Yolk Sac Hematopoietic Progenitors', *Cell*, 109: 29-37.

Lacaud, G., V. Kouskoff, A. Trumble, S. Schwantz, and G. Keller. 2004. 'Haploinsufficiency of Runx1 results in the acceleration of mesodermal development and hemangioblast specification upon in vitro differentiation of ES cells', *Blood*, 103: 886-9.

Ladewig, Julia, Philipp Koch, and Oliver Brüstle. 2013. 'Leveling Waddington: the emergence of direct programming and the loss of cell fate hierarchies', *Nature reviews. Molecular cell biology*, 14: 225-36.

Lancrin, Christophe, Milena Mazan, Monika Stefanska, Rahima Patel, Monika Lichtinger, Guilherme Costa, Özge Vargel, Nicola K. Wilson, Tarik Möröy, Constanze Bonifer, Berthold Göttgens, Valerie Kouskoff, and Georges Lacaud. 2012. 'GFI1 and GFI1B control the loss of endothelial identity of hemogenic endothelium during hematopoietic commitment', *Blood*, 120: 314-22.

Lancrin, Christophe, Patrycja Sroczynska, Catherine Stephenson, Terry Allen, Valerie Kouskoff, and Georges Lacaud. 2009. 'The haemangioblast generates haematopoietic cells through a haemogenic endothelium stage', *Nature*, 457: 892-95.

Lanner, Fredrik, Marcus Sohl, and Filip Farnebo. 2007. 'Functional Arterial and Venous Fate Is Determined by Graded VEGF Signaling and Notch Status During Embryonic Stem Cell Differentiation', *Arteriosclerosis, Thrombosis, and Vascular Biology*, 27: 487-93.

Lawrence, Jeffrey H., Julie Christensen, Stephen Fong, Yu-Long Hu, Irving Weissman, Guy Sauvageau, Keith R. Humphries, and Corey Largman. 2005. 'Loss of expression of the

Hoxa-9 homeobox gene impairs the proliferation and repopulating ability of hematopoietic stem cells', *Blood*, 106: 3988-94.

Lawson, N. D., N. Scheer, V. N. Pham, C. H. Kim, A. B. Chitnis, J. A. Campos-Ortega, and B. M. Weinstein. 2001. 'Notch signaling is required for arterial-venous differentiation during embryonic vascular development', *Development*, 128: 3675-83.

le Noble, Ferdinand, Delphine Moyon, Luc Pardanaud, Li Yuan, Valentin Djonov, Robert Matthijsen, Christiane Bréant, Vincent Fleury, and Anne Eichmann. 2003. 'Flow regulates arterial-venous differentiation in the chick embryo yolk sac', *Development (Cambridge, England)*: 361-75.

Lee, Lydia K., Yasamine Ghorbanian, Wenyuan Wang, Yanling Wang, Yeon Kim, Irving L. Weissman, Matthew A. Inlay, and Hanna Mikkola. 2016. 'LYVE1 Marks the Divergence of Yolk Sac Definitive Hemogenic Endothelium from the Primitive Erythroid Lineage', *Cell Reports*, 17: 2286-98.

Lemischka, I. R. 1991. 'Clonal, in vivo behavior of the totipotent hematopoietic stem cell', *Seminars in immunology*, 3: 349-55.

Lengerke, Claudia, Sabine Schmitt, Teresa V. Bowman, Il Jang, Leila Maouche-Chretien, Shannon McKinney-Freeman, Alan J. Davidson, Matthias Hammerschmidt, Fabian Rentzsch, Jeremy Green, Leonard I. Zon, and George Q. Daley. 2008. 'BMP and Wnt Specify Hematopoietic Fate by Activation of the Cdx-Hox Pathway', *Cell Stem Cell*, 2: 72-82.

Leung, Amy, Aldo Ciau-Uitz, Philip Pinheiro, Rui Monteiro, Jie Zuo, Paresh Vyas, Roger Patient, and Catherine Porcher. 2013. 'Uncoupling VEGFA Functions in Arteriogenesis and Hematopoietic Stem Cell Specification', *Developmental Cell*, 24: 144-58.

Li, Yan, Long Gao, Brandon Hadland, Kai Tan, and Nancy A. Speck. 2017. 'CD27 marks murine embryonic hematopoietic stem cells and type II prehematopoietic stem cells', *Blood*, 130: 372-76.

Liakhovitskaia, Anna, Stanislav Rybtsov, Tom Smith, Antoniana Batsivari, Natalia Rybtsova, Christina Rode, Marella de Bruijn, Frank Buchholz, Sabrina Gordon-Keylock, Suling Zhao, and Alexander Medvinsky. 2014. 'Runx1 is required for progression of CD41+ embryonic precursors into HSCs but not prior to this', *Development*, 141: 3319-23.

Lichtinger, Monika, Richard Ingram, Rebecca Hannah, Dorothee Müller, Deborah Clarke, Salam A. Assi, Michael Lie-A-Ling, Laura Noailles, M. S. Vijayabaskar, Mengchu Wu, Daniel G. Tenen, David R. Westhead, Valerie Kouskoff, Georges Lacaud, Berthold Göttgens, and Constanze Bonifer. 2012. 'RUNX1 reshapes the epigenetic landscape at the onset of haematopoiesis', *The EMBO Journal*, 31: 4318-33.

Lie-A-Ling, Michael, Elli Marinopoulou, Andrew J. Lilly, Mairi Challinor, Rahima Patel, Christophe Lancrin, Valerie Kouskoff, and Georges Lacaud. 2018. 'Regulation of RUNX1 dosage is crucial for efficient blood formation from hemogenic endothelium', *Development*, 145.

Lis, Raphael, Charles C. Karrasch, Michael G. Poulos, Balvir Kunar, David Redmond, Jose G. Duran, Chaitanya R. Badwe, William Schachterle, Michael Ginsberg, Jenny Xiang, Arash Tabrizi, Koji Shido, Zev Rosenwaks, Olivier Elemento, Nancy A. Speck, Jason M. Butler, Joseph M. Scandura, and Shahin Rafii. 2017. 'Conversion of adult endothelium to immunocompetent haematopoietic stem cells', *Nature*, 545: 439-45.

Lizama, Carlos O., John S. Hawkins, Christopher E. Schmitt, Frank L. Bos, Joan P. Zape, Kelly M. Cautivo, Hugo Pinto, Alexander M. Rhyner, Hui Yu, Mary E. Donohoe, Joshua D. Wythe, and Ann C. Zovein. 2015. 'Repression of arterial genes in hemogenic endothelium is sufficient for haematopoietic fate acquisition', *Nature Communications*, 6: 7739.

Loh, K. M., A. Chen, P. W. Koh, T. Z. Deng, R. Sinha, J. M. Tsai, A. A. Barkal, K. Y. Shen, R. Jain, R. M. Morganti, N. Shyh-Chang, N. B. Fernhoff, B. M. George, G. Wernig, R. E. A. Salomon, Z. Chen, H. Vogel, J. A. Epstein, A. Kundaje, W. S. Talbot, P. A. Beachy, L. T. Ang, and I. L. Weissman. 2016. 'Mapping the Pairwise Choices Leading from Pluripotency to Human Bone, Heart, and Other Mesoderm Cell Types', *Cell*, 166: 451-67.

Lu, Yi-Fen, Patrick Cahan, Samantha Ross, Julie Sahalie, Patricia M. Sousa, Brandon K. Hadland, Wenqing Cai, Erik Serrao, Alan N. Engelman, Irwin D. Bernstein, and George Q. Daley. 2016. 'Engineered Murine HSCs Reconstitute Multi-lineage Hematopoiesis and Adaptive Immunity', *Cell Reports*, 17: 3178-92.

Lux, Christopher T., Momoko Yoshimoto, Kathleen McGrath, Simon J. Conway, James Palis, and Mervin C. Yoder. 2008. 'All primitive and definitive hematopoietic progenitor cells emerging before E10 in the mouse embryo are products of the yolk sac', *Blood*, 111: 3435-38.

Maecker, H. T., and J. Trotter. 2006. 'Flow cytometry controls, instrument setup, and the determination of positivity', *Cytometry A*, 69: 1037-42.

Masumura, Tomomi, Kimiko Yamamoto, Nobutaka Shimizu, Syotaro Obi, and Joji Ando. 2009. 'Shear Stress Increases Expression of the Arterial Endothelial Marker EphrinB2 in Murine ES Cells via the VEGF-Notch Signaling Pathways', *Arteriosclerosis, Thrombosis, and Vascular Biology*, 29: 2125-31.

Matsuoka, Sahoko, Kohichiro Tsuji, Hiroaki Hisakawa, Ming-jiang Xu, Yasuhiro Ebihara, Takefumi Ishii, Daisuke Sugiyama, Atsushi Manabe, Ryuhei Tanaka, Yasuo Ikeda, Shigetaka Asano, and Tatsutoshi Nakahata. 2001. 'Generation of definitive hematopoietic stem cells from murine early yolk sac and paraaortic splanchnopleures by aorta-gonad-mesonephros region–derived stromal cells', *Blood*, 98: 6-12.

McGrath, Kathleen E., Jenna M. Frame, Katherine H. Fegan, James R. Bowen, Simon J. Conway, Seana C. Catherman, Paul D. Kingsley, Anne D. Koniski, and James Palis. 2015. 'Distinct Sources of Hematopoietic Progenitors Emerge before HSCs and Provide Functional Blood Cells in the Mammalian Embryo', *Cell Reports*, 11: 1892-904.

McGrath, Kathleen E., Anne D. Koniski, Jeffrey Malik, and James Palis. 2003. 'Circulation is established in a stepwise pattern in the mammalian embryo', *Blood*, 101: 1669-75.

McKinney-Freeman, Shannon, Patrick Cahan, Hu Li, Scott A. Lacadie, Hsuan-Ting T. Huang, Matthew Curran, Sabine Loewer, Olaia Naveiras, Katie L. Kathrein, Martina Konantz, Erin M. Langdon, Claudia Lengerke, Leonard I. Zon, James J. Collins, and George Q. Daley. 2012. 'The transcriptional landscape of hematopoietic stem cell ontogeny', *Cell Stem Cell*, 11: 701-14.

Medvinsky, A., and E. Dzierzak. 1996. 'Definitive hematopoiesis is autonomously initiated by the AGM region', *Cell*, 86: 897-906.

Mikkola, Hanna K. A., and Stuart H. Orkin. 2006. 'The journey of developing hematopoietic stem cells', *Development*, 133: 3733-44.

Mills, Jason A., Prasuna Paluru, Mitchell J. Weiss, Paul Gadue, and Deborah L. French. 2014. 'Hematopoietic Stem Cell Protocols', *Methods in molecular biology (Clifton, N.J.)*, 1185: 181-94.

Minot, CS, HM Evans, J Tandler, and FR Sabin. 1913. 'Development of the Blood, the Vascular System, and the Spleen.' in, *Manual of Human Embryology* (J.B. Lippincott Company).

Monteiro, Rui, Philip Pinheiro, Nicola Joseph, Tessa Peterkin, Jana Koth, Emmanouela Repapi, Florian Bonkhofer, Arif Kirmizitas, and Roger Patient. 2016. 'Transforming Growth Factor β Drives Hemogenic Endothelium Programming and the Transition to Hematopoietic Stem Cells', *Developmental Cell*, 38: 358-70.

Moyon, D., L. Pardanaud, L. Yuan, C. Bréant, and A. Eichmann. 2001. 'Plasticity of endothelial cells during arterial-venous differentiation in the avian embryo', *Development (Cambridge, England)*: 3359-70.

Müller, Albrecht M., Alexander Medvinsky, John Strouboulis, Frank Grosveld, and Elaine Dzierzakt. 1994. 'Development of hematopoietic stem cell activity in the mouse embryo', *Immunity*, 1: 291-301.

Murray, P.D.F. 1932. 'The development *in vitro* of the blood of the early chick embryo', *Proc. Roy. Soc. London*, 11: 497-521.

Nakamura-Ishizu, A., H. Takizawa, and T. Suda. 2014. 'The analysis, roles and regulation of quiescence in hematopoietic stem cells', *Development*, 141: 4656-66.

Ng, Elizabeth S., Lisa Azzola, Freya F. Bruveris, Vincenzo Calvanese, Belinda Phipson, Katerina Vlahos, Claire Hirst, Vanta J. Jokubaitis, Qing C. Yu, Jovana Maksimovic, Simone Liebscher, Vania Januar, Zhen Zhang, Brenda Williams, Aude Conscience, Jennifer Durnall, Steven Jackson, Magdaline Costa, David Elliott, David N. Haylock, Susan K. Nilsson, Richard Saffery, Katja Schenke-Layland, Alicia Oshlack, Hanna K. A. Mikkola, Edouard G. Stanley, and Andrew G. Elefanty. 2016. 'Differentiation of human embryonic stem cells to HOXA+ hemogenic vasculature that resembles the aorta-gonad-mesonephros', *Nature Biotechnology*, 34: 1168-79.

Ng, Elizabeth S., Lisa Azzola, Koula Sourris, Lorraine Robb, Edouard G. Stanley, and Andrew G. Elefanty. 2005. 'The primitive streak gene Mixl1 is required for efficient haematopoiesis and BMP4-induced ventral mesoderm patterning in differentiating ES cells', *Development*, 132: 873-84.

Nishikawa, S. I., S. Nishikawa, H. Kawamoto, H. Yoshida, M. Kizumoto, H. Kataoka, and Y. Katsura. 1998. 'In vitro generation of lymphohematopoietic cells from endothelial cells purified from murine embryos', *Immunity*, 8: 761-69.

North, T. E., W. Goessling, M. Peeters, P. Li, C. Ceol, A. M. Lord, G. J. Weber, J. Harris, C. C. Cutting, P. Huang, E. Dzierzak, and L. I. Zon. 2009. 'Hematopoietic stem cell development is dependent on blood flow', *Cell*, 137: 736-48.

North, T. E., W. Goessling, C. R. Walkley, C. Lengerke, K. R. Kopani, A. M. Lord, G. J. Weber, T. V. Bowman, I. H. Jang, T. Grosser, G. A. Fitzgerald, G. Q. Daley, S. H. Orkin, and L. I. Zon. 2007. 'Prostaglandin E2 regulates vertebrate haematopoietic stem cell homeostasis', *Nature*, 447: 1007-11.

North, T., T. L. Gu, T. Stacy, Q. Wang, L. Howard, M. Binder, M. Marin-Padilla, and N. A. Speck. 1999. 'Cbfa2 is required for the formation of intra-aortic hematopoietic clusters', *Development*, 126: 2563-75.

Nostro, Cristina M., Xin Cheng, Gordon M. Keller, and Paul Gadue. 2008. 'Wnt, Activin, and BMP Signaling Regulate Distinct Stages in the Developmental Pathway from Embryonic Stem Cells to Blood', *Cell Stem Cell*, 2: 60-71.

Notta, Faiyaz, Sergei Doulatov, Elisa Laurenti, Armando Poeppl, Igor Jurisica, and John E. Dick. 2011. 'Isolation of Single Human Hematopoietic Stem Cells Capable of Long-Term Multilineage Engraftment', *Science*, 333: 218-21.

Nottingham, W. T., A. Jarratt, M. Burgess, C. L. Speck, J. F. Cheng, S. Prabhakar, E. M. Rubin, P. S. Li, J. Sloane-Stanley, A. San J. Kong, and M. F. de Bruijn. 2007. 'Runx1-mediated hematopoietic stem-cell emergence is controlled by a Gata/Ets/SCL-regulated enhancer', *Blood*, 110: 4188-97.

Oberlin, Estelle, Manuela Tavian, Istvàn Blazsek, and Bruno Péault. 2002. 'Blood-forming potential of vascular endothelium in the human embryo', *Development (Cambridge, England)*, 129: 4147-57.

Ohishi, Kohshi, Barbara Varnum-Finney, and Irwin D. Bernstein. 2002. 'Delta-1 enhances marrow and thymus repopulating ability of human CD34+CD38– cord blood cells', *Journal of Clinical Investigation*, 110: 1165-74.

Okuda, T., J. van Deursen, S. W. Hiebert, G. Grosveld, and J. R. Downing. 1996. 'AML1, the target of multiple chromosomal translocations in human leukemia, is essential for normal fetal liver hematopoiesis', *Cell*, 84: 321-30.

Org, Tõnis, Dan Duan, Roberto Ferrari, Amelie Montel-Hagen, Ben Handel, Marc A. Kerényi, Rajkumar Sasidharan, Liudmilla Rubbi, Yuko Fujiwara, Matteo Pellegrini, Stuart H. Orkin, Siavash K. Kurdistani, and Hanna K. A. Mikkola. 2015. 'Scl binds to primed enhancers in mesoderm to regulate hematopoietic and cardiac fate divergence', *The EMBO Journal*, 34: 759-77.

Othman-Hassan, Karim, Ketan Patel, Maria Papoutsi, Marc Rodriguez-Niedenführ, Bodo Christ, and Jörg Wilting. 2001. 'Arterial Identity of Endothelial Cells Is Controlled by Local Cues', *Developmental Biology*, 237: 398-409.

Padrón-Barthe, Laura, Susana Temiño, Cristina del Campo, Laura Carramolino, Joan Isern, and Miguel Torres. 2014. 'Clonal analysis identifies hemogenic endothelium as the source of the blood-endothelial common lineage in the mouse embryo', *Blood*, 124: 2523-32.

Palis, J. 2014. 'Primitive and definitive erythropoiesis in mammals', *Front Physiol*, 5: 3.

Palis, J., S. Robertson, M. Kennedy, C. Wall, and G. Keller. 1999. 'Development of erythroid and myeloid progenitors in the yolk sac and embryo proper of the mouse', *Development (Cambridge, England)*, 126: 5073-84.

Pardanaud, L., C. Altmann, P. Kitos, F. Dieterlen-Lievre, and C. A. Buck. 1987. 'Vasculogenesis in the early quail blastodisc as studied with a monoclonal antibody recognizing endothelial cells', *Development (Cambridge, England)*, 100: 339-49.

Park, Changwon, Iva Afrikanova, Yun Chung, Wen Zhang, Elizabeth Arentson, Guo hua Fong, Alexander Rosendahl, and Kyunghee Choi. 2004. 'A hierarchical order of factors in the generation of FLK1- and SCL-expressing hematopoietic and endothelial progenitors from embryonic stem cells', *Development*, 131: 2749-62.

Park, J. E., G. A. Keller, and N. Ferrara. 1993. 'The vascular endothelial growth factor (VEGF) isoforms: differential deposition into the subepithelial extracellular matrix and bioactivity of extracellular matrix-bound VEGF', *Molecular Biology of the Cell*, 4: 1317-26.

Park, Mi, Akhilesh Kumar, Ho Jung, Gene Uenishi, Oleg V. Moskvin, James A. Thomson, and Igor I. Slukvin. 2018. 'Activation of the Arterial Program Drives Development of Definitive Hemogenic Endothelium with Lymphoid Potential', *Cell Reports*, 23: 2467-81.

Pearson, Stella, Sara Cuvertino, Maud Fleury, Georges Lacaud, and Valerie Kouskoff. 2015. 'In Vivo Repopulating Activity Emerges at the Onset of Hematopoietic Specification during Embryonic Stem Cell Differentiation', *Stem Cell Reports*, 4: 431-44.

Pearson, Stella, Patrycja Sroczynska, Georges Lacaud, and Valerie Kouskoff. 2008. 'The stepwise specification of embryonic stem cells to hematopoietic fate is driven by sequential exposure to Bmp4, activin A, bFGF and VEGF', *Development*, 135: 1525-35.

Pijuan-Sala, B., J. A. Griffiths, C. Guibentif, T. W. Hiscock, W. Jawaid, F. J. Calero-Nieto, C. Mulas, X. Ibarra-Soria, R. C. V. Tyser, D. L. L. Ho, W. Reik, S. Srinivas, B. D. Simons, J. Nichols, J. C. Marioni, and B. Gottgens. 2019. 'A single-cell molecular map of mouse gastrulation and early organogenesis', *Nature*, 566: 490-95.

Pindyurin, Alexey V., and Bas van Steensel. 2012. 'Hox in space: gene cluster regulation linked to folding of chromatin', *Nucleus (Austin, Tex.)*, 3: 118-22.

Porcher, Catherine, Hedia Chagraoui, and Maiken S. Kristiansen. 2017. 'SCL/TAL1: a multifaceted regulator from blood development to disease', *Blood*, 129: 2051-60.

Quillien, A., J. C. Moore, M. Shin, A. F. Siekmann, T. Smith, L. Pan, C. B. Moens, M. J. Parsons, and N. D. Lawson. 2014. 'Distinct Notch signaling outputs pattern the developing arterial system', *Development*, 141: 1544-52.

Reese, David E., Christopher E. Hall, and Takashi Mikawa. 2004. 'Negative Regulation of Midline Vascular Development by the Notochord', *Developmental Cell*: 699-708.

Richard, Charlotte, Cécile Drevon, Pierre-Yves Canto, Gaelle Villain, Karine Bollérot, Aveline Lempereur, Marie-Aimée Teillet, Christine Vincent, Catalina Rosselló Castillo, Miguel Torres, Eileen Piwarzyk, Nancy A. Speck, Michèle Souyri, and Thierry Jaffredo. 2013. 'Endothelio-Mesenchymal Interaction Controls runx1 Expression and Modulates the notch Pathway to Initiate Aortic Hematopoiesis', *Developmental Cell*, 24: 600-11.

Robert-Moreno, A., L. Espinosa, J. L. de la Pompa, and A. Bigas. 2005. 'RBPjkappa-dependent Notch function regulates Gata2 and is essential for the formation of intra-embryonic hematopoietic cells', *Development*, 132: 1117-26.

Robert-Moreno, Alex, Jordi Guiu, Cristina Ruiz-Herguido, M. E. López, Julia Inglés-Esteve, Lluis Riera, Alex Tipping, Tariq Enver, Elaine Dzierzak, Thomas Gridley, Lluis Espinosa, and Anna Bigas. 2008. 'Impaired embryonic haematopoiesis yet normal arterial development in the absence of the Notch ligand Jagged1', *The EMBO Journal*, 27: 1886-95.

Ruhrberg, Christiana, Holger Gerhardt, Matthew Golding, Rose Watson, Sofia Ioannidou, Hajime Fujisawa, Christer Betsholtz, and David T. Shima. 2002. 'Spatially restricted patterning cues provided by heparin-binding VEGF-A control blood vessel branching morphogenesis', *Genes & Development*, 16: 2684-98.

Rybtsov, S., A. Ivanovs, S. Zhao, and A. Medvinsky. 2016. 'Concealed expansion of immature precursors underpins acute burst of adult HSC activity in foetal liver', *Development*, 143: 1284-9.

Rybtsov, Stanislav, Antoniana Batsivari, Kateryna Bilotkach, Daria Paruzina, Jordi Senserrich, Oleg Nerushev, and Alexander Medvinsky. 2014. 'Tracing the Origin of the HSC Hierarchy Reveals an SCF-Dependent, IL-3-Independent CD43− Embryonic Precursor', *Stem Cell Reports*, 3: 489-501.

Rybtsov, Stanislav, Malgorzata Sobiesiak, Samir Taoudi, Céline Souilhol, Jordi Senserrich, Anna Liakhovitskaia, Andrejs Ivanovs, Jon Frampton, Suling Zhao, and Alexander Medvinsky. 2011. 'Hierarchical organization and early hematopoietic specification of the developing HSC lineage in the AGM region', *The Journal of Experimental Medicine*, 208: 1305-15.

Sabin, Florence R. 1920. 'Studies on the origin of blood-vessels and of red blood-corpuscles as seen in the living blastoderm of chicks during the second day of incubation', *Contrib. Embryol Carneg Inst.*, 9: 214-62.

Saito, Tetsuya, Norihiko Takeda, Eisuke Amiya, Tomoko Nakao, Hajime Abe, Hiroaki Semba, Katsura Soma, Katsuhiro Koyama, Yumiko Hosoya, Yasushi Imai, Takayuki Isagawa, Masafumi Watanabe, Ichiro Manabe, Issei Komuro, Ryozo Nagai, and Koji Maemura. 2013. 'VEGF-A induces its negative regulator, soluble form of VEGFR-1, by modulating its alternative splicing', *FEBS Letters*, 587: 2179-85.

Sakurai, H., T. Era, L. M. Jakt, M. Okada, S. Nakai, S. Nishikawa, and S. Nishikawa. 2006. 'In vitro modeling of paraxial and lateral mesoderm differentiation reveals early reversibility', *STEM CELLS*, 24: 575-86.

Samokhvalov, Igor M., Natalia I. Samokhvalova, and Shin-ichi Nishikawa. 2007. 'Cell tracing shows the contribution of the yolk sac to adult haematopoiesis', *Nature*, 446.

Sandler, V. M., R. Lis, Y. Liu, A. Kedem, D. James, O. Elemento, J. M. Butler, J. M. Scandura, and S. Rafii. 2014. 'Reprogramming human endothelial cells to haematopoietic cells requires vascular induction', *Nature*, 511: 312-8.

Sanjuan-Pla, A., I. C. Macaulay, C. T. Jensen, P. S. Woll, T. C. Luis, A. Mead, S. Moore, C. Carella, S. Matsuoka, T. Bouriez Jones, O. Chowdhury, L. Stenson, M. Lutteropp, J. C. Green, R. Facchini, H. Boukarabila, A. Grover, A. Gambardella, S. Thongjuea, J. Carrelha, P. Tarrant, D. Atkinson, S. A. Clark, C. Nerlov, and S. E. Jacobsen. 2013. 'Platelet-biased stem cells reside at the apex of the haematopoietic stem-cell hierarchy', *Nature*, 502: 232-6.

Sauvageau, G., P. M. Lansdorp, C. J. Eaves, D. E. Hogge, W. H. Dragowska, D. S. Reid, C. Largman, H. J. Lawrence, and R. K. Humphries. 1994. 'Differential expression of homeobox genes in functionally distinct CD34+ subpopulations of human bone marrow cells', *Proceedings of the National Academy of Sciences*, 91: 12223-27.

Schulz, C., E. Gomez Perdiguero, L. Chorro, H. Szabo-Rogers, N. Cagnard, K. Kierdorf, M. Prinz, B. Wu, S. E. Jacobsen, J. W. Pollard, J. Frampton, K. J. Liu, and F. Geissmann. 2012a. 'A lineage of myeloid cells independent of Myb and hematopoietic stem cells', *Science*, 336: 86-90.

Schulz, Christian, Elisa Perdiguero, Laurent Chorro, Heather Szabo-Rogers, Nicolas Cagnard, Katrin Kierdorf, Marco Prinz, Bishan Wu, Sten W. Jacobsen, Jeffrey W. Pollard, Jon

Frampton, Karen J. Liu, and Frederic Geissmann. 2012b. 'A Lineage of Myeloid Cells Independent of Myb and Hematopoietic Stem Cells', *Science*, 336: 86-90.
Shin, M., T. J. Beane, A. Quillien, I. Male, L. J. Zhu, and N. D. Lawson. 2016. 'Vegfa signals through ERK to promote angiogenesis, but not artery differentiation', *Development*, 143: 3796-805.
Sitnicka, E., N. Lin, G. V. Priestley, N. Fox, V. C. Broudy, N. S. Wolf, and K. Kaushansky. 1996. 'The effect of thrombopoietin on the proliferation and differentiation of murine hematopoietic stem cells', *Blood*, 87: 4998-5005.
Sjöqvist, Marika, and Emma R. Andersson. 2017. 'Do as I say, Not(ch) as I do: lateral control of cell fate', *Developmental Biology*.
Slukvin, Igor I. 2016. 'Generating human hematopoietic stem cells in vitro –exploring endothelial to hematopoietic transition as a portal for stemness acquisition', *FEBS Letters*, 590: 4126-43.
Smith, R. A., and C. A. Glomski. 1982. '"Hemogenic endothelium" of the embryonic aorta: Does it exist?', *Dev Comp Immunol*, 6: 359-68.
Souilhol, C., J. G. Lendinez, S. Rybtsov, F. Murphy, H. Wilson, D. Hills, A. Batsivari, A. Binagui-Casas, A. C. McGarvey, H. R. MacDonald, R. Kageyama, C. Siebel, S. Zhao, and A. Medvinsky. 2016. 'Developing HSCs become Notch independent by the end of maturation in the AGM region', *Blood*, 128: 1567-77.
Spangrude, G. J., L. Smith, N. Uchida, K. Ikuta, S. Heimfeld, J. Friedman, and I. L. Weissman. 1991. 'Mouse hematopoietic stem cells', *Blood*, 78: 1395-402.
Sriram, Gopu, Jia Tan, Intekhab Islam, Abdul Rufaihah, and Tong Cao. 2015. 'Efficient differentiation of human embryonic stem cells to arterial and venous endothelial cells under feeder- and serum-free conditions', *Stem Cell Research & Therapy*, 6: 1-17.
Stefanska, M., K. Batta, R. Patel, M. Florkowska, V. Kouskoff, and G. Lacaud. 2017. 'Primitive erythrocytes are generated from hemogenic endothelial cells', *Sci Rep*, 7: 6401.
Sturgeon, Christopher M., Andrea Ditadi, Geneve Awong, Marion Kennedy, and Gordon Keller. 2014. 'Wnt signaling controls the specification of definitive and primitive hematopoiesis from human pluripotent stem cells', *Nature Biotechnology*, 32: 554-61.
Sugimura, Ryohichi, Deepak Jha, Areum Han, Clara Soria-Valles, Edroaldo da Rocha, Yi-Fen Lu, Jeremy A. Goettel, Erik Serrao, Grant R. Rowe, Mohan Malleshaiah, Irene Wong, Patricia Sousa, Ted N. Zhu, Andrea Ditadi, Gordon Keller, Alan N. Engelman, Scott B. Snapper, Sergei Doulatov, and George Q. Daley. 2017. 'Haematopoietic stem and progenitor cells from human pluripotent stem cells', *Nature*, 545.
Sugiyama, D., M. Ogawa, I. Hirose, T. Jaffredo, K. Arai, and K. Tsuji. 2003. 'Erythropoiesis from acetyl LDL incorporating endothelial cells at the preliver stage', *Blood*, 101: 4733-8.
Suzuki, N., S. Yamazaki, T. Yamaguchi, M. Okabe, H. Masaki, S. Takaki, M. Otsu, and H. Nakauchi. 2013. 'Generation of engraftable hematopoietic stem cells from induced pluripotent stem cells by way of teratoma formation', *Mol Ther*, 21: 1424-31.
Swiers, G., C. Baumann, J. O'Rourke, E. Giannoulatou, S. Taylor, A. Joshi, V. Moignard, C. Pina, T. Bee, K. D. Kokkaliaris, M. Yoshimoto, M. C. Yoder, J. Frampton, T. Schroeder, T. Enver, B. Gottgens, and Mftr de Bruijn. 2013. 'Early dynamic fate changes in haemogenic endothelium characterized at the single-cell level', *Nat Commun*, 4: 2924.
Swift, Matthew R., Van N. Pham, Daniel Castranova, Kameha Bell, Richard J. Poole, and Brant M. Weinstein. 2014. 'SoxF factors and Notch regulate nr2f2 gene expression during venous differentiation in zebrafish', *Developmental Biology*: 116-25.
Takahashi, Kazutoshi, and Shinya Yamanaka. 2006. 'Induction of Pluripotent Stem Cells from Mouse Embryonic and Adult Fibroblast Cultures by Defined Factors', *Cell*, 126: 663-76.
Tamplin, Owen J., Ellen M. Durand, Logan A. Carr, Sarah J. Childs, Elliott J. Hagedorn, Pulin Li, Amanda D. Yzaguirre, Nancy A. Speck, and Leonard I. Zon. 2015. 'Hematopoietic Stem Cell Arrival Triggers Dynamic Remodeling of the Perivascular Niche', *Cell*, 160: 241-52.

Tang, Yuefeng, Hao Bai, Sumithra Urs, Zack Wang, and Lucy Liaw. 2013. 'Notch1 activation in embryonic VE-cadherin populations selectively blocks hematopoietic stem cell generation and fetal liver hematopoiesis', *Transgenic Research*, 22: 403-10.

Taoudi, Samir, Christèle Gonneau, Kate Moore, Julie M. Sheridan, C. Clare Blackburn, Erin Taylor, and Alexander Medvinsky. 2008. 'Extensive Hematopoietic Stem Cell Generation in the AGM Region via Maturation of VE-Cadherin+CD45+ Pre-Definitive HSCs', *Cell Stem Cell*, 3: 99-108.

Taoudi, Samir, and Alexander Medvinsky. 2007. 'Functional identification of the hematopoietic stem cell niche in the ventral domain of the embryonic dorsal aorta', *Proceedings of the National Academy of Sciences of the United States of America*, 104: 9399-403.

Thambyrajah, Roshana, Milena Mazan, Rahima Patel, Victoria Moignard, Monika Stefanska, Elli Marinopoulou, Yaoyong Li, Christophe Lancrin, Thomas Clapes, Tarik Möröy, Catherine Robin, Crispin Miller, Shaun Cowley, Berthold Göttgens, Valerie Kouskoff, and Georges Lacaud. 2016. 'GFI1 proteins orchestrate the emergence of haematopoietic stem cells through recruitment of LSD1', *Nature Cell Biology*, 18: 21-32.

Thompson, M. A., D. G. Ransom, S. J. Pratt, H. MacLennan, M. W. Kieran, H. W. Detrich, B. Vail, T. L. Huber, B. Paw, A. J. Brownlie, A. C. Oates, A. Fritz, M. A. Gates, A. Amores, N. Bahary, W. S. Talbot, H. Her, D. R. Beier, J. H. Postlethwait, and L. I. Zon. 1998. 'The cloche and spadetail genes differentially affect hematopoiesis and vasculogenesis', *Developmental Biology*, 197: 248-69.

Torres-Vázquez, Jesús, Makoto Kamei, and Brant M. Weinstein. 2003. 'Molecular distinction between arteries and veins', *Cell and tissue research*, 314: 43-59.

Tukey, J. W. 1949. 'Comparing individual means in the analysis of variance', *Biometrics*, 5: 99-114.

Uenishi, G. I., H. S. Jung, A. Kumar, M. A. Park, B. K. Hadland, E. McLeod, M. Raymond, O. Moskvin, C. E. Zimmerman, D. J. Theisen, S. Swanson, J. Tamplin O, L. I. Zon, J. A. Thomson, I. D. Bernstein, and Slukvin, II. 2018. 'NOTCH signaling specifies arterial-type definitive hemogenic endothelium from human pluripotent stem cells', *Nat Commun*, 9: 1828.

Ueno, H., and I. L. Weissman. 2006. 'Clonal analysis of mouse development reveals a polyclonal origin for yolk sac blood islands', *Dev Cell*, 11: 519-33.

Vargel, Özge, Yang Zhang, Kinga Kosim, Kerstin Ganter, Sophia Foehr, Yannicka Mardenborough, Maya Shvartsman, Anton J. Enright, Jeroen Krijgsveld, and Christophe Lancrin. 2016. 'Activation of the TGFβ pathway impairs endothelial to haematopoietic transition', *Scientific Reports*, 6: 21518.

Villa, N., L. Walker, C. E. Lindsell, J. Gasson, M. L. Iruela-Arispe, and G. Weinmaster. 2001. 'Vascular expression of Notch pathway receptors and ligands is restricted to arterial vessels', *Mechanisms of development*, 108: 161-64.

Vokes, S. A., T. A. Yatskievych, R. L. Heimark, J. McMahon, A. P. McMahon, P. B. Antin, and P. A. Krieg. 2004. 'Hedgehog signaling is essential for endothelial tube formation during vasculogenesis', *….*.

Wang, Q., T. Stacy, M. Binder, M. Marin-Padilla, A. H. Sharpe, and N. A. Speck. 1996. 'Disruption of the Cbfa2 gene causes necrosis and hemorrhaging in the central nervous system and blocks definitive hematopoiesis', *Proc Natl Acad Sci U S A*, 93: 3444-9.

Yamamizu, Kohei, Taichi Matsunaga, Hideki Uosaki, Hiroyuki Fukushima, Shiori Katayama, Mina Hiraoka-Kanie, Kohnosuke Mitani, and Jun K. Yamashita. 2010. 'Convergence of Notch and β-catenin signaling induces arterial fate in vascular progenitors', *The Journal of Cell Biology*, 189: 325-38.

Yoder, M. C., and K. Hiatt. 1997. 'Engraftment of embryonic hematopoietic cells in conditioned newborn recipients', *Blood*, 89: 2176-83.

Yoder, Mervin C. 2014. 'Inducing definitive hematopoiesis in a dish', *Nature Biotechnology*, 32: 539-41.

Yoder, Mervin C., Kelly Hiatt, and Pinku Mukherjee. 1997. 'In vivo repopulating hematopoietic stem cells are present in the murine yolk sac at day 9.0 postcoitus', *Proceedings of the National Academy of Sciences*, 94: 6776-80.

Yokomizo, T., N. Watanabe, T. Umemoto, J. Matsuo, R. Harai, Y. Kihara, E. Nakamura, N. Tada, T. Sato, T. Takaku, A. Shimono, H. Takizawa, N. Nakagata, S. Mori, M. Kurokawa, D. G. Tenen, M. Osato, T. Suda, and N. Komatsu. 2019. 'Hlf marks the developmental pathway for hematopoietic stem cells but not for erythro-myeloid progenitors', *J Exp Med*.

Yoshimoto, Momoko, Encarnacion Montecino-Rodriguez, Michael J. Ferkowicz, Prashanth Porayette, Christopher W. Shelley, Simon J. Conway, Kenneth Dorshkind, and Mervin C. Yoder. 2011. 'Embryonic day 9 yolk sac and intra-embryonic hemogenic endothelium independently generate a B-1 and marginal zone progenitor lacking B-2 potential', *Proceedings of the National Academy of Sciences*, 108: 1468-73.

Yoshimoto, Momoko, Prashanth Porayette, Nicole L. Glosson, Simon J. Conway, Nadia Carlesso, Angelo A. Cardoso, Mark H. Kaplan, and Mervin C. Yoder. 2012. 'Autonomous murine T-cell progenitor production in the extra-embryonic yolk sac before HSC emergence', *Blood*, 119: 5706-14.

Yurugi-Kobayashi, T., H. Itoh, Schroeder - T. …, and biology and vascular. 2006. 'Adrenomedullin/cyclic AMP pathway induces Notch activation and differentiation of arterial endothelial cells from vascular progenitors', *…*

Yvernogeau, Laurent, Rodolphe Gautier, Hanane Khoury, Sara Menegatti, Melanie Schmidt, Jean-Francois Gilles, and Thierry Jaffredo. 2016. 'An in vitro model of hemogenic endothelium commitment and hematopoietic production', *Development*, 143: 1302-12.

Zhang, Gang, Jianye Zhou, Quanxin Fan, Zhe Zheng, Fusheng Zhang, Xuebin Liu, and Shengshou Hu. 2008a. 'Arterial–venous endothelial cell fate is related to vascular endothelial growth factor and Notch status during human bone mesenchymal stem cell differentiation', *FEBS Letters*, 582: 2957-64.

Zhang, Panpan, Qiuping He, Dongbo Chen, Weixiao Liu, Lu Wang, Chunxia Zhang, Dongyuan Ma, Wei Li, Bing Liu, and Feng Liu. 2015. 'G protein-coupled receptor 183 facilitates endothelial-to-hematopoietic transition via Notch1 inhibition', *Cell Research*, 25: 1093-107.

Zhang, X., A. A. Lanahan, and M. Simons. 2013. 'VEGFR2 trafficking: speed doesn't kill', *Cell Cycle*, 12: 2163-4.

Zhang, Xiao-Bing, Brian C. Beard, Grant D. Trobridge, Brent L. Wood, George E. Sale, Reeteka Sud, Keith R. Humphries, and Hans-Peter Kiem. 2008b. 'High incidence of leukemia in large animals after stem cell gene therapy with a HOXB4-expressing retroviral vector', *Journal of Clinical Investigation*, 118: 1502-10.

Zhong, Tao P., Sarah Childs, James P. Leu, and Mark C. Fishman. 2001. 'Gridlock signalling pathway fashions the first embryonic artery', *Nature*, 414: 35102599.

Zhou, Fan, Xianlong Li, Weili Wang, Ping Zhu, Jie Zhou, Wenyan He, Meng Ding, Fuyin Xiong, Xiaona Zheng, Zhuan Li, Yanli Ni, Xiaohuan Mu, Lu Wen, Tao Cheng, Yu Lan, Weiping Yuan, Fuchou Tang, and Bing Liu. 2016. 'Tracing haematopoietic stem cell formation at single-cell resolution', *Nature*, 533: 487-92.

Zovein, Ann C., Jennifer J. Hofmann, Maureen Lynch, Wendy J. French, Kirsten A. Turlo, Yanan Yang, Michael S. Becker, Lucia Zanetta, Elisabetta Dejana, Judith C. Gasson, Michelle D. Tallquist, and Luisa M. Iruela-Arispe. 2008. 'Fate Tracing Reveals the Endothelial Origin of Hematopoietic Stem Cells', *Cell Stem Cell*, 3: 625-36.